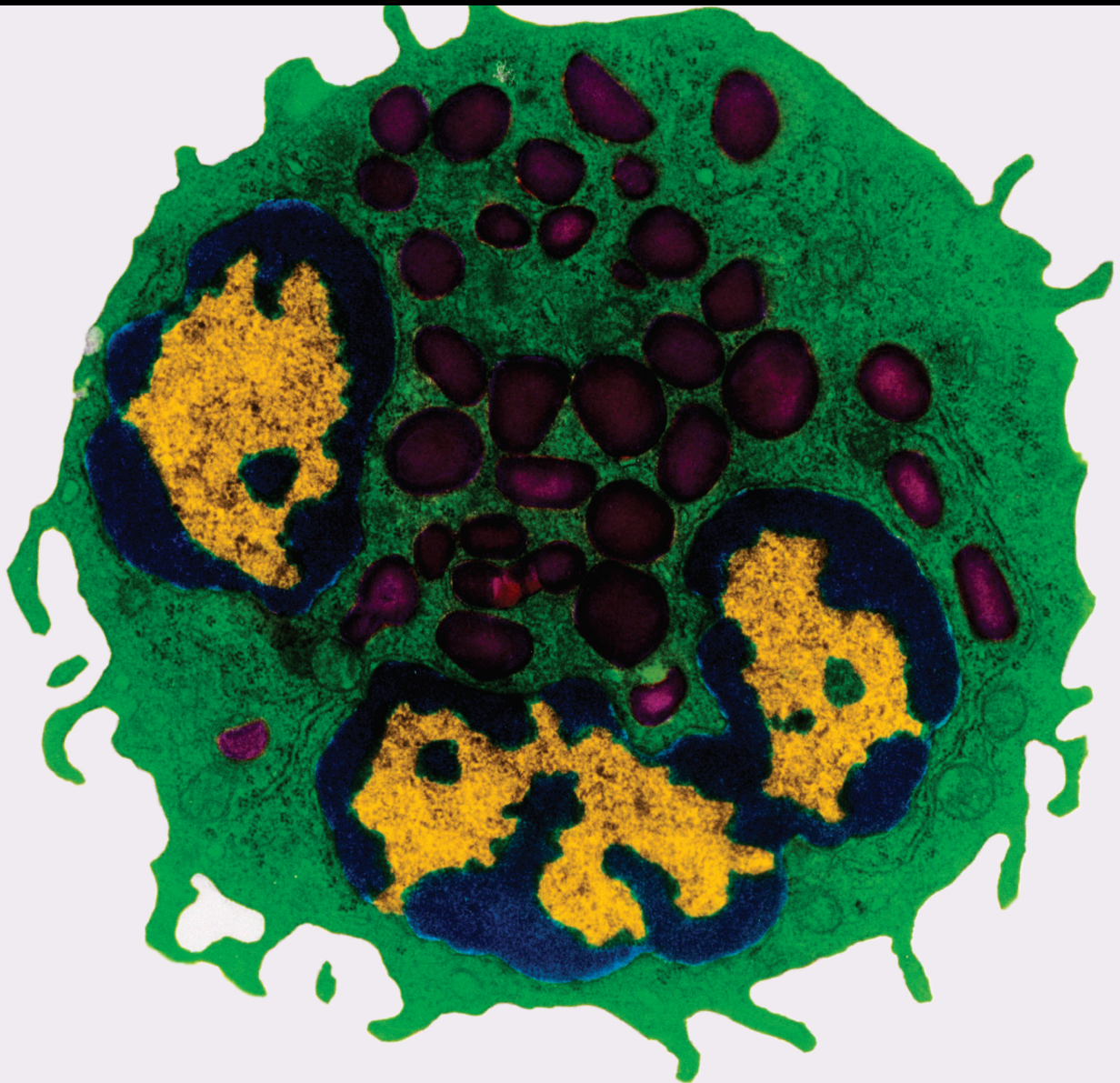


Role of Inflammasomes in Inflammatory and Infectious Diseases

Lead Guest Editor: Young-Su Yi

Guest Editors: Tae Jin Lee and Sehyun Kim





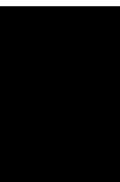
Role of Inflammasomes in Inflammatory and Infectious Diseases

Mediators of Inflammation

**Role of Inflammasomes in
Inflammatory and Infectious Diseases**

Lead Guest Editor: Young-Su Yi

Guest Editors: Tae Jin Lee and Sehyun Kim



Copyright © 2021 Hindawi Limited. All rights reserved.

This is a special issue published in “Mediators of Inflammation.” All articles are open access articles distributed under the Creative Commons Attribution License, which permits unrestricted use, distribution, and reproduction in any medium, provided the original work is properly cited.

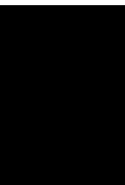
Chief Editor

Anshu Agrawal, USA

Editorial Board

Amedeo Amedei, Italy
Oleh Andrukhov, Austria
Emiliano Antiga, Italy
Zsolt J. Balogh, Australia
Adone Baroni, Italy
Jagadeesh Bayry, France
Tomasz Brzozowski, Poland
Elisabetta Buommino, Italy
Daniela Caccamo, Italy
Luca Cantarini, Italy
Raffaele Capasso, Italy
Calogero Caruso, Italy
Maria Rosaria Catania, Italy
Carlo Cervellati, Italy
Cristina Contreras, Spain
Robson Coutinho-Silva, Brazil
Jose Crispin, Mexico
Fulvio D'Acquisto, United Kingdom
Eduardo Dalmarco, Brazil
Pham My-Chan Dang, France
Carlos Dieguez, Spain
Agnieszka Dobrzyn, Poland
Elena Dozio, Italy
Emmanuel Economou, Greece
Ulrich Eisel, The Netherlands
Mirvat El-Sibai, Lebanon
Giacomo Emmi, Italy
Claudia Fabiani, Italy
Fabiola B Filippin Monteiro, Brazil
Antonella Fioravanti, Italy
Stefanie B. Flohé, Germany
Jan Fric, Czech Republic
Tânia Silvia Fröde, Brazil
Julio Galvez, Spain
Mirella Giovarelli, Italy
Denis Girard, Canada
Ronald Gladue, USA
Markus H. Gräler, Germany
Oreste Gualillo, Spain
Qingdong Guan, Canada
Elaine Hatanaka, Brazil
Tommaso Iannitti, United Kingdom
Byeong-Churl Jang, Republic of Korea
Yasumasa Kato, Japan

Yona Keisari, Israel
Alex Kleinjan, The Netherlands
Elzbieta Kolaczowska, Poland
Vladimir A. Kostyuk, Belarus
Dmitri V. Krysko, Belgium
Martha Lappas, Australia
Francesca Lembo, Italy
Eduardo López-Collazo, Spain
Andreas Ludwig, Germany
Ariadne Malamitsi-Puchner, Greece
Joilson O. Martins, Brazil
Donna-Marie McCafferty, Canada
Barbro N. Melgert, The Netherlands
Paola Migliorini, Italy
Vinod K. Mishra, USA
Eeva Moilanen, Finland
Alexandre Morrot, Brazil
Kutty Selva Nandakumar, China
Nadra Nilsen, Norway
Daniela Novick, Israel
Marja Ojaniemi, Finland
Sandra Helena Penha Oliveira, Brazil
Carla Pagliari, Brazil
Martin Pelletier, Canada
Vera L. Petricevich, Mexico
Sonja Pezelj-Ribarić, Croatia
Rituraj Purohit, India
Michal A. Rahat, Israel
Zoltan Rakonczay Jr., Hungary
Marcella Reale, Italy
Emanuela Roscetto, Italy
Carlos Rossa, Brazil
Settimio Rossi, Italy
Bernard Ryffel, France
Elena Silvestri, Italy
Carla Sipert, Brazil
Helen C. Steel, South Africa
Saravanan Subramanian, USA
Veendamali S. Subramanian, USA
Jacek Cezary Szepietowski, Poland
Taina Tervahartiala, Finland
Kathy Triantafilou, United Kingdom
Fumio Tsuji, Japan
Maria Letizia Urban, Italy



Giuseppe Valacchi, Italy
Luc Vallières, Canada
Kerstin Wolk, Germany
Suowen Xu, USA
Soh Yamazaki, Japan
Shin-ichi Yokota, Japan
Teresa Zelante, Singapore


Contents

Role of Inflammasomes in Inflammatory and Infectious Diseases

Young-Su Yi  and Tae Jin Lee 


Editorial (2 pages), Article ID 9832912, Volume 2021 (2021)

Antituberculosis Drugs (Rifampicin and Isoniazid) Induce Liver Injury by Regulating NLRP3 Inflammasomes

Qiang Su, Wei Kuang, Weiyi Hao, Jing Liang, Liang Wu, Chunmei Tang, Yali Wang, and Tao Liu 




Research Article (13 pages), Article ID 8086253, Volume 2021 (2021)

Expression and Potential Role of MMP-9 in Intrauterine Adhesion

Congqing Li , Wenyan Wang, Shiyang Sun, Youjiang Xu, Ziang Fang, and Lin Cong



Research Article (9 pages), Article ID 6676510, Volume 2021 (2021)

Cryptococcus neoformans Secretes Small Molecules That Inhibit IL-1 β Inflammasome-Dependent Secretion

Pedro Henrique Bürgel, Clara Luna Marina, Pedro H. V. Saavedra, Patrícia Albuquerque , Stephan Alberto Machado de Oliveira, Paulo Henrique de Holanda Veloso Janior, Raffael Araújo de Castro, Heino M. Heyman, Carolina Coelho, Radames J. B. Cordero, Arturo Casadevall, Joshua D. Nosanchuk, Ernesto S. Nakayasu, Robin C. May, Aldo Henrique Tavares , and Anamelia Lorenzetti Bocca 



Research Article (20 pages), Article ID 3412763, Volume 2020 (2020)

Involvement of the Inflammasome and Th17 Cells in Skin Lesions of Human Cutaneous Leishmaniasis Caused by Leishmania (Viannia) panamensis

K. Gonzalez , J. E. Calzada, C. E. P. Corbett, A. Saldaña, and M. D. Laurenti 


Research Article (10 pages), Article ID 9278931, Volume 2020 (2020)

Expression of AIM2 in Rheumatoid Arthritis and Its Role on Fibroblast-Like Synoviocytes

Yong Chen, Qiu Fujuan , Ensheng Chen, Beijia Yu, Fangfang Zuo, Yi Yuan, Xiaofeng Zhao, and Changhong Xiao 


Research Article (10 pages), Article ID 1693730, Volume 2020 (2020)

Molecularly Distinct NLRP3 Inducers Mediate Diverse Ratios of Interleukin-1 β and Interleukin-18 from Human Monocytes

Kristine Midtbö , Daniel Eklund , Eva Särndahl , and Alexander Persson 


Research Article (11 pages), Article ID 4651090, Volume 2020 (2020)

The Role of Inflammation in the Pathogenesis of Preeclampsia

Michał Michalczyk, Aleksander Celewicz, Marta Celewicz, Paula Woźniakowska-Gondek, and Rafał Rzepka 



Review Article (9 pages), Article ID 3864941, Volume 2020 (2020)

P2Y2 Receptor Induces L. amazonensis Infection Control in a Mechanism Dependent on Caspase-1 Activation and IL-1 β Secretion

Maria Luiza Thorstenberg, Monique Daiane Andrade Martins, Vanessa Figliuolo, Claudia Lucia Martins Silva, Luiz Eduardo Baggio Savio, and Robson Coutinho-Silva 

Research Article (11 pages), Article ID 2545682, Volume 2020 (2020)

Molecular Mechanisms Contributing Bacterial Infections to the Incidence of Various Types of Cancer

Salah A. Sheweita  and Awad S. Alsamghan 

Review Article (10 pages), Article ID 4070419, Volume 2020 (2020)

Amelioration of Coagulation Disorders and Inflammation by Hydrogen-Rich Solution Reduces Intestinal Ischemia/Reperfusion Injury in Rats through NF- κ B/NLRP3 Pathway

Ling Yang , Yan Guo , Xin Fan , Ye Chen , Bo Yang , Ke-Xuan Liu , and Jun Zhou 

Research Article (12 pages), Article ID 4359305, Volume 2020 (2020)

Intravenous Arginine Administration Downregulates NLRP3 Inflammasome Activity and Attenuates Acute Kidney Injury in Mice with Polymicrobial Sepsis

Sharon Angela Tanuseputero, Ming-Tsan Lin, Sung-Ling Yeh , and Chiu-Li Yeh 

Research Article (11 pages), Article ID 3201635, Volume 2020 (2020)

Editorial

Role of Inflammasomes in Inflammatory and Infectious Diseases

Young-Su Yi¹ and Tae Jin Lee²

¹Department of Life Sciences, Kyonggi University, Suwon 16227, Republic of Korea

²Department of Neurosurgery, University of Texas Health Science Center at Houston, Houston 77030, USA

Correspondence should be addressed to Young-Su Yi; ysyi@kgu.ac.kr

Received 28 July 2021; Accepted 28 July 2021; Published 15 August 2021

Copyright © 2021 Young-Su Yi and Tae Jin Lee. This is an open access article distributed under the Creative Commons Attribution License, which permits unrestricted use, distribution, and reproduction in any medium, provided the original work is properly cited.

Inflammation is an innate immune response protecting the body from invading pathogens and intracellular danger signals. However, chronic inflammation, that is, a repeated and prolonged inflammatory response, involves a progressive change in the type of cells present at the site of inflammation and has been regarded as a major risk factor for a variety of human diseases, including inflammatory, autoimmune, metabolic, and cardiovascular diseases and even cancer.

The inflammatory response consists of two main steps, “priming” and “triggering.” Priming is the preparatory step of inflammatory response by increasing the expression of inflammatory genes and the production of inflammatory mediators, while triggering is the activating step of inflammatory response by inducing inflammasome activation and inflammatory cell death, called pyroptosis.

In the last several decades, a large number of studies have mostly focused on the priming step of inflammatory responses; however, there have been recent advances in the understanding that triggering plays a crucial role in inflammatory responses by activating inflammasomes, intracellular protein complexes comprising intracellular pattern recognition receptor (PRR), and inflammatory molecules in response to various extracellular and intracellular activating ligands.

In this special issue, we invited investigators to contribute the latest original research and review articles investigating *in vitro*, *in vivo*, nonclinical, and clinical/translational studies focusing not only on the roles of inflammasomes in inflammatory and infectious diseases but also on the potential therapeutic strategies selectively targeting inflammasomes to prevent and treat various inflammatory and infectious dis-

eases. In this special issue, nine original and two review articles were published regarding the role of inflammasomes in inflammatory and infectious diseases.

The research article by S. A. Tanuseputero et al. investigated the effect of intravenous L-arginine (Arg) supplementation on modulating NLRP3 inflammasome activity in relation to septic acute kidney injury (AKI) and demonstrated that intravenous Arg supplementation immediately after sepsis restores plasma Arg levels and is beneficial for attenuating septic AKI, partly via nitric oxide- (NO-) mediated NLRP3 inflammasome inhibition.

The research article by L. Yang et al. investigated whether hydrogen-rich solution (HRS) could attenuate coagulation disorders and inflammation to improve intestinal injury and poor survival following intestinal ischemia/reperfusion (I/R) and demonstrated the amelioration of coagulation disorders and inflammation by HRS as a mechanism to improve intestinal I/R-induced intestinal injury and poor survival, which might be partially related to inhibition of the nuclear factor kappa B (NF- κ B)/NLRP3 pathway.

The research article by M. L. Thorstenberg et al. investigated the involvement of the P2 purinergic receptor P2Y₂R in the activation of NLRP3 inflammasome elements (caspase-1 and 11) and interleukin- (IL-) 1 β secretion during *Leishmania amazonensis* infection in peritoneal macrophages as well as in a murine model of cutaneous leishmaniasis. This study suggests that P2Y₂R activation induces caspase-1 activation and IL-1 β secretion during *Leishmania amazonensis* infection and that IL-1 β /IL-1R signaling is crucial for P2Y₂R-mediated protective immune response in an experimental model of cutaneous leishmaniasis.

Another research article by K. Gonzalez et al. also investigated the Th17 and inflammasome responses in the skin lesions of patients with localized cutaneous leishmaniasis (LCL) caused by *Leishmania (Viannia) panamensis* and demonstrated the participation of Th17 cells and the inflammasome in the *in situ* inflammatory response in localized cutaneous leishmaniasis caused by *Leishmania (Viannia) panamensis* infection and their roles in the control of the parasites through IL-17 and the IL-1 β -dependent NLRP3 inflammasome activation.

The research article by K. Midtbö et al. described the outcome of NLRP3 inflammasome activation and the functional effects of diverse inflammasome inducers and suggests that NLRP3 inflammasome response should be considered a dynamic process, which can be described by taking the ratio between IL-1 β and IL-18 into account and moving away from an on/off perspective of inflammasome activation.

The research article by Y. Chen et al. investigated the differences in absent in melanoma 2 (AIM2) inflammasome expression levels between rheumatoid arthritis (RA) and osteoarthritis (OA) and the role of AIM2 in RA fibroblast-like synoviocytes (RA-FLS). This study demonstrated that the AIM2 inflammasome pathway involves in the pathogenesis of RA and suggests that AIM2 inflammasome may be a promising therapeutic strategy for the treatment of RA.

The research article by P. H. Bürgel et al. analyzed the impact of molecules secreted by *Cryptococcus neoformans* B3501 strain and its acapsular mutant $\Delta cap67$ on inflammasome activation in an *in vitro* model. This study demonstrated that conditioned media from a wild-type strain inhibit a vital recognition pathway and subsequent fungicidal function of macrophages, contributing to fungal survival *in vitro* and *in vivo*, which suggests that the secretion of aromatic metabolites, such as DL-indole-3-lactic acid (ILA), during cryptococcal infections fundamentally impacts pathogenesis.

Canonical inflammasomes, such as NLRP3 inflammasome can activate matrix metalloproteinase-9 (MMP-9) in inflammatory responses and diseases, and the research article by C. Li et al. investigated the role of MMP-9 in intrauterine adhesion (IUA) in rats and patients. This study established an animal model for studying IUA mechanisms and suggests that MMP-9 plays an important role in IUA by decreasing MMP-9 expression.

The research article by Q. Su et al. investigated the mechanism by which patients being treated for pulmonary tuberculosis often suffer liver injury due to the effects of anti-TB drugs. This study demonstrated that isoniazid (INH) and rifampin (RIF) can destroy the normal liver tissue, induce an inflammatory response and oxidative stress, and can regulate drug-metabolizing enzymes and the antioxidant defense system by accelerating the activation of NLRP3 inflammasomes, which provide the strong evidence that NLRP3 inflammasomes could be the key factors involved in INH- and RIF-induced liver injuries.

The review article by S. A. Sheweita et al. discussed different bacteria, such as *Helicobacter pylori*, *Salmonella typhi*, *Staphylococcus aureus*, *Klebsiella* spp., and *Proteus mirabilis* that induced cancer via different molecular mechanisms

and concluded that a certain bacterium is linked with induction of a specific type of cancer via different molecular and biochemical mechanisms, such as the induction of inflammatory responses. This study suggests that bacterial infection could potentially affect human health in different ways and that it is important to know the possible factors involved in cancer induction for better treatment of cancer patients.

Another review article by M. Michalczyk et al. discussed the current understanding of the mechanisms which underlie the development of preeclampsia (PE) and the significant factors responsible for PE development. This review suggests the mechanisms causing the immune imbalance leading to an enhanced systemic inflammatory response that occurs in PE and potential future researches which may contribute to the identification of new targets for PE therapies. This review also helps readers understand that the pathophysiology of the inflammatory process in PE can largely contribute to the design of new, targeted anti-inflammatory therapies, such as selective NLRP3 inflammasome inhibitors. This review provides a key impact on the development of a targeted therapy that can improve perinatal outcomes in women affected with PE.

We hope that readers will be interested in understanding the roles of inflammasomes in inflammatory response and various human inflammatory and infectious diseases. We also hope that this special issue attracts the interest of the scientific community, thereby contributing and driving further investigations leading to the discovery of unknown inflammasome targets and the development of novel therapeutics to prevent and treat various human inflammatory and infectious diseases.

Conflicts of Interest

The editors declare that there is no conflict of interest regarding the publication of this special issue.

Acknowledgments

We appreciate all authors who submitted the articles and all reviewers for their valuable contributions to this special issue. We also would like to express our thanks to Dr. Sehyun Kim for his contribution to this special issue.

Young-Su Yi
Tae Jin Lee
Sehyun Kim

Research Article

Antituberculosis Drugs (Rifampicin and Isoniazid) Induce Liver Injury by Regulating NLRP3 Inflammasomes

Qiang Su,^{1,2} Wei Kuang,³ Weiyi Hao,^{1,2} Jing Liang,^{1,2} Liang Wu,^{1,2} Chunmei Tang,^{1,2} Yali Wang,^{1,2} and Tao Liu^{2,4} 

¹Department of Pharmacy, Nanchong Central Hospital, The Second Clinical Medical College, North Sichuan Medical College, Nanchong, Sichuan, China

²Nanchong Key Laboratory of Individualized Drug Therapy, Nanchong, Sichuan, China

³School of Pharmacy, North Sichuan Medical College, Nanchong, Sichuan, China

⁴Department of Cardiology, Nanchong Central Hospital, The Second Clinical Medical College, North Sichuan Medical College, Nanchong, Sichuan, China

Correspondence should be addressed to Tao Liu; nclt456@sina.com

Qiang Su and Wei Kuang contributed equally to this work.

Received 1 August 2020; Revised 13 January 2021; Accepted 23 January 2021; Published 20 February 2021

Academic Editor: Young-Su Yi

Copyright © 2021 Qiang Su et al. This is an open access article distributed under the Creative Commons Attribution License, which permits unrestricted use, distribution, and reproduction in any medium, provided the original work is properly cited.

Patients being treated for pulmonary tuberculosis often suffer liver injury due to the effects of anti-TB drugs, and the underlying mechanisms for those injuries need to be clarified. In this study, rats and hepatic cells were administrated isoniazid (INH) and rifampin (RIF) and then treated with NLRP3-inflammasome inhibitors (INF39 and CP-456773) or NLRP3 siRNA. Histopathological changes that occurred in liver tissue were examined by H&E staining. Additionally, the levels IL-33, IL-18, IL-1 β , NLRP3, ASC, and cleaved-caspase 1 expression in the liver tissues were also determined. NAT2 and CYP2E1 expression were identified by QRT-PCR analysis. Finally, *in vitro* assays were performed to examine the effects of siRNA targeting NLRP3. Treatment with the antituberculosis drugs caused significant liver injuries, induced inflammatory responses and oxidative stress (OS), activated NLRP3 inflammasomes, reduced the activity of drug-metabolizing enzymes, and altered the antioxidant defense system in rats and hepatic cells. The NLRP3 inflammasome was required for INH- and RIF-induced liver injuries that were produced by inflammatory responses, OS, the antioxidant defense system, and drug-metabolizing enzymes. This study indicated that the NLRP3 inflammasome is involved in antituberculosis drug-induced liver injuries (ATLIs) and suggests NLRP3 as a potential target for attenuating the inflammation response in ATLIs.

1. Introduction

Tuberculosis (TB) is a disease caused by infection with *Mycobacterium tuberculosis* [1]. In recent years, extrapulmonary TB infections and atypical TB infections have become more frequently diagnosed [2], and TB remains one of the leading causes of illness and death worldwide [3]. According to a 2016 report by the World Health Organization (WHO), one-third of the world's population (~2 billion people) has been infected with TB [4]. In 2015, there were 10.4 million new cases of TB worldwide, 580,000 multidrug-resistant TB patients, and 1.4 million people died from TB [5]. At present,

TB is mainly treated using anti-TB drugs [6], which can be divided into categories of new, first-line, and second-line drugs. First-line anti-TB drugs are currently the first choice for treating TB and include rifampicin (RIF), isoniazid (INH), ethambutol (E), and pyrazinamide (Z) [7–9]. However, when used in combination, these drugs produce different degrees of adverse effects [10, 11]; among which, anti-TB drug-induced liver injuries (ATLIs) are the most common and serious effect.

The WHO still regards INH and RFP to be irreplaceable first-line anti-TB drugs [12, 13]. INH inhibits the synthesis of mycolic acid, which is specific to *Mycobacterium tuberculosis*

cells, and such inhibition causes the bacteria to die due to loss of acid resistance, hydrophobicity, and proliferation [13]. RIF inhibits bacterial RNA polymerase and prevents mRNA synthesis, resulting in bacteriostatic and bactericidal effects [14]. INH and RFP exert strong bactericidal and bacteriostatic effects on bacteria in both the breeding and resting stages [15]. The combined application of INH and RFP synergistically increases the killing of intracellular and extracellular tuberculosis bacilli and reduces drug resistance [16]. However, the incidence of hepatotoxicity becomes significantly increased when INH and RFP are administered in combination [17]. Although the liver injuries produced by clinical anti-TB drugs pose a serious problem, the mechanism for those injuries has not been fully elucidated.

Inflammation is a defensive response to the removal of dangerous stimuli from the body [18]. Inflammasomes, as a class of protein complexes distributed in the cytoplasm, can regulate inflammation via proinflammatory cytokines [19]. The NLRP3 inflammasome is one of the most widely studied and characterized inflammasomes [20]. When influenced by endogenous (e.g., ROS, lysosomal disruption) or exogenous (e.g., lipopolysaccharides) danger signals, NLRP3 inflammasomes become activated and induce immune and inflammatory responses [21]. NLRP3 inflammasomes play roles in a variety of diseases, such as atherosclerosis [22] and chronic glomerulosclerosis [23]. Studies have also revealed that NLRP3 inflammasomes significantly affect the development of liver diseases and that inhibition of NLRP3 inflammasomes can reduce liver inflammation [24]. However, it has not been proven whether NLRP3 inflammasomes participate in causing INH- and RFP-induced liver injuries.

We hypothesized that RIF- and INH-induced liver injuries might be ameliorated by inhibiting NLRP3 inflammasomes and that NLRP3 inflammasome inhibitors (INF39 and CP-456773) might help to protect against RIF- and INH-induced liver injuries.

2. Materials and Methods

2.1. Animals. Equal numbers of SPF grade Sprague-Dawley (SD) rats (aged 8-9 weeks; weight range, 250-350 g) were purchased from the animal experimental center of North Sichuan Medical College and fed a normal diet for 7 days in a SPF laboratory. All experiments were carried out in strict accordance with regulations concerning the management and protection of experimental animals at North Sichuan Medical College. The study protocol was approved by the Ethics Committee of SLAS (Approval No. SLAS-20200113-02).

2.2. Grouping and Antituberculosis Drug-Induced Hepatotoxicity (ATDH). The SD rats were randomly assigned to a normal group ($n = 6$) or the INH+RIF group ($n = 18$), with equal numbers of males and females in each group. SD rats in the normal control group received 2 mL of normal saline solution via intragastric administration. SD rats in the INH+RIF group received INH (50 mg/kg, Novus Life Sciences Pvt. Ltd., Mumbai, India) and RIF (50 mg/kg, Novus Life Sciences Pvt. Ltd.) in a total volume of 2 mL once a day for 28 days. The rats in the INH+RIF group were also randomly assigned to an INF39

group ($n = 6$) and a CP-456773 group ($n = 6$). Samples of blood serum and liver tissue were collected from the rats in each group at 28 days after continuous drug administration. The serum was stored at -80°C ; one portion of each liver sample was immersed in 4% formaldehyde, and the other portion of liver tissue was stored at -80°C for use in subsequent experiments.

2.3. Extraction and Culture of Hepatic Cells. After being fasted for 12 hrs, the SD rats were deeply anesthetized by intraperitoneal injection of 3% pentobarbital sodium (30 mg/kg). Calcium-free perfusion fluid and type IV collagenase solution (Sigma) were consecutively injected into the hepatic portal vein of the rats. Under aseptic conditions, the liver was carefully removed, placed in high-glucose DMEM (Procell; cat. no. PM150210), and then cut into pieces. After filtration, the liver cells were resuspended in a high-glucose DMEM and purified with Percoll reagent. After centrifugation, the pelleted liver cells were diluted with moderate low-glucose DMEM (HyClone; GE Healthcare Life Sciences, Marlborough, MA, USA) and incubated overnight in a 6-well plate. The medium was then replaced with a low-glucose DMEM containing 0.25% BSA. Albumin-conjugated oleic acid was used to induce the hepatic cells. The different groups of hepatic cells were then treated with INH and RIF, followed by treatment with INF39 or CP-456773, respectively.

2.4. RNA Interference. NLRP3 siRNA and a negative control (NC) were purchased from Genepharma Company (Shanghai, China). The isolated hepatic cells were transfected with NC siRNA or NLRP3 siRNAs using Lipofectamine 3000 Reagent (Invitrogen; Thermo Fisher Scientific, Inc., Waltham, MA, USA): siRNA 1 (5'-3'): GGCUAUGUACUAUCUGCGUA; siRNA 2 (5'-3'): GGAUCUUUGCAGCGAUCAA; siRNA 3 (5'-3'): GGAUAGGUUUGCUGGGGAUA; NC: GAGAUCUGCUUAGAUCGCA.

2.5. H&E Staining. The right lobe of each liver (5 mm \times 5 mm \times 3 mm) was fixed with 4% formaldehyde solution and embedded in paraffin. Next, tissue slices were prepared and stained with hematoxylin (Servicebio, China) for 5 mins, differentiated by exposure to hydrochloric acid alcohol solution for 20 s, and then exposed to a weak ammonia solution (Sinopharm, Ecuador, 100021600) for 20 s. After staining with eosin (Solarbio, Turkey; G1100), the slices were dehydrated and made transparent. Finally, the pathological characteristics of the liver tissues were observed under a microscope (Nikon, Japan).

2.6. ELISA Assay. The levels of IL-33, IL-18, and IL-1 β were examined using an IL-33 ELISA kit (GenWay Biotech, Inc., San Diego, CA, USA), IL-18 ELISA kit (MBL, Nagoya, Japan), and IL-1 β ELISA kit (R&D Systems, Minneapolis, MN, USA), respectively, according to instructions provided by the manufacturers. The absorbance of each sample was determined at 450 nm.

2.7. RNA Extraction and Real-Time Quantitative PCR (QRT-PCR) Assay. The total RNA was extracted from tissue samples and cells using Trizol reagent (Takara, Japan, cat.

no. 9109). The concentration and purity of RNA were monitored by an ultraviolet detector at wavelengths of 260 nm and 280 nm, respectively. cDNA was synthesized using a reverse transcription kit (Takara) and subsequently used as a template for PCR amplification that was performed using the SYBR GREEN PCR Master Mix (Applied Biosystems, Foster City, CA, USA). The levels of mRNA expression were determined using the $2^{-\Delta\Delta C_t}$ method [25].

2.8. Western Blotting Analysis. The liver tissues in each group were ground, and the hepatic cells in each group were harvested and washed with PBS. Total proteins were extracted using a protein extraction kit (BestBio; BB-3101), and the protein concentration in each extract was determined using the bicinchoninic acid (BCA) method. Next, a 20 μ g aliquot of total protein from each extract was separated by 10% SDS-PAGE performed at 120 V. The separated protein bands were electrophoretically (200 mA for 90 mins) transferred onto PVDF membranes (Roche, Basal Switzerland, cat. no. 3010040001), which were subsequently blocked with 5% powdered skim milk. Next, the PVDF membranes were incubated with primary antibodies at 4°C overnight. After washing, the PVDF membranes were soaked with an HRP-labeled secondary antibody for 1 h and the immunostained protein bands were detected using the ECL chemiluminescence reagent (Millipore; KLS0500). The primary antibodies used in the study were as follows: NLRP3 (1:1000, Abcam, Cambridge, UK, ab214185), ASC (1:1000, Abcam, ab180799), and caspase 1 (1:1000, Abcam, ab62698).

2.9. Biochemistry Parameters. The liver tissues from the SD rats in each group were accurately weighed and then homogenized in normal saline. Liver tissue homogenates with a 10% mass fraction were prepared and stored at 4°C. After centrifugation at 3000g for 10 mins, the levels of superoxide dismutase (SOD), catalase (CAT), and glutathione peroxidase (GPX) activity as well as the levels of reduced glutathione (GSH) and lipid peroxidation products (LPOs) in the supernatants were determined using assay kits according to instructions provided by the manufacturers.

2.10. Immunohistochemistry (IHC) Assay. Immunohistochemistry was performed using the MaxVision (TM) method as previously described [26]. The tissue sections were dewaxed with xylene and then dehydrated using a gradient alcohol series. After soaking in 1% H₂O₂ for 10 mins, the sections were treated with citrate buffer for antigen retrieval. Next, the sections were blocked with goat serum for 1 h and treated with anti-NLRP3 (Abcam) at 4°C overnight; after which, they were incubated with a secondary antibody (Abcam) for 30 mins. Finally, the tissue sections were stained with DAB, dehydrated, and blocked. NLRP3 expression was confirmed under a microscope.

2.11. Immunofluorescence (IF) Assay. Treated hepatic cells were incubated for 8 hrs in a 6-well plate (5×10^4 cells/well). Next, the cells were fixed in 4% paraformaldehyde (Sigma-Aldrich, St. Louis, MO, USA, cat. no. P6148-500G) for 30 mins and permeated in 0.1% Triton X100 for 10 mins. The cells were then blocked with 5% BSA for 1 h, incubated

with anti-NLRP3 (Abcam) overnight at 4°C, and subsequently treated with a secondary antibody (Abcam) for 2 hrs in the dark. The cells were then stained with DAPI (Life Technologies, Carlsbad, CA, USA, cat. no. D1306,) for 10 mins, and their fluorescence was photographed under a fluorescence microscope.

2.12. Flow Cytometry Detection. Hepatic cells in each group were collected and counted. Next, a 200 μ L aliquot of suspended cells was added to 20 μ L of H2DCF-DA (10 μ mol/L; Beyotime, cat. no. S0033-1) and incubated for 15 mins in the dark. After washing with Earle's solution, the hepatic cells were suspended in 400 μ L of Earle's solution, and the ROS level was confirmed by flow cytometry.

2.13. Statistical Analysis. All experiments were independently repeated at least three times, and results are expressed as a mean value \pm standard deviation (SD). Student's *t* test was used to analyze differences between two groups, and one-way analysis of variance (ANOVA) was used to evaluate the significance of differences between more than two groups. All experimental data were analyzed using IBM SPSS Statistics for Windows, Version 19.0 software (IBM Corp., Armonk, NY, USA). A *P* value < 0.05 was considered to be statistically significant.

3. Results

3.1. INH and RIF Induced Liver Injury, Enhanced the Inflammatory Response, and Activated the NLRP3 Inflammasome in Rats. In order to determine the effects of INH and RIF on the histopathological characteristics of liver tissues, an inflammatory response and NLRP3 inflammasome ATDH model was established in SD rats by dosing the rats with INH (70 mg/kg) and RIF (70 mg/kg) for 28 consecutive days. Subsequent H&E staining showed that the liver tissues from control rats had a normal morphology and intact structure, and no degeneration or necrosis was observed. In contrast, liver tissues from the rats dosed with INH and RIF contained necrotic hepatocytes and showed signs of inflammatory cell infiltration (Figure 1(a)). Moreover, the levels of inflammatory cytokines (IL-33, IL-18, and IL-1 β) in the INH and RIF group were significantly elevated when compared with those in the normal group ($P < 0.01$, Figures 1(b)–1(d)). We also found that the levels of NLRP3 inflammasome-related proteins (NLRP3, ASC, and cleaved-caspase 1) were markedly upregulated in the INH and RIF group when compared with those in the normal group ($P < 0.01$, Figure 1(e)). When taken together, these findings indicated that the antituberculosis drugs INH and RIF could cause liver injury, induce an inflammatory response, and activate NLRP3 inflammasomes in rats.

3.2. INH and RIF Markedly Regulated the OS-Antioxidant Defense System and Drug-Metabolizing Enzymes in Rats. As the most active metabolic organ in the body, the liver performs crucial functions, such as material metabolism, energy metabolism, and biological transformation of various molecules. In subsequent experiments, we investigated the effects of INH and RIF on liver drug-metabolizing enzymes, oxidative stress (OS), and antioxidant enzyme activity in rats.

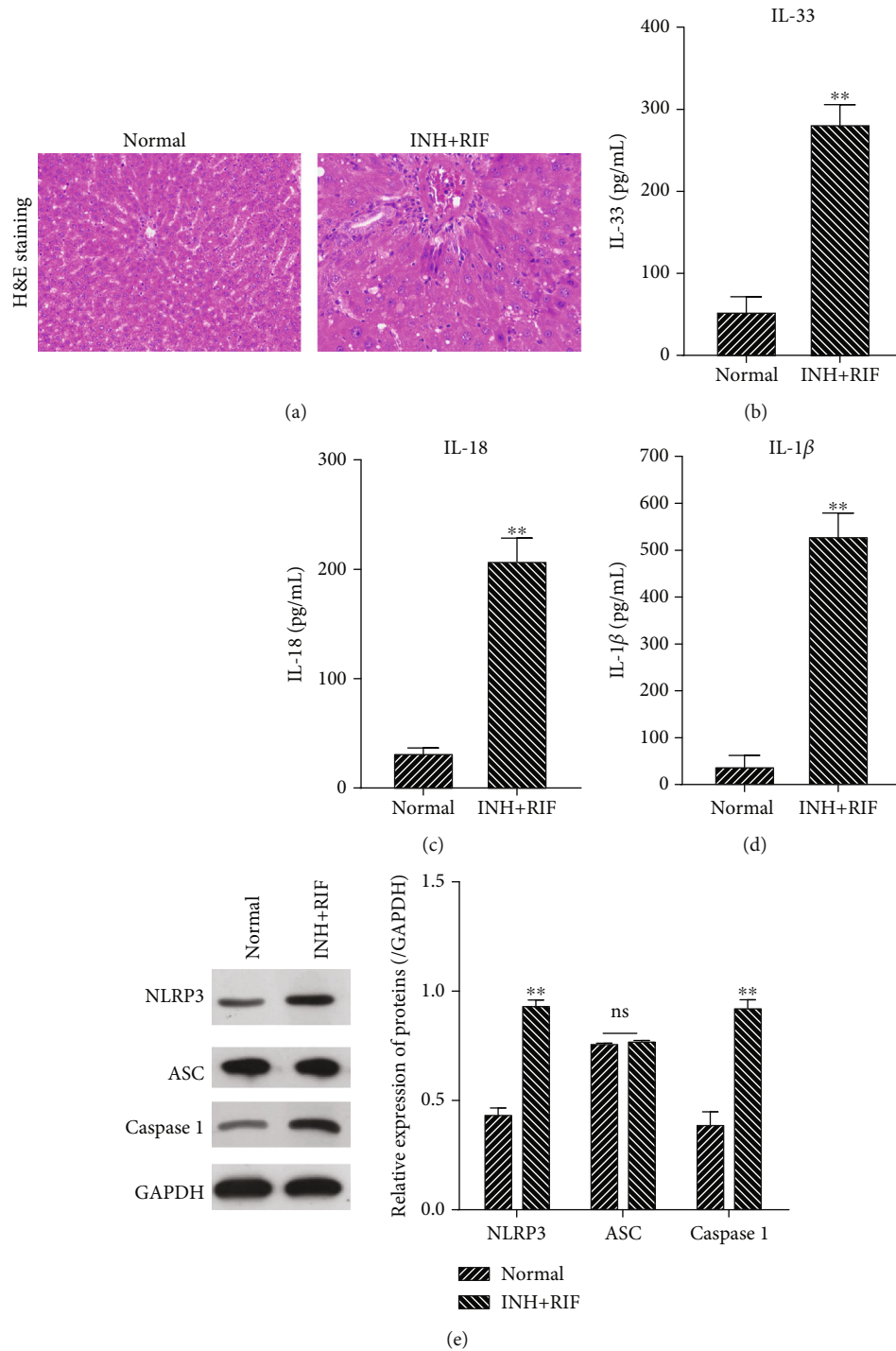


FIGURE 1: INH and RIF induced liver injury, enhanced the inflammatory response, and activated NLRP3 inflammasomes in rats. Rats were administrated 70 mg/kg INH and 70 mg/kg RIF for 28 consecutive days. (a) The liver tissues in each group were collected, and histopathological changes in the liver tissues were observed after H&E staining. Samples of blood serum were obtained from each group of rats; the levels of IL-33 (b), IL-18 (c), and IL-1 β (d) in serum were detected by ELISA. (e) Western blot assays were performed to verify the levels of NLRP3, ASC, and cleaved-caspase 1 protein expression in each group of liver tissues. GAPDH served as an internal reference. A quantitative analysis of each protein expression was conducted according to the gray value. ** $P < 0.01$ vs. the normal group.

We found that the levels of OS indices (LPOs) in the INH and RIF group were significantly higher than those in the normal group ($P < 0.01$, Figure 2(a)). We also found that the levels of

antioxidant enzymes (SOD, CAT, GSH, and GPx) in the INH and RIF group were significantly lower than those in the normal group ($P < 0.01$, Figures 2(b)–2(e)). Moreover, NAT2

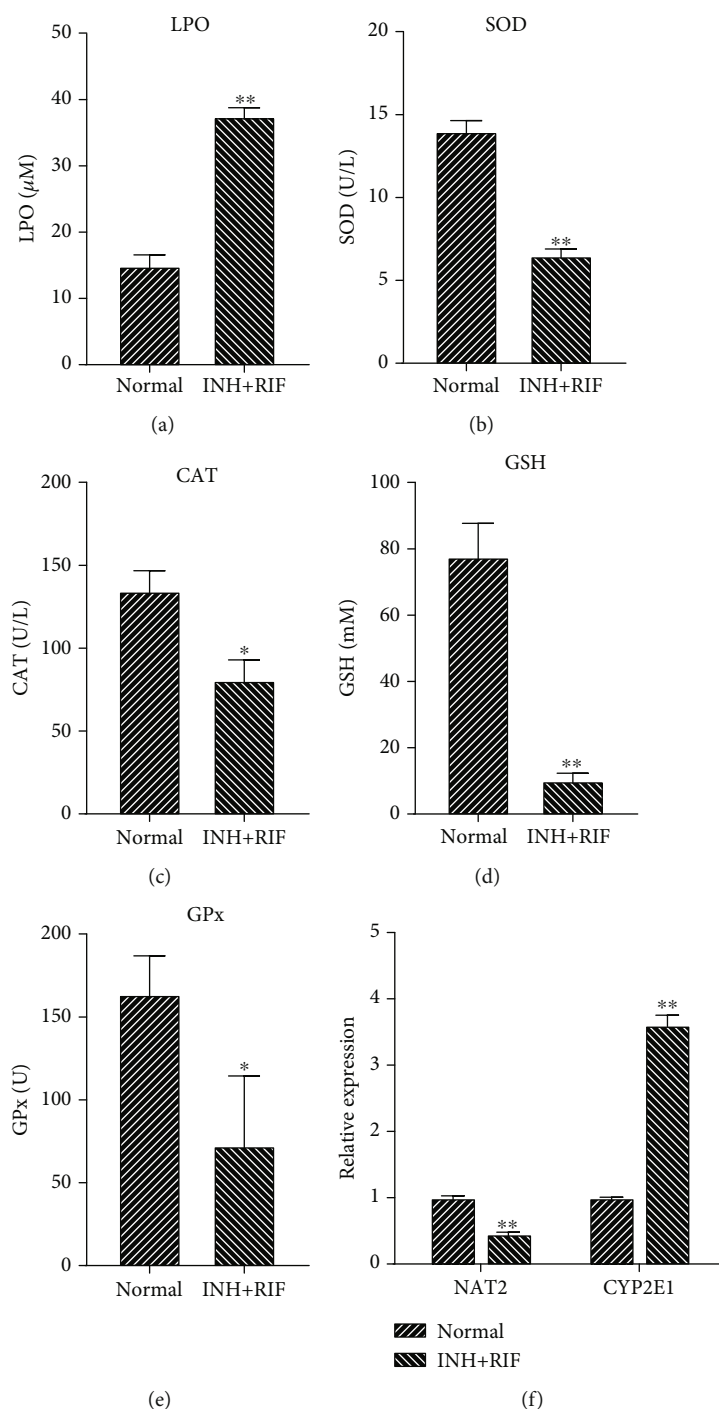


FIGURE 2: INH and RIF markedly regulated the OS-antioxidant defense system and drug-metabolizing enzymes in rats. (a–e) The OS indices (LPOs) and levels of antioxidant enzymes (SOD, CAT, GSH, and GPx) in rats treated with INH and RIF were determined using specific commercial kits. (f) QRT-PCR analyses of NAT2 and CYP2E1 in the liver tissues of rats treated with INH and RIF. * $P < 0.05$ and ** $P < 0.01$ vs. the normal group.

expression was markedly downregulated and CYP2E1 expression was markedly upregulated in the INH and RIF group when compared with the normal group ($P < 0.01$, Figure 2(f)). Thus, our data revealed that INH and RIF could significantly reduce antioxidant functions and also the activity of drug-metabolizing enzymes in rat liver tissue.

3.3. The NLRP3 Inflammasome Was Required for the INH/RIF-Induced Inflammatory Response in Rats. Next, we explored whether the NLRP3 inflammasome helps to facilitate the inflammatory response in INH- and RIF-induced rats by treating the rats with NLRP3-inflammasome inhibitors (INF39 or CP-45677, respectively). Subsequent ELISA assays showed that

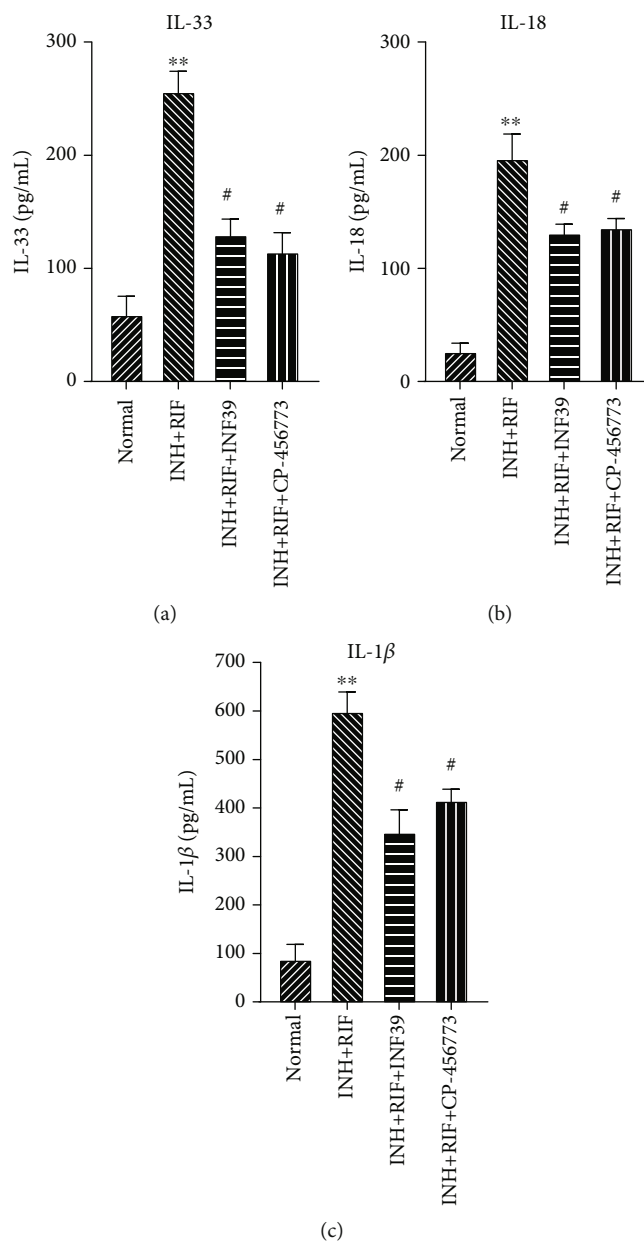


FIGURE 3: Continued.

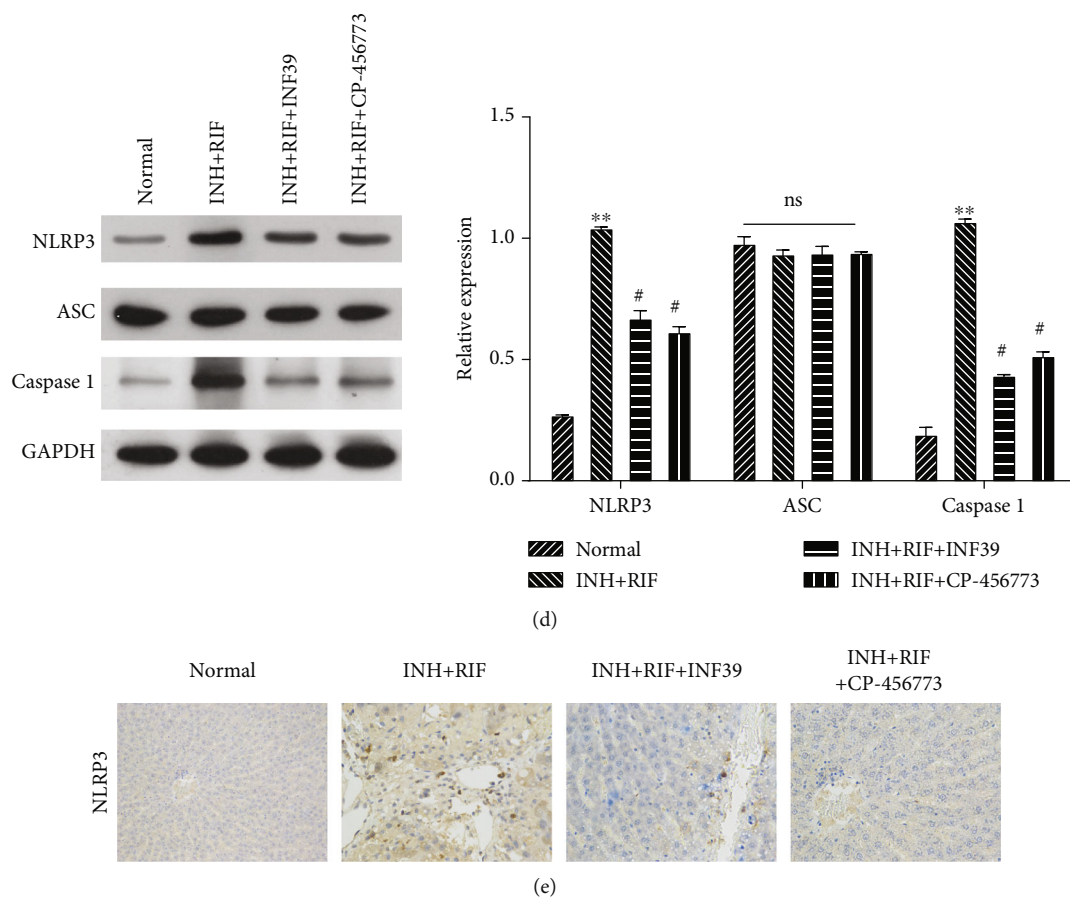


FIGURE 3: NLRP3 inflammasomes were required for INH- and RIF-induced inflammatory responses in rats. Rats were treated with INH and RIF for 28 consecutive days and then treated with an NLRP3-inflammasome inhibitor (INF39 or CP-456773, respectively). (a–c) ELISA assays were performed to evaluate the effects of NLRP3 inhibitors on INH- and RIF-induced inflammatory factors (IL-33, IL-18, and IL-1 β) in the serum of each group of rats. (d) The levels of NLRP3, ASC, and cleaved-caspase 1 protein expression were assessed by western blot assays, and the relative levels of the proteins were analyzed based on the gray value. (e) IHC assays revealed the expression and distribution of NLRP3 in the liver tissues of rats in each group. Magnification, $\times 100$. ** $P < 0.01$ vs. the normal group; # $P < 0.05$ vs. the INH and RIF group.

the levels of IL-33, IL-18, and IL-1 β in rats treated with INH and RIF were significantly enhanced when compared to rats in the normal group, and rescue experiments verified that treatment with INF39 or CP-456773 could partly attenuate the INH- and RIF-mediated increases in IL-33, IL-18, and IL-1 β levels in rat serum ($P < 0.05$ and $P < 0.01$, Figures 3(a)–3(c)). Additionally, we also found that the significant increases in NLRP3, ASC, and cleaved-caspase 1 expression in rat liver tissue caused by RIF and INH administration could be markedly reduced by an NLRP3-inflammasome inhibitor (INF39 or CP-456773) ($P < 0.05$ and $P < 0.01$, Figure 3(d)). Similarly, the results of IHC assays verified that INF39 or CP-456773 could notably weaken the promoting effect of RIF and INH on NLRP3 expression in the liver tissues of rats (Figure 3(e)). When taken together, our data showed that INH and RIF induced a strong inflammatory response in rat liver tissue by activating NLRP3 inflammasomes.

3.4. NLRP3 Inflammasomes Altered the INH- and RIF-Mediated OS-Antioxidant Defense System and the Levels of Drug-Metabolizing Enzymes in Rats. Likewise, we also exam-

ined the effects of NLRP3 inflammasomes on antioxidant and drug-metabolizing enzymes in rats. Our data showed that the increases in LPOs that were mediated by INH and RIF in rats could be significantly attenuated by INF39 or CP-456773 ($P < 0.05$ and $P < 0.01$, Figure 4(a)). Subsequently, we also found that either INF39 or CP-456773 could reverse the decreases in antioxidant enzyme levels (SOD, CAT, GSH, and GPx) caused by treatment with INH and RIF ($P < 0.05$ and $P < 0.01$, Figures 4(b)–4(e)). Moreover, our data also showed that the downregulation of NAT2 expression and upregulation of CYP2E1 expression in INH- and RIF-stimulated rats could also be markedly changed by INF39 or CP-456773 ($P < 0.01$, Figure 4(f)). These findings indicated that NLRP3 inflammasome inhibitors (INF39 or CP-456773) could significantly reduce INH- and RIF-induced hepatotoxicity in rats.

3.5. INH and RIF Regulated Drug-Metabolizing Enzymes and Induced an Inflammatory Response and OS by Activating NLRP3 Inflammasomes in Hepatic Cells. We performed *in vitro* experiments to determine whether NLRP3

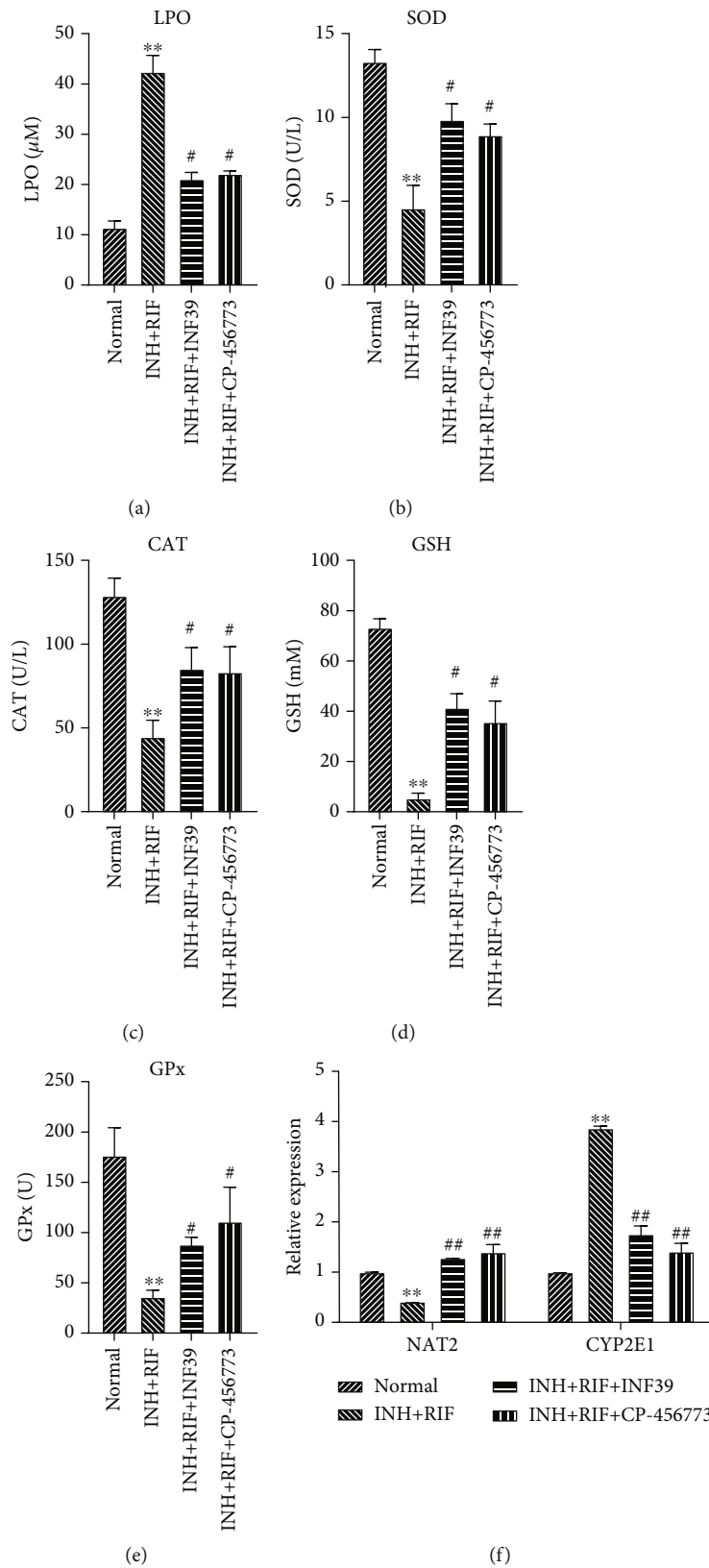


FIGURE 4: The NLRP3 inflammasome was involved in regulating the INH- and RIF-mediated OS-antioxidant defense system and drug-metabolizing enzymes in rats. INF39 or CP-456773 was administered to the INH- and RIF-induced rats, respectively. (a–e) Specific commercial kits were used to monitor the levels of LPO and antioxidant enzymes (SOD, CAT, GSH, and GPx). (f) NAT2 and CYP2E1 expression were detected by QRT-PCR assays. ** $P < 0.01$ vs. the normal group; # $P < 0.05$ and ## $P < 0.01$ vs. the INH and RIF group.

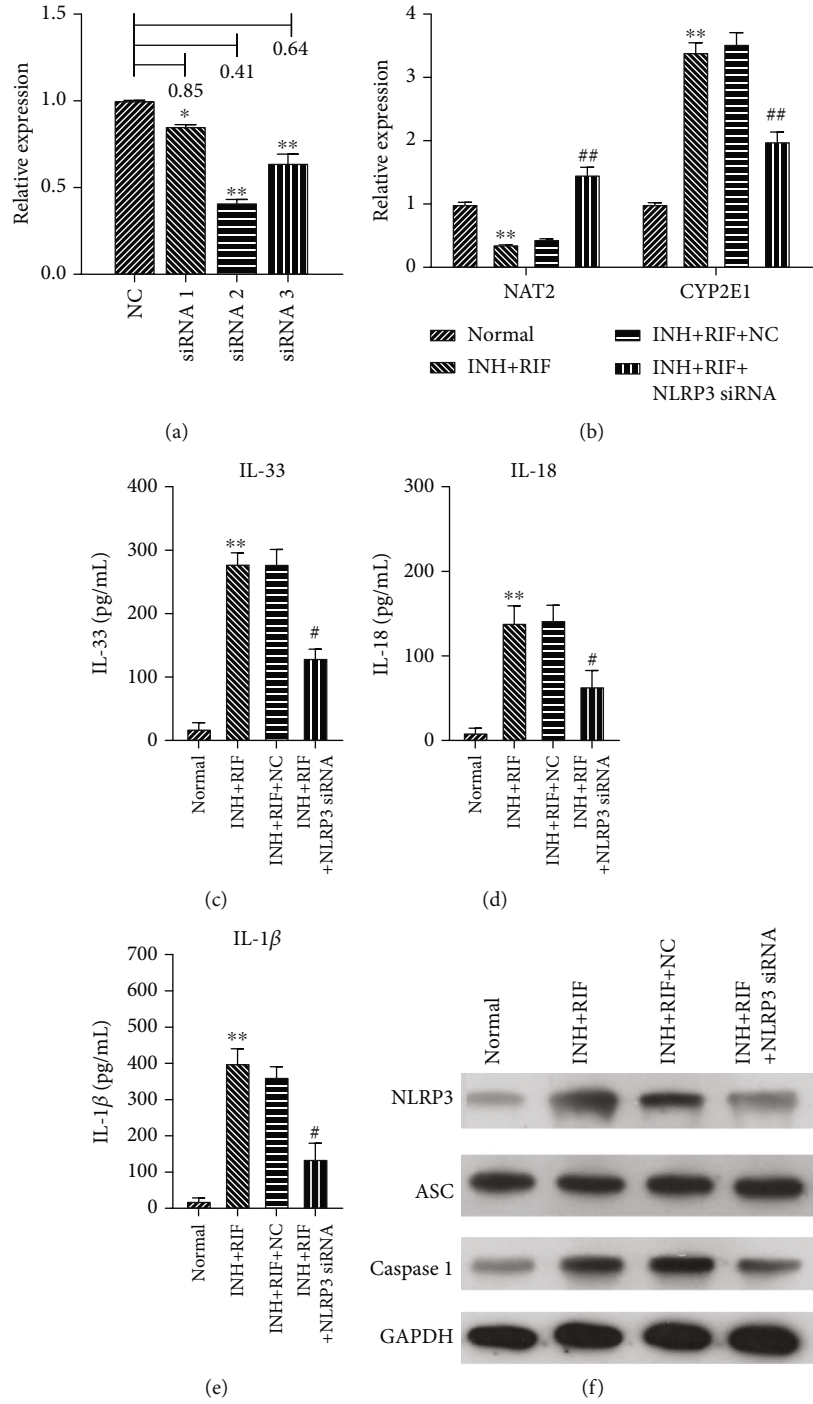


FIGURE 5: Continued.

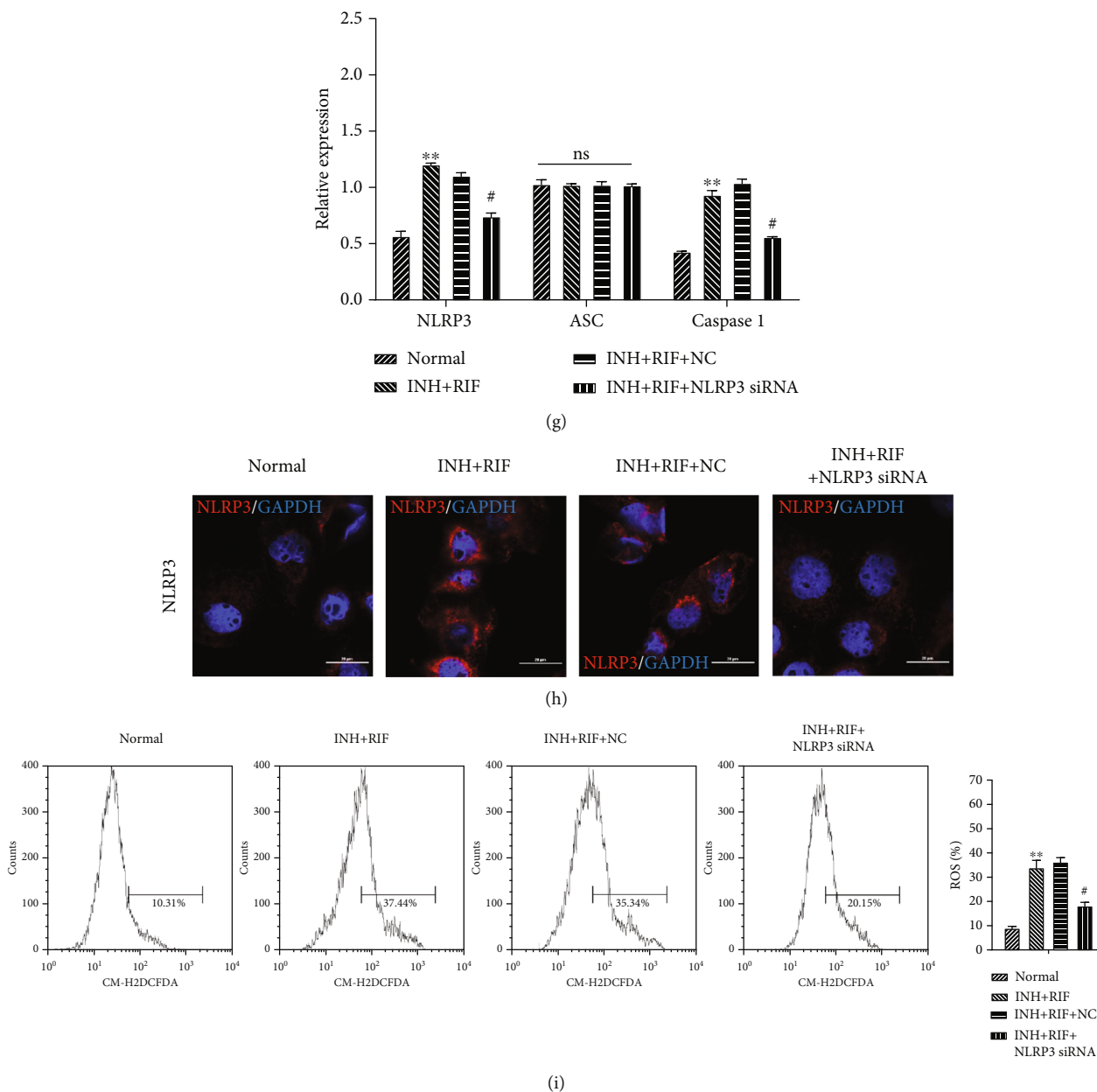


FIGURE 5: INH and RIF regulated drug-metabolizing enzymes and induced an inflammatory response and OS in hepatic cells by activating the NLRP3 inflammasome. Hepatic cells were treated with INH and RIF and then transfected with NLRP3 siRNA. (a) Transfection efficiency of siRNAs was detected by using QRT-PCR. (b) QRT-PCR analyses were performed to detect the levels of NAT2 and CYP2E1 expression in each group of hepatocytes. ELISA assays were performed to detect the levels of IL-33 (c), IL-18 (d), and IL-1 β (e) in hepatic cells treated with INH and RIF, and INF39 or CP-456773. (f) Western blot analyses revealed changes in the levels of NLRP3, ASC. And cleaved-caspase 1 protein expression in the treated hepatic cells. (g) Protein expression was quantified based on the gray values obtained from western blotting. (h) IF assays were performed to determine the expression and distribution of NLRP3 protein in treated hepatic cells. Magnification, $\times 200$; scale bar = 20 μm . (i) ROS levels were monitored by flow cytometry. ** $P < 0.01$ vs. the normal group; # $P < 0.05$ and ## $P < 0.01$ vs. the INH and RIF group.

inflammasomes affected drug-metabolizing enzymes, the inflammatory response, and OS in INH- and RIF-induced hepatic cells. Firstly, siRNA was transfected into cells and transfection efficiency was detected by using QRT-PCR. Results showed that siRNA 2 presented the highest efficiency of knockdown on NLRP3 (Figure 5(a)). QRT-PCR analyses showed that when compared to hepatic cells from the normal

group, the levels of NAT2 were downregulated and the levels of CYP2E1 were upregulated in the INH- and RIF-induced hepatic cells, while NLRP3 knockdown dramatically reversed the levels NAT2 and CYP2E1 expression in INH- and RIF-induced hepatic cells ($P < 0.01$, Figure 5(b)). Secondly, we found that INH and RIF significantly increased the levels of IL-33, IL-18, and IL-1 β in hepatic cells, and those increases

could be significantly attenuated by NLRP3 knockdown ($P < 0.05$ and $P < 0.01$, Figures 5(c)–5(e)). Additionally, western blot studies showed that treatment with INH and RIF increased the levels of NLRP3 and cleaved-caspase 1 expression in hepatic cells, while those increases were attenuated by NLRP3 knockdown ($P < 0.05$ and $P < 0.01$, Figures 5(f) and 5(g)). Graphical results of IF assays showed the same trend in NLRP3 expression as western blotting results and also showed that NLRP3 protein was mainly located in the cytoplasm (Figure 5(h)). Furthermore, we verified that the levels of ROS were significantly elevated in hepatic cells in the INH plus RIF group when compared with hepatic cells in the normal group, and those increases could be attenuated by NLRP3 knockdown (Figure 5(i)). Therefore, we proved that INH and RIF dramatically reduced the activity of drug-metabolizing enzymes and induced an inflammatory response and OS in hepatic cells by regulating NLRP3 inflammasomes.

4. Discussion

Our study showed that the anti-TB drugs INH and RIF could significantly change the structure of normal liver tissues and induce inflammation. The mechanism by which anti-TB drugs cause liver injury is quite complicated [27, 28]. Current studies have indicated that the pathogenesis of ATLJ involves both hepatotoxicity and metabolic specificity [29]. Anti-TB drugs are initially transported to the liver, where they are transformed into metabolites via enzymatic reactions [30]. Subsequently, the metabolites, as immunogens, bind to endogenous proteins and subsequently cause liver immune damage or hepatotoxicity [31]. The toxic metabolites of INH can lead to heterogeneous drug reactions, which are the main cause for ADLI in most heterogeneous patients [32]. RIF can induce a variety of metabolic enzymes in the liver, and those enzymes can further aggravate the toxicity of the drug to the liver [33]. RIF- and INH-induced liver injuries have been previously reported in several studies. For instance, *Tamarix gallica* leaf extract was shown to protect against RIF- and INH-induced liver injury in rats [34]; pyrrolidine dithiocarbamate was shown to alleviate liver injuries induced by RIF and INH in rats [35]; *naringenin* was found to significantly mitigate the effects RIF- and INH-induced hepatotoxicity [36]. However, the mechanisms for these effects remain unclear.

The body's OS-antioxidant defense system can quickly remove endogenously produced ROS from the body under normal physiological conditions [37]. However, continuous external stimulation can result in excessive ROS production that causes tissue damage [38]. Drug-metabolizing enzymes are key factors that determine how drugs are metabolized in the body [39]. It has been reported that slow NAT2 acetylator genotypes and a CYP2E1 C1/C1 genotype can lead to an accumulation of toxic metabolites during the metabolism of INH in the liver [40]. It was also found that the quantities of toxic metabolites generated by breakdown of INH and RIF were significantly increased in patients with slow NAT2 acetylator genotypes [41]. Research has confirmed that RIF can induce INH hydrolase and thereby cause liver injury in patients with slow NAT2 acetylator genotypes

[41]. In our study, we verified that INH and RIF markedly increased the levels of OS indices (LPOs) and reduced the levels of antioxidant enzymes, suggesting that INH and RIF could affect the OS-antioxidant defense system. We also verified that INH and RIF could downregulate NAT2 expression and upregulate CYP2E1 expression, indicating that INH and RIF could regulate the activity of drug-metabolizing enzymes.

NOD-like receptor protein 3 inflammasomes (NLRP3 inflammasomes) comprise a class of polyprotein complexes that exist in the cytoplasm [21]. Activation of NLRP3 inflammasomes can cause downstream inflammatory cascades (Dougherty et al. 2019). The NLRP3 inflammasome is composed of NLRP3, apoptosis-associated speck-like protein containing a CARD (ASC), and procaspase 1 [42]. When stimulated by exogenous pathogens such as bacteria, viruses, and fungi, or by endogenous stimuli, NLRP3 activates caspase 1 by recruiting the adaptor protein ASC to bind to procaspase 1 [43]. Activated caspase 1 then causes activation of pro-interleukin-1 β (pro-IL-1 β) and pro-interleukin-18 (pro-IL-18) to form IL-1 β and IL-18 [42, 44]. Numerous studies have verified that NLRP3 inflammasomes are involved in regulating liver injuries [45, 46]. In our study, we verified that INH and RIF could activate NLRP3 inflammasomes in the liver tissues of rats and hepatocytes cultured *in vitro*. We also demonstrated that an NLRP3-inflammasome inhibitor (INF39 or CP-456773) could markedly reverse the regulatory effects of INH and RIF on drug-metabolizing enzymes, the OS-antioxidant defense system, and inflammatory response in rats. Additionally, we showed that silencing of NLRP3 also could lessen the influence of INH and RIF on hepatic cells. Therefore, we proved that the NLRP3 inflammasome is required for INH- and RIF-induced liver injuries.

5. Conclusions

Our findings suggest that INH and RIF can destroy the normal liver tissue, induce an inflammatory response and OS, and also regulate drug-metabolizing enzymes and the antioxidant defense system by accelerating the activation of NLRP3 inflammasomes. Therefore, NLRP3 inflammasomes might be the key factors involved in INH- and RIF-induced liver injuries.

Data Availability

The datasets used and/or analyzed during the present study are available from the corresponding author on reasonable request.

Ethical Approval

All animal experiments were approved by the Ethics Committee of SLAS (Approval No. SLAS-20200113-02).

Conflicts of Interest

All authors declare having no competing interests.

Authors' Contributions

QS, WK, and TL proposed the project and designed the experiments. QS and WK performed the experiments. TL provided administrative support. WYH and JL collected and analyzed the data. LW and CMT illustrated the results. YLW validated the data analysis. QS organized the draft manuscript. TL supervised the project and revised the draft manuscript. All authors reviewed and approved the manuscript prior to submission. Qiang Su and Wei Kuang contributed equally to this work.

Acknowledgments

This study was supported by the Scientific Research Projects on Basic Scientific and Technological Strategic Cooperation of Nanchong Municipal Schools (No. 18SXHZ0362), Scientific Research Projects of Sichuan Education Department (No. 18ZB0221), and Nanchong Key Laboratory of Individualized Drug Therapy (No. NCKL201711).

References

- [1] K. Dheda, C. E. Barry 3rd, and G. Maartens, "Tuberculosis," *Lancet*, vol. 387, no. 10024, pp. 1211–1226, 2016.
- [2] S. Subramani, P. K. Saravanam, and R. Rajendran, "Extrapulmonary tuberculosis: atypical presentation in otorhinolaryngology," *BMJ Case Reports*, vol. 2018, 2018.
- [3] S. Sobhy, Z. O. E. Babiker, J. Zamora, K. S. Khan, and H. Kunst, "Maternal and perinatal mortality and morbidity associated with tuberculosis during pregnancy and the postpartum period: a systematic review and meta-analysis," *BJOG: An International Journal of Obstetrics & Gynaecology*, vol. 124, no. 5, pp. 727–733, 2017.
- [4] A. Lam, R. Prabhu, C. M. Gross, L. A. Riesenber, V. Singh, and S. Aggarwal, "Role of apoptosis and autophagy in tuberculosis," *American Journal of Physiology-Lung Cellular and Molecular Physiology*, vol. 313, no. 2, pp. L218–L229, 2017.
- [5] G. Churchyard, P. Kim, N. S. Shah et al., "What we know about tuberculosis transmission: an overview," *The Journal of Infectious Diseases*, vol. 216, suppl_6, pp. S629–S635, 2017.
- [6] M. M. Islam, H. A. Hameed, J. Mugweru et al., "Drug resistance mechanisms and novel drug targets for tuberculosis therapy," *Journal of Genetics and Genomics*, vol. 44, no. 1, pp. 21–37, 2017.
- [7] R. Fatima, M. Ashraf, S. Ejaz et al., "In vitro toxic action potential of anti tuberculosis drugs and their combinations," *Environmental Toxicology and Pharmacology*, vol. 36, no. 2, pp. 501–513, 2013.
- [8] V. J. Gómez-Tangarife, A. J. Gómez-Restrepo, J. Robledo-Restrepo, and J. M. Hernández-Sarmiento, "Drug resistance in Mycobacterium tuberculosis: contribution of constituent and acquired mechanisms," *Revista de Salud Pública*, vol. 20, no. 4, pp. 491–497, 2018.
- [9] J. P. Sarathy, L. E. Via, D. Weiner et al., "Extreme drug tolerance of Mycobacterium tuberculosis in caseum," *Antimicrobial Agents and Chemotherapy*, vol. 62, no. 2, 2018.
- [10] Y. Li, Y. Zhu, Q. Zhong, X. Zhang, M. Shu, and C. Wan, "Serious adverse reactions from anti-tuberculosis drugs among 599 children hospitalized for tuberculosis," *The Pediatric Infectious Disease Journal*, vol. 36, no. 8, pp. 720–725, 2017.
- [11] S. K. Sharma and A. Mohan, "Miliary tuberculosis," *Microbiology Spectrum*, vol. 5, no. 2, 2017.
- [12] S. Hofmann-Thiel, N. Molodtsov, C. Duffner et al., "Capacity of Abbott RealTimeMTB RIF/INH to detect rifampicin- and isoniazid-resistant tuberculosis," *The International Journal of Tuberculosis and Lung Disease*, vol. 23, no. 4, pp. 458–464, 2019.
- [13] A. N. Unissa, S. Subbian, L. E. Hanna, and N. Selvakumar, "Overview on mechanisms of isoniazid action and resistance in Mycobacterium tuberculosis," *Infection, Genetics and Evolution*, vol. 45, pp. 474–492, 2016.
- [14] T. Idowu, G. Arthur, G. G. Zhanel, and F. Schweizer, "Heterodimeric rifampicin-tobramycin conjugates break intrinsic resistance of Pseudomonas aeruginosa to doxycycline and chloramphenicol in vitro and in a Galleria mellonella in vivo model," *European Journal of Medicinal Chemistry*, vol. 174, pp. 16–32, 2019.
- [15] A. Jacobino, G. Piccaro, F. Giannoni, A. Mustazzolu, and L. Fattorini, "Fighting tuberculosis by drugs targeting nonreplicating Mycobacterium tuberculosis bacilli," *International Journal of Mycobacteriology*, vol. 6, no. 3, pp. 213–221, 2017.
- [16] L. He, Y. Guo, Y. Deng, C. Li, C. Zuo, and W. Peng, "Involvement of protoporphyrin IX accumulation in the pathogenesis of isoniazid/rifampicin-induced liver injury: the prevention of curcumin," *Xenobiotica*, vol. 47, no. 2, pp. 154–163, 2017.
- [17] F. Li, J. Zhou, Y. Li, K. Sun, and J. Chen, "Mitochondrial damage and Drp1 overexpression in rifampicin- and isoniazid-induced liver injury cell model," *Journal of Clinical and Translational Hepatology*, vol. 7, no. 1, pp. 40–45, 2019.
- [18] J. H. Check, M. P. Dougherty, and D. L. Check, "Long standing post-herpetic neuralgia resistant to standard anti-neuropathy medication showing quick dramatic improvement following treatment with sympathomimetic amines," *Clinical and Experimental Obstetrics & Gynecology*, vol. 46, no. 2, pp. 335–336, 2019.
- [19] P. Broz and V. M. Dixit, "Inflammasomes: mechanism of assembly, regulation and signalling," *Nature Reviews Immunology*, vol. 16, no. 7, pp. 407–420, 2016.
- [20] T. Karasawa and M. Takahashi, "Role of NLRP3 inflammasomes in atherosclerosis," *Journal of Atherosclerosis and Thrombosis*, vol. 24, no. 5, pp. 443–451, 2017.
- [21] N. Kelley, D. Jeltema, Y. Duan, and Y. He, "The NLRP3 inflammasome: an overview of mechanisms of activation and regulation," *International Journal of Molecular Sciences*, vol. 20, no. 13, p. 3328, 2019.
- [22] A. Grebe, F. Hoss, and E. Latz, "NLRP3 inflammasome and the IL-1 pathway in atherosclerosis," *Circulation Research*, vol. 122, no. 12, pp. 1722–1740, 2018.
- [23] O. Foresto-Neto, V. F. Ávila, S. C. A. Arias et al., "NLRP3 inflammasome inhibition ameliorates tubulointerstitial injury in the remnant kidney model," *Laboratory Investigation*, vol. 98, no. 6, pp. 773–782, 2018.
- [24] K. Neumann, B. Schiller, and G. Tiegs, "NLRP3 inflammasome and IL-33: novel players in sterile liver inflammation," *International Journal of Molecular Sciences*, vol. 19, no. 9, p. 2732, 2018.
- [25] K. J. Livak and T. D. Schmittgen, "Analysis of relative gene expression data using real-time quantitative PCR and the $2^{-\Delta\Delta C_T}$ method," *Methods*, vol. 25, no. 4, pp. 402–408, 2001.
- [26] Z. Xu, L. Wang, J. Tian, H. Man, P. Li, and B. Shan, "High expression of B7-H3 and CD163 in cancer tissues indicates

- malignant clinicopathological status and poor prognosis of patients with urothelial cell carcinoma of the bladder," *Oncology Letters*, vol. 15, no. 5, pp. 6519–6526, 2018.
- [27] Y. Bao, X. Ma, T. P. Rasmussen, and X. B. Zhong, "Genetic variations associated with anti-tuberculosis drug-induced liver injury," *Current Pharmacology Reports*, vol. 4, no. 3, pp. 171–181, 2018.
- [28] T. E. Chang, Y. S. Huang, W. J. Su, C. L. Perng, Y. H. Huang, and M. C. Hou, "The role of regular liver function monitoring in anti-tuberculosis drug-induced liver injury," *Journal of the Chinese Medical Association*, vol. 82, no. 7, pp. 535–540, 2019.
- [29] J. G. Chamorro, J. P. Castagnino, R. M. Musella et al., "tagSNP rs1495741 as a useful molecular marker to predict antituberculosis drug-induced hepatotoxicity," *Pharmacogenetics and Genomics*, vol. 26, no. 7, pp. 357–361, 2016.
- [30] Y. Bao, P. Wang, X. Shao et al., "Acetaminophen-induced liver injury alters expression and activities of cytochrome P450 enzymes in an age-dependent manner in mouse liver," *Drug Metabolism and Disposition*, vol. 48, no. 5, pp. 326–336, 2020.
- [31] X. Liu, Y. Liu, M. Cheng, and H. Xiao, "Application of ultra high performance liquid chromatography-mass spectrometry to metabolomics study of drug-induced hepatotoxicity," *Chinese Journal of Chromatography*, vol. 33, no. 7, pp. 683–690, 2015.
- [32] C. Genestet, F. Bernard-Barret, E. Hodille et al., "Antituberculous drugs modulate bacterial phagolysosome avoidance and autophagy in *Mycobacterium tuberculosis* -infected macrophages," *Tuberculosis*, vol. 111, pp. 67–70, 2018.
- [33] M. T. Zaw, N. A. Emran, and Z. Lin, "Mutations inside rifampicin-resistance determining region of *rpoB* gene associated with rifampicin-resistance in *Mycobacterium tuberculosis*," *Journal of Infection and Public Health*, vol. 11, no. 5, pp. 605–610, 2018.
- [34] M. K. Urfi, M. Mujahid, M. A. Rahman, and M. A. Rahman, "The role of *Tamarix gallica* leaves extract in liver injury induced by rifampicin plus isoniazid in Sprague Dawley rats," *Journal of Dietary Supplements*, vol. 15, no. 1, pp. 24–33, 2017.
- [35] X. He, Y. Song, L. Wang, and J. Xu, "Protective effect of pyrrolidine dithiocarbamate on isoniazid/rifampicin-induced liver injury in rats," *Molecular Medicine Reports*, vol. 21, no. 1, pp. 463–469, 2020.
- [36] C. Wang, R. Q. Fan, Y. X. Zhang, H. Nie, and K. Li, "Naringenin protects against isoniazid- and rifampicin-induced apoptosis in hepatic injury," *World Journal of Gastroenterology*, vol. 22, no. 44, pp. 9775–9783, 2016.
- [37] K. Szentmihályi, "Metal element homeostasis and oxidative stress in pathological processes," *Orvosi Hetilap*, vol. 160, no. 36, pp. 1407–1416, 2019.
- [38] J. Liu, X. Wang, Z. Peng et al., "The effects of insulin pre-administration in mice exposed to ethanol: alleviating hepatic oxidative injury through anti-oxidative, anti-apoptotic activities and deteriorating hepatic steatosis through SRBEP-1c activation," *International Journal of Biological Sciences*, vol. 11, no. 5, pp. 569–586, 2015.
- [39] E. Cobbina and F. Akhlaghi, "Non-alcoholic fatty liver disease (NAFLD) - pathogenesis, classification, and effect on drug metabolizing enzymes and transporters," *Drug Metabolism Reviews*, vol. 49, no. 2, pp. 197–211, 2017.
- [40] M. Stettner, D. Steinberger, C. J. Hartmann et al., "Isoniazid-induced polyneuropathy in a tuberculosis patient - implication for individual risk stratification with genotyping?," *Brain and Behavior*, vol. 5, no. 8, article e00326, 2015.
- [41] H. Guio, K. S. Levano, C. Sánchez, and D. Tarazona, "The role of pharmacogenomics in the tuberculosis treatment regime," *Revista Peruana de Medicina Experimental y Salud Publica*, vol. 32, no. 4, pp. 794–800, 2015.
- [42] Q. Liu, D. Zhang, D. Hu, X. Zhou, and Y. Zhou, "The role of mitochondria in NLRP3 inflammasome activation," *Molecular Immunology*, vol. 103, pp. 115–124, 2018.
- [43] L. Sun, W. Ma, W. Gao et al., "Propofol directly induces caspase-1-dependent macrophage pyroptosis through the NLRP3-ASC inflammasome," *Cell Death & Disease*, vol. 10, no. 8, p. 542, 2019.
- [44] A. Dolunay, S. P. Senol, M. Temiz-Resitoglu et al., "Inhibition of NLRP3 inflammasome prevents LPS-induced inflammatory hyperalgesia in mice: contribution of NF- κ B, caspase-1/11, ASC, NOX, and NOS isoforms," *Inflammation*, vol. 40, no. 2, pp. 366–386, 2017.
- [45] A. R. Mridha, A. Wree, A. A. B. Robertson et al., "NLRP3 inflammasome blockade reduces liver inflammation and fibrosis in experimental NASH in mice," *Journal of Hepatology*, vol. 66, no. 5, pp. 1037–1046, 2017.
- [46] J. Qu, Z. Yuan, G. Wang, X. Wang, and K. Li, "The selective NLRP3 inflammasome inhibitor MCC950 alleviates cholestatic liver injury and fibrosis in mice," *International Immunopharmacology*, vol. 70, pp. 147–155, 2019.

Research Article

Expression and Potential Role of MMP-9 in Intrauterine Adhesion

Congqing Li ¹, Wenyan Wang,¹ Shiyong Sun,¹ Youjiang Xu,¹ Ziang Fang,¹ and Lin Cong²

¹Department of Obstetrics and Gynecology, The Second Hospital of Anhui Medical University, No. 678 Furong Road, Hefei, Anhui 230601, China

²Department of Obstetrics and Gynecology, The First Affiliated Hospital of Anhui Medical University, No. 218 Jixi Road, Hefei 230022, China

Correspondence should be addressed to Congqing Li; licongqing@139.com

Received 7 November 2020; Revised 11 January 2021; Accepted 20 January 2021; Published 29 January 2021

Academic Editor: Young-Su Yi

Copyright © 2021 Congqing Li et al. This is an open access article distributed under the Creative Commons Attribution License, which permits unrestricted use, distribution, and reproduction in any medium, provided the original work is properly cited.

Objective. Intrauterine adhesions affect menstruation and fertility, and endometrial fibrosis is the final manifestation of IUA. MMP-9 is closely related to fibrosis. The purpose of the study was to assess the role of MMP-9 in intrauterine adhesion (IUA) in rats and patients. **Methods.** 40 rats and 24 women were enrolled in this study. 40 rats were randomly divided into 3 groups: IUA group ($n = 20$), sham group ($n = 10$), and control group ($n = 10$). Rat IUA models were established by intrauterine mechanical and chemical injured. In this study, 12 patients of intrauterine adhesions were detected and underwent TCRA (transcervical resection of adhesion) surgery, and endometrial tissue specimens were obtained during operation. One month later, an office hysteroscopy procedure was performed, and endometrial tissue specimens were obtained during operation again (postoperative group). A group of 12 normal age-matched control individuals served as controls underwent hysteroscopy and endometrial sampling. We used immunohistochemistry to detect MMP-9 expressions in rats and human endometrial tissues and to detect MMP-9 protein levels by Western blotting. In addition, we detected mRNA expression levels with qRT-PCR. **Results.** The expression of MMP-9 in the IUA rats was reduced compared with that in the sham group and Ctrl group ($P < 0.05$), and the expression of MMP-9 was also reduced in the IUA patients compared with that in the Ctrl group ($P < 0.05$). The mRNA levels of MMP-9 in the endometrium reflected similar results ($P < 0.05$). The MMP-9 clearly increased even in the endometrium after TCRA surgery ($P < 0.05$). **Conclusion.** Our study suggests that MMP-9 may play an important role in IUA. In the future, more in-depth research should be conducted on MMP-9.

1. Introduction

Intrauterine adhesion (IUA) is a condition that was identified more than a century ago [1]. IUA is a very common problem encountered in clinical practice and is the main cause of menstrual volume reduction, infertility, and recurrent abortion. It has been identified that uterine cavity injury, especially induced abortion, can lead to endometrial basal layer injury. Injury is one of the direct causes of uterine cavity adhesion, and endometrial fibrosis is the final manifestation of IUA [2]. Fibrosis is a common and difficult problem to treat in the clinic. During the healing process of normal wounds, the deposition of extracellular matrix (ECM) leads to the occurrence and development of tissue fibrosis. The excessive accumulation or degradation of ECM components in the organs leads to an increase in ECM, fibrosis of the tis-

sue, and ultimately to a decrease in or loss of function due to liver fibrosis, kidney fibrosis, pulmonary fibrosis, and intestinal fibrosis [3]. The mechanism of endometrial fibrosis due to intrauterine adhesions is still unclear. According to conventional speculation, the persistence of ECM components and the reduced deposition or degradation of the extracellular matrix may be the main causes of fibrosis [3]. The process of fibrosis involves many factors and is intricate. Fibrosis involves the deposition of ECM proteins and related molecules/factors that crosslink various ECM elements, the hydrolysis of ECM proteins, and the enzymatic degradation of ECM. Among proteolytic ECM enzymes, matrix metalloproteinases (MMPs) have been a frequent topic of research by scholars [3]. MMPs play a key role in the balance between fibrosis and antifibrosis; when fibrosis and antifibrosis are out of balance, and the degradation of the extracellular

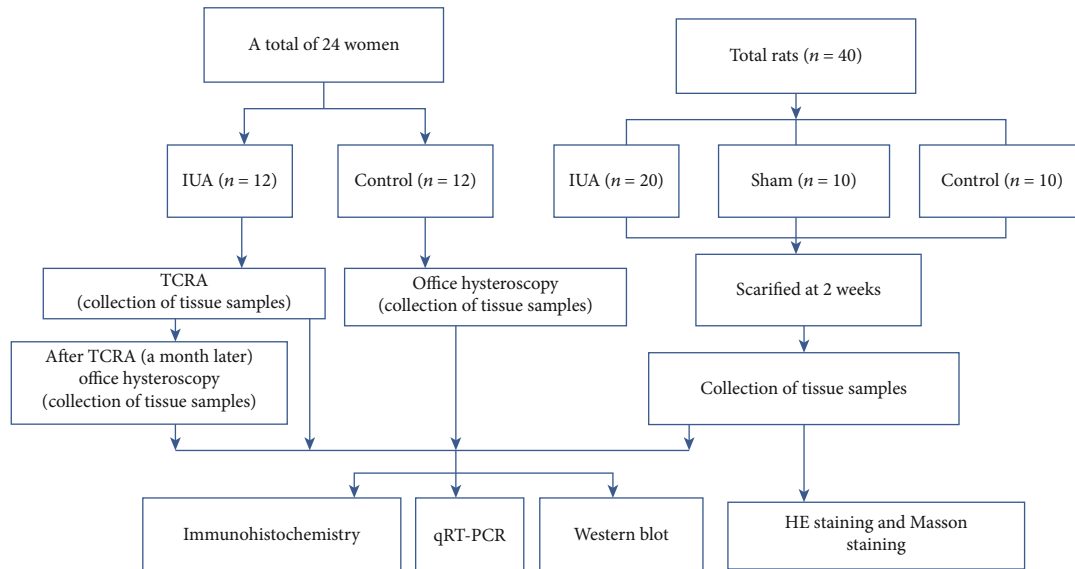


FIGURE 1: Master plan route for this study.

matrix eventually leads to the generation of tissue fibrosis [4, 5]. MMP-9 is a member of the metzincin family of mostly extracellular proteases. Although all of these enzymes might be promiscuous in their targeting of proteins, MMP-9 is a particular concern of researchers [6–9]. We aimed to investigate whether MMP-9 may also be involved in fibrosis in IUA. In this study, we evaluated the potential role of MMP-9 in fibrosis in IUA by measuring the expression of MMP-9 in endometrial tissues.

2. Materials and Methods

The master plan for this study is shown in Figure 1.

2.1. IUA Patients and Controls. 24 patients were included in our study, of which 12 were IUA patients. The ethics committee of the Second Hospital of Anhui Medical University approved the research plan (PJ-YX2019-016F1). The average age of the IUA patients was 29.5 years (24–40 years), and that of the control group was 24.75 years (21–39 years). We collected samples of the endometrial fibrosis tissue from May 2018 to July 2018. IUA patients were scored and graded according to criteria designed by the American Fertility Association (AFS) [10]. 12 patients underwent TCRA (transcervical resection of adhesion) surgery, and endometrial tissue specimens were obtained during operation (IUA group, $n = 12$). One month later, an office hysteroscopy procedure was performed, and it can be used to evaluate the uterine cavity and obtained endometrial tissue specimens (TCRA post-operative group, $n = 12$). A group of 12 normal age-matched control individuals served as controls underwent hysteroscopy and endometrial sampling. The criteria for the inclusion of surgical specimens excluded the presence of infection, any disease of the uterus, chronic inflammation, and malignant diseases. All patients signed written informed consent forms before surgery and agreed to the use of endometrial tissue specimens for scientific research.

2.2. Rat Experimental Protocol. The experimental animals used for this project were purchased from the Animal Experimental Center of Anhui Medical University under the animal certificate number: SCXK (Anhui) 2005-001. The experimental protocol followed the requirements of animal ethics and was implemented in accordance with the regulations of the Animal Ethics Committee of Anhui Medical University. The studies were approved by the Institutional Animal Care and Use Committee at the Anhui Medical University (LLSC20180085). From January 5th to February 26th, 2017, 40 mature fertile female SD rats were enrolled in this study (weighing 200–250 g, age 8 weeks). The experimental animals were kept in the animal breeding room of the Experimental Center of the Second Affiliated Hospital of Anhui Medical University. Under standard laboratory conditions, the ambient temperature of the animal breeding room is $25 \pm 2^\circ\text{C}$, and the maximum temperature difference must not exceed 2°C ; the humidity is controlled at $60\% \pm$, the indoor noise is less than 55 decibels (dB), and the rats were given one week to adapt to the breeding environment.

2.2.1. IUA Rat Models. The experimental surgery in all rats was performed by the same person, and the method of anesthesia was intraperitoneal administration of sterile sodium pentobarbital (30 mg/kg). Our goal was to use the rat uterus to generate an animal model to simulate human uterine adhesions. In clinical work, phenol mucus is used in female sterilization surgery and is safe and reliable [11]. 40 rats were randomly divided into three groups. Rats were sacrificed 2 weeks after surgery via the administration of carbon dioxide. Then, the uterus was removed, and the endometrial tissue specimens were obtained. After the specimens were removed, the bodies of the rats were harmlessly treated.

2.2.2. IUA Model Group, Sham Group, and Control Group. 20 rats were included in the IUA group. We used a uterine cavity from one rat as the experimental research object and injected

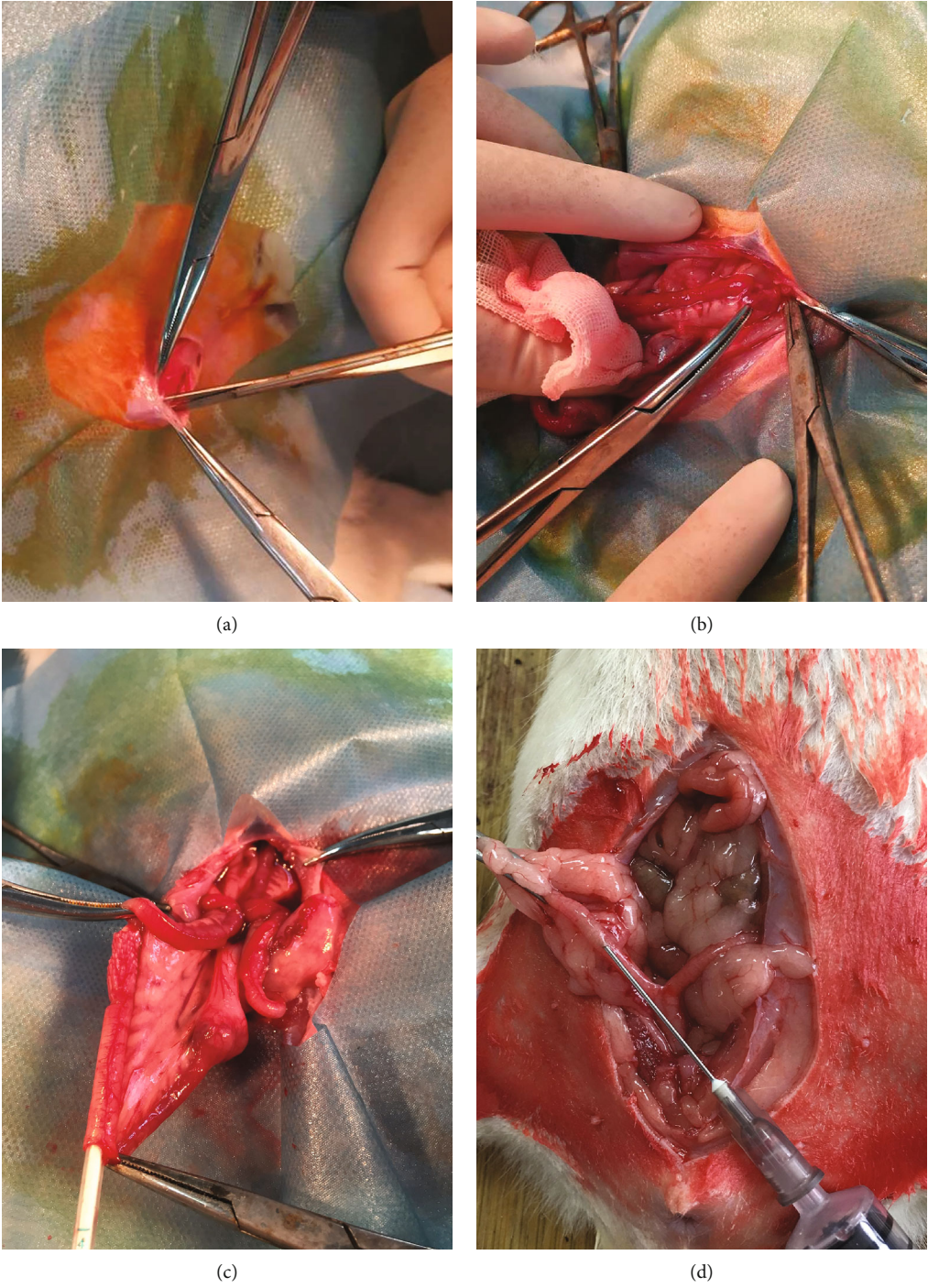


FIGURE 2: Continued.

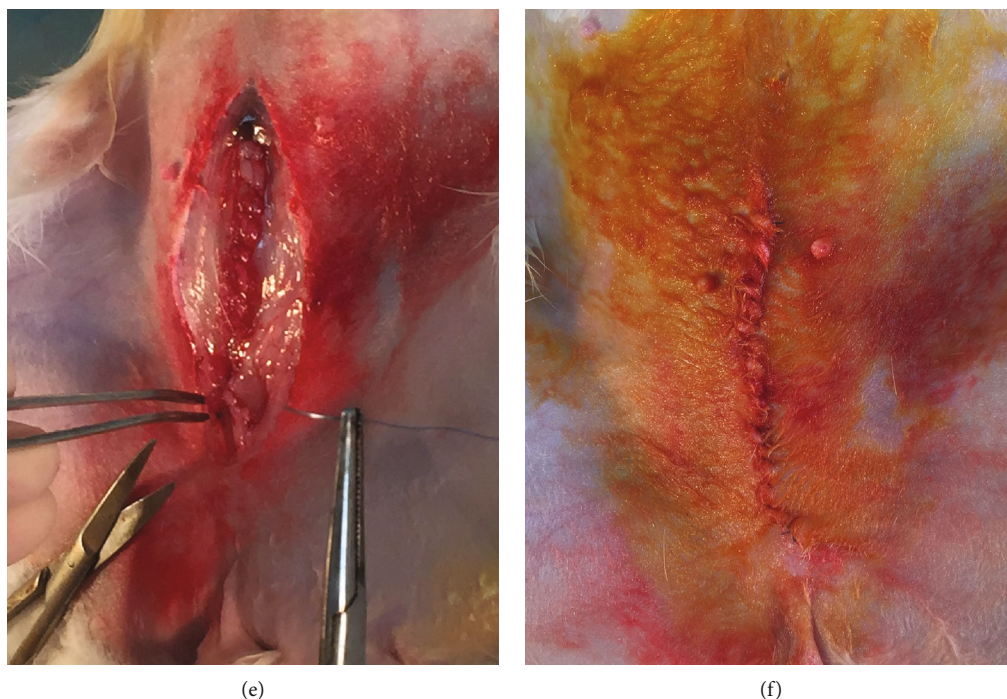


FIGURE 2: The operation procedure of the IUA rat model. (a) Select the incision sign. (b) Incise the skin and subcutaneous tissue. (c) Rat uterus was observed, and one side uterine cavity was probed. (d) Phenol mucilage was slowly injected into rat uterine cavity with syringe. (e) After the operation, the abdominal incision was closed. (f) After suturing the skin, sterilize the incision again.

0.04 ml of phenol mucilage into the selected uterine cavity; the phenol mucilage was composed of 25% v/v phenol solution, 5% v/v gum Arabic, and 20% glycerol v/v. This method resulted in the formation of adhesions within 2 weeks. The surgical procedure is shown in Figure 2. 10 rats were subjected to sham surgery, and the surgical procedure was the same as that used for the IUA group; the only difference was that normal saline was injected into the right uterine cavity instead of phenol mucilage. The control group also comprised 10 rats, which were not injected in the right uterine cavity.

2.3. Collection of Tissue Samples from Patients and Rats. The endometrial tissue samples were divided into two groups: one group was kept at room temperature in formalin, and the other was stored at -80°C until use.

2.4. HE Staining and Masson Trichrome Staining of the Rat Tissue Samples. The tissue specimens were fixed in 4% neutral buffered formalin, and paraffin sections were routinely made and then stained according to the HE staining procedure. The Masson trichrome staining methods and procedures were performed according to the instructions of the reagent manufacturer [11].

2.5. Immunohistochemistry of Human and Rat Tissue Samples. Tissue specimen sections were stained with conventional immunohistochemistry (IHC) procedures [12, 13], and the IHC reagents were used according to the manufacturer's instructions (ZhongShanJinQiao, Beijing, China). To measure the relative expression of MMP-9 in different

TABLE 1: Primers used for PCR analysis.

Target mRNA	Primer sequence
MMP-9-forwards:	5'-TTGACAGCGACAAGAAGTGG-3'
MMP-9-reverse:	5'-CCCTCAGTGAAGCGGTACAT-3'
GADPH-forwards:	5'-GGTTGAGCAGGTACTTT-3'
GADPH-reverse:	5'-AGCAAGAGCACAAAGAGGAAG-3'

groups of endometrial tissues, we calculated the expression score by evaluating the percentage of positive cells and the intensity of the staining signal. The expression score was calculated by multiplying the percentage of positive cells by the intensity score and then converting the result to determine the relative expression.

2.6. Western Blot Analysis. Western blotting was performed according to the manufacturer's instructions (Beyotime, Shanghai, China). Molecular imaging systems (Bio-Rad, Philadelphia, PA, USA) were used to visualize the bands, and finally, the relative expression value was calculated. Repeat three times for each sample.

2.7. Analysis of MMP-9 mRNA by RT-qPCR. Total RNA was extracted using TRIzol reagent (Invitrogen), and an RT kit (Takara) was used for the reverse transcription reactions according to the instructions. The MMP-9 mRNA was detected by PCR using cDNA as a template. Real-time quantitative PCR was used to detect the relative mRNA levels. The internal control was GAPDH. The primer sequences are shown in Table 1. The PCR conditions consisted of 5 min

TABLE 2: IUA patients' clinical data.

IUA patient	Age	Pregnancy history	Before TCRA surgery		After TCRA surgery	
			Grade	Score	Grade	Score
1	34	Gravida 1, Para 0	Severe	9	Mild	2
2	28	Gravida 4, Para 1	Severe	10	Moderate	6
3	35	Gravida 2, Para 1	Severe	10	Mild	1
4	32	Gravida 2, Para 0	Moderate	8	Mild	4
5	25	Gravida 1, Para 1 (a stillbirth,2016, fetal weight 5 kg)	Severe	10	Mild	3
6	34	Gravida 3, Para 1	Severe	10	Mild	2
7	30	Gravida 2, Para 0	Severe	9	Moderate	5
8	24	Gravida 1, Para 0	Severe	10	Mild	3
9	40	Gravida 3, Para 1	Severe	10	Mild	2
10	28	Gravida 2, Para 0	Severe	9	Moderate	5
11	29	Gravida 4, Para 0	Moderate	8	Mild	2
12	35	Gravida 6, Para 1	Severe	9	Moderate	5

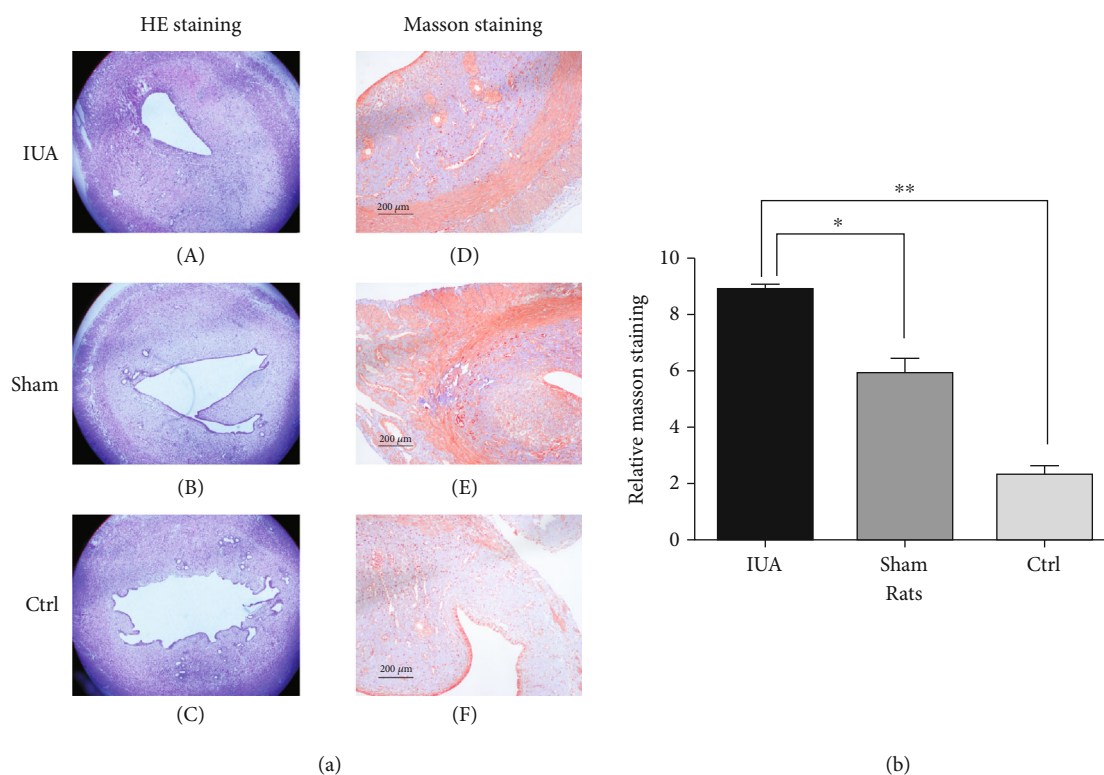


FIGURE 3: (a) HE and Masson staining revealed in rats. (A, D) IUA group (phenol mucilage treatment), (B, E) sham group (saline treatment), and (C, F) control group (no treatment), scale bar = 200 μm. (b) Relative Masson staining in rats, comparison of IUA to sham and Ctrl, * $P < 0.05$, ** $P < 0.05$.

at 95°C for one cycle followed by 45 cycles of 95°C for 10 s, 60°C for 40 s, and 72°C for 90 s. Repeat three times for each sample.

2.8. Statistical Analyses. All statistical analyses were performed using SPSS software (version 19.0, SPSS, Chicago, IL), and the differences between groups were analyzed using Student's *t*-test, the Mann-Whitney *U* test, or one-way analysis of variance with the Kruskal-Wallis test for

correction. A P value < 0.05 was considered to be statistically significant.

3. Results

3.1. Clinical Characteristics of Patients with IUA. 12 patients with intrauterine adhesions were included in this study, and their average age was 29.5 years. The IUA grade was 83% severe (score ≥ 9 points) and 17% moderate (score 5-8 points)

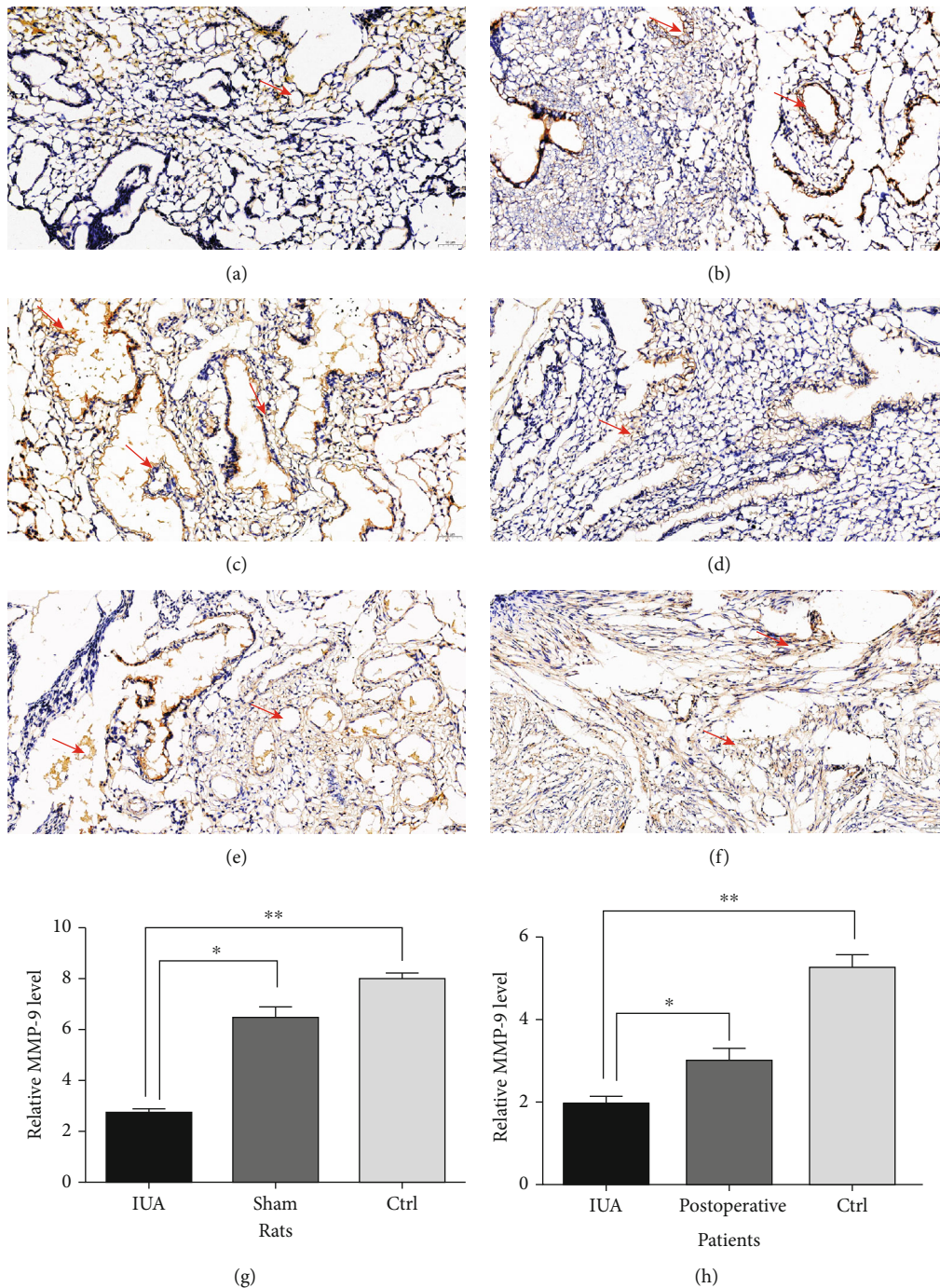


FIGURE 4: IHC of MMP-9 in rats and patients. Rat groups: (a) (IUA), (b) (sham), and (c) (control). Patient group: (d) (IUA), (e) (postoperative), and (f) (control). Scale bar = 50 μ M. (g) Relative MMP-9 level in rats, comparison of IUA to Sham and Ctrl, * $P < 0.05$, ** $P < 0.05$. (h) Relative MMP-9 level in patients, comparison of IUA to postoperative and Ctrl, * $P < 0.05$, ** $P < 0.05$.

according to the American Fertility Association (AFS) criteria. 6 of the 12 patients with intrauterine adhesions had children, but one of them was stillborn, and they all have fertility needs. TCRA was performed under general anesthesia. One month later, outpatient hysteroscopy was performed to evaluate the uterine cavity morphology. 8 cases had filmy membranous adhesions at the bottom of the uterus, and 4 cases had dense uterine segment adhesion. During the hysteroscopy procedure, the adhesion tissue is bluntly separated

through the sheath. Patients' clinical data are shown in Table 2.

3.2. HE Staining and Masson Trichrome Staining of Rat Tissue Samples. HE staining showed a narrowing of the uterine cavity in the IUA group. The Masson trichrome staining results showed that more severe fibrosis occurred in the endometrial tissue of the IUA group compared with that of the control group and the sham operation group (Figure 3).

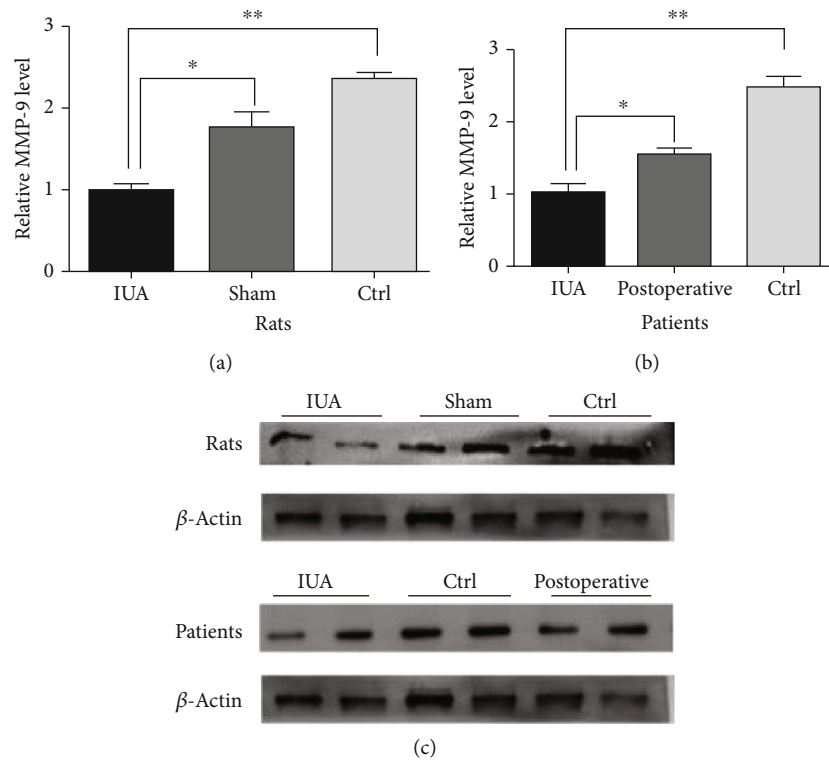


FIGURE 5: Determination of the MMP-9 protein expression in IUA rats and patients. (a) Relative MMP-9 protein expression in rat groups. Comparison of IUA to Ctrl and sham group, $*P < 0.05$, $**P < 0.05$. (b) Relative MMP-9 protein expression in patients. Comparison of IUA to postoperative and Ctrl, $*P < 0.05$, $**P < 0.05$. (c) Gel electrophoresis picture of MMP-9.

3.3. MMP-9 Expression in IUA Rats and Patients. It is known that MMP-9 plays an important role in fibrosis, and we measured the tissue sample expression by IHC, protein detection, and RT-PCR of MMP-9 mRNA in IUA rats and patients to assess whether there was differential expression of MMP-9 in IUA. We performed IHC staining of the tissue samples from IUA rats and patients, which revealed that the IUA groups were negative for MMP-9 staining. The differences were significant in the analysis ($P < 0.05$) (Figure 4). We detected the protein expression of MMP-9 by Western blotting and observed significant decreases in the protein expression in IUA rats and patients compared to that in controls. The MMP-9 protein expression was significantly different ($P < 0.05$) (Figure 5). In addition, the mRNA expression of MMP-9 was significantly decreased ($P < 0.05$) in IUA rats and patients compared with that in controls ($P < 0.05$) (Figure 6).

4. Discussion

In general, massive granulation, tissue hyperplasia, and fibrosis in the uterine cavity after abortion or curettage and IUAs occur 5 to 7 days after injury. When a sufficient amount of fibrosis occurs, regulatory mechanisms can hinder the regeneration of the endometrium and cause the formation of intrauterine adhesions [14]. Generally, in the initial stage of tissue damage, damaged and dead cells release antifibrinolytic coagulation factors, which trigger platelet activation, generate high levels of MMPs, destroy

the ECM, and allow inflammatory mediators to recruit inflammatory cells to the injury site. On the other hand, the microenvironment of the injury site will also change accordingly. The proinflammatory response will lead to the activation of matrix-producing cells and will also enhance the formation of fibers [4]. The MMP-9 expression is not isolated in the body; it is affected by other members of the MMP family, and it is controlled by metalloproteinase tissue inhibitors (TIMPs) [4]. MMP-9 has been extensively studied by scholars, especially in the fibrosis of the lung, liver, and heart [15]. Basic research has found that MMPs are not only a physiological effector of extracellular matrix turnover but also a key factor in the remodeling process under pathological conditions [16, 17]. The specific details of the fibrosis process are unknown, but we should realize that the functions of specific MMPs may not be the same in different organ systems [18].

IUA is the manifestation of tissue fibrosis. Here, we found that the MMP-9 expression was decreased in both IUA rats and patients. IHC, Western blotting, and RT-qPCR were used to detect MMP-9 mRNA and protein. Saribas and colleagues used a needle tube to injure the uterine cavity to establish a rat IUA model. Twenty-four rats were divided into four groups on average. The endometrium was obtained from the IUA group for the detection of MMP-9 and other related tests 8 weeks after modeling. Based on the IUA model, stem cells and exosomes were used for follow-up intervention. MMP-2 and MMP-9 expression were enhanced by MSC and exosomal

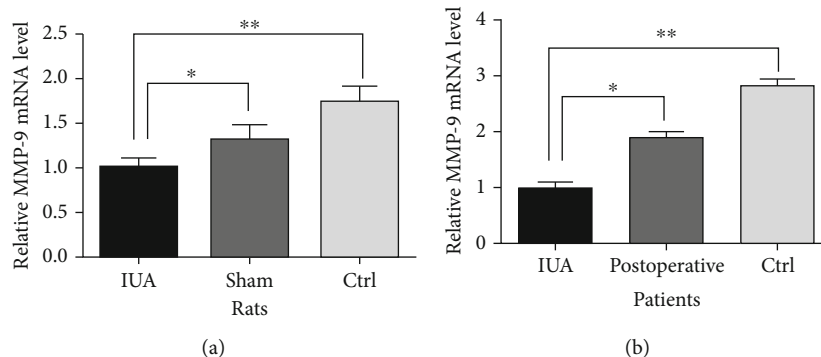


FIGURE 6: qRT-PCR analysis of the MMP-9 mRNA expression. (a) IUA rats. * $P < 0.05$, ** $P < 0.01$. (b) IUA patients, comparison of IUA to postoperative and Ctrl, * $P < 0.05$, ** $P < 0.01$.

therapy; in addition, the TIMP-2 expression was decreased [19]. Despite the different damage formation methods, the end results were quite similar. Of course, this study was simply based on the IUA rat model, and the time point for obtaining the endometrium was fixed. For human IUA patients, the expression of MMP-9 and TIMPs in the endometrium may not be consistent with those in animal models due to the differences in the IUA time course. In our study, the phenol mucilage method was used to establish the IUA model of rats, and MMP-9 detection was performed, the results of which were consistent with the previous research results. At the same time, we also collected specimens from patients with different disease durations for MMP-9 detection in the endometrium. The study results did not change significantly due to the length of the disease course. Human IUA endometrium showed low expression of MMP-9. Coincidentally, Chen and colleagues also used 24 rats to study uterine adhesions. The rats were divided into 2 groups on average. For the IUA group, the endometria of the left uteri were scraped without treatment. The right uteri were used as the control group. At 3, 7, 14, and 28 days after transplantation, the uteri were sampled for evaluation. Postoperative test results showed that the expression of MMP-9 in the endometrium was increased, but the thickness of endometrial glands and endometrium in fibrotic tissues was not different from those in the IUA group [20]. Our study found that MMP-9 showed low expression in the endometrial tissue of IUA rats, which is consistent with the previous two results [19, 20]. The value of freeze-drying the amniotic membrane was assessed using the rat IUA model. The expression of MMP-9 in human IUA intima was not tested. In the rat models and IUA patients, why was MMP-9 expressed at a low level? The reasons may be as follows. First, the MMP-9 expression changes dynamically in different stages of fibrosis and may be high in the early stage. MMP-9 appears to be downregulated as fibrosis progresses. However, the rat animal model did not show that the MMP-9 expression changes significantly with the operation time [20]. Second, in this study, perhaps the degree of fibrosis in IUA had an impact on the results, and the IUA patients included in this study all had third degree fibrosis, with certain limitations. In addition, patients with intrauterine adhesions have an urgent desire for childbirth.

The classical therapeutic approaches for infertile patients with IUA are hysteroscopic adhesiolysis, removing visible intrauterine adhesions [21]. In this study, the uterine cavity after intrauterine adhesion separation was significantly improved. MMP-9 in the endometrium after operation also increased, and the difference is statistically significant. It further suggests that MMP-9 is involved in the occurrence of IUA. Further study is needed to confirm the involvement of the intracellular MMP-9 signaling pathway in IUA, especially to identify and verify other key factors and the relationship between these key factors, such as MMP-2, MMP-3, MMP-7, IMP-1, and TIMP-2.

5. Conclusion

In summary, this study established an animal model for studying IUA mechanisms. In addition, we determined that MMP-9 is an important factor involved in IUA. In future research, we can carry out follow-up studies on MMP-9 to explore new ideas for mechanisms in IUA.

Abbreviations

IUA: Intrauterine adhesion
 MMP-9: Matrix metalloproteinases 9
 IHC: Immunohistochemistry
 mRNA: Messenger RNA.

Data Availability

Data supporting these study findings are available from the corresponding authors upon reasonable request.

Conflicts of Interest

The authors declare no conflicts of interest.

Authors' Contributions

Congqing Li conceived and designed the study, performed the analysis, interpretation of data, and drafted the manuscript. Wenyan Wang and Shiyang Sun assisted with the design, conception, and interpretation of data and critically reviewed the manuscript. Youjiang Xu assisted with the design, conception, and interpretation of data. Ziang Fang

assisted with the design, conception, and interpretation of data. All authors read and approved the final manuscript.

Acknowledgments




We extend our appreciation to Shun Yao, Yu He, and Chao Sun from the Department of Obstetrics and Gynecology of The Second Hospital of Anhui Medical University for their technical assistance, facilities, and support throughout this study. The manuscript's preprint is found in the link below: <https://www.researchsquare.com/article/rs-24240/v1>

References

- [1] H. E. Fritsch, "Fall von volligen Schwund der Gebärmutterhohlenach Auskratzung," *Zentralblatt für Gynäkologie*, vol. 18, pp. 1337–1342, 1894.
- [2] M. P. Diamond and M. L. Freeman, "Clinical implications of postsurgical adhesions," *Human Reproduction Update*, vol. 6, pp. 567–576, 2001.
- [3] Y. Liu, "Cellular and molecular mechanisms of renal fibrosis," *Nature Reviews Nephrology*, vol. 12, pp. 684–696, 2011.
- [4] N. A. Afratis, M. Klepfish, N. K. Karamanos, and I. Sagi, "The apparent competitive action of ECM proteases and cross-linking enzymes during fibrosis: applications to drug discovery," *Advanced Drug Delivery Reviews*, vol. 129, pp. 4–15, 2018.
- [5] B. Eckes, P. Zigrino, D. Kessler et al., "Fibroblast-matrix interactions in wound healing and fibrosis," *Matrix Biology*, vol. 19, no. 4, pp. 325–332, 2000.
- [6] B. Vafadari, A. Salamian, and L. Kaczmarek, "MMP-9 in translation: from molecule to brain physiology, pathology, and therapy," *Journal of Neurochemistry*, vol. 139, no. 2, pp. 91–114, 2016.
- [7] R. A. Nascimento, J. S. Possomato-Vieira, G. F. Bonacio, E. Rizzi, and C. A. Dias-Junior, "Reductions of circulating nitric oxide are followed by hypertension during pregnancy and increased activity of matrix metalloproteinases-2 and -9 in rats," *Cell*, vol. 8, no. 11, p. 1402, 2019.
- [8] H. Wang, M. Gao, J. Li et al., "MMP-9-positive neutrophils are essential for establishing profibrotic microenvironment in the obstructed kidney of UUO mice," *Acta Physiologica (Oxford, England)*, vol. 227, no. 2, 2019.
- [9] E. Hernández-Aquino, M. A. Quezada-Ramírez, A. Silva-Olivares et al., "Naringenin attenuates the progression of liver fibrosis via inactivation of hepatic stellate cells and profibrogenic pathways," *European Journal of Pharmacology*, vol. 865, p. 172730, 2019.
- [10] American Fertility Society, "The American Fertility Society classifications of adnexal adhesions, distal tubal occlusion, tubal occlusion secondary to tubal ligation, tubal pregnancies, Müllerian anomalies and intrauterine adhesions," *Fertility and Sterility*, vol. 49, pp. 944–955, 1988.
- [11] X. Wang, N. Ma, Q. Sun, C. Huang, Y. Liu, and X. Luo, "Elevated NF- κ B signaling in Asherman syndrome patients and animal models," *Oncotarget*, vol. 8, no. 9, pp. 15399–15406, 2017.
- [12] S. Zhang, P. Li, Z. Yuan, and J. Tan, "Platelet-rich plasma improves the appetite effects of menstrual blood-derived stromal cells in the rat model of intrauterine adhesion," *Stem Cell Research & Therapy*, vol. 10, pp. 1–12, 2019.
- [13] S. Kobayashi, H. Yamada-Okabe, M. Suzuki et al., "LGR5-positive colon cancer stem cells interconvert with drug-resistant LGR5-negative cells and are capable of tumor reconstitution," *Stem Cells*, vol. 30, no. 12, pp. 2631–2644, 2012.
- [14] J. G. Schenker, "Etiology of and therapeutic approach to synechia uteri," *European Journal of Obstetrics Gynecology and Reproductive Biology*, vol. 65, no. 1, pp. 109–113, 1996.
- [15] T. Vu and Z. Werb, "Gelatinase B structure, regulation, and function," in *Matrix Metalloproteinases*, W. C. Parks and R. P. Mecham, Eds., pp. 115–148, Academic Press, San Diego, 1998.
- [16] J. D. Mott and Z. Werb, "Regulation of matrix biology by matrix metalloproteinases," *Current Opinion in Cell Biology*, vol. 16, no. 5, pp. 558–564, 2004.
- [17] S. Robert, T. Gicquel, T. Victoni et al., "Involvement of matrix metalloproteinases (MMPs) and inflammatory pathway in molecular mechanisms of fibrosis," *Bioscience Reports*, vol. 36, pp. 1–11, 2016.
- [18] M. Giannandrea and W. C. Parks, "Diverse functions of matrix metalloproteinases during fibrosis," *Disease Models and Mechanisms*, vol. 7, no. 2, pp. 193–203, 2014.
- [19] G. S. Saribas, C. Ozogul, M. Tiryaki, F. Alpaslan Pinarli, and K. S. Hamdemir, "Effects of uterus derived mesenchymal stem cells and their exosomes on Asherman's syndrome," *Acta Histochemica*, vol. 122, no. 1, p. 151465, 2020.
- [20] X. Chen, J. Sun, X. Li et al., "Antifibrotic effects of decellularized and lyophilized human amniotic membrane transplant on the formation of intrauterine adhesion," *Experimental and Clinical Transplantation*, vol. 17, no. 2, pp. 236–242, 2019.
- [21] K. H. Tsui, L. T. Lin, J. T. Cheng, S. W. Teng, and P. H. Wang, "Comprehensive treatment for infertile women with severe Asherman syndrome," *Taiwanese Journal of Obstetrics & Gynecology*, vol. 53, no. 3, pp. 372–375, 2014.

Research Article

***Cryptococcus neoformans* Secretes Small Molecules That Inhibit IL-1 β Inflammasome-Dependent Secretion**

Pedro Henrique Bürgel,^{1,2} Clara Luna Marina,¹ Pedro H. V. Saavedra,³ Patrícia Albuquerque ,^{4,5} Stephan Alberto Machado de Oliveira,¹ Paulo Henrique de Holanda Veloso Junior,¹ Raffael Araújo de Castro,¹ Heino M. Heyman,^{6,7} Carolina Coelho,^{8,9} Radames J. B. Cordero,⁸ Arturo Casadevall,⁸ Joshua D. Nosanchuk,¹⁰ Ernesto S. Nakayasu,⁶ Robin C. May,² Aldo Henrique Tavares ,⁵ and Anamelia Lorenzetti Bocca ¹

¹Laboratory of Applied Immunology, Department of Cellular Biology, Institute of Biological Sciences, University of Brasilia, Brazil

²Institute of Microbiology and Infection and School of Biosciences, University of Birmingham, Edgbaston, UK B15 2TT

³Immunology Program, Sloan Kettering Institute, Memorial Sloan Kettering Cancer Center, New York, NY, USA

⁴Laboratory of Molecular Biology of Pathogenic Fungi, University of Brasilia, Brasilia, Brazil

⁵Faculty of Ceilândia, University of Brasília, Brazil

⁶Biological Sciences Division, Pacific Northwest National Laboratory, Richland, Washington, USA

⁷Bruker Daltonics Inc., Billerica, MA, USA

⁸Department of Molecular Microbiology and Immunology, Johns Hopkins Bloomberg School of Public Health, Baltimore, MD, USA

⁹Medical Research Council Centre for Medical Mycology, College of Medicine and Health, University of Exeter and University of Aberdeen, Aberdeen, UK

¹⁰Departments of Medicine (Division of Infectious Diseases) and Microbiology and Immunology, Albert Einstein College of Medicine, Bronx, NY, USA

Correspondence should be addressed to Aldo Henrique Tavares; atavares@unb.br and Anamelia Lorenzetti Bocca; albocca@unb.br

Received 9 July 2020; Revised 22 October 2020; Accepted 4 November 2020; Published 7 December 2020

Academic Editor: Young-Su Yi

Copyright © 2020 Pedro Henrique Bürgel et al. This is an open access article distributed under the Creative Commons Attribution License, which permits unrestricted use, distribution, and reproduction in any medium, provided the original work is properly cited.

Cryptococcus neoformans is an encapsulated yeast that causes disease mainly in immunosuppressed hosts. It is considered a facultative intracellular pathogen because of its capacity to survive and replicate inside phagocytes, especially macrophages. This ability is heavily dependent on various virulence factors, particularly the glucuronoxylomannan (GXM) component of the polysaccharide capsule. Inflammasome activation in phagocytes is usually protective against fungal infections, including cryptococcosis. Nevertheless, recognition of *C. neoformans* by inflammasome receptors requires specific changes in morphology or the opsonization of the yeast, impairing proper inflammasome function. In this context, we analyzed the impact of molecules secreted by *C. neoformans* B3501 strain and its acapsular mutant $\Delta cap67$ in inflammasome activation in an *in vitro* model. Our results showed that conditioned media derived from B3501 was capable of inhibiting inflammasome-dependent events (i.e., IL-1 β secretion and LDH release via pyroptosis) more strongly than conditioned media from $\Delta cap67$, regardless of GXM presence. We also demonstrated that macrophages treated with conditioned media were less responsive against infection with the virulent strain H99, exhibiting lower rates of phagocytosis, increased fungal burdens, and enhanced vomocytosis. Moreover, we showed that the aromatic metabolite DL-Indole-3-lactic acid (ILA) and DL-p-Hydroxyphenyllactic acid (HPLA) were present in B3501's conditioned media and that ILA alone or with HPLA is involved in the regulation of inflammasome activation by *C. neoformans*. These results were confirmed by *in vivo* experiments, where exposure to conditioned media led to higher fungal burdens in *Acanthamoeba castellanii* culture as well as in higher fungal loads in the lungs of infected mice. Overall, the results presented show that conditioned media from a wild-type strain can inhibit a vital recognition pathway and subsequent

fungicidal functions of macrophages, contributing to fungal survival *in vitro* and *in vivo* and suggesting that secretion of aromatic metabolites, such as ILA, during cryptococcal infections fundamentally impacts pathogenesis.

1. Introduction

Cryptococcus neoformans is a fungal pathogen that primarily affects immunocompromised patients with acquired immunodeficiency syndrome (AIDS) [1]. *C. neoformans* is responsible for over 180 thousand deaths yearly worldwide [2]. Human infection is usually initiated by the inhalation of environmental spores or yeasts that are present in environmental sources [3–7]. Once in the lung, the fungus is cleared by the host or survives within granulomas. In the context of immunosuppression, primary acquisition or relapse of previously contained yeast can result in disseminated disease, especially involving the central nervous system [5, 8, 9].

The ability of *C. neoformans* to remain viable and survive inside the host is dependent on its many virulence factors, which allow the fungus to modulate and evade the immune response [10, 11]. These virulence factors include enzymes (laccase, urease, phospholipases, proteases, and others) that can be secreted freely or encapsulated in extracellular vesicles [10, 12–14], melanin deposition in the cell wall [14, 15], and the formation of capsular polysaccharides, which are considered the most important of these factors [16–18]. Glucuronoxylomannan (GXM) is the most prevalent of these capsular polysaccharides, facilitating *C. neoformans* resistance against phagocytosis and suppressing various immune responses [19–26]. Altogether, these virulence factors enable this fungus to effectively survive and thrive as a facultative intracellular pathogen, particularly within macrophages [27–33]. Depletion of alveolar macrophages in mice is associated with a worse prognosis during infection with a glucosylceramide mutant, indicating that they might be co-opted by *C. neoformans* during pathogenesis to facilitate fungal growth and dissemination [34]. Phagocytic cells that are unable to kill intracellular yeast cells can return fungal cells to the extracellular environment, either through nonlytic exocytosis called vomocytosis [35–38] or a rapid, highly inflammatory and inflammasome-dependent cell death referred to as pyroptosis [39–41].

The inflammasome is an intracellular multiprotein complex that usually requires an intracellular damage-associated molecular pattern (DAMP) for its oligomerization and proper function [42]. The canonical activation step requires the engagement of an intracellular receptor from the NOD-like receptor (NLR) or AIM2-like receptor (ALR) family, an adaptor protein ASC and the cleavage of procaspase-1. Although some cell types can activate inflammasome pathways from basal expression levels, most of them require extracellular signaling, promoted by membrane-bound pattern-recognition receptors, to initiate inflammasome activation [43]. The activated caspases in this context are responsible for the previously described pyroptosis cell death and, most importantly, for the processing of interleukin- (IL-) 1 β and IL-18, essential mediators of inflammatory Th1/Th17-driven responses [44].

Among the receptors associated with inflammasome oligomerization, NLRP3 is one of the best described and well characterized in fungal recognition [45]. This receptor is involved in recognition of various fungal species, between yeast and hyphal forms, and opportunistic and primary pathogens [46–51]. The activation of NLRP3 is usually dependent on one or more intracellular stress signals (i.e., potassium efflux; mitochondrial reactive oxygen species production and cathepsin release), which are associated with the interaction between the host cell and the fungus [42, 45]. NLRP3 activation in response to *C. neoformans* only occurs when the yeast is in specific conditions such as biofilms [52], lacking capsule [53], or opsonized before phagocytosis [54]. Moreover, all three classical stress signals are required to activate NLRP3 during these interactions [52]. Notably, mice lacking NLRP3 or ASC are more susceptible to cryptococcal infection with encapsulated yeast cells, whereas infection with acapsular yeast cells results in higher fungal burdens in the lungs in NLRP3 knockout mice [52, 53]. Likewise, susceptibility to cryptococcal infection has also been observed in murine knockout models for IL-1 β and IL-18 receptors [55, 56].

Different strains of *C. neoformans* elicit variable IL-1 β induction, especially in *in vitro* models. Although GXM participates in inflammasome inhibition when macrophages are challenged with acapsular strains [53], capsule-independent inhibition of the inflammasome remains poorly understood. Here, we show that other secreted molecules besides GXM can specifically interfere with intracellular signals during inflammasome activation, suppressing various processes associated with this activation and reducing the overall antifungal capacity of macrophages. Furthermore, we have defined two molecules present in *C. neoformans* conditioned media that participate in inhibiting inflammasome activation in the presence of this remarkable fungus.

2. Material and Methods

2.1. Ethics Statement. All experimental procedures were approved by the Animal Ethics Committee of the University of Brasilia (UnBDoc number 55924/2016) and conducted according to the Brazilian Council for the Control of Animal Experimentation (CONCEA) guidelines.

2.2. Fungal Strains. Cryptococcal species complex strains H99 (var. *grubii*/*Cryptococcus neoformans*), B3501 (var. *neoformans*/*Cryptococcus deneoformans*), and *cap67* (acapsular strain derived from B3501) were grown for 18 h in Sabouraud dextrose broth, rotating (120 rpm) at 30°C. Yeast cells were retrieved from culture by centrifugation (5 min, 1800 g) and washed twice in PBS before experiments.

2.3. Conditioned Medium, GXM Isolation, and Subsequent Treatments. B3501 and *cap67* strains were grown for 5 days in minimal media (MM) (glucose 15 mM, magnesium sulfate 10 mM, monopotassium phosphate 29.4 mM, glycine

13 mM, and thiamine 3 μ M) rotating (120 rpm) at 30°C [57]. Yeast cells were removed from culture by centrifugation (2 \times 15 min 5500 g). The supernatant was collected and filtered (0.45 μ m) for complete yeast removal. The filtrate was lyophilized and suspended in deionized water, with a tenfold concentration. The products obtained from the B3501 and Δ cap67 strains were denominated conditioned media 35 (CM35) and conditioned media CAP (CMCAP), respectively [58]. CM35 was treated and/or fractionated for subsequent experiments. The size fractions were obtained utilizing an ultrafiltration Amicon system (Millipore), with filtration membranes varying from 100 to 1 kilodalton (kDa). In between fractions (e.g., 100 kDa > CM35 > 10 kDa) were also obtained, by recovering molecules retained in the filtration membrane. Polarity fractions were obtained by Blight-Dyer technique. Additionally, CM35 was treated by autoclaving (20 min at 123°C) and with the following proteases (24 h at 37°C): trypsin, thermolysin, and pronase. CM35 was also processed to remove GXM using a GXM-capture enzyme-linked immunosorbent assay (ELISA), as described by Rodrigues et al. [59]. Briefly, an ELISA high-binding plate was coated with mAb 18B7 (a monoclonal antibody (Ab) specific for GXM) [60] for 2 h at room temperature, preceded by a blocking step with 1% BSA solution for 1 h. Finally, conditioned media or minimal media were added to the wells for an additional 2 h and recovered at the end. The bound GXM was recovered by elution with Tris-glycine (pH 7.4) buffer. Yeast capsular polysaccharides from B3501 were harvested [61] and kindly supplied by Julie M. Wolf (Albert Einstein College of Medicine). Exopolysaccharides were obtained by the collection of a viscous layer in the 10 kDa membrane during CM35 ultrafiltration, as described [62].

2.4. Polysaccharide (PS) Attachment and Immunofluorescence. Polysaccharide (PS) attachment to Δ cap67 cell wall was performed as described [63]. Δ cap67 cells were incubated in yeast-free B3501 conditioned medium (grown in a minimal medium for 4 days) overnight at 37°C. B3501, Δ cap67, and Δ cap67-PS were fixed with 4% paraformaldehyde for 30 minutes at room temperature and incubated with PBS+1% bovine serum albumin for 1 h at room temperature. Yeast cells were then incubated with 0.01% Uvitex2B (a chitin marker; Polysciences) and mAb 18B7 (10 μ g/ml) for 30 minutes followed by incubation with Alexa Fluor 546 anti-mouse IgG1 (5 μ g/ml; Invitrogen) for 30 minutes at 37°C. Cells were then suspended in an antifading agent, mounted on glass slides, and analyzed with a confocal microscope (Leica TCS SP5).

2.5. Generation of Bone Marrow-Derived Macrophages (BMDMs and BMMs) and Dendritic Cells (BMDCs). Bone marrow cells were obtained from C57BL/6 isogenic mice (8–10 weeks old), as previously described [49]. Briefly, femurs and tibias were flushed with RPMI-1640 to harvest the bone marrow cells. Cells were submitted to erythrocyte lysis under a Tris-buffered ammonium chloride solution, seeded (2 \times 10⁵ cells/ml), and cultured for 8 days at 37°C in non-tissue culture-treated Petri dishes in 10 ml/dish of RPMI-1640 medium that contained 50 mM 2-mercapto-

ethanol. The medium was supplemented with 20 ng/ml murine granulocyte-macrophage colony-stimulating factor (GM-CSF, PeproTech) to obtain BMDCs and BMDMs or 30% conditioned medium from macrophage colony-stimulating factor-secreting L929 fibroblasts (M-CSF) to obtain BMMs. On the third day, an additional 10 ml of a complete medium that contained differentiation-inducing cytokines was added. Half the medium was exchanged on the sixth day of culturing the BMDCs. On the eight-day, non- and loosely adherent BMDCs or firmly adherent BMMs were stripped with TrypLE™ Express (Gibco), harvested, and plated in RPMI-1640 medium supplemented with Fetal Bovine Serum (FBS) and gentamicin.

2.6. Murine Cell Culture Interaction with Conditioned Media. BMMs or BMDCs (1 \times 10⁶/ml) were incubated at 37°C in a humidified 5% CO₂ atmosphere. Cells were stimulated with lipopolysaccharide (LPS; 500 ng/ml for 4 h, Sigma-Aldrich), providing the first signal for inflammasome activation. Additionally, cells were incubated for 18 h with or without potential inhibitors: CM35 (and its fractions), CMCAP, minimal medium, glycine (Sigma-Aldrich), glucuronoxylomannan (GXM), and aromatic metabolites: (Sigma) 3-Phenyllactic acid (PLA); DL-p-Hydroxyphenyllactic acid (HPLA) and DL-Indole-3-lactic acid (ILA), alone or in combination. After that, cells were treated with nigericin (20 μ M for 40 or 90 minutes, InvivoGen), providing the second signal for inflammasome activation. Alternatively, cells stimulated with LPS were infected with the fungal strains opsonized with mAb 18B7 (a kind gift from A. Casadevall, Johns Hopkins Bloomberg School of Public Health) [60]. Controls included conditions without LPS or nigericin.

2.7. Cytokine Quantification by ELISA and Lactate Dehydrogenase (LDH) Detection. The cell-free supernatants of the BMM and BMDC cultures were harvested for measurements of IL-1 β and tumor necrosis factor- (TNF-) α (Ready-Set-Go! Kit, eBioscience) concentrations using ELISA. The determination of intracellular pro-IL-1 β was performed with the cell lysates (Ready-Set-Go! Kit, eBioscience). The data were expressed as pg/ml \pm the standard deviation (SD) of two to three independent experiments, which were conducted in triplicate.

The cell-free supernatants of the BMM cultures were harvested to quantify LDH release, as a cell death marker (Cytotox 96® Non-Radioactive Cytotoxicity Assay, Promega) after treatment with nigericin for 90 minutes. The data were expressed as percentage \pm the standard deviation (SD) of two to three independent experiments, which were conducted in triplicate, considering cells without any treatment as 0% and cells treated with 15% dimethyl sulfoxide (DMSO) as 100% of cell death.

2.8. Active Caspase-1 Detection by Flow Cytometry. BMMs challenged with *C. neoformans* strains (MOI 5 : 1) opsonized with mAb 18B7 were harvested from the tissue culture well plates with a dissociation agent (TrypLE Express, Thermo Fisher Scientific). 5 \times 10⁵ were collected per group before staining. Staining for caspase-1 (FAM-FLICA™ Caspase-1

Assay Kit, Immunochemistry) was performed according to the manufacturer's instructions. The cells were then analyzed in a flow cytometer (FACSVerse, BD Biosciences) with the FITC filter channel (FL-1), and data were processed (FlowJo X, LLC).

2.9. cDNA Synthesis and Real-Time Reverse Transcription Polymerase Chain Reaction (RT-PCR). Total RNA from the cultured BMDMs was extracted using TRIzol reagent (Invitrogen), and cDNA synthesis was performed using a high-capacity RNA-to-cDNA kit (Applied Biosystems), according to the manufacturer's instructions. qRT-PCR was performed using SYBR Green Master Mix and StepOne Real-Time PCR System (Applied Biosystems). The primer sequences were as follows: IL-1 β forward, 5'-GTGTGTGACGTTCCCATTA GACA-3'; IL-1 β reverse, 5'-CAGCACGAGGCTTTTTTGT TG-3'; Nf- κ B forward, 5'-AGCCAGCTTCCGTGTTTGT T-3'; nuclear factor kappa-light-chain-enhancer of activated B cells (Nf- κ B) reverse, 5'-AGGGTTTCGGTTCCTACTAGT TTCC-3'; GAPDH forward, 5'-TGAAGCAGGCATCTGA GGG-3'; glyceraldehyde 3-phosphate dehydrogenase (GAPDH) reverse, 5'-CGAAGGTGGAAGAGTGGGAG-3'; IL-1 β or Nf- κ B to GAPDH relative expression was calculated using the $2^{-(Ct)}$ method and normalized to the level of unstimulated BMDMs.

2.10. Vomocytosis Scoring by Flow Cytometry. BMDMs challenged with stained H99 with Calcofluor White (10 μ g/ml, 10 min, Sigma-Aldrich) were treated concomitantly with CM35 or left untreated [64]. After 2 h of interaction, all wells were gently washed three times with warm PBS. The last wash from the 2 h time point wells were collected, and the cells were lysed. RPMI with fluconazole (10 μ g/ml, Sigma-Aldrich) was added in the other wells, and the cells were treated again with CM35 or left untreated. The supernatant and cell lysate were collected in determined time points (6, 12, and 24 h). Right after the collection, both supernatant and lysate samples were centrifuged (2,000 \times g, 5 min) for yeast recovery and fixated in paraformaldehyde 4% in PBS until flow cytometry analysis. Samples were accessed by flow cytometry (FACS Fortessa, BD Biosciences), at low-speed acquisition for 4 minutes. Parent yeast cells were detected using a high Calcofluor fluorescence gate. Using the specification provided by the manufacturer, the number of yeast/ml was calculated.

2.11. Coincubation Assays (Phagocytic Index, Fungicidal Activity, and Transwell Assays). BMDMs were challenged with H99 opsonized with mAb 18B7 (MOI 2 : 1), and the phagocytosis rates and fungal burdens were analyzed at 37°C. For the phagocytosis assay, BMDMs were primed with LPS (500 ng/ml) for 4 h followed by treatment overnight with conditioned media. Controls were left untreated. After this period, the cells were challenged with opsonized H99. After 2 h, the wells were gently washed three times with warm PBS, and the remaining coculture was fixed and stained with modified Wright-Giemsa stain. The phagocytic index was calculated by multiplying the number of macrophages engag-

ing phagocytosis and the number of yeasts phagocytosed per 100 macrophages analyzed. For the yeast intracellular growth assay, BMDMs primed with LPS (500 ng/ml) or not were challenged with opsonized H99 and concomitantly treated with conditioned media or left untreated. After 2 h, all the wells were gently washed three times with warm PBS to remove extracellular yeast. Right after the washes as well as 24 h later, macrophages were lysed with 0.05% SDS and intracellular yeasts recovered and measured by colony forming units (CFU) by plating on Sabouraud dextrose agar. The intracellular growth rate was determined by dividing 2 h CFU by 24 h CFU. For the transwell assay, BMDMs were seeded in both upper and lower chambers and primed with LPS (500 ng/ml). The BMDMs in the lower chamber were challenged with opsonized *Cryptococcus* strains (MOI 5 : 1) or left uninfected, while the BMDMs in the upper chamber were not challenged. After 24 h at 37°C, macrophages from the upper chambers were challenged with opsonized green fluorescent protein (GFP) expressing H99 (MOI 2 : 1) and lysed with 0.05% sodium dodecyl sulfate SDS at 24 h postinfection. Alternatively, the lower chambers contained only yeast cells from *Cryptococcus* strains in a media with LPS (500 ng/ml) throughout the assay. The recovered intracellular yeast cells were quantified using flow cytometry.

2.12. Detection of GXM Internalization Using Fluorescence Microscopy. BMDMs primed with LPS were treated with CMCAP or CM35 and their fractioned derivatives, as described earlier. BMDMs were plated in glass inserts, and after 18 h of interaction with conditioned media, cells were permeabilized and fixed with cold methanol (Vetec) for 10 minutes. After consecutive washes, cells were blocked for 1 h with a 10% FBS solution and stained for GXM with mAb 18B7 (10 μ g/ml) as a primary Ab and "Alexa Fluor® 633 Goat Anti-Mouse IgG" (Life Technologies) as a secondary Ab. Cells were also stained with a DAPI solution (Life Technologies). The glass inserts were then recovered, and GXM content internalized by the BMDMs was observed under a confocal microscope (Leica TCS SP5).

2.13. Gas Chromatography-Mass Spectrometry Analysis. Metabolites from conditioned culture media were derivatized as described [65]. Ketone groups of metabolites were derivatized by adding 20 μ l of 30 mg/ml methoxyamine in pyridine (Sigma-Aldrich) and incubating at 37°C for 90 minutes with shaking (1000 RPM). Then, amine, hydroxyl, and carboxyl groups were modified with 80 μ l of N-methyl-N-(trimethylsilyl)trifluoroacetamide (MSTFA) (Sigma-Aldrich) with 1% trimethylchlorosilane (TMCS) (Sigma-Aldrich) by shaking (1000 rpm) at 37°C for 30 minutes. Derivatized samples were analyzed in an Agilent GC 7890A using a HP-5MS column (30 m \times 0.25 mm \times 0.25 μ m; Agilent Technologies) coupled with a single quadrupole MSD 5975C (Agilent Technologies). Samples were injected in the splitless mode with the port temperature set at 250°C and oven temperature equilibrated at 60°C. The oven temperature was kept at 60°C for 1 minute and then raised to 325°C at a rate of 10°C/minute and finally finished with 5 minutes hold at 325°C. A fatty acid methyl ester (FAME) standard mix was analyzed with each

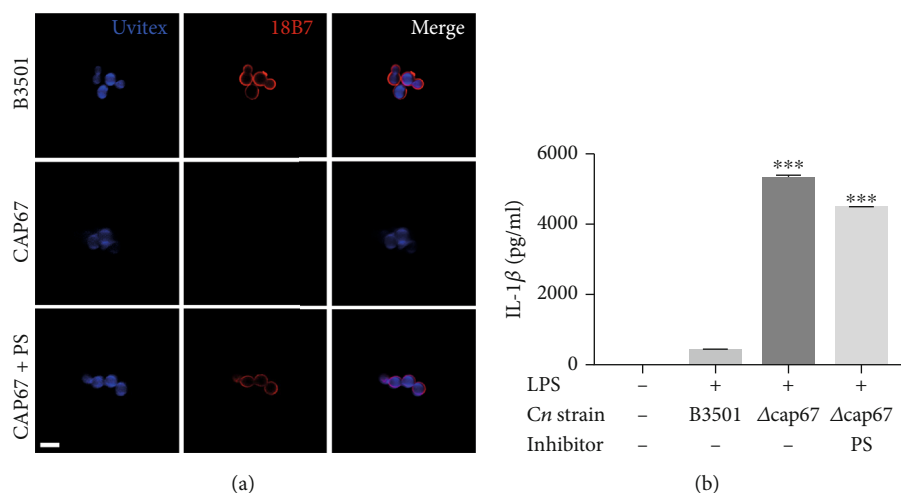


FIGURE 1: Exopolysaccharide incorporation on an acapsular mutant does not impair macrophage inflammasome activation. (a) GXM detection by immunofluorescence of B3501, CAP67 ($\Delta cap67$), and CAP67+PS ($\Delta cap67$ coated with polysaccharides from B3501) labeled with Uvitex2B (blue) and mAb against GXM (18B7) (red). (b) BMDMs were stimulated with LPS (500 ng/ml) and infected with opsonized B3501, $\Delta cap67$, or $\Delta cap67$ +PS strains (MOI 2:1) for 24 h. Statistical analysis was performed using one-way ANOVA, where *** $P \leq 0.001$. Comparisons were made with the B3501-infected group.

batch for subsequent retention time calibration purposes. Collected data files were processed with MetaboliteDetector [66], by calibrating retention indices (RI) based on FAME standards and deconvoluting and chromatographically aligning features. Metabolites were identified by matching spectral features and retention indices against a PNNL augmented version of the FiehnLib library containing more than 900 metabolites [67]. Unidentified metabolites were also searched against the NIST14 GC-MS library by comparing spectral features only. All identifications were manually validated. Extracted metabolite intensities were subjected to multivariate data analysis (MVDA) using MetaboAnalyst [68]. The data were median normalized and log transformed followed by principal component, hierarchical cluster, and heat map analysis to identify natural clustering within the data.

2.14. Acanthamoeba Infection and Treatment with Conditioned Media. *Acanthamoeba castellanii* was cultivated in liquid Yeast Peptone Dextrose Medium (YPD, 2% peptone, 1.8% D-glucose, 0.1% yeast extract) supplemented with 0.0034 M tribasic sodium citrate, 0.004 sodium sulfate, 0.0025% monobasic sodium phosphate, 0.0025% monobasic potassium phosphate, 0.00005% iron ammonium sulfate hexahydrate, and 0.00004% calcium chloride dihydrate at 30°C. *A. castellanii* (5×10^5 cells/ml) and *C. neoformans* H99 (1×10^6 cells/ml) were concomitantly added to culture plates with treatments (10% of the volume): PBS, <1 kDa CM35, minimal medium, or aromatic metabolites (1 mM): ILA alone or in combination with HPLA or with HPLA and PLA. After 24 h, the cells were washed three times with PBS to withdraw any fungi not internalized by amoebas. To lysate the amoebas but not the yeasts, 0.01% Triton X-100 was added, and they were sonicated for 10 minutes. Afterward, the lysate was

plated in Sabouraud agar plates, which were incubated for 48 h at 30°C for quantification of CFU.

2.15. Murine Infection and Treatment with Conditioned Media. The influence of CM treatment in the host immune response was analyzed using three groups of male C57Bl/6 wild-type mice 8-12 weeks old infected with the virulent strain H99 of *C. neoformans* followed by treatment with <1 kDa CM35 or aromatic metabolites. Each group was formed with eight mice, and all of them were challenged with 8×10^4 cryptococcal cells by intratracheal inoculation. Before the surgery, animals were anesthetized following the instruction of Ethics Committee, injecting a solution of Ketamine-Vetnil and Xylazine-Ceva (1:1) in the intramuscular region of one of the hind paws of the mice. The volumes used for anesthesia were according to animal weight. Two and seven days after infection, each group received a treatment of 20 μ l of intranasal MM, PBS, <1 kDa CM35, or ILA+HPLA (1 mM). Fourteen days after infection, the mice were euthanized by hypoxia using a CO₂ chamber, and the lungs and brain were surgically removed to the analysis of fungal burden and cytokine production. For quantification of fungal burden, the tissues obtained were weighed and macerated in 1 ml of PBS using a glass macerator. The homogenized tissues were plated in a Sabouraud agar plate and incubated at 30°C for 48 h, allowing the counting of CFU.

2.16. Statistical Analysis. Statistical analysis was conducted using GraphPad Prism v.7.0 software. Data were analyzed by one-way ANOVA followed by Tukey's post hoc test. P values less than 0.05 were considered significant. The metabolomics assay was analyzed by t -test, PCA, and OPLS, and the metabolite figure was generated from an Excel spreadsheet that was extracted from a heat map using the t -test

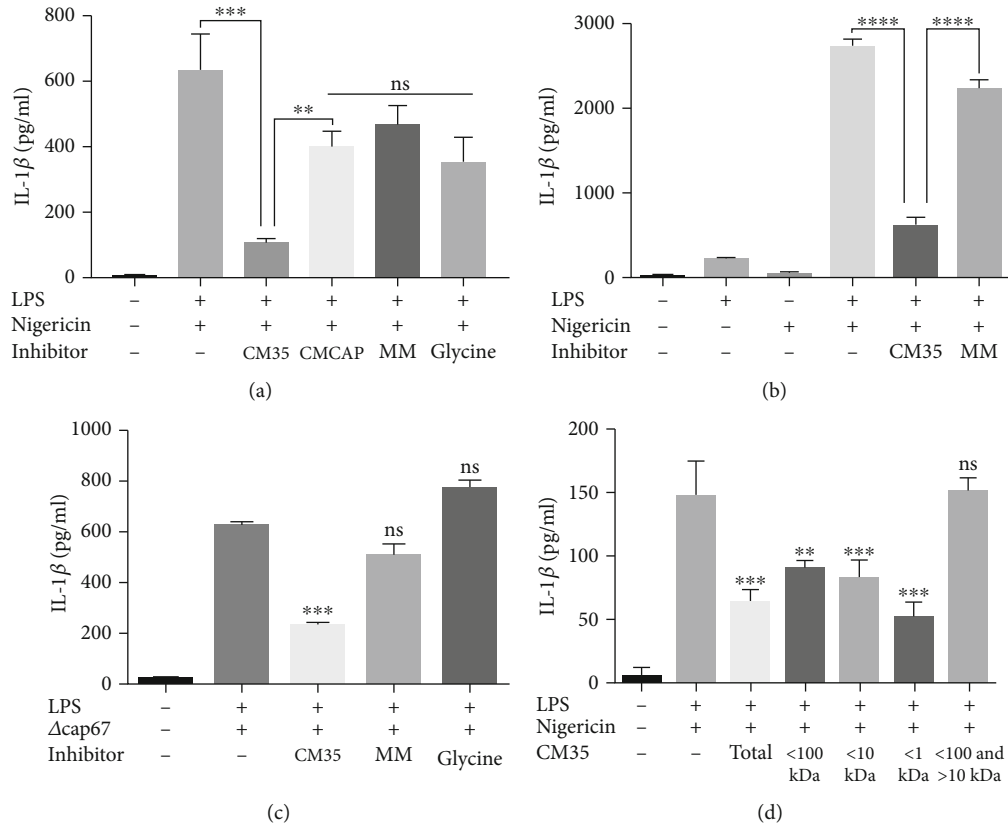


FIGURE 2: CM35, but not CMCAP or minimal media reduces IL-1 β secretion. (a) BMMs were stimulated with LPS (500 ng/ml) and/or nigericin (20 μ M), added or not by mediums (CM35; CMCAP or MM 10% v/v) or glycine (13 mM) overnight (18 h). (b) BMDCs were stimulated with LPS (500 ng/ml) and/or nigericin (20 μ M), added by media (CM35 or MM 10% v/v) overnight (18 h). (c) BMDMs were stimulated with LPS (500 ng/ml), infected with $\Delta cap67$ strain (MOI 5 : 1), added or not by mediums (CM35 or MM 10% v/v) or glycine (13 mM) overnight (18 h). (d) BMDMs stimulated with LPS (500 ng/ml) and/or nigericin (20 μ M), added by CM35 >100 kDa, <100 and >10 kDa, <10 kDa and <1 kDa (10% v/v) overnight (18 h). Supernatants were collected after stimulus and cytokines were quantified by ELISA technique. CM35 = conditioned media from B3501; CMCAP = conditioned media from $\Delta cap67$; MM = minimal media. Statistical analysis was performed utilizing one-way ANOVA, where ns: not significant; ** $P \leq 0.002$; *** $P \leq 0.001$. Comparisons were made with the positive control group (LPS+nigericin) when not indicated (c, d).

values. For normalization, the data were median centered and log transformed.

3. Results

3.1. Exopolysaccharide Incorporation on Acapsular Mutant Does Not Impair Macrophage Inflammasome Activation. As described previously [53, 54], *C. neoformans* mutants lacking GXM expression and proper capsule formation triggered inflammasome activation more effectively than wild-type encapsulated yeast cells presumably due to the presence of immunomodulatory exopolysaccharides, including GXM, in the fungal capsule. However, we found that $\Delta cap67$ coated with exo-PS which consists mostly of GXM molecules (Figure 1(a)) induced significantly more IL-1 β secretion compared to the wild-type B3501 (Figure 1(b)). This result suggested that the presence of GXM on the yeast surface by itself was not sufficient to explain the differences in inflammasome activation observed between acapsular mutants and their wild-type counterparts.

3.2. CM35, But Not CMCAP or Minimal Media, Reduces IL-1 β Secretion. Since many of the virulence factors presented by *C. neoformans* are secreted [10, 15], we evaluated whether components released by the fungus (CM) were able to inhibit inflammasome canonical activation. The addition of CM35 to activated macrophages (Figure 2(a)) and dendritic cells (Figure 2(b)) significantly reduced the secretion of IL-1 β by these cells, while CMCAP, MM, and glycine inhibited IL-1 β secretion to a lesser degree (Figures 2(a) and 2 (b), S1A Fig). Interestingly, CM35, CMCAP, and MM did not reduce the secretion of TNF- α (S1B-D Fig), even if added before LPS priming (S1E Fig). The same pattern was observed when conditioned media from H99 strain was used as treatment (S1G-H Fig). The specific interference of conditioned media in the secretion of IL-1 β , an inflammasome-dependent cytokine, but not in TNF- α , an inflammasome-independent cytokine, indicates that the canonical inflammasome pathway is being inhibited. The reduction in IL-1 β observed with CMCAP and MM is likely explained by the presence of glycine (Figure 2(a)). We tested if the same results were found when using a different stimulus for inflammasome; we primed

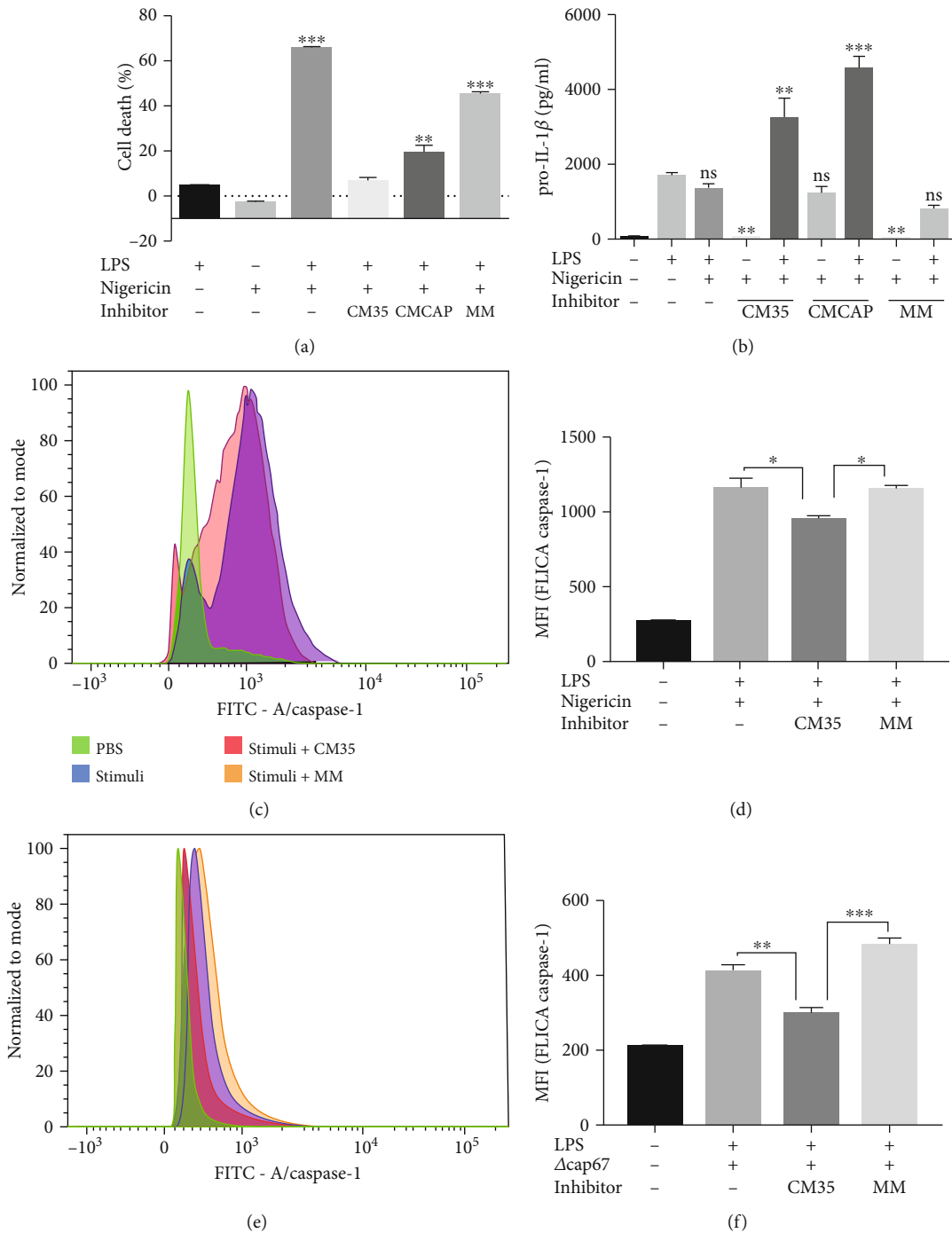


FIGURE 3: 1 kDa CM35 inhibits caspase-1 activation, promotes pro-IL-1β accumulation, and inhibits cell death. (a) LDH release from supernatants of BMMs stimulated with LPS (500 ng/ml) and/or nigericin (20 μM), with or without inhibitors (10% v/v). The medium group was utilized as negative control (0% of cell death) and the DMSO (15%) group was used as positive control (100% of cell death). (b) pro-IL-1β production measured from cell lysates of BMMs stimulated with LPS (500 ng/ml) and/or nigericin (20 μM), with or without inhibitors (10% v/v). (c–f) BMMs stimulated with LPS (500 ng/ml) and nigericin (20 μM) or Δcap67 (MOI 5:1), with or without inhibitors, were analyzed for caspase-1 activation (FLICA). LDH release was measured by colorimetric assay (a), cytokine was measured by ELISA (b), and caspase activation was measured by flow cytometry. (c, d) LPS and nigericin or (e, f) Cap67 was used as stimuli, and the mean fluorescence intensity (MFI) was assessed (d, f). Statistical analysis was performed by one-way ANOVA, where ns: not significant; *P ≤ 0.033; **P ≤ 0.002; ***P ≤ 0.001. Comparisons were made with the LPS only group (a, b).

macrophages with LPS followed by challenging with the acapsular strain Δcap67. In these conditions, BMMs still show a marked reduction in IL-1β levels in the presence of

CM35, while in these conditions MM and glycine did not affect IL-1β secretion (Figure 2(c)), indicating that CM35 is able to decrease the inflammasome activation in the context

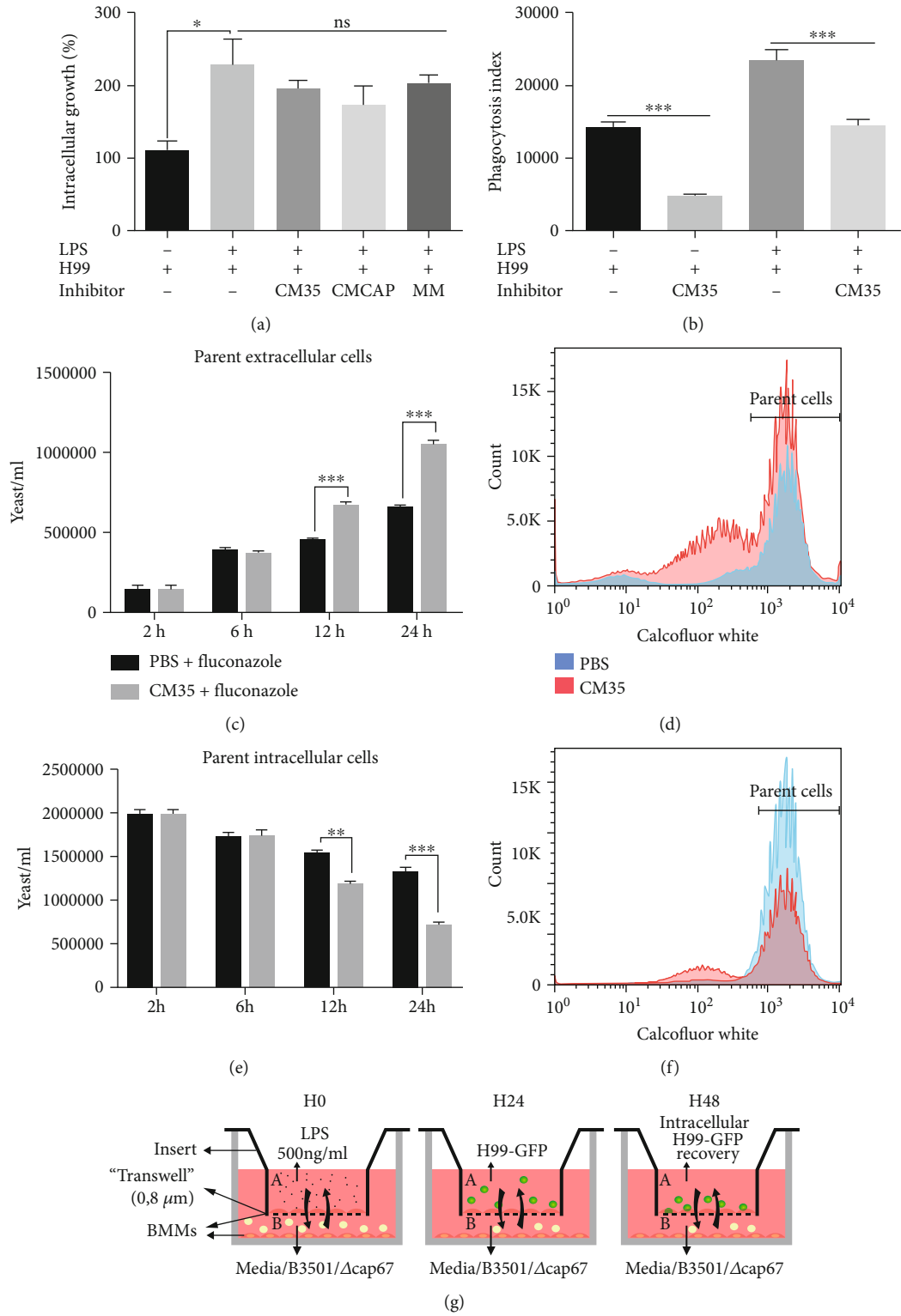


FIGURE 4: Continued.

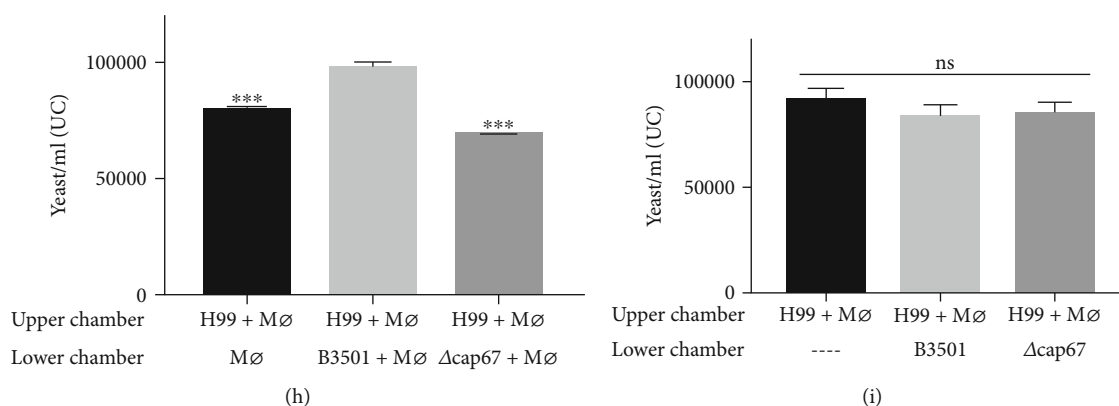


FIGURE 4: 1 kDa CM35 impacts phagocytic capacity and vomocytosis events in interactions between macrophages and *C. neoformans*. (a) Intracellular growth (CFU of 3 h vs. 24 h postinfection) of yeasts cells in BMMs stimulated with LPS (500 ng/ml) and H99 (2:1), with or without inhibitors (10% v/v). (b) Phagocytosis index (2 h postinfection) from BMMs stimulated with LPS (500 ng/ml) and H99 (5:1), with or without 1 kDa CM35 (10% v/v). (c–f) Flow cytometry analysis of (c, d) extracellular and (e, f) intracellular yeast cells (Calcofluor White high 2 h, 6 h, 12 h, and 24 h postinfection) from BMMs infected with H99 (10:1), with or without 1 kDa CM35 (10% v/v). (g) Scheme for transwell infection assay, illustrating the steps taken during the assay. (h, i) Flow cytometry measurement (24 h postinfection) of intracellular yeast cells in BMMs infected with H99 (2:1), in the upper chamber of a transwell apparatus. In the lower chambers, BMMs were stimulated with LPS (500 ng/ml) and B3501 or $\Delta cap67$ (5:1) (g). Alternatively, only yeast cells from B3501 or $\Delta cap67$ in a media with LPS (500 ng/ml) were included in the lower chambers (h). Statistical analysis was performed utilizing one-way ANOVA, where ns: not significant; * $P \leq 0.033$; ** $P \leq 0.002$; *** $P \leq 0.001$. Comparisons were made with the B3501 lower chamber infected group (g).

of different activators. To investigate the molecular identity of the component affecting the inflammasome, we further fractionated our media using ultrafiltration devices with nominal molecular weight cutoffs. From CM35, all these molecular weights separated inhibited IL-1 β secretion with the exception of the fraction where the high molecular weight components were removed (>10 kDa) (Figure 2(d)), indicating that molecules below the 1 kDa range are responsible for inhibition of inflammasome. Since the strongest effect was achieved with the fractions below 1 kDa, the next assays were conducted utilizing this small size fraction (<1 kDa CM35), unless stated otherwise.

3.3. <1 kDa CM35 Inhibits Caspase-1 Activation, Promoting pro-IL-1 β Accumulation and Cell Death Inhibition. Canonical inflammasome activation triggers various processes in the cell, including, but not limited to, IL-1 β maturation and secretion. In that context, we analyzed other cell processes related to inflammasome activation, such as intracellular pro-IL-1 β cleavage and cellular lysis due to caspase-1-mediated pyroptosis. When macrophages were treated with <1 kDa CM35, LDH release was largely abrogated, while treatment with <1 kDa CMCAP or MM resulted in a smaller inhibition of macrophage cell death (Figure 3(a)), which again is likely partly explained by the presence of glycine in the media [69]. <1 kDa CM35 inhibited cell death (as measured by LDH release) following the same pattern seen for IL-1 β secretion (Figure 3(a)). Regarding pro-IL-1 β , the results showed that macrophages must be primed with LPS for this cytokine production and that the presence of nigericin does not alter its intracellular levels, indicating LPS-dependent production of the inactive IL-1 β (Figure 3(b)). When treated with <1 kDa CM35, primed macrophages exhibited an increase in intracellular pro-IL-1 β protein, while cells treated with MM did not (Figure 3(b)). Surpris-

ingly, treatment with <1 kDa CMCAP also induced a high accumulation of intracellular pro-IL-1 β (Figure 3(b)). The pro-IL-1 β production might be explained by the fact that <1 kDa CMCAP was the only treatment able to induce pro-IL-1 β production without LPS. Both conditioned media increased IL-1 β (i.e., pro-IL-1 β) transcription levels in primed macrophages, while not similarly inducing *nfkB* transcription, even after 24 h after LPS stimuli (S2 Fig). <1 kDa CMCAP alone was also able to induce TNF- α secretion by unprimed macrophages (S1F Fig), corroborating the assumption that this conditioned media can induce first signaling via NF- κ B activation.

Having confirmed that <1 kDa CM35 inhibited various signals related to inflammasome activation, the next step was to observe inflammasome activation itself, analyzing the last step in the multiprotein complex assembly: the autocleavage of procaspase-1 into the caspase-1 active form via flow cytometry (Figures 3(c)–3(f)). Results showed that primed macrophages treated with <1 kDa CM35 decreased the caspase-1 active form, compared to untreated cells or cells treated with MM. Moreover, this was independent of nigericin (Figures 3(c) and 3(d)) or infection with *C. neoformans* strains (Figures 3(e) and 3(f)). These results are consistent with the finding that <1 kDa CM35 inhibits IL-1 β secretion, showing that <1 kDa CM35 can inhibit inflammasome activation induced via different stimuli (i.e., nigericin and infection with $\Delta cap67$). Altogether, these results indicate that <1 kDa CM35 decreased inflammasome activation, including pyroptotic cell death, pro-IL-1 β cleavage, the later stages of caspase-1 activation, and consequently IL-1 β secretion.

3.4. <1 kDa CM35 Impacts Phagocytic Capacity and Vomocytosis Events in Interactions between Macrophages and *C. neoformans*. Macrophages are critical for defense

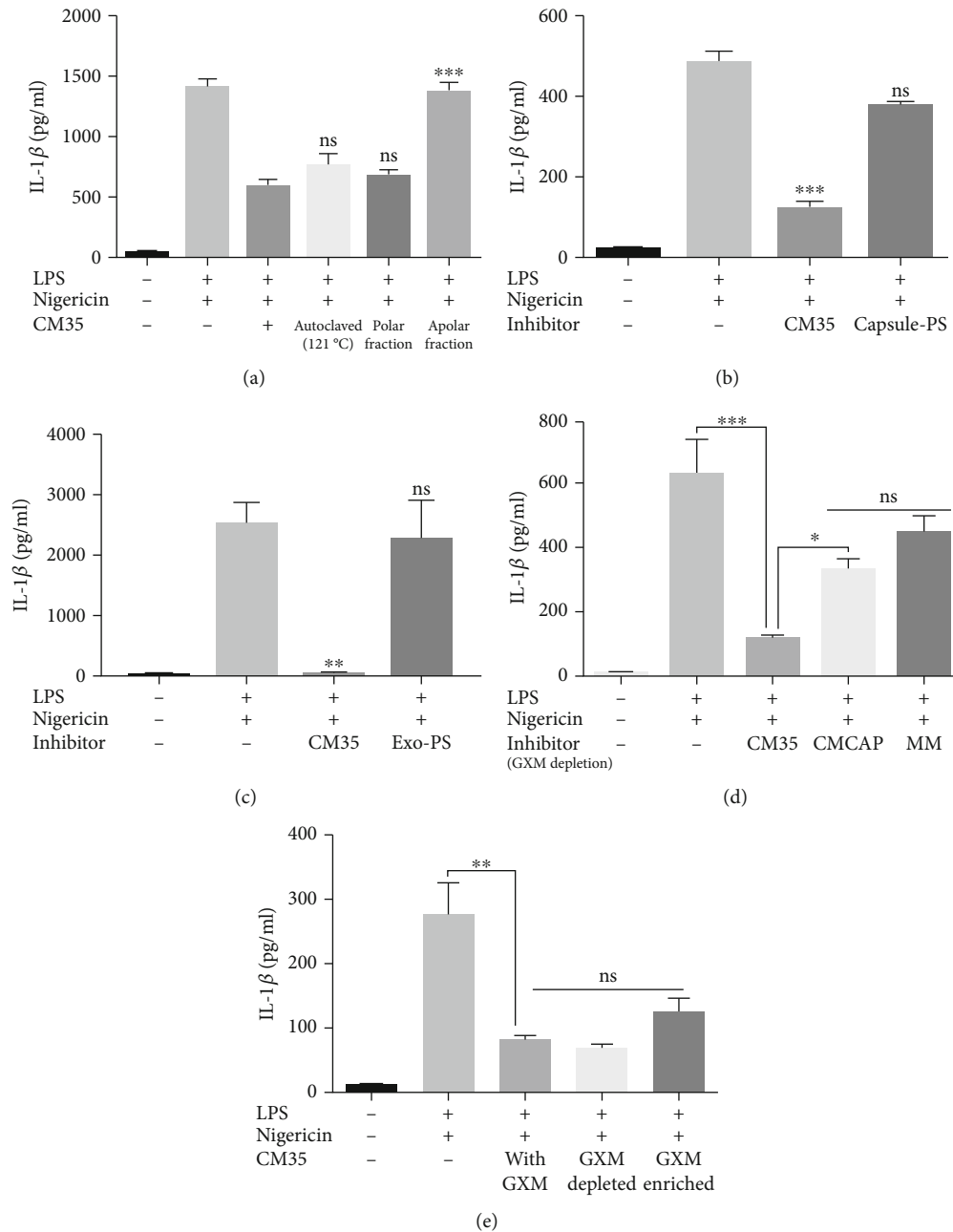


FIGURE 5: 1 kDa CM35 inhibition characteristics indicate a small, polar molecule that does not derive from a polysaccharide origin. (a) BMMs were stimulated with LPS (500 ng/ml) and nigericin (20 μ M), with or without 1 kDa CM35 fractioned by water affinity or autoclaved (10% v/v) overnight (18 h). (b, c) BMMs were stimulated with LPS (500 ng/ml) and nigericin (20 μ M), with or without potential inhibitor (10% v/v) overnight (18 h). Polysaccharides (200ug/mL) extracted from the (c) capsule or secreted in (d) minimal medium were used as inhibitors. (d, e) BMMs were stimulated with LPS (500 ng/ml) and/or nigericin (20 μ M), with or without possible inhibitor (10% v/v) overnight (18 h). Conditioned medium and minimal media (1 kDa CM35, 1 kDa CMCAP, and MM) were treated for GXM depletion utilizing capture ELISA and used as inhibitors (10% v/v) (e). GXM recovered from ELISA was mixed with 1 kDa CM35 and utilized as an inhibitor (10% v/v) (f). Supernatants were recovered after stimuli and IL-1 β secretion was quantified using ELISA. Statistical analysis was performed by one-way ANOVA, where ns: not significant; * $P \leq 0.033$; ** $P \leq 0.002$; *** $P \leq 0.001$. Comparisons were made with the (a) 1 kDa CM35-treated group or the (b, c) positive control group (LPS+nigericin).

against cryptococcosis [70]. We analyzed if >1 kDa CM35 treatment caused a functional impairment of macrophages when infected with *C. neoformans* strain H99. We initially evaluated intracellular fungal burdens in macrophages when yeast cells were added simultaneously with <1 kDa CM35 or minimal media. Interestingly, none of the treat-

ments impacted fungal intracellular growth in primed macrophages (Figure 4(a)). However, when macrophages were primed for 18 h with the conditioned medium, <1 kDa CM35 before infection, we observed a significant reduction in the phagocytic capacity of macrophages (Figure 4(b)).

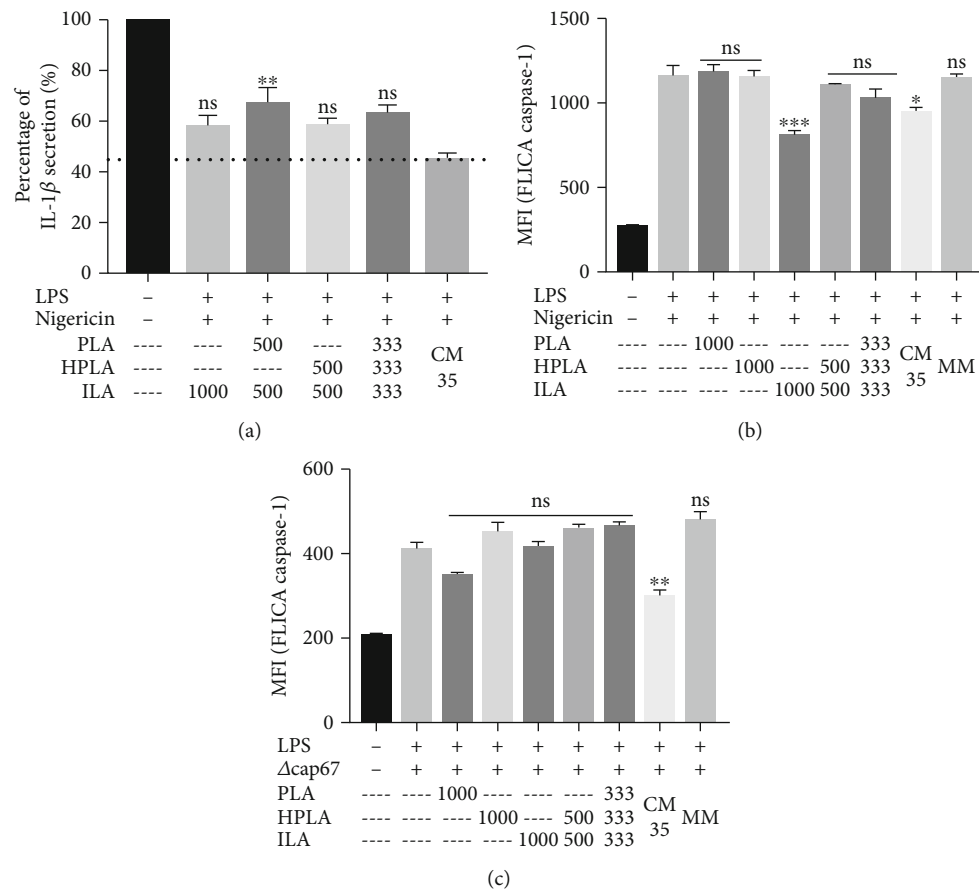


FIGURE 6: ILA is partly responsible for the inhibitory activity of 1 kDa CM35. (a, b) Percentage of cytokine secretion, measured by IL-1 β (a) release by BMMS stimulated with LPS+nigericin and the addition of possible inflammasome inhibitors (CM35, PLA, HPLA, and ILA). Positive group LPS+nigericin was normalized for a 100% cytokine secretion. The numbers below the bars represent the concentration of the respective metabolite in μ M, except for 1 kDa CM35 and MM (10% v/v). The graph shows the metabolites alone, followed by double combinations and a triple combination of all metabolites. The bars represent three independent assays. (b, c) BMMS stimulated with LPS (500 ng/ml) and nigericin (20 μ M) or Δ cap67 (MOI 5:1), with or without inhibitors, were analyzed for caspase-1 activation (FLICA). 1 kDa CM35=conditioned media from *C. neoformans* B3501; MM=minimal media; PLA=DL-3-Phenyllactic acid; HPLA=DL-p-Hydroxyphenyllactic acid; ILA=DL-Indole-3-lactic acid. Statistical analysis was made utilizing one-way ANOVA, where ns: not significant; * $P \leq 0.033$; ** $P \leq 0.002$; *** $P \leq 0.001$. Comparisons were made with 1 kDa CM35 group. ns means that the inhibition level achieved by the metabolites is similar to the inhibition achieved by 1 kDa CM35 (a, b). Comparisons were made with the positive control (LPS+nigericin or LPS+ Δ cap67) (c, d).

Another important aspect of macrophage-*Cryptococcus* interaction is vomocytosis. We analyzed vomocytosis in the presence of 1 kDa CM35. Macrophages were concomitantly exposed to <1 kDa CM35, infected with H99 strain and treated with fluconazole, an antifungal drug used for extracellular growth control [29, 71]. We stained H99 cells with Uvitex and allowed macrophages to ingest. If vomocytosis occurs then that would originate highly fluorescent cells in the extracellular space as demonstrated previously. Yeast cells with lower fluorescence were considered to be derived from extracellular growth (daughter cells). We observed that macrophages treated with 1 kDa CM35 had a higher percentage of extracellular parent cells compared to untreated macrophages (Figures 4(c) and 4(d)). The difference between groups starts to increase at 12 h of infection ($P > 0.001$), increasing once again after 24 h while simultaneously intracellular parent yeast cells number showed an inverse pattern,

reducing after 12 h of infection in the groups treated with <1 kDa CM35 (Figures 4(e) and 4(f)). Knowing that macrophages treated with 1 kDa CM35 present an equal rate of cell death when compared to untreated cells (Figure 3(a)), the increase of extracellular cells observed in this assay likely indicates an increase in vomocytosis rate in the presence of <1 kDa CM35.

To further study the impact of secreted molecules by *C. neoformans* strains, in macrophage function, a transwell assay involving two sequential infections in different chambers physically separated was carried out (Figure 4(g)). After 24 h, all yeast cells recovered from the upper chamber exhibited high GFP fluorescence, indicating no crossing from yeast cells present in the lower chamber. H99 cells expressing GFP were used for the infection of the macrophages in the upper chamber, while nonfluorescent B3501 or Δ cap67 was used for infection in the lower chamber. A

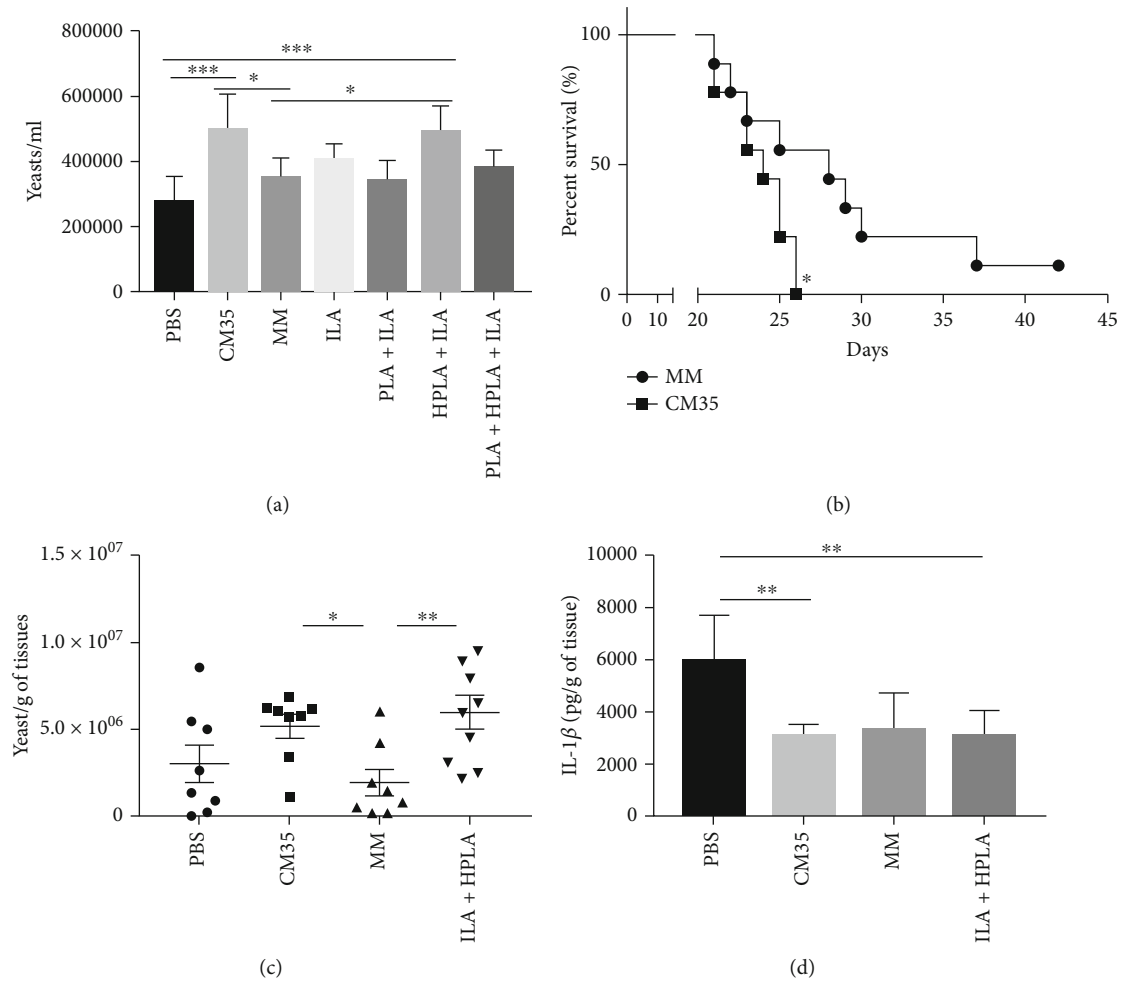


FIGURE 7: ILA and HPLA increased fungal survival in *Acanthamoeba castellanii* and mice experimentally infected. Intracellular growth (CFU of 3 h vs. 24 h postinfection) inside *A. castellanii* was measured by CFU after treatment with 1 kDa CM35, MM, and ILA associated or not with PLA and HPLA. (b) The survival curve of C57Bl/6 infected with 1×10^4 H99 strain treated with 1 kDa CM35 or MM during each 5 days intranasally. (c) The lung fungal burden from C57Bl/e infected with 1×10^4 H99 strain treated with 1 kDa CM35, MM, or ILA+HPLA each 5 days intranasal repeated after 15 days postinfection. (d) IL-1 β release in lung tissue after 15 days postinfection from C57Bl/e infected with 1×10^4 H99 strain treated with 1 kDa CM35, MM, or ILA+HPLA each 5 days intranasal repeated. 1 kDa CM35 = conditioned media from *C. neoformans* B3501; MM = minimal media; PLA = DL-3-Phenyllactic acid; HPLA = DL-p-Hydroxyphenyllactic acid; ILA = DL-Indole-3-lactic acid. Statistical analysis was made utilizing one-way ANOVA, where ns: not significant; * $P \leq 0.033$; ** $P \leq 0.002$; *** $P \leq 0.001$. Comparisons were made with the PBS group (a, b). Comparisons were made with the (c) MM or (d) PBS group.

significantly higher intracellular fungal burden was observed in macrophages infected with H99 strain in a chamber vertically adjacent to the bottom chamber containing macrophages infected with B3501 strain compared to fungal burden when the adjacent chamber contained macrophages alone or macrophages infected with $\Delta cap67$ strain or uninfected macrophages (Figure 4(h)). Interestingly, the increase in fungal burden derived by B3501 was not observed when only yeast cells were seeded in the bottom chambers, i.e., the factor produced by B3501 strain is only produced in a stressed milieu, as in the presence of macrophages (Figure 4(i)).

Overall, these experiments indicate that <1 kDa CM35 secreted by B3501 alters macrophage function such that macrophage antifungal activity is affected, potentially by secreting molecules that inhibit a proinflammatory environment.

3.5. <1 kDa CM35 Inhibition Characteristics Indicate That a Small, Polar, and Nonpolysaccharide Molecule Is Responsible for the Effects. To further characterize the conditioned medium, <1 kDa CM35 was submitted to autoclaving and separated into polar and nonpolar soluble fractions. Autoclaved and polar fraction of CM35 retained its inhibitory properties (Figure 5(a)). Crude <1 kDa CM35 was also treated with various proteases before its addition to primed macrophages. None of the treatments eliminated the inhibition promoted by the conditioned media, and the proteases themselves also did not significantly alter IL-1 β secretion (data not shown). Overall, the analysis showed that a small, polar, and heat and protease-resistant molecule (or molecules) resulted in the <1 kDa CM35 inhibitory properties.

GXM is a known virulence factor that matches the characteristics possessed by our candidate molecule. While

generally depicted as a high molecular weight polysaccharide, this polymer can also exist as lower molecular weight species [72]. We decided to investigate the role of GXM and GXM-derived molecules when interacting with activated macrophages and in the context of <1 kDa CM35 treatment, i.e., if we could detect these molecules in macrophages treated with CM35 below 1 kDa size fraction, but not if treated with <1 kDa CMCAP (S3 Fig). Firstly, polysaccharides derived from the yeast capsule (Figure 5(b)) or exopolysaccharides obtained from the culture media (Figure 5(c)) were used to treat macrophages primed with LPS and nigericin. None of these treatments were able to significantly reduce IL-1 β secretion compared to <1 kDa CM35, suggesting that GXM is not enough to promote inflammasome inhibition.

Similarly, depleting GXM from <1 kDa CM35 using mAb 18B7 capture protocol [59] did not alter IL-1 β secretion by activated macrophages (Figure 5(d)). Supporting the hypothesis that GXM is not the candidate molecule, the recovery of GXM from the coated ELISA plate and enrichment of its content in the <1 kDa CM35 did not significantly affect IL-1 β secretion (Figure 5(e)). Although GXM may be isolated together with our candidate molecule, these assays indicate that GXM does not affect inflammasome inhibition seen in our model.

3.6. DL-p-Hydroxyphenyllactic Acid (HPLA) and DL-Indole-3-Lactic Acid (ILA) Participate in Inflammasome Inhibition Property Possessed by <1 kDa CM35. Given that GXM did not interfere in our inflammasome activation model, we pursued the identification of our active candidate molecule by analyzing <1 kDa CM35 and <1 kDa CMCAP using mass spectrometry. Three candidates met our criteria of being enriched in CM35 vs. CMCAP, small, polar, and heat and protease-resistant molecules: DL-3-Phenyllactic acid (PLA), DL-p-Hydroxyphenyllactic acid (HPLA), and DL-Indole-3-lactic acid (ILA) (S4 Fig). All three are aromatic metabolites derived from amino acid metabolism and are produced by several species of prokaryotes and eukaryotes [73, 74]. Testing these three metabolites separately revealed that ILA, alone or with HPLA, mimicked the activity of >1 kDa CM35 (Figure 6(a)), and ILA alone or associated with HPLA inhibited IL1 β secretion and did not affect TNF- α secretion (Figure 6(a)). Notably, ILA alone reduced caspase-1 activation to levels similar to that achieved with <1 kDa CM35 (Figure 6(b)). Interestingly, ILA did not reduce caspase-1 activation when macrophages were activated with $\Delta cap67$ infection instead of nigericin (Figure 6(c)). This result suggests that ILA may participate in <1 kDa CM35 inhibition properties, but that it is not the single molecule responsible for this capacity. Hence, it is possible that <1 kDa CM35 inhibitory properties are due to a combination of molecules. At this point, we identify ILA and HPLA as immunomodulatory metabolites produced by *C. neoformans*.

3.7. Conditioned Media Also Promotes Survival of *C. neoformans* in *Acanthamoeba castellanii* and Mouse Infection. To evaluate the properties of <1 kDa CM35 in promoting *C. neoformans* survival during infection in other organisms, *A. castellanii* were infected with H99 strain of *C.*

neoformans and treated or not with <1 kDa CM35 or aromatic metabolites. The quantification of CFU was performed 24 h postinfection and showed a significantly higher fungal load inside amoebas in the groups treated with <1 kDa CM35 and ILA combined with HPLA, compared to the other groups (Figure 7(a)), indicating that both ILA+HPLA and <1 kDa CM35 enhance fungal survival inside *A. castellanii*. To evaluate if <1 kDa CM35 was effectively favoring *C. neoformans* survival and increasing infection in a more complex host, we treated or not infected mice with <1 kDa CM35 or MM, each 5 days, and analyzed their survival for 45 days (Figure 7(b)). Mice treated with MM survived longer than mice treated with <1 kDa CM35, showing that active metabolites in <1 kDa CM35 enhance infection. Furthermore, when infected C57BL/6 mice were treated with <1 kDa CM35 or ILA plus HPLA at two and seven days postinfection, the fungal load was significantly higher in the lungs of mice treated with <1 kDa CM35 or ILA+HPLA (Figure 7(c)) compared to the lungs of mice treated with PBS or MM at 14 days of infection. Contributing to this result, we found significantly lower levels of IL-1 β in the lungs of mice treated with <1 kDa CM35 or ILA+HPLA, but not with MM (Figure 7(d)).

4. Discussion

The processes by which fungi manipulate the mammalian immune systems and in particular their interaction with inflammasome pathways remain unknown. Although the significant receptors involved and most of the stress signals required for inflammasome activation are known, the mechanisms by which fungal pathogens modulate and/or evade these responses are still poorly understood, when compared to its bacterial counterparts. Here, we demonstrate that molecules secreted by *C. neoformans* can specifically inhibit the canonical activation of the inflammasome pathway and dampen macrophage anticryptococcal activity and mouse immune response, potentiating fungal survival and growth during the host-pathogen interaction. Furthermore, we determined that GXM did not participate in this process, and we identified one molecule partially responsible for the effect promoted by the fungal conditioned media.

Inflammasome activation is associated with a proinflammatory response, mainly due to its IL-1 β and IL-18 processing properties. Both are critical cytokines for macrophage activation as well as in the development of Th17 and Th1 polarization, respectively [44]. Therefore, inflammasome activation critically affects Th1/Th17 polarization which is widely reported as a protective response against pathogenic fungi. NLRP3 defects are therefore associated with a poor prognosis upon fungal infection, ranging from severe susceptibility in invasive candidiasis [46] to milder susceptibility to cryptococcosis [52]. On the other hand, NLRP3 defects have also been associated with a better prognosis in aspergillosis associated with cystic fibrosis [75], and these defects had no impact in chromoblastomycosis [50]. Hence, inflammasome activation has different effects depending on the fungal pathogen and the associated pathologies of the host.

As the canonical inflammasome scaffold involves various proteins and downstream signaling, numerous steps can be inhibited to prevent scaffold formation, thus preventing the cascade at several steps with different consequences to the cell activation. A single point of interference is sufficient to disrupt the entirety of downstream signaling and inflammasome function, from receptor activation to caspase autolysis [76]. Inflammasome activation can also be partially prevented by the use of cytoprotective agents like glycine [69]. Our study demonstrated that conditioned media from *C. neoformans* strain B3501 promoted robust inhibition of IL-1 β secretion and complete inhibition of LDH release, although it had less of an impact on caspase-1 activation. IL-1 β can be secreted by various mechanisms, depending on the cell status, for example, through membrane pores formed by Gasdermin D or through cell membrane defects during pyroptosis [77]. In this model, glycine was not able to prevent pore formation in immortalized macrophages, consequently preventing LDH release but not cytokine secretion. Studies also depicted that dying macrophages undergoing pyroptosis were the primary source of IL-1 β secretion in an *in vitro* model, with peritoneal macrophages exhibiting caspase-1 activation and a cytokine burst that coincided with the moment of cell death. Interestingly, caspase-1 activation inhibition prevented IL-1 β secretion, but it did not alter cell death events [78, 79]. Taken together, these findings show that both events can occur independently, even if they are mostly caspase-1 dependent and depend on the inflammasome stimuli, cell type, and inhibition scheme utilized.

In our model, glycine and MM containing glycine dampened IL-1 β and LDH release if nigericin was used as stimuli when interacting with the cells for an extended period before inflammasome activation, but not when inflammasome activation was promoted by $\Delta cap67$ infection [69]. Another interesting feature presented in our inflammasome inhibition model was the accumulation of pro-IL-1 β intracellularly in cells treated with CM35. It is well characterized that neither caspase-1 activation nor inhibition has any impact on pro-IL-1 β intracellular levels in activated cells, indicating that IL-1 β translation is stable regardless of whether it is subsequently cleaved [80]. One explanation for this stability of intracellular levels during caspase-1 inhibition is that pro-IL-1 β , along with other inflammasome unrelated proteins, are present in the supernatant of necrotic cells undergoing NLRP3 activation [79]. On the other hand, changes in the intracellular cytokine reservoir can impact the secretion of its mature form [81]. In our work, an increase in pro-IL-1 β intracellular levels occurred concomitantly with a decrease in IL-1 β mature form release, which is not fully explained by the inhibition seen in caspase-1 activation. One aspect of our model is that pyroptosis is prevented in the presence of CM35, suggesting that intracellular proteins are retained during NLRP3 activation in this group. Furthermore, transcripts of IL-1 β were highly expressed in the cells treated with CM35. Regarding inflammasome inhibition and pro-IL-1 β , Folco et al. demonstrated that macrophages primed with LPS and treated with bafilomycin, a known inhibitor of the NLRP3-dependent receptor activation, exhibited increased intracellular levels of this cytokine [82].

The first studies depicting inflammasome activation by fungi demonstrated that morphogenesis is important to promote NLRP3 inflammasome activation; hence, some morphotypes of a pathogen can induce a more robust response than others [48, 83]. *C. neoformans* is also known to be a weak inflammasome activator. In this context, GXM has been considered the main factor for the yeast to evade inflammasome activation, promoting the evasion of phagocytosis and prevention of recognition by extracellular receptors [52–54].

The only well-described direct modulation of the inflammasome pathway to date with a focus on fungicidal activity has been with *C. albicans* internalized hyphae in which the secretion of a candidalysin leads to cell piercing, NLRP3 inflammasome activation, and host cell death via pyroptosis [84–87]. Despite the lack of further published evidence for fungal inhibition of inflammasome activation, many other intracellular pathogens, like bacteria and viruses, have well-described mechanisms for NLRP3 suppression. The human pathogenic bacteria of the genus *Yersinia* express a conserved type III secretion system (T3SS) as a virulence trait, which is associated with inflammasome activation. This secretion system is responsible for the release of effector proteins called *Yersinia* outer proteins (Yops), and two Yops can inhibit inflammasome activation: YopK is related to prevention of T3SS recognition by NLR receptors [88], and YopM is related to blockage of pyrin inflammasome activation [89]. Defects in both effector proteins lead to more robust inflammasome activation and bacterial clearance, highlighting the importance of the inhibition promoted by the pathogen. Poxviruses produce proteins homologous to mammalian proteins responsible for inflammasome inhibition, known as pyrin domain-only proteins (POP) and serpins. These viral proteins bind to ASC or caspase domains, preventing proper inflammasome assembly and activity from promoting the intracellular survival of the poxvirus [90]. Therefore, it is not surprising to demonstrate that *C. neoformans*-derived molecules can specifically inhibit inflammasome activity, and it is feasible to hypothesize that other fungal-driven mechanisms for inflammasome inhibition will be discovered soon.

While most studies have shown that IL-18 is important during cryptococcosis, IL-1 β itself is sometimes depicted as unnecessary for host protection [55]. However, a recent study has shown that IL-1R signaling is essential for a Th1/Th17 polarization in a chronic infection model, consequently facilitating fungal clearance by the host [56]. These data corroborate the importance of the NLRP3 components during cryptococcosis [52]. We demonstrate that macrophages treated with CM35 had a reduced capacity to control *C. neoformans*; the secretion of inflammasome-related cytokines is usually accompanied by cell death via pyroptosis. This cellular lysis releases a high content of proinflammatory IL-1 family cytokines, therefore activating neighboring cells thus promoting the maintenance of a proinflammatory environment [78]. Overall, inflammasome activation is related to a more effective response against *C. neoformans*, eliciting polarization towards Th1 and promoting antimicrobial macrophage activation; consequently, inhibition of this pathway

reduces the responsiveness of the macrophages against the fungus.

The mechanisms and causes of vomocytosis are still poorly understood, but it is accepted that macrophages undergo vomocytosis because they cannot control their intracellular fungal burden [77]. Therefore, macrophages release the fungus to the extracellular environment instead of permitting themselves to serve as a protected niche for cryptococcal replication. Extracellular yeasts are less capable of evading the immune killing, and therefore, vomocytosis should lead to milder disease and is considered relatively protective [91]. Alanio and colleagues demonstrated that the outcome of human patients was highly correlated with the intracellular growth rate of virulent strains of *C. neoformans* [64], supporting this vomocytosis immune evasion hypothesis. Our results indicate that macrophages treated with CM35 have a higher rate of vomocytosis events, suggesting that the inhibition in the inflammatory response and pyroptosis promoted by the conditioned media might also enhance vomocytosis as an alternative mechanism to expel fungal burden to mitigate against host cell death.

ILA is an aromatic metabolite derived from the tryptophan pathway. It is produced by a wide variety of organisms and microorganisms, ranging from soil bacteria to humans [73, 74]. ILA production in fungi is mostly commonly seen in endophytic and phytopathogenic species and necessary for plant tissue colonization [92]. The tryptophan degradation pathway that leads to ILA production has an intermediate product denominated indolepyruvate, which is transformed in ILA as a result of a reduction-oxidation reaction by the NADPH-dependent enzyme indole-3-lactate dehydrogenase. Although this pathway and responsible enzymes have not yet been fully annotated in *C. neoformans* or *C. albicans*, the presence of ILA has been observed in conditioned media from both pathogenic yeasts [93]. Zelante et al. correlated the production of tryptophan catabolites by mouse gut microbiota, among them ILA, with mucosal protection from inflammation and resistance in a candidiasis infection model, which is mediated via IL-22 production [94].

In recent years, various enzymes and proteins related to biosynthesis metabolic pathways have been depicted as important for pathogenesis in cryptococcosis infection models, especially those associated with glucose metabolism. Defects in pyruvate and hexose kinases and in acetyl-CoA production impact virulence traits of the yeast, resulting in a reduction in host mortality [95, 96]. Nevertheless, our knowledge regarding aromatic metabolites derived from amino acid metabolism secreted by *C. neoformans* and their impact on the host during infection is severely limited. Notably, amino acid permeases are essential for the protection of the yeast when challenged by environmental or host-promoted stress conditions. *C. neoformans* mutants with a defect in these enzymes are less virulence, highlighting the importance of amino acid uptake during infection [97]. Yeast cells deficient in a small protein allegedly involved in the citric acid cycle had a higher expression of amino acids (i.e., tryptophan), and the mutant cells were more lethal in mice compared to wild-type yeast cells [98]. Another interesting

aspect of this study was the demonstration that the intracellular fungal burden in macrophages infected with the mutant was only higher in the presence of exogenous NADPH, a cofactor that is essential to produce ILA from indol-3-pyruvate [86].

Although there is no report correlating aromatic metabolites and inflammasome inhibition, some small molecules with structures similar to aromatic metabolites are known to inhibit inflammasome. Glyburide is one of the most well-described inhibitors for NLRP3 activation, acting on ATP-sensitive potassium channels to block potassium efflux, which prevents inflammasome activation. Glyburide is a sulfonylurea drug with aromatic hydrocarbons in its structure [99]. Interestingly, not all sulfonylurea drugs are able to prevent IL-1 β secretion via inflammasome inhibition, and there are reports of sulfonylurea drugs that prevent inflammasome activation by mechanisms other than potassium efflux blockage [100] which we hypothesize may be similar to the effects of ILA.

5. Conclusions

This work identifies new effects mediated by *C. neoformans* wild-type secreted molecules, especially in the ability to modify the activation of the intracellular inflammasome pathway. Treating macrophages with conditioned media reduced such critical functions such as phagocytosis and intracellular killing in *in vitro* infection models, suggesting a possible new mechanism for fungal persistence inside the host. We also found that the aromatic metabolite ILA mimics the inhibitory properties of CM35. Future studies regarding ILA and CM35 effects in fungal infection are essential to determine the detailed mechanism of action, to define where along the signaling pathway that the inflammasome is being affected and identifying other molecules that participate in inflammasome inhibition. An in-depth analysis of how these molecules impact cryptococcal infection would significantly enhance our understanding of cryptococcosis and perhaps lead to new strategies to prevent and treat *C. neoformans* disease.

Abbreviations

ASC:	Apoptosis-associated speck-like protein containing a CARD
BMDC:	Bone marrow-derived dendritic cells with GM-CSF stimulus
BMDM:	Bone marrow-derived macrophages with GM-CSF stimulus
BMM:	Bone marrow-derived macrophages with M-CSF stimulus
CFU:	Colony forming units
CM35:	Conditioned media obtained from B3501 culture
CMCAP:	Conditioned media obtained from $\Delta cap67$ culture
ELISA:	Enzyme-linked immunosorbent assay
GM-CSF:	Granulocyte-macrophage colony-stimulating factor
GXM:	Glucuronoxylomannan
HPLA:	DL-p-Hydroxyphenyllactic acid
IL-18:	Interleukin 18

IL-1 β :	Interleukin 1 beta
ILA:	DL-Indole-3-lactic acid
kDa:	Kilodalton
LDH:	Lactate dehydrogenase
LPS:	Lipopolysaccharide
mAb:	Monoclonal antibody
M-CSF:	Macrophage colony-stimulating factor
MM:	Minimal media
NLRP3:	NLR pyrin domain-containing 3
PBS:	Phosphate-buffered saline
PLA:	3-Phenyllactic acid
PS:	Polysaccharide
TNF- α :	Tumor necrosis factor alpha.

Data Availability

The data used to support the findings of this study are available from the corresponding author upon request.

Conflicts of Interest

The authors declare that there is no conflict of interest regarding the publication of this paper.

Authors' Contributions

A.H.T. and A.L.B. share senior authorship of this article.

Acknowledgments

We thank Guillaume E. Desanti (University of Birmingham) for technical assistance. We thank Julie M. Wolf (Albert Einstein College of Medicine) for providing capsule polysaccharides. We thank Dario Zamboni (University of São Paulo) and Kelly Magalhães (University of Brasília) for initial discussions. This study was financially supported by the Conselho Nacional de Desenvolvimento Científico e Tecnológico (CNPq) (470059/2014-1) and the Coordenação de Aperfeiçoamento de Pessoal de Nível Superior (CAPES) (005/2012). "RCM is supported by the European Research Council under the European Union's Seventh Framework Programme (FP/2007-2013)/ERC Grant Agreement No. 614562 Wolfson Royal Society Research Merit Award."

Supplementary Materials

S1 Fig: CM35, but not CMCAP or minimal media, is able to reduce IL-1 β secretion. Secretion of IL-1 β was measured from BMDMs stimulated with LPS (500 ng/ml) and nigericin (20 μ M), with or without possible inhibitor (10% v/v) overnight (18 h) (A). Secretion of TNF- α was measured from BMDMs (B), BMMs (C), and DCs (D) stimulated with LPS (500 ng/ml) and nigericin (20 μ M), with or without possible inhibitor (10% v/v) overnight (18 h). Alternatively, BMDMs were treated with possible inhibitors overnight (18 h) previously to stimulation with LPS (500 ng/ml) for 4 h (E). TNF- α release measured from supernatants of BMMs stimulated with nigericin (20 μ M), with or without CMCAP (F). Secretion of IL-1 β (G) or TNF- α (H) was measured from BMMs stimulated with LPS (500 ng/ml) and nigericin (20 μ M), with

or without possible inhibitor (10% v/v) overnight (18 h). Supernatants were collected after stimulus and cytokines measured by ELISA technique. CM35 = conditioned media from B3501; CMCAP = conditioned media from $\Delta cap67$; MM = minimal media; CM99 = conditioned media from H99. Statistical analysis was performed utilizing one-way ANOVA, where ns: not significant; * $P \leq 0.033$; *** $P \leq 0.001$. S2 Fig: CMs induce IL-1 β transcription in activated macrophages. Transcript levels of IL-1 β (A) and Nf- κ B (B) from cDNA extracted from BMMs stimulated with LPS (500 ng/ml) and/or nigericin (20 μ M), with or without potential inhibitor (10% v/v) overnight (18 h). IL-1 β or Nf- κ B to GAPDH relative expression was calculated using the $2^{(-ct)}$ method and normalized to the level of unstimulated BMMs. Statistical analysis was achieved by one-way ANOVA, where ns: not significant; * $P \leq 0.033$; *** $P \leq 0.001$. Comparisons were made with the LPS+nigericin group. S3 Fig: GXM detection in CM samples. (A–C) BMMs interacting with inhibitors CM35 (A), CM35<1 kDa (B), and CMCAP (C). (D–F) BMMs interacting with CM35 inhibitor before GXM depletion treatment by capture ELISA (D), after treatment (E) and enriched with GXM eluted from the ELISA plate (F). Cells were stained for the nucleus (blue) and GXM (red). Images were taken in a confocal fluorescence microscope. S4 Fig: mass spectrometry comparative CM analysis. (A) Heat map based on extracted metabolite significant intensities from CM35 and CMCAP. (B–D) Comparative data from each aromatic metabolite detected in the analysis. (*Supplementary Materials*)

References

- [1] B. J. Park, K. A. Wannemuehler, B. J. Marston, N. Govender, P. G. Pappas, and T. M. Chiller, "Estimation of the current global burden of cryptococcal meningitis among persons living with HIV/AIDS," *AIDS*, vol. 23, no. 4, pp. 525–530, 2009.
- [2] R. Rajasingham, R. M. Smith, B. J. Park et al., "Global burden of disease of HIV-associated cryptococcal meningitis: an updated analysis," *The Lancet Infectious Diseases*, vol. 17, no. 8, pp. 873–881, 2017.
- [3] M. S. Lazera, M. A. S. Cavalcanti, A. T. Londero, L. Trilles, M. M. Nishikawa, and B. Wanke, "Possible primary ecological niche of *Cryptococcus neoformans*," *Medical Mycology*, vol. 38, no. 5, pp. 379–383, 2000.
- [4] D. T. Takahara, M. d. S. Lazera, B. Wanke et al., "First report on *Cryptococcus neoformans* in pigeon excreta from public and residential locations in the metropolitan area of Cuiabá, state of Mato Grosso, Brazil," *Revista do Instituto de Medicina Tropical de São Paulo*, vol. 55, no. 6, pp. 371–376, 2013.
- [5] X. Lin and J. Heitman, "The biology of the *Cryptococcus neoformans* species complex," *Annual Review of Microbiology*, vol. 60, no. 1, pp. 69–105, 2006.
- [6] X. Lin, "Cryptococcus neoformans: morphogenesis, infection, and evolution," *Infection, Genetics and Evolution*, vol. 9, no. 4, pp. 401–416, 2009.
- [7] T. Sorrell and D. Ellis, "Ecology of *Cryptococcus neoformans*," *Revista Iberoamericana de Micología*, vol. 14, no. 2, pp. 42–43, 1997.

- [8] A. Idnurm, Y.-S. Bahn, K. Nielsen, X. Lin, J. A. Fraser, and J. Heitman, "Deciphering the model pathogenic fungus *Cryptococcus neoformans*," *Nature Reviews. Microbiology*, vol. 3, no. 10, pp. 753–764, 2005.
- [9] T. Mitchell and J. Perfect, "Cryptococcosis in the era of AIDS—100 years after the discovery of *Cryptococcus neoformans*," *Clinical Microbiology Reviews*, vol. 8, no. 4, pp. 515–548, 1995.
- [10] F. Almeida, J. M. Wolf, and A. Casadevall, "Virulence-associated enzymes of *Cryptococcus neoformans*," *Eukaryotic Cell*, vol. 14, no. 12, pp. 1173–1185, 2016.
- [11] L. M. Taylor-Smith and R. C. May, "New weapons in the *Cryptococcus* infection toolkit," *Current Opinion in Microbiology*, vol. 34, pp. 67–74, 2016.
- [12] M. L. Rodrigues, E. S. Nakayasu, D. L. Oliveira et al., "Extracellular vesicles produced by *Cryptococcus neoformans* contain protein components associated with virulence," *Eukaryotic Cell*, vol. 7, no. 1, pp. 58–67, 2008.
- [13] D. L. Oliveira, C. G. Freire-de-Lima, J. D. Nosanchuk, A. Casadevall, M. L. Rodrigues, and L. Nimrichter, "Extracellular vesicles from *Cryptococcus neoformans* modulate macrophage functions," *Infection and Immunity*, vol. 78, no. 4, pp. 1601–1609, 2010.
- [14] P. R. Williamson, "Laccase and melanin in the pathogenesis of *Cryptococcus neoformans*," *Frontiers in Bioscience*, vol. 2, no. 5, pp. e99–107, 1997.
- [15] J. W. Kronstad, R. Attarian, B. Cadieux et al., "Expanding fungal pathogenesis: *Cryptococcus* breaks out of the opportunistic box," *Nature Reviews. Microbiology*, vol. 9, no. 3, pp. 193–203, 2011.
- [16] T. R. O'Meara and J. Alspaugh, "The *Cryptococcus neoformans* capsule: a sword and a shield," *Clinical Microbiology Reviews*, vol. 25, no. 3, pp. 387–408, 2012.
- [17] S. Frases, B. Pontes, L. Nimrichter, M. L. Rodrigues, N. B. Viana, and A. Casadevall, "The elastic properties of the *Cryptococcus neoformans* capsule," *Biophysical Journal*, vol. 97, no. 4, pp. 937–945, 2009.
- [18] O. Zaragoza, M. L. Rodrigues, M. De Jesus, S. Frases, E. Dadachova, and A. Casadevall, *The capsule of the fungal pathogen Cryptococcus neoformans*, vol. 68 Elsevier Inc, 1st edition, 2009.
- [19] T. Kozel and E. Gotschlich, "The capsule of *Cryptococcus neoformans* passively inhibits phagocytosis of the yeast by macrophages," *The Journal of Immunology*, vol. 129, pp. 1675–1680, 1982.
- [20] S. M. Levitz and D. J. DiBenedetto, "Paradoxical role of capsule in murine bronchoalveolar macrophage-mediated killing of *Cryptococcus neoformans*," *The Journal of Immunology*, vol. 142, no. 2, pp. 659–665, 1989.
- [21] A. Vecchiarelli, D. Pietrella, P. Lupo, F. Bistoni, D. C. Mcfadden, and A. Casadevall, "The polysaccharide capsule of *Cryptococcus neoformans* interferes with human dendritic cell maturation and activation solar strains of *Cryptococcus neoformans* to anti-differentiation, as documented by the enhance-maturation, indicating a new pathway by," *Journal of Leukocyte Biology*, vol. 74, no. 3, pp. 370–378, 2003.
- [22] C. Monari, E. Pericolini, G. Bistoni, A. Casadevall, T. R. Kozel, and A. Vecchiarelli, "*Cryptococcus neoformans* Capsular glucuronoxylomannan induces expression of Fas ligand in macrophages," *Journal of Immunology*, vol. 174, no. 6, pp. 3461–3468, 2005.
- [23] C. Monari, F. Bistoni, A. Casadevall et al., "Glucuronoxylomannan, a microbial compound, regulates expression of costimulatory molecules and production of cytokines in macrophages," *The Journal of Infectious Diseases*, vol. 191, no. 1, pp. 127–137, 2005.
- [24] C. Monari, F. Bistoni, and A. Vecchiarelli, "Glucuronoxylomannan exhibits potent immunosuppressive properties," *FEMS Yeast Research*, vol. 6, no. 4, pp. 537–542, 2006.
- [25] A. Vecchiarelli, C. Retini, D. Pietrella et al., "Downregulation by cryptococcal polysaccharide of tumor necrosis factor alpha and interleukin-1 beta secretion from human monocytes," *Infection and Immunity*, vol. 63, pp. 2919–2923, 1995.
- [26] A. Vecchiarelli, E. Pericolini, E. Gabrielli et al., "Elucidating the immunological function of the *Cryptococcus neoformans* capsule," *Future Microbiology*, vol. 8, no. 9, pp. 1107–1116, 2013.
- [27] M. Feldmesser, S. Tucker, and A. Casadevall, "Intracellular parasitism of macrophages by *Cryptococcus neoformans*," *Trends in Microbiology*, vol. 9, no. 6, pp. 273–278, 2001.
- [28] C. M. Leopold Wager, C. R. Hole, K. L. Wozniak, and F. L. Wormley, "*Cryptococcus* and phagocytes: complex interactions that influence disease outcome," *Frontiers in Microbiology*, vol. 7, 2016.
- [29] M. J. Davis, A. J. Eastman, Y. Qiu et al., "*Cryptococcus neoformans*-induced macrophage lysosome damage crucially contributes to fungal virulence," *Journal of Immunology*, vol. 194, no. 5, pp. 2219–2231, 2015.
- [30] K. Voelz and R. C. May, "Cryptococcal interactions with the host immune system," *Eukaryotic Cell*, vol. 9, no. 6, pp. 835–846, 2010.
- [31] S. M. Levitz, S. H. Nong, K. F. Seetoo, T. S. Harrison, R. A. Speizer, and E. R. Simons, "*Cryptococcus neoformans* resides in an acidic phagolysosome of human macrophages," *Infection and Immunity*, vol. 67, no. 2, pp. 885–890, 1999.
- [32] L. M. Smith, E. F. Dixon, and R. C. May, "The fungal pathogen *Cryptococcus neoformans* manipulates macrophage phagosome maturation," *Cellular Microbiology*, vol. 17, no. 5, pp. 702–713, 2015.
- [33] A. S. Gilbert, R. T. Wheeler, and R. C. May, "Fungal pathogens: survival and replication within macrophages," *Cold Spring Harbor Perspectives in Medicine*, vol. 5, no. 7, p. a019661, 2015.
- [34] T. B. Kechichian, J. Shea, and M. Del Poeta, "Depletion of alveolar macrophages decreases the dissemination of a glucosylceramide-deficient mutant of *Cryptococcus neoformans* in immunodeficient mice," *Infection and Immunity*, vol. 75, no. 10, pp. 4792–4798, 2007.
- [35] M. Alvarez and A. Casadevall, "Phagosome extrusion and host-cell survival after *Cryptococcus neoformans* phagocytosis by macrophages," *Current Biology*, vol. 16, no. 21, pp. 2161–2165, 2006.
- [36] H. Ma, J. E. Croudace, D. A. Lammas, and R. C. May, "Expulsion of live pathogenic yeast by macrophages," *Current Biology*, vol. 16, no. 21, pp. 2156–2160, 2006.
- [37] F. Real, P. T. V. Florentino, L. C. Reis et al., "Cell-to-cell transfer of *Leishmania amazonensis* amastigotes is mediated by immunomodulatory LAMP-rich parasitophorous extrusions," *Cellular Microbiology*, vol. 16, no. 10, pp. 1549–1564, 2014.
- [38] J. M. Bain, L. E. Lewis, B. Okai, J. Quinn, N. A. R. Gow, and L. P. Erwig, "Non-lytic expulsion/exocytosis of *Candida*

- albicans* from macrophages,” *Fungal Genetics and Biology*, vol. 49, no. 9, pp. 677–678, 2012.
- [39] T. Bergsbaken, S. L. Fink, and B. T. Cookson, “Pyroptosis: host cell death and inflammation,” *Nature Reviews. Microbiology*, vol. 7, no. 2, pp. 99–109, 2009.
- [40] T. Bergsbaken, S. L. Fink, A. B. den Hartigh, W. P. Loomis, and B. T. Cookson, “Coordinated host responses during pyroptosis: caspase-1-dependent lysosome exocytosis and inflammatory cytokine maturation,” *Journal of Immunology*, vol. 187, no. 5, pp. 2748–2754, 2011.
- [41] I. Jorgensen and E. A. Miao, “Pyroptotic cell death defends against intracellular pathogens,” *Immunological Reviews*, vol. 265, no. 1, pp. 130–142, 2015.
- [42] S. K. Vanaja, V. A. K. Rathinam, and K. A. Fitzgerald, “Mechanisms of inflammasome activation: recent advances and novel insights,” *Trends in Cell Biology*, vol. 25, no. 5, pp. 308–315, 2015.
- [43] F. Martinon, A. Mayor, and J. Tschopp, “The inflammasomes: guardians of the body,” *Annual Review of Immunology*, vol. 27, no. 1, pp. 229–265, 2009.
- [44] F. L. van de Veerdonk, L. A. B. Joosten, P. J. Shaw et al., “The inflammasome drives protective Th1 and Th17 cellular responses in disseminated candidiasis,” *European Journal of Immunology*, vol. 41, no. 8, pp. 2260–2268, 2011.
- [45] A. H. Tavares, P. H. Bürgel, and A. L. Bocca, “Turning up the heat: inflammasome activation by fungal pathogens,” *PLoS Pathogens*, vol. 11, no. 7, article e1004948, 2015.
- [46] O. Gross, H. Poeck, M. Bscheider et al., “Syk kinase signalling couples to the Nlrp3 inflammasome for anti-fungal host defence,” *Nature*, vol. 459, no. 7245, pp. 433–436, 2009.
- [47] A. G. Hise, J. Tomalka, S. Ganesan et al., “An essential role for the NLRP3 inflammasome in host defense against the human fungal pathogen *Candida albicans*,” *Cell Host & Microbe*, vol. 5, no. 5, pp. 487–497, 2009.
- [48] N. Saïd-Sadier, E. Padilla, G. Langsley, and D. M. Ojcius, “*Aspergillus fumigatus* stimulates the NLRP3 inflammasome through a pathway requiring ROS production and the Syk tyrosine kinase,” *PLoS One*, vol. 5, no. 4, article e10008, 2010.
- [49] A. H. Tavares, K. G. Magalhães, R. D. N. Almeida, R. Correa, P. H. Bürgel, and A. L. Bocca, “NLRP3 inflammasome activation by *Paracoccidioides brasiliensis*,” *PLoS Neglected Tropical Diseases*, vol. 7, no. 12, article e2595, 2013.
- [50] R. J. A. de Castro, I. M. Siqueira, M. S. Jerônimo et al., “The major chromoblastomycosis etiologic agent *Fonsecaea pedrosoi* activates the NLRP3 inflammasome,” *Frontiers in Immunology*, vol. 8, p. 8, 2017.
- [51] L. Mao, L. Zhang, H. Li et al., “Pathogenic fungus *Microsporium canis* activates the NLRP3 inflammasome,” *Infection and Immunity*, vol. 82, no. 2, pp. 882–892, 2014.
- [52] G. Lei, M. Chen, H. Li et al., “Biofilm from a clinical strain of *Cryptococcus neoformans* activates the NLRP3 inflammasome,” *Cell Research*, vol. 23, no. 7, pp. 965–968, 2013.
- [53] C. Guo, M. Chen, Z. Fa et al., “Acapsular *Cryptococcus neoformans* activates the NLRP3 inflammasome,” *Microbes and Infection*, vol. 16, no. 10, pp. 845–854, 2014.
- [54] M. Chen, Y. Xing, A. Lu et al., “Internalized *Cryptococcus neoformans* activates the canonical caspase-1 and the noncanonical caspase-8 inflammasomes,” *Journal of Immunology*, vol. 195, no. 10, pp. 4962–4972, 2015.
- [55] J. P. Wang, C. K. Lee, A. Akalin, R. W. Finberg, and S. M. Levitz, “Contributions of the MyD88-dependent receptors IL-18R, IL-1R, and TLR9 to host defenses following pulmonary challenge with *Cryptococcus neoformans*,” *PLoS One*, vol. 6, no. 10, article e26232, 2011.
- [56] M. Shourian, B. Ralph, I. Angers, D. C. Sheppard, and S. T. Qureshi, “Contribution of IL-1RI signaling to protection against *Cryptococcus neoformans* 52D in a mouse model of infection,” *Frontiers in Immunology*, vol. 8, p. 19, 2018.
- [57] S. Frases, B. Pontes, L. Nimrichter, N. B. Viana, M. L. Rodrigues, and A. Casadevall, “Capsule of *Cryptococcus neoformans* grows by enlargement of polysaccharide molecules,” *Proceedings of the National Academy of Sciences of the United States of America*, vol. 106, no. 4, pp. 1228–1233, 2009.
- [58] P. Albuquerque, A. M. Nicola, E. Nieves et al., “Quorum sensing-mediated, cell density-dependent regulation of growth and virulence in *Cryptococcus neoformans*,” *MBio*, vol. 5, no. 1, article e00986, 2013.
- [59] M. L. Rodrigues, L. Nimrichter, D. L. Oliveira et al., “Vesicular polysaccharide export in *Cryptococcus neoformans* is a eukaryotic solution to the problem of fungal trans-cell wall transport,” *Eukaryotic Cell*, vol. 6, no. 1, pp. 48–59, 2007.
- [60] A. Casadevall, W. Cleare, M. Feldmesser et al., “Characterization of a murine monoclonal antibody to *Cryptococcus neoformans* polysaccharide that is a candidate for human therapeutic studies,” *Antimicrobial Agents and Chemotherapy*, vol. 42, no. 6, pp. 1437–1446, 1998.
- [61] R. A. Bryan, O. Zaragoza, T. Zhang, G. Ortiz, A. Casadevall, and E. Dadachova, “Radiological studies reveal radial differences in the architecture of the polysaccharide capsule of *Cryptococcus neoformans*,” *Eukaryotic Cell*, vol. 4, no. 2, pp. 465–475, 2005.
- [62] L. Nimrichter, S. Frases, L. P. Cinelli et al., “Self-aggregation of *Cryptococcus neoformans* capsular glucuronoxylomannan is dependent on divalent cations,” *Eukaryotic Cell*, vol. 6, no. 8, pp. 1400–1410, 2007.
- [63] G. d. S. Araujo, F. L. Fonseca, B. Pontes et al., “Capsules from pathogenic and non-pathogenic *Cryptococcus* spp. manifest significant differences in structure and ability to protect against phagocytic cells,” *PLoS One*, vol. 7, no. 1, article e29561, 2012.
- [64] A. Alanio, M. Desnos-Ollivier, and F. Dromer, “Dynamics of *Cryptococcus neoformans*-macrophage interactions reveal that fungal background influences outcome during cryptococcal meningoencephalitis in Humans,” *MBio*, vol. 2, no. 4, pp. 1–10, 2011.
- [65] Y.-M. Kim, B. J. Schmidt, A. S. Kidwai et al., “Salmonella modulates metabolism during growth under conditions that induce expression of virulence genes,” *Molecular BioSystems*, vol. 9, no. 6, pp. 1522–1534, 2013.
- [66] K. Hiller, J. Hangebrauk, C. Jäger, J. Spura, K. Schreiber, and D. Schomburg, “MetaboliteDetector: comprehensive analysis tool for targeted and nontargeted GC/MS based metabolome analysis,” *Analytical Chemistry*, vol. 81, no. 9, pp. 3429–3439, 2009.
- [67] T. Kind, G. Wohlgemuth, D. Y. Lee et al., “FiehnLib: mass spectral and retention index libraries for metabolomics based on quadrupole and time-of-flight gas chromatography/mass spectrometry,” *Analytical Chemistry*, vol. 81, no. 24, pp. 10038–10048, 2009.
- [68] J. Xia, I. V. Sinelnikov, B. Han, and D. S. Wishart, “MetaboAnalyst 3.0—making metabolomics more meaningful,” *Nucleic Acids Research*, vol. 43, no. W1, pp. W251–W257, 2015.

- [69] S. L. Fink and B. T. Cookson, "Caspase-1-dependent pore formation during pyroptosis leads to osmotic lysis of infected host macrophages," *Cellular Microbiology*, vol. 8, no. 11, pp. 1812–1825, 2006.
- [70] A. C. Herring, J. Lee, R. A. McDonald, G. B. Toews, and G. B. Huffnagle, "Induction of interleukin-12 and gamma interferon requires tumor necrosis factor alpha for protective T1-cell-mediated immunity to pulmonary *Cryptococcus neoformans* infection," *Infection and Immunity*, vol. 70, no. 6, pp. 2959–2964, 2002.
- [71] E. W. van Etten, N. E. van de Rhee, K. M. van Kampen, and I. A. J. M. Bakker-Woudenberg, "Effects of amphotericin B and fluconazole on the extracellular and intracellular growth of *Candida albicans*," *Antimicrobial Agents and Chemotherapy*, vol. 35, no. 11, pp. 2275–2281, 1991.
- [72] D. C. McFadden, M. de Jesus, and A. Casadevall, "The physical properties of the capsular polysaccharides from *Cryptococcus neoformans* suggest features for capsule construction," *The Journal of Biological Chemistry*, vol. 281, no. 4, pp. 1868–1875, 2006.
- [73] I. Morita, M. Kawamoto, and H. Yoshida, "Difference in the concentration of tryptophan metabolites between maternal and umbilical foetal blood," *Journal of Chromatography. B, Biomedical Sciences and Applications*, vol. 576, no. 2, pp. 334–339, 1992.
- [74] S. Gilbert, J. Xu, K. Acosta, A. Poulev, S. Lebeis, and E. Lam, "Bacterial production of indole related compounds reveals their role in association between duckweeds and endophytes," *Frontiers in Chemistry*, vol. 6, p. 265, 2018.
- [75] S. Moretti, S. Bozza, V. Oikonomou et al., "IL-37 inhibits inflammasome activation and disease severity in murine aspergillosis," *PLoS Pathogens*, vol. 10, no. 11, article e1004462, 2014.
- [76] H. H. Shen, Y. X. Yang, X. Meng et al., "NLRP3: a promising therapeutic target for autoimmune diseases," *Autoimmunity Reviews*, vol. 17, no. 7, pp. 694–702, 2018.
- [77] C. L. Evavold, J. Ruan, Y. Tan, S. Xia, H. Wu, and J. C. Kagan, "The pore-forming protein gasdermin D regulates interleukin-1 secretion from living macrophages," *Immunity*, vol. 48, no. 1, pp. 35–44.e6, 2018.
- [78] T. Liu, Y. Yamaguchi, Y. Shirasaki et al., "Single-cell imaging of caspase-1 dynamics reveals an all-or-none inflammasome signaling response," *Cell Reports*, vol. 8, no. 4, pp. 974–982, 2014.
- [79] S. P. Cullen, C. J. Kearney, D. M. Clancy, and S. J. Martin, "Diverse activators of the NLRP3 inflammasome promote IL-1 β secretion by triggering necrosis," *Cell Reports*, vol. 11, no. 10, pp. 1535–1548, 2015.
- [80] J. M. Sanz and F. D. Virgilio, "Kinetics and mechanism of ATP-dependent IL-1 β release from microglial cells," *Journal of Immunology*, vol. 164, no. 9, pp. 4893–4898, 2000.
- [81] Z. Zaslona, E. M. Pålsson-McDermott, D. Menon et al., "The induction of pro-IL-1 β by lipopolysaccharide requires endogenous prostaglandin E2 production," *Journal of Immunology*, vol. 198, no. 9, pp. 3558–3564, 2017.
- [82] E. J. Folco, G. K. Sukhova, T. Quillard, and P. Libby, "Moderate hypoxia potentiates interleukin-1 β production in activated human macrophages," *Circulation Research*, vol. 115, no. 10, pp. 875–883, 2014.
- [83] S.-C. Cheng, F. L. van de Veerdonk, M. Lenardon et al., "The dectin-1/inflammasome pathway is responsible for the induction of protective T-helper 17 responses that discriminate between yeasts and hyphae of *Candida albicans*," *Journal of Leukocyte Biology*, vol. 90, no. 2, pp. 357–366, 2011.
- [84] M. Wellington, K. Koselny, F. S. Sutterwala, and D. J. Krysan, "*Candida albicans* triggers NLRP3-mediated pyroptosis in macrophages," *Eukaryotic Cell*, vol. 13, no. 2, pp. 329–340, 2014.
- [85] L. Kasper, A. König, P.-A. Koenig et al., "The fungal peptide toxin Candidalysin activates the NLRP3 inflammasome and causes cytolysis in mononuclear phagocytes," *Nature Communications*, vol. 9, no. 1, p. 4260, 2018.
- [86] T. R. O'Meara, K. Duah, C. X. Guo et al., "High-throughput screening identifies genes required for *Candida albicans* induction of macrophage pyroptosis," *MBio*, vol. 9, no. 4, 2018.
- [87] S. Vylkova and M. C. Lorenz, "Phagosomal neutralization by the fungal pathogen *Candida albicans* induces macrophage pyroptosis," *Infection and Immunity*, vol. 85, no. 2, 2017.
- [88] I. E. Brodsky, N. W. Palm, S. Sadanand et al., "A *Yersinia* effector protein promotes virulence by preventing inflammasome recognition of the type III secretion system," *Cell Host & Microbe*, vol. 7, no. 5, pp. 376–387, 2010.
- [89] D. Ratner, M. P. A. Orning, M. K. Proulx et al., "The *Yersinia pestis* effector YopM inhibits pyrin inflammasome activation," *PLoS Pathogens*, vol. 12, no. 12, article e1006035, 2016.
- [90] D. J. Taxman, M. T.-H. Huang, and J. P.-Y. Ting, "Inflammasome inhibition as a pathogenic stealth mechanism," *Cell Host & Microbe*, vol. 8, no. 1, pp. 7–11, 2010.
- [91] A. S. Gilbert, P. I. Seoane, P. Sephton-Clark et al., "Vomocytosis of live pathogens from macrophages is regulated by the atypical MAP kinase ERK5," *Science Advances*, vol. 3, no. 8, article e1700898, 2017.
- [92] M. Hilbert, L. M. Voll, Y. Ding, J. Hofmann, M. Sharma, and A. Zuccaro, "Indole derivative production by the root endophyte *Piriformospora indica* is not required for growth promotion but for biotrophic colonization of barley roots," *The New Phytologist*, vol. 196, no. 2, pp. 520–534, 2012.
- [93] M. Gunasekaran, "Synthesis of tryptophol and indolelactic acid by *Cryptococcus neoformans*," *Mycologia*, vol. 72, no. 3, p. 578, 1980.
- [94] T. Zelante, R. G. Iannitti, C. Cunha et al., "Tryptophan catabolites from microbiota engage aryl hydrocarbon receptor and balance mucosal reactivity via interleukin-22," *Immunity*, vol. 39, no. 2, pp. 372–385, 2013.
- [95] G. Hu, P.-Y. Cheng, A. Sham, J. R. Perfect, and J. W. Kronstad, "Metabolic adaptation in *Cryptococcus neoformans* during early murine pulmonary infection," *Molecular Microbiology*, vol. 69, no. 6, pp. 1456–1475, 2008.
- [96] M. S. Price, M. Betancourt-Quiroz, J. L. Price et al., "*Cryptococcus neoformans* requires a functional glycolytic pathway for disease but not persistence in the host," *MBio*, vol. 2, no. 3, 2011.
- [97] K. F. C. Martho, A. T. de Melo, J. P. F. Takahashi et al., "Amino acid permeases and virulence in *Cryptococcus neoformans*," *PLoS One*, vol. 11, no. 10, article e0163919, 2016.
- [98] E. E. McClelland, U. A. Ramagopal, J. Rivera et al., "A small protein associated with fungal energy metabolism affects the virulence of *Cryptococcus neoformans* in mammals," *PLoS Pathogens*, vol. 12, no. 9, article e1005849, 2016.

- [99] D. G. Perregaux, P. McNiff, R. Laliberte et al., "Identification and characterization of a novel class of interleukin-1 post-translational processing inhibitors," *The Journal of Pharmacology and Experimental Therapeutics*, vol. 299, no. 1, pp. 187–197, 2001.
- [100] R. C. Coll, A. A. B. Robertson, J. J. Chae et al., "A small-molecule inhibitor of the NLRP3 inflammasome for the treatment of inflammatory diseases," *Nature Medicine*, vol. 21, no. 3, pp. 248–255, 2015.

Research Article

Involvement of the Inflammasome and Th17 Cells in Skin Lesions of Human Cutaneous Leishmaniasis Caused by *Leishmania (Viannia) panamensis*

K. Gonzalez ^{1,2}, J. E. Calzada,^{1,3} C. E. P. Corbett,² A. Saldaña,^{1,4} and M. D. Laurenti ²

¹Departamento de Parasitología Molecular, Instituto Conmemorativo Gorgas de Estudios de la Salud, Ave. Justo Arosemena, Calidonia, 0816-02593 Panama City, Panama

²Departamento de Patología, Laboratorio de Patología de Moléstias Infecciosas, Faculdade de Medicina, Universidade de São Paulo, Ave. Doutor Arnaldo 455, 01246-903 São Paulo Cerqueira César, Brazil

³Facultad de Medicina Veterinaria, Universidad de Panamá, Campus Harmodio Arias Madrid, Av. Juan Pablo II, Albrook, Panama City, Panama

⁴Centro de Investigación y Diagnóstico de Enfermedades Parasitarias, Facultad de Medicina, Universidad de Panamá, Ave. Octavio Méndez Pereira, Panama City, Panama

Correspondence should be addressed to M. D. Laurenti; mdlauren@usp.br

Received 6 July 2020; Revised 24 July 2020; Accepted 19 September 2020; Published 28 October 2020

Academic Editor: Young-Su Yi

Copyright © 2020 K. Gonzalez et al. This is an open access article distributed under the Creative Commons Attribution License, which permits unrestricted use, distribution, and reproduction in any medium, provided the original work is properly cited.

Localized cutaneous leishmaniasis (LCL) caused by *Leishmania (Viannia) panamensis* is an endemic disease in Panama. This condition causes ulcerated skin lesions characterized by a mixed Th1/Th2 immune response that is responsible for disease pathology. However, the maintenance of the *in situ* inflammatory process involves other elements, such as Th17 and inflammasome responses. Although these processes are associated with parasite elimination, their role in the increase in disease pathology cannot be discarded. Thus, the role in *Leishmania* infection is still unclear. In this sense, the present study aimed at characterizing the Th17 and inflammasome responses in the skin lesions of patients with LCL caused by *L. (V.) panamensis* to help elucidate the pathogenesis of this disease in Panama. Th17 and inflammasome responses were evaluated by immunohistochemistry (IHC) in 46 skin biopsies from patients with LCL caused by *L. (V.) panamensis*. The Th17 immune response was assessed using CD3, CD4, RoRyt, IL-17, IL-6, IL-23, and TGF- β 1 antibodies, and the inflammasome response was assessed by IL-1 β , IL-18, and caspase-1 antibodies. The presence of the Th17 and inflammasome responses was evidenced by a positive reaction for all immunological markers in the skin lesions. An inverse correlation between the density of amastigotes and the density of RoRyt⁺, IL-17⁺, IL-1 β ⁺, and caspase-1⁺ cells was observed, but no correlation between Th17 and the inflammasome response with evolutionary disease pathology was reported. These data showed the participation of Th17 cells and the inflammasome in the inflammatory response of the skin lesions of LCL caused by *L. (V.) panamensis* infection. These results suggest a role in the control of tissue parasitism of IL-17 and the activation of the NLRP3 inflammasome dependent on IL-1 β but cannot exclude their role in the development of disease pathology.

1. Introduction

Cutaneous leishmaniasis (CL) caused by *Leishmania (Viannia) panamensis* is an endemic disease in Panama [1, 2]. The most prevalent clinical manifestation is ulcerated skin lesions, and a small percentage of patients develop mucosal leishmaniasis (ML) concomitantly with or after CL, leading

to tissue damage and occasionally disfiguring facial lesions [1, 3]. Tissue damage in murine and human leishmaniasis has been associated with the exacerbated response of cytokines such as IL-17, IL-1, and TNF α , especially in *L. (V.) braziliensis* infection [4–6]. IL-17 is principally produced by Th17 cells [7, 8], and IL-1 has been related to the differentiation of Th17 cells [9, 10] and inflammasome

activation [11–13]. Recently, the participation of Th17 cells and the inflammasome in the immune response against *Leishmania* spp. have been described [6, 12, 14, 15]. Both factors promote the activation of inflammatory processes in infections by *Leishmania* sp. [12, 16, 17], and they seem to have a different role depending on the species of the parasite [13, 15, 16, 18]. Th17 cells play an important role in eliminating pathogens that are not adequately destroyed by Th1 cells [8, 18]. However, Th17 may play an ambiguous role in leishmaniasis since, in visceral disease, they are associated with parasite elimination, and in CL, they are related to the exacerbation of cutaneous lesions and consequently the pathogenesis of the disease [15, 18]. In a murine study with *L. (L.) major* and in human infection with *L. (V.) braziliensis*, the effect of Th17 cells was related to the progression of leishmaniasis [5, 6]. In contrast, other studies of *L. (V.) panamensis* and *L. (V.) braziliensis* correlated Th17 cells with control and elimination of the parasite [15, 19].

In addition to activation of Th17 cells in response to *Leishmania* sp. infection, we observed activation of the inflammasome that contributes to the inflammatory process at the site of infection. Inflammasomes are multiprotein complexes assembled in the cytoplasm of innate immune cells that regulate the processing of caspase-1 to activate pro-inflammatory cytokines such as IL-1 β and IL-18 in response to microbial molecules or stress signals [11, 12, 20, 21]. The NLRP3 inflammasome is the best characterized inflammasome and is composed of the sensor (NLR protein NLRP3) [12, 22], the adapter protein ASC [20], and the inflammatory caspase-1 [11, 23]. Among inflammatory caspases, caspase-1 is the most studied, and its catalytic activity is strongly regulated by the signal-dependent autoactivation of the inflammasome that mediates caspase-1-dependent processing of cytokines, such as IL-1 β [11]. Several studies have reported that the NLRP3 inflammasome is activated by *Leishmania* spp. and plays an important role in the outcome of the infection [13, 24–27]. The ambiguous role of the inflammasome in the immune response against *Leishmania* sp. has been described [13, 16, 24, 28]. An experimental study in a murine model infected with *L. amazonensis*, *L. braziliensis*, and *L. infantum chagasi* showed that IL-1 β production derived from the activation of the NLRP3 inflammasome led to host resistance to infection by the production of nitric oxide (NO) [13]. In contrast, activation of the NLRP3 inflammasome and production of IL-1 β led to an increase in the pathology of murine infection by *L. braziliensis* [16].

Despite the increasing knowledge of the immunopathological mechanisms that contribute to disease progression, the role of Th17 and the inflammasome during *L. (V.) panamensis* infection remains unclear. Therefore, in this study, we evaluated the Th17 and inflammasome responses in the skin lesions of patients with LCL caused by *L. (V.) panamensis* to better understand their roles in the immune response against this species of parasite in Panama County, where studies are rare.

2. Materials and Methods

2.1. Study Design. Samples of skin biopsies ($n = 46$) from patients with positive laboratory and clinical diagnoses of

LCL were analysed. The samples were collected at the Clínica de Medicina Tropical of the Instituto Conmemorativo Gorgas de Estudios de la Salud (ICGES), Panama, between January and December 2012. All patients were adults without previous treatment for leishmaniasis and agreed, freely and voluntarily, to participate in the study by providing informed consent. Samples were taken under local anaesthesia and aseptically [29] and analysed by immunohistochemistry at the Laboratorio de Patología de Moléstias Infecciosas, Universidade de São Paulo, Brazil. *Leishmania* infection was confirmed by direct microscopic observation of amastigotes in Giemsa staining and/or isolation of promastigotes in Schneider's medium from skin scrape samples [29]. The *Leishmania* species was assessed by polymerase chain reaction by kDNA PCR as previously described [30] and characterized as *L. (V.) panamensis* by PCR-Hsp70/RFLP [31]. After diagnosis, all patients were treated with 20 mg/kg/day of intramuscular glucantime according to the Panamanian guidelines for leishmaniasis control [32].

2.2. Ethical Statements. This study was approved by the National Committee of Bioethics of Research of the Gorgas Memorial Institute of Health Studies, Panama, and by the Ethics of Research Committee of the Faculty of Medicine of the University of São Paulo, Brazil, under protocol number 141/13. All the participants signed an informed consent form and voluntarily agreed to participate in the study.

3. Sample Collection and Immunohistochemistry Assay

3.1. Biopsy Collection. The biopsy samples were taken from the outer edge of the ulcer with a 4 mm Harris punch (Whatman International, Ltd.; UK), followed by the application of local anaesthesia and aseptically [33, 34].

3.2. Histopathological Processing. All samples were fixed in 10% buffered formalin and processed within a period of no more than 48 hours to dispose of the paraffin tissue block. All tissue samples were dehydrated, cleared, embedded in paraffin, cut into 4–5 μm thick sections, and prepared for analysis by immunohistochemistry [34–36]. The lesion sections were characterized microscopically based on the histological alterations found in the epidermis and the dermis to correlate with the different markers used to analyse the Th17 and inflammasome responses. The results of the histopathological findings were described in a previous study [37].

3.3. Immunohistochemistry. The *in situ* Th17 inflammatory immune response was assessed by immunohistochemistry using anti-IL-6, anti-IL-23, anti-RoR γ t, and anti-CD4 monoclonal antibodies and anti-IL-17, anti-TGF- β 1, and anti-CD3 polyclonal antibodies. The participation of the inflammasome was assessed by immunohistochemistry using anti-IL-1 β , anti-IL-18, and anti-caspase-1 polyclonal antibodies. Hyperimmune serum from a mouse chronically infected with *L. (L.) amazonensis* produced in the Laboratory of Pathology of Infectious Diseases was used to confirm tissue parasitism. The histological sections were deparaffinized in

xylene for 15 minutes, followed by hydration with a descending series of alcohols. Endogenous peroxidase was blocked with 3% hydrogen peroxide solution (88597, Sigma-Aldrich, USA). Antigen retrieval for the IL-17 and CD4 markers was conducted using 1 mM EDTA buffer at pH 8.0, for the IL-18 marker was conducted with 10 mM Tris/1 mM EDTA at pH 9.0, and for the other markers was conducted with 10 mM citrate buffer at pH 6.0, all in a boiling water bath. Then, primary antibodies were added to the tissues in the following dilutions: anti-*Leishmania* (mouse hyperimmune serum) [38] diluted at 1:1000, anti-CD3 (A0452, DakoCytomation, USA), and anti-CD4 (NC-L-CD4-1F6, Novocastra, Leica, USA) diluted at 1:50; anti-IL-6 (SC-130326, Santa Cruz Biotechnology, USA) diluted at 1:100; anti-TGF- β 1 (V: SC-146, Santa Cruz Biotechnology, USA) diluted at 1:200; anti-IL-17 (H-132: SC-7927, Santa Cruz Biotechnology, USA) diluted at 1:200; anti-RoR γ t (MABF81, 6F3.1, Sigma-Aldrich, USA) diluted at 1:2000; anti-IL-23 (C-3: SC-271279, Santa Cruz Biotechnology, USA) diluted at 1:2500; anti-IL-1 β (ab2105, Abcam, UK) diluted 1:300; anti-caspase-1 (G6231-3D2, Sigma-Aldrich, USA) diluted at 1:500; and anti-IL-18 (ab68435, Abcam, UK) diluted at 1:1500. As a negative control, a solution containing phosphate-buffered saline (PBS) and bovine serum albumin (A9647-BSA, Sigma-Aldrich, St. Louis, MO, USA) with the omission of a primary antibody was used, and human amygdala was employed to standardize the reactions. The slides were incubated in a humidified chamber overnight at 4°C. For all markers, the Novolink kit (RE7280-K-Novovastra, Leica, IL, USA) was used. The chromogenic substrate DAB + H₂O₂ (K0690-diaminobenzidine with hydrogen peroxide, DakoCytomation, CO, USA) was added to the tissue, incubated for 5 minutes, and counterstained with eosin (Sigma-Aldrich, St. Louis, MO, USA) for anti-RoR γ t antibody and Harris haematoxylin (VWR International, PA, USA) for the other antibodies. Finally, the slides were dehydrated in a series of ascending alcohols and mounted with Permount (SP15-500, Fisher Scientific, Waltham, MA, USA) and glass coverslips. Ten skin samples from healthy adult individuals undergoing plastic surgery without current or previous diagnosis of leishmaniasis or any dermatological infection were included as controls.

3.4. Quantitative Analysis of Immunostained Cells. Sequential images were obtained using an optical microscope coupled to the microcomputer, and quantification of immunostained cells was performed using the AxioVision 4.8.2 software (Zeiss, San Diego, CA, USA). The images were obtained in the dermis where the inflammatory infiltrate was observed. Ten microscopic fields of each histological section for the different markers were photographed using a 40x objective. Cells were quantified according to cell morphology and brown immunostaining, and cellular density (number of cells per square millimetre) was determined by the ratio of the immunolabeled cells to the area of each image.

3.5. Statistical Analysis. The GraphPad Prism 5.0 software (GraphPad Software, San Diego, CA, USA) was used for the statistical analysis of the results. For analysis of the differ-

ences between the groups, a *t* test was performed for data with a Gaussian distribution, and the Mann-Whitney test was used for data with a non-Gaussian distribution. For correlation of different markers, Pearson's correlation test was performed for data with a Gaussian distribution and Spearman's correlation test for data with a non-Gaussian distribution. Graphics were made using the Origin 8.0 programme (OriginLab Corporation, Northampton, MA, USA).

4. Results

4.1. Patient Profile. Forty-six samples from patients with LCL were analysed. Patients came from areas known to be endemic for leishmaniasis in Panama, and most of them were male (72%). The mean age was 33 years, ranging between 21 and 72 years. The median lesion number was 2, ranging between 1 and 8 lesions, with an average of 35 days for the time of evolution, varying from 10 to 90 days. The majority of patients (65%) had lesions with an evolution time \leq 30 days. Forty-three percent of the patients had ulcerated lesions. The lesions were distributed mostly in the upper extremities (63%), followed by the lower extremities (18%), face/neck (10%), back (5%), and abdomen (4%). All parasites isolated from the skin lesions were characterized as *L. (V.) panamensis* by PCR-Hsp70/RFLP.

4.2. Evaluation of the In Situ Th17 Immune Response. To analyse the Th17 immune response in the skin lesions of the patients with LCL caused by *L. (V.) panamensis*, we assessed the CD3, CD4, RoR γ t, IL-17, IL-6, TGF- β , and IL-23 markers by immunohistochemistry (see Figure 1). The cellular densities (mean \pm the standard error) of these markers were 2593.00 \pm 112.00 cells/mm² for CD3⁺, 914.50 \pm 51.76 cells/mm² for CD4⁺, 229.20 \pm 13.49 cells/mm² for RoR γ t⁺, 859.80 \pm 70.66 cells/mm² for IL-17⁺, 132.20 \pm 9.50 cells/mm² for TGF- β ⁺, 273.20 \pm 15.89 cells/mm² for IL-6⁺, and 669.80 \pm 34.73 cells/mm² for IL-23⁺ (see Table 1). The density of different markers observed in the skin biopsies from individuals infected with *L. (V.) panamensis* was higher than that observed in healthy skin ($p < 0.0001$) (see Table 1).

Considering the time of infection (\leq 30 days versus $>$ 30 days), gender (male versus female), or histopathological tissue response (granulomas versus nongranuloma reaction and presence versus absence of ulcer), no significant difference was observed between the markers used to analyse the Th17 immune response ($p > 0.05$).

According to the linear correlation analysis between the evaluated markers, we observed a positive correlation between RoR γ t⁺ and CD4⁺ (moderate: $\rho = 0.519$; $p < 0.0001$), IL-17⁺ (weak: $\rho = 0.362$; $p = 0.01$), IL-6⁺ (weak: $\rho = 0.453$; $p = 0.002$), and TGF- β ⁺ (weak: $\rho = 0.334$; $p = 0.02$) (see Figure 2). In addition, there was a positive correlation between IL-17⁺ and IL-23⁺ (weak: $\rho = 0.409$; $p = 0.006$) and CD3⁺ (weak: $\rho = 0.314$; $p = 0.03$) (see Figure 3) and a positive correlation between TGF- β ⁺ and IL-6⁺ (moderate: $\rho = 0.541$; $p < 0.0001$). Although not statistically significant, an inverse correlation was observed between the density of amastigotes and the density of RoR γ t⁺ ($\rho = -0.213$; $p > 0.05$) and IL-17⁺ cells ($\rho = -0.200$; $p > 0.05$) (see Figure 4).

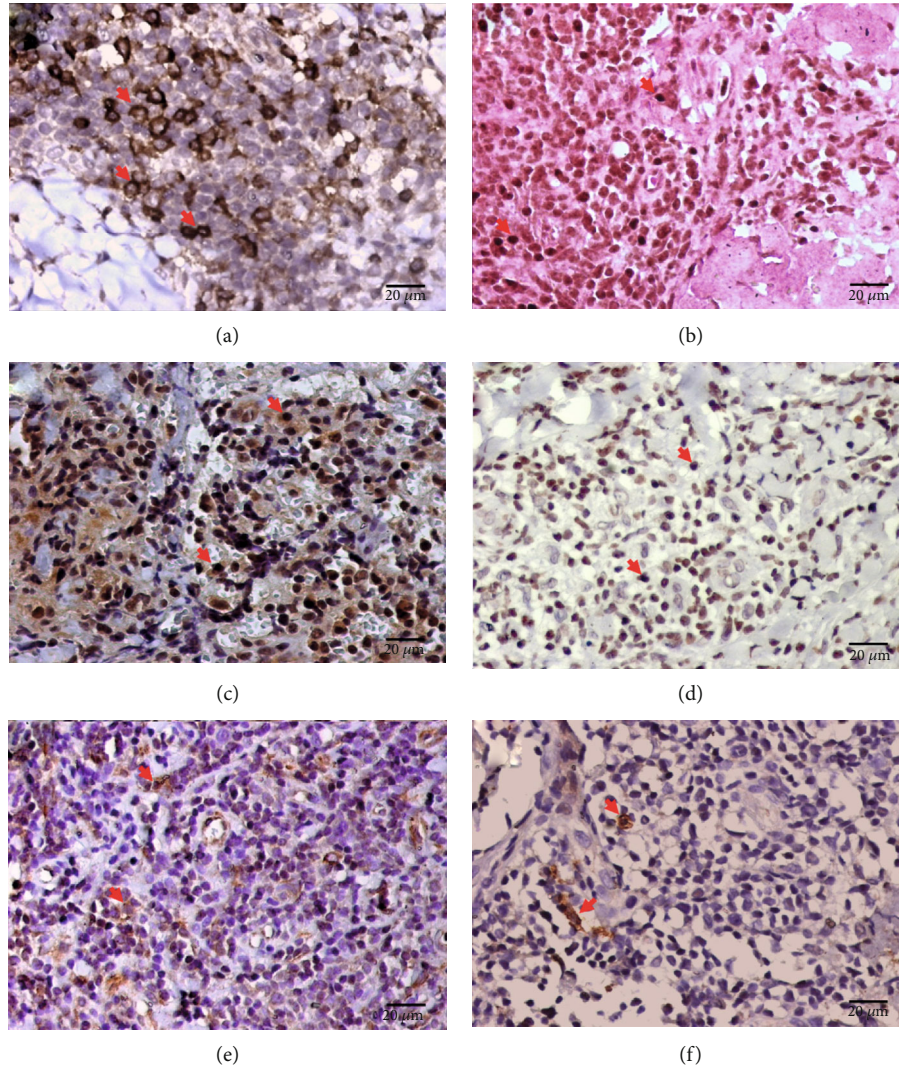


FIGURE 1: Immunohistochemistry of the skin sections from the patients with LCL; brown CD4⁺ cells (a), RoRyt⁺ cells (b), IL-17⁺ cells (c), IL-23⁺ cells (d), IL-6⁺ cells (e), and TGF-β⁺ (f) cells can be observed. The red arrow shows positive cells.

TABLE 1: Mean and standard error of the cellular densities (cells/mm²) of the different markers used to evaluate the Th17 immune response in the skin lesions of the patients with localized cutaneous leishmaniasis (LCL) caused by *L. (V.) panamensis* and in healthy skin.

Antibody	LCL skin (n = 46)	Healthy skin (n = 10)	p value
CD3	2593.00 ± 112.00	37.30 ± 8.13	p < 0.0001
CD4	914.50 ± 51.76	46.25 ± 11.55	p < 0.0001
RoRyt	229.20 ± 13.49	0.10 ± 0.01	p < 0.0001
IL-17	859.80 ± 70.66	18.64 ± 5.03	p < 0.0001
IL-6	273.20 ± 15.89	7.31 ± 2.14	p < 0.0001
TGF-β	132.20 ± 9.50	0.10 ± 0.01	p < 0.0001
IL-23	669.80 ± 34.73	0.10 ± 0.01	p < 0.0001

4.3. Evaluation of Inflammasomes in the In Situ Immune Response against *L. (V.) panamensis*. The markers IL-1β, IL-18, and caspase-1 were assessed to evaluate the participation of the canonical NLRP3 inflammasome in the immune response against *L. (V.) panamensis* infection (see Figure 5). The cellular density (mean ± the standard error) of IL-1β⁺ was 645.90 ± 72.33 cells/mm², that of IL-18⁺ was 73.45 ± 8.84 cells/mm² and that of caspase-1⁺ was 485.00 ± 64.17 cells/mm² (see Table 2). The cellular density of these markers was higher in the skin sections of the *L. (V.) panamensis*-infected patients than the control skin sections (p < 0.0001) (see Table 2).

Considering the time of infection (≤30 days versus >30 days), gender (male versus female), and histopathological tissue response (granulomas versus nongranuloma reaction and presence versus absence of ulcer), no significant difference was observed in the cellular densities of IL-1β, IL-18, and caspase-1 (p > 0.05).

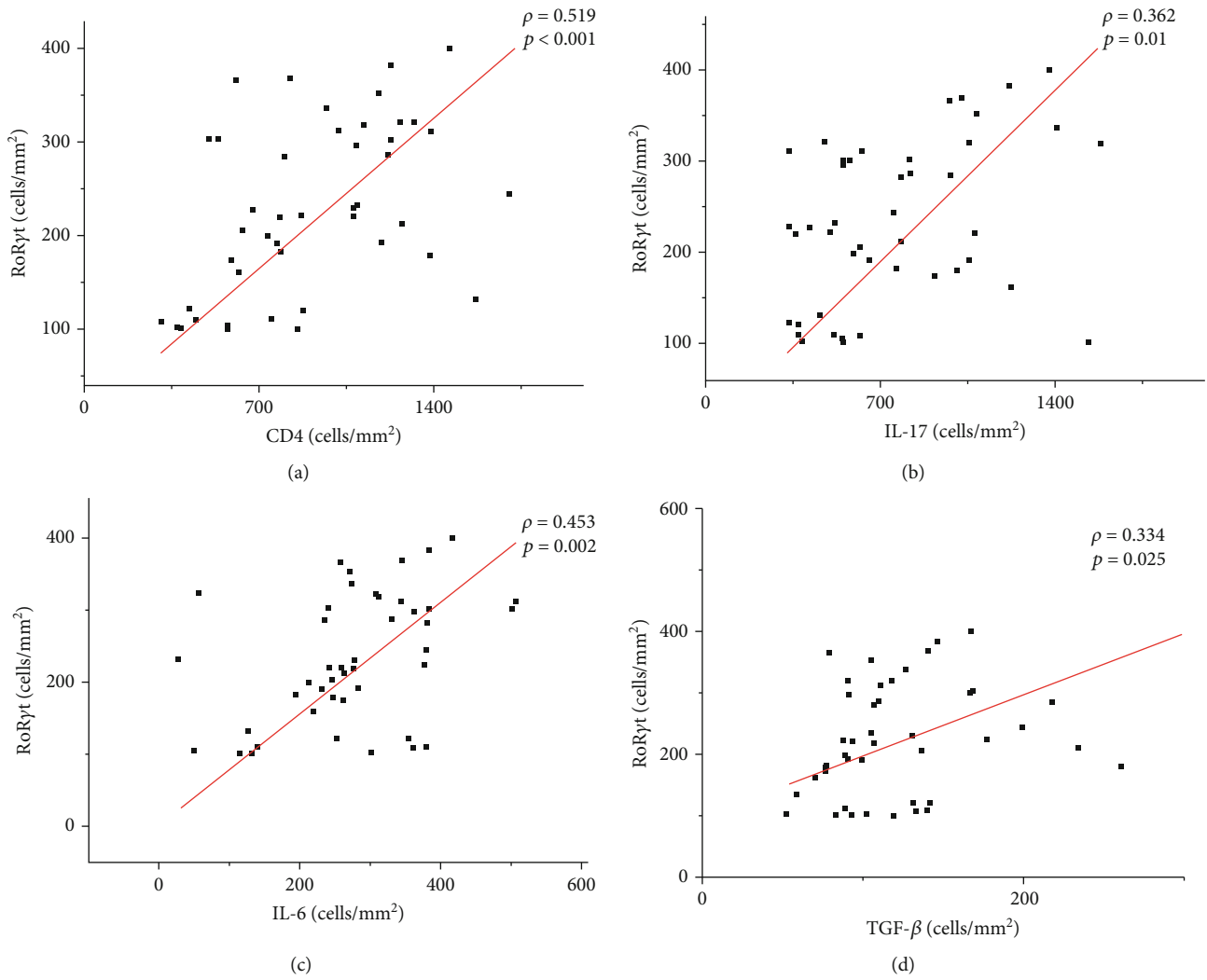


FIGURE 2: Graphs showing the correlation between the cellular density of RoRyt⁺ cells and CD4⁺ cells (a), IL-17⁺ cells (b), IL-6⁺ cells (c), and TGF- β ⁺ cells (d). The value of ρ is Spearman's correlation coefficient, and p is the p value. The red line indicates a positive correlation.

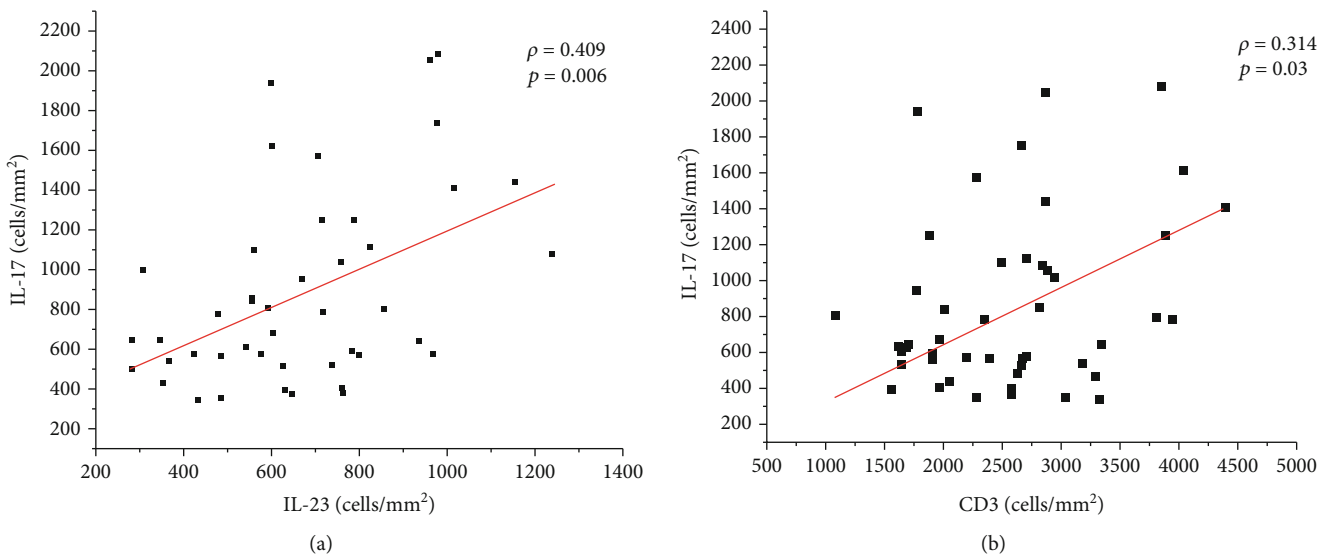


FIGURE 3: Graphs showing the correlation between the cellular density of IL-17⁺ cells and IL-23⁺ cells (a) and CD3⁺ cells (b). The value of ρ is Spearman's correlation coefficient, and p is the p value. The red line indicates a positive correlation.

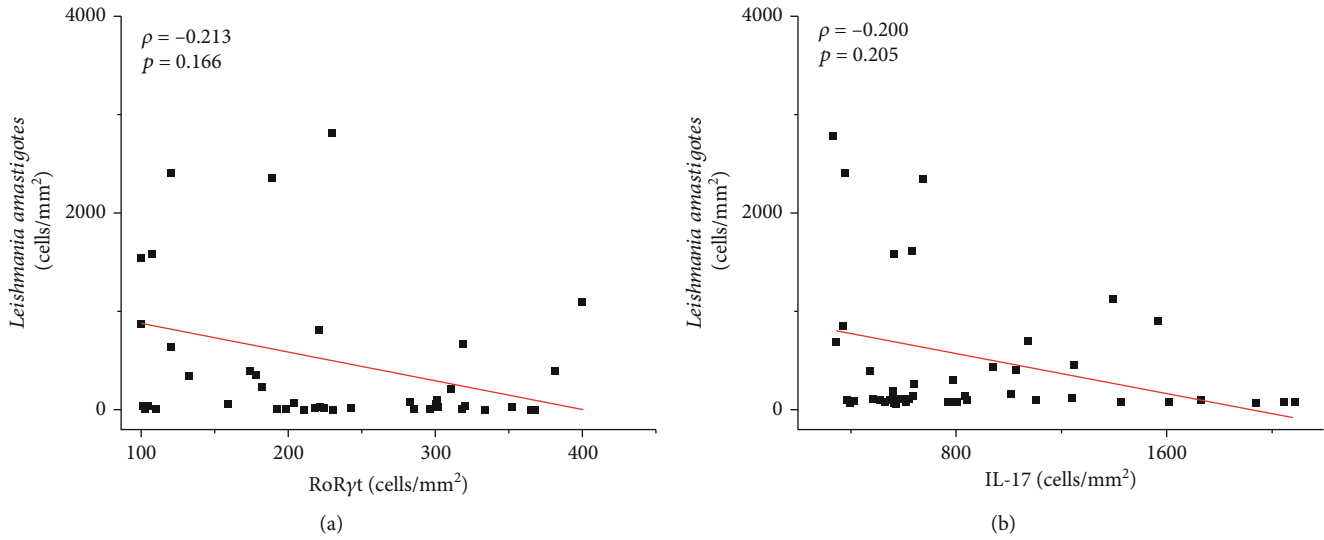


FIGURE 4: Graph showing the correlation between the density of *Leishmania* amastigotes and RoRyt⁺ cells (a) and IL-17⁺ cells (b). The value of ρ is Spearman's correlation coefficient, and p is the p value. The red line indicates a negative correlation.

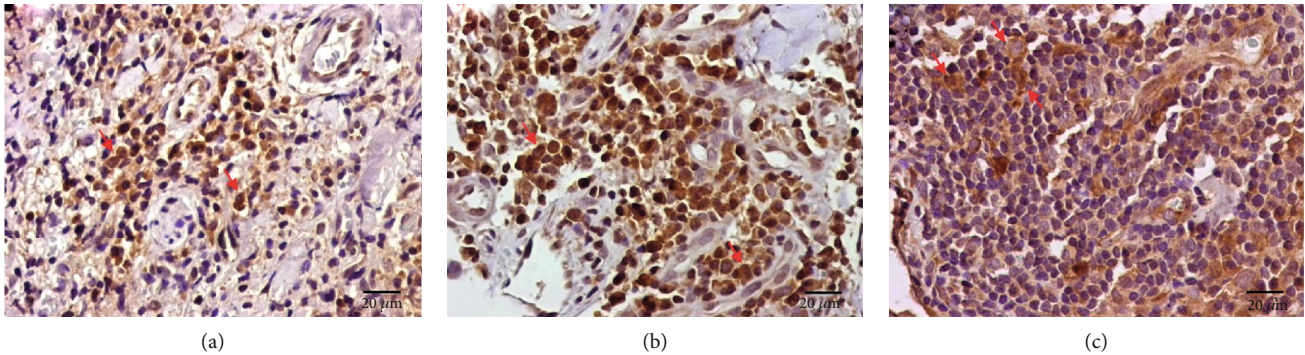


FIGURE 5: Immunohistochemistry of the skin sections from the patients with LCL showing brown IL-1 β ⁺ cells (a), IL-18⁺ cells (b), and caspase-1⁺ cells (c). The red arrow indicates positive cells.

TABLE 2: Mean and standard error of the cellular densities (cells/mm²) of the different markers used to evaluate the inflammasome response in the skin lesions of the patients with localized cutaneous leishmaniasis (LCL) caused by *L. (V.) panamensis* and in healthy skin.

Antibody	LCL skin $n = 46$	Healthy skin $n = 10$	p value
IL-1 β	645.90 \pm 72.33	0.10 \pm 0.01	$p < 0.0001$
IL-18	73.45 \pm 8.84	0.10 \pm 0.01	$p < 0.0001$
Caspase-1	485.00 \pm 64.17	0.10 \pm 0.01	$p < 0.0001$

A positive correlation was observed between caspase-1 and IL-1 β (strong: $\rho = 0.679$; $p < 0.0001$) as well as between caspase-1 and IL-18 (moderate: $\rho = 0.600$; $p < 0.0001$) and between IL-1 β and IL-18 (weak: $\rho = 0.483$; $p = 0.003$) (see Figure 6). Although not statistically significant, an inverse correlation was observed between the density of amastigotes and the cellular density of IL-1 β ⁺ ($\rho = -0.020$; $p > 0.05$) and caspase-1⁺ cells ($\rho = -0.010$; $p > 0.05$) (see Figure 7).

5. Discussion

Recent studies have shown the participation of Th17 cells and the inflammasome in the immune response against *Leishmania* sp. infection. Both factors contribute to the production of proinflammatory cytokines by favouring the inflammatory response at the site of infection [6, 12, 14, 15]. Among the proinflammatory cytokines, IL-1 is related to the differentiation of Th17 cells and the activation of the inflammasome [9–13]. Th17 (RoRyt) cells produce IL-17 [8, 39], whose main function is the induction of tissue inflammation and protection of the host against pathogens [8]. The present study showed the presence of CD4⁺, RoRyt⁺, and IL-17⁺ cells, as evidenced by immunohistochemistry, and the linear correlation analysis of these data showed a positive correlation among these markers, suggesting the presence of Th17 cells (CD4⁺RoRyt⁺) producing IL-17 in the skin biopsies of the patients with LCL caused by *L. (V.) panamensis*. The cellular density of IL-17⁺ cells was greater than the density of RoRyt⁺ cells, indicating that other cells could produce this cytokine in the cutaneous lesions. According to the literature, most IL-17 produced in the

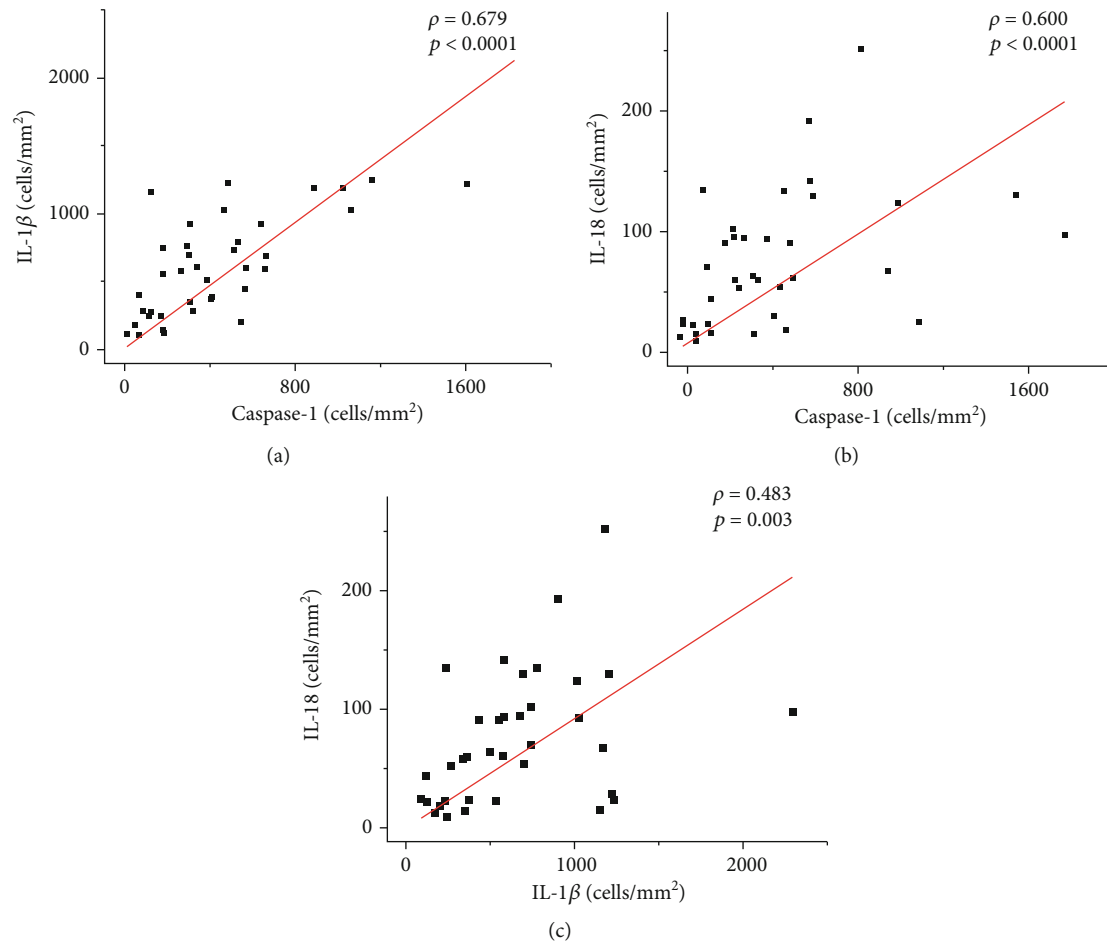


FIGURE 6: Graphs showing the correlation between the cellular density of Caspase-1⁺ cells with IL-1 β ⁺ cells (a) and IL-18⁺ cells (b). The positive correlation between IL-1 β ⁺ cells and IL-18⁺ cells (c). The value of ρ is Spearman's correlation coefficient, and p is the p value. The red line indicates a positive correlation.

CL is mainly from TCD4⁺RoR γ t⁺ cells; however, IL-17 can also be secreted by other cell types, such as TCD8, T γ δ , and NK cells and monocytes [40]. Therefore, in the present study, we cannot rule out the possibility that other cellular types, such as T γ δ cells and double-negative CD3 lymphocytes, are producing IL-17 [41].

Correlations between RoR γ t⁺ cells and IL-6⁺ and TGF- β ⁺ cells were observed ($p < 0.002$ and $p < 0.02$, respectively), which suggests the participation of these cytokines in the differentiation of Th17 cells [42–44]. We also observed a weak positive correlation between IL-1 β ⁺ cells and RoR γ t⁺ cells ($\rho = 0.320$; $p = 0.04$), suggesting the possible participation of IL-1 β in the development of Th17 cells, as has been described elsewhere [9, 10]. In addition, there was a correlation between IL-17 and IL-23 ($p = 0.006$), suggesting the important role of IL-23 in the maintenance of IL-17-producing Th17 cells [8, 18]. Although not statistically significant, an inverse correlation was observed between the density of amastigotes and the density of RoR γ t⁺ and IL-17⁺ cells, suggesting the control of tissue parasitism as described in murine studies since IL-17 together with IFN- γ has been demonstrated to have an important role in the resolution

of the disease caused by *Leishmania (Viannia)* parasites [15, 19]. However, the presence of IL-17 has also been associated with the worsening of the disease outcome due to the increase in the lesion size and the presence of ulcers [5]. Unfortunately, in the present study, due to the absence of data about lesion size, we were unable to establish these correlations and associate them with disease severity. Despite the presence of ulcers in 43% of the skin biopsies, we did not observe a correlation indicating a detrimental role of Th17 cells, probably due to the presence of other mechanisms or cytokines, such as TNF- α , that could be involved in the tissue damage observed in the cutaneous lesions [4, 45]. Notably, the lesions analysed in this study were relatively recent, and the majority of patients (65%) had lesions with an evolution time ≤ 30 days, varying from 10 to 90 days. The results suggest that Th17 cells can help eliminate parasites through IL-17 in the activation of host cells; however, their role in the progression of the disease pathology caused by *L. (V.) panamensis* cannot be disregarded.

An imbalanced immune response in *L. (V.) panamensis* infection involving the production of both inflammatory and anti-inflammatory cytokines is responsible for the

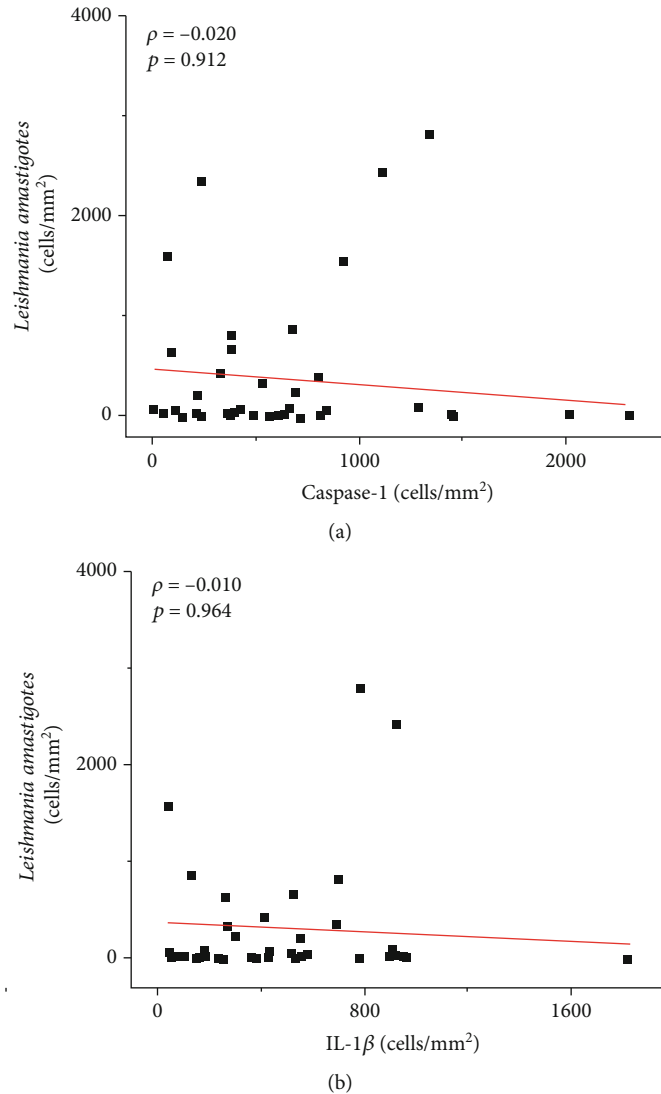


FIGURE 7: Graphs showing the correlation between the density of *Leishmania amastigotes* and caspase-1⁺ cells (a) and IL-1 β ⁺ cells (b). The value of ρ is Spearman's correlation coefficient, and p is the p value. The red line indicates a negative correlation.

maintenance of inflammation, which plays an important role in the pathogenesis of leishmaniasis [46, 47]. In this way, other inflammatory cytokines, such as IL-1 and IL-18, that are directly related to inflammasome activation could be part of this process and be directly involved in the skin lesions caused by this species of parasite [12, 13]. The data obtained in our study showed the presence of IL-1 β and IL-18 cytokines as well as caspase-1, which are canonical markers to assess the presence of NLRP3 inflammasome activation in *Leishmania (Viannia)* infection, in the inflammatory response against *L. (V.) panamensis* [11, 12]. Their presence, evidenced by immunohistochemistry, is correlated with the moderate to intense inflammatory infiltrate observed in the skin lesions of LCL caused by *L. (V.) panamensis*. Although the activation of the NLRP3 inflammasome and the production of IL-1 β lead to an increase in the pathology of murine infection by *L. braziliensis* [16], we observed an inverse correlation between the density of amastigotes and the densities of IL-1 β and caspase-1, suggesting the role of

the inflammasome in the control of *L. (V.) panamensis* infection as has been described previously [13, 28]. Inflammasome activation was shown to be important for the restriction of parasite replication in a murine model of infection induced by *L. amazonensis*, *L. braziliensis*, and *L. infantum chagasi* infection [13]. These species of the *Leishmania* parasite trigger the activation of caspase-1 in macrophages, leading to the production of nitric oxide (NO), which is important for clearance of the parasite. Another *in vitro* study showed that the activation of the NLRP3 inflammasome promotes host resistance against *L. braziliensis* infection through NO production by macrophages [28]. Although these data suggest the important role of the inflammasome in the control of *Leishmania* parasites, its pathogenic role in the infection caused by *L. (V.) panamensis* cannot be discarded. Further studies regarding the role of inflammasomes in *L. (V.) panamensis* infection, including correlations with the evolution of infection and mucous involvement, are needed.

6. Conclusions

These data suggest the participation of Th17 cells and the inflammasome in the *in situ* inflammatory response in localized cutaneous leishmaniasis caused by *L. (V.) panamensis* infection and their roles in the control of the parasites, probably through IL-17 and the IL-1 β -dependent NLRP3 inflammasome activation; however, the results cannot exclude their inflammatory role in the development of disease pathology.

Data Availability

The datasets generated for this study are available upon request from the corresponding author.

Conflicts of Interest

The authors declare that they have no conflict of interest.

Authors' Contributions

KG, AS, JEC, and CEPC contributed to the acquisition of the data and drafted the manuscript. KG and MDL critically helped to interpret the data and revised the manuscript. All authors agreed to be fully accountable for ensuring the integrity and accuracy of the work and read and approved the manuscript.

Acknowledgments

This project was carried out with the support of the Sistema Nacional de Investigación (SNI-SENACYT, Panamá), IFHARU-SENACYT, and the São Paulo Research Foundation (FAPESP) grants No 2014/50315-0 and No 2017/03141-5. We acknowledge the people who helped in a great way the first steps of this study: GAF, CMP, AM, VG, RD, TT, HP, and CMG; and the institutions: HST, ICGES, and LIM50-FMUSP for their support with its facilities, equipment, and administrative help. AS and JEC are members of the SNI-SENACYT, Panamá, and MDL is a research fellow from National Research Council/CNPq, Brazil.

References

- [1] H. A. Christensen, G. B. Fairchild, A. Herrer, C. M. Johnson, D. G. Young, and A. M. de Vásquez, "The ecology of cutaneous leishmaniasis in the Republic of Panama," *Journal of Medical Entomology*, vol. 20, no. 5, pp. 463–484, 1983.
- [2] A. Vásquez, H. Paz, J. Alvar, and H. C. Perez, *Informe Final: Estudios Sobre la Epidemiología de la Leishmaniasis Panamá, en la parte Occidental de la República de Panamá*, Instituto Conmemorativo Gorgas de Estudio de la Salud, MINSA, 1998.
- [3] R. Lainson and J. J. Shaw, "Evolution, classification and geographical distribution," in *The leishmaniases in biology and medicine*, W. Peters and R. Killick-Kendric, Eds., vol. 1, pp. 1–120, Biology and epidemiology Academic Press, London, 1988.
- [4] L. R. V. Antonelli, W. O. Dutra, R. P. Almeida, O. Bacellar, E. M. Carvalho, and K. J. Gollub, "Activated inflammatory T cells correlate with lesion size in human cutaneous leishmaniasis," *Immunology Letters*, vol. 101, no. 2, pp. 226–230, 2005.
- [5] S. Lopez Kostka, S. Dinges, K. Griewank, Y. Iwakura, M. C. Udey, and E. von Stebut, "IL-17 promotes progression of cutaneous Leishmaniasis in susceptible mice," *Journal of Immunology*, vol. 182, no. 5, pp. 3039–3046, 2009.
- [6] O. Bacellar, D. Faria, M. Nascimento et al., "Interleukin 17 Production among Patients with American Cutaneous Leishmaniasis," *The Journal of infectious diseases*, vol. 200, no. 1, pp. 75–78, 2009.
- [7] L. A. Tesmer, S. K. Lundy, S. Sarkar, and D. A. Fox, "Th17 cells in human disease," *Immunological Reviews*, vol. 223, no. 1, pp. 87–113, 2008.
- [8] E. Bettelli, T. Korn, M. Oukka, and V. K. Kuchroo, "Induction and effector functions of TH17 cells," *Nature*, vol. 453, no. 7198, pp. 1051–1057, 2008.
- [9] N. J. Wilson, K. Boniface, J. R. Chan et al., "Development, cytokine profile and function of human interleukin 17-producing helper T cells," *Nature Immunology*, vol. 8, no. 9, pp. 950–957, 2007.
- [10] E. V. Acosta-Rodriguez, G. Napolitani, A. Lanzavecchia, and F. Sallusto, "Interleukins 1 β and 6 but not transforming growth factor- β are essential for the differentiation of interleukin 17-producing human T helper cells," *Nature Immunology*, vol. 8, no. 9, pp. 942–949, 2007.
- [11] F. Martinon, K. Burns, and J. Tschopp, "The inflammasome," *Molecular Cell*, vol. 10, no. 2, pp. 417–426, 2002.
- [12] D. S. Zamboni and D. S. Lima-Junior, "Inflammasomes in host response to protozoan parasites," *Immunological Reviews*, vol. 265, no. 1, pp. 156–171, 2015.
- [13] D. S. Lima-Junior, D. L. Costa, V. Carregaro et al., "Inflammasome-derived IL-1 β production induces nitric oxide-mediated resistance to *Leishmania*," *Nature Medicine*, vol. 19, no. 7, pp. 909–915, 2013.
- [14] D. S. Zamboni and D. L. Sacks, "Inflammasomes and Leishmania: in good times or bad, in sickness or in health," *Current Opinion in Microbiology*, vol. 52, pp. 70–76, 2019.
- [15] T. M. Castilho, K. Goldsmith-Pestana, C. Lozano, L. Valderrama, N. G. Saravia, and D. McMahon-Pratt, "Murine model of chronic *L. (Viannia) panamensis* infection: role of IL-13 in disease," *European Journal of Immunology*, vol. 40, no. 10, pp. 2816–2829, 2010.
- [16] D. Santos, T. M. Campos, M. Saldanha et al., "IL-1 β production by intermediate monocytes is associated with immunopathology in cutaneous Leishmaniasis," *The Journal of Investigative Dermatology*, vol. 138, no. 5, pp. 1107–1115, 2018.
- [17] H. Park, Z. Li, X. O. Yang et al., "A distinct lineage of CD4 T cells regulates tissue inflammation by producing interleukin 17," *Nature Immunology*, vol. 6, no. 11, pp. 1133–1141, 2005.
- [18] A. Banerjee, P. Bhattacharya, A. B. Joshi, N. Ismail, R. Dey, and H. L. Nakhasi, "Role of pro-inflammatory cytokine IL-17 in *Leishmania* pathogenesis and in protective immunity by *Leishmania* vaccines," *Cellular Immunology*, vol. 309, pp. 37–41, 2016.
- [19] D. A. Vargas-Inchaustegui, L. Xin, and L. Soong, "*Leishmania braziliensis* infection induces dendritic cell activation, ISG15 transcription, and the generation of protective immune responses," *Journal of Immunology*, vol. 180, no. 11, pp. 7537–7545, 2008.
- [20] K. Schroder and J. Tschopp, "The inflammasomes," *Cell*, vol. 140, no. 6, pp. 821–832, 2010.

- [21] H. Guo, J. B. Callaway, and J. P.-Y. Ting, "Inflammasomes: mechanism of action, role in disease, and therapeutics," *Nature Medicine*, vol. 21, no. 7, pp. 677–687, 2015.
- [22] L. D. Cunha and D. S. Zamboni, "Subversion of inflammasome activation and pyroptosis by pathogenic bacteria," *Frontiers in Cellular and Infection Microbiology*, vol. 3, pp. 1–14, 2013.
- [23] T. D. Kanneganti, N. Özören, M. Body-Malapel et al., "Bacterial RNA and small antiviral compounds activate caspase-1 through cryopyrin/Nalp3," *Nature*, vol. 440, no. 7081, pp. 233–236, 2006.
- [24] M. Charmoy, B. P. Hurrell, A. Romano et al., "The Nlrp3 inflammasome, IL-1 β , and neutrophil recruitment are required for susceptibility to a nonhealing strain of *Leishmania major* in C57BL/6 mice," *European Journal of Immunology*, vol. 46, no. 4, pp. 897–911, 2016.
- [25] P. Gurung, R. Karki, P. Vogel et al., "An NLRP3 inflammasome-triggered Th2-biased adaptive immune response promotes leishmaniasis," *The Journal of Clinical Investigation*, vol. 125, no. 3, pp. 1329–1338, 2015.
- [26] F. O. Novais, A. M. Carvalho, M. L. Clark et al., "CD8⁺ T cell cytotoxicity mediates pathology in the skin by inflammasome activation and IL-1 β production," *PLoS Pathogens*, vol. 13, no. 2, article e1006196, 2017.
- [27] R. V. H. de Carvalho, D. S. Lima-Junior, M. V. G. da Silva et al., "*Leishmania* RNA virus exacerbates Leishmaniasis by subverting innate immunity via TLR3-mediated NLRP3 inflammasome inhibition," *Nature communications*, vol. 10, no. 1, 2019.
- [28] D. M. Santos, M. W. Carneiro, T. R. de Moura et al., "PLGA nanoparticles loaded with KMP-11 stimulate innate immunity and induce the killing of *Leishmania*," *Biology and Medicine*, vol. 9, no. 7, pp. 985–995, 2013.
- [29] F. Samudio, G. Santamaría, J. E. Calzada et al., "Molecular epidemiology of American tegumentary leishmaniasis in Panama," *The American Journal of Tropical Medicine and Hygiene*, vol. 81, no. 4, pp. 565–571, 2009.
- [30] A. Miranda, A. Saldaña, K. González et al., "Evaluation of PCR for cutaneous leishmaniasis diagnosis and species identification using filter paper samples in Panama, Central America," *Transactions of the Royal Society of Tropical Medicine and Hygiene*, vol. 106, no. 9, pp. 544–548, 2012.
- [31] A. M. Montalvo Alvarez, J. F. Nodarse, I. M. Goodridge et al., "Differentiation of *Leishmania (Viannia) panamensis* and *Leishmania (V.) guyanensis* using BccI for *hsp70* PCR-RFLP," *Transactions of the Royal Society of Tropical Medicine and Hygiene*, vol. 104, no. 5, pp. 364–367, 2010.
- [32] "Organización Panamericana de la Salud/Organización Mundial de la Salud," *Guía para el abordaje integral de la leishmaniasis en Panamá*, 2015.
- [33] R. Restrepo, G. Caceres-Dittmar, F. J. Tapia, D. M. Isaza, and M. Restrepo, "Immunocytochemical and histopathologic characterization of lesions from patients with localized cutaneous leishmaniasis caused by *Leishmania panamensis*," *The American journal of tropical medicine and hygiene*, vol. 55, no. 4, pp. 365–369, 1996.
- [34] A. V. Magalhães, M. A. P. Moraes, A. N. Raick et al., "Histopatologia da leishmaniose tegumentar por *Leishmania braziliensis braziliensis*: 4. Classificação histopatológica," *Revista do Instituto de Medicina Tropical de São Paulo*, vol. 28, no. 6, pp. 421–430, 1986.
- [35] F. Tresserra, M. A. Martinez Lanao, and M. T. Soler, "Manejo de las muestras para test inmunohistoquímicos, moleculares y genéticos en el cáncer de mama," *Revista de Senología y Patología Mamaria*, vol. 29, no. 1, pp. 26–31, 2016.
- [36] K. B. Engel and H. M. Moore, "Effects of preanalytical variables on the detection of proteins by immunohistochemistry in formalin-fixed, paraffin-embedded tissue," *Archives of Pathology & Laboratory Medicine*, vol. 135, no. 5, pp. 537–543, 2011.
- [37] K. González, R. Diaz, A. F. Ferreira et al., "Histopathological characteristics of cutaneous lesions caused by *Leishmania Viannia panamensis* in Panama," *Revista do Instituto de Medicina Tropical de São Paulo*, vol. 60, 2018.
- [38] M. Moreira, M. Luvizotto, J. Garcia, C. Corbett, and M. D. Laurenti, "Comparison of parasitological, immunological and molecular methods for the diagnosis of leishmaniasis in dogs with different clinical signs," *Veterinary Parasitology*, vol. 145, no. 3-4, pp. 245–252, 2007.
- [39] C. L. Langrish, Y. Chen, W. M. Blumenschein et al., "IL-23 drives a pathogenic T cell population that induces autoimmune inflammation," *Journal of Experimental Medicine*, vol. 201, no. 2, pp. 233–240, 2005.
- [40] Y. Belkaid and K. Tarbell, "Regulatory T cells in the control of host-microorganism interactions," *Annual Review of Immunology*, vol. 27, no. 1, pp. 551–589, 2009.
- [41] E. Lockhart, A. M. Green, and J. L. Flynn, "IL-17 production is dominated by $\gamma\delta$ T cells rather than CD4 T cells during *Mycobacterium tuberculosis* Infection," *Journal of Immunology*, vol. 177, no. 7, pp. 4662–4669, 2006.
- [42] P. R. Mangan, L. E. Harrington, D. B. O'Quinn et al., "Transforming growth factor- β induces development of the T_H17 lineage," *Nature*, vol. 441, no. 7090, pp. 231–234, 2006.
- [43] M. Veldhoen, R. J. Hocking, C. J. Atkins, R. M. Locksley, and B. Stockinger, "TGF β in the context of an inflammatory cytokine milieu supports de novo differentiation of IL-17-producing T cells," *Immunity*, vol. 24, no. 2, pp. 179–189, 2006.
- [44] E. Bettelli, Y. Carrier, W. Gao et al., "Reciprocal developmental pathways for the generation of pathogenic effector T_H17 and regulatory T cells," *Nature*, vol. 441, no. 7090, pp. 235–238, 2006.
- [45] O. Bacellar, H. Lessa, A. Schriefer et al., "Up-regulation of Th1-type responses in mucosal leishmaniasis patients," *Infection and Immunity*, vol. 70, no. 12, pp. 6734–6740, 2002.
- [46] F. T. Silveira, R. Lainson, and C. E. P. Corbett, "Clinical and immunopathological spectrum of American cutaneous leishmaniasis with special reference to the disease in Amazonian Brazil: a review," *Memórias do Instituto Oswaldo Cruz*, vol. 99, no. 3, pp. 239–251, 2004.
- [47] F. T. Silveira, R. Lainson, C. M. C. Gomes, M. D. Laurenti, and C. E. P. Corbett, "Reviewing the role of the dendritic Langerhans cells in the immunopathogenesis of American cutaneous leishmaniasis," *Transactions of the Royal Society of Tropical Medicine and Hygiene*, vol. 102, no. 11, pp. 1075–1080, 2008.

Research Article

Expression of AIM2 in Rheumatoid Arthritis and Its Role on Fibroblast-Like Synoviocytes

Yong Chen, Qiu Fujuan , Ensheng Chen, Beijia Yu, Fangfang Zuo, Yi Yuan, Xiaofeng Zhao, and Changhong Xiao 

Rheumatology Department, Integrated Traditional Chinese and Western Medicine Hospital, Southern Medical University, Guangzhou 510315, China

Correspondence should be addressed to Changhong Xiao; xiaochh_388@163.com

Received 7 March 2020; Revised 8 June 2020; Accepted 24 June 2020; Published 26 October 2020

Guest Editor: Young-Su Yi

Copyright © 2020 Yong Chen et al. This is an open access article distributed under the Creative Commons Attribution License, which permits unrestricted use, distribution, and reproduction in any medium, provided the original work is properly cited.

Objectives. To determine differences in AIM2 inflammasome expression levels between rheumatoid arthritis (RA) and osteoarthritis (OA) and to investigate the role of AIM2 in RA fibroblast-like synoviocytes (RA-FLS). **Methods.** Serum AIM2 levels among health controls (HC, $n = 20$), OA ($n = 25$), and RA ($n = 49$) patients were compared via ELISA. The different expression levels of AIM2, ASC, caspase-1, and IL-1 β between RA and OA synovium were semiquantified by qRT-PCR and immunohistochemical (IHC) staining. IHC staining was recorded by H scores, and its correlation with the ESR and CRP levels of RA patients was determined. siRNA AIM2 was transferred to RA-FLS and its effects on the proliferation and migration via CCK-8 assay and Transwell test, respectively. **Results.** In RA sera, the HC expressed higher level of AIM2 than OA and RA patients, and ASC, caspase-1, and IL-1 β expressed higher in RA patients than HC; no significant differences were observed between sera of OA and RA patients. However, in affected knee synovium, AIM2, ASC, caspase-1, and IL-1 β were expressed higher in RA than that of OA. Moreover, the H scores of AIM2, ASC, and IL-1 β were positively correlated with the ESR and CRP levels in RA patients. The proliferation of FLS was significantly inhibited after transferring with AIM2 siRNA to FLS. There were no differences in apoptosis and migration assay between the si-AIM2 group and the control group. **Conclusion.** AIM2 inflammasome pathway involves in the pathogenesis of RA. si-AIM2 inhibits the proliferation of RA-FLS, which may be a promising therapeutic strategy for the treatment of RA.

1. Introduction

Rheumatoid arthritis (RA) is a chronic autoimmune inflammatory disease characterised by the hyperproliferation of synovial cells, infiltration of mononuclear cells into the synovium, and early destruction of the articular cartilage and bone, causing damage to the musculoskeletal system and consequently loss of physical ability and quality of life [1, 2]. Past studies regarding the genetic architecture of RA have been well characterised through conventional and genome-wide approaches, and more than 100 loci were found to be associated with disease risk and progression [3], among which, absent in melanoma 2 (AIM2) was one of the genes detected [4, 5].

AIM2 is involved in innate immune responses through the recognition of cytosolic double-stranded DNA and the induction of caspase-1-activating inflammasome formation in macrophages [6]. Upon binding to DNA, AIM2 is thought to undergo oligomerization and to associate with PYCARD (PYD and CARD domain containing/ASC, apoptosis-associated speck-like protein containing a CARD) initiating the recruitment of caspase-1 precursors and the processing of interleukin- (IL-) 1 β and IL-18 [7, 8]. Inappropriate recognition of cytoplasmic self-DNA by AIM2 contributes to the development of psoriasis, dermatitis, arthritis, and other autoimmune or inflammatory diseases [9]. AIM2 was reported upregulated in RA synovium than that of OA [5], and AIM2 inflammasome plays role in the activation of

TABLE 1: General information of patients and health controls recruited for ELISA in this study.

General information	HC ($n = 20$)	OA ($n = 25$)	RA ($n = 49$)
Gender (male/female)	8/12	7/18	11/38
Age (y/o)	45.87 \pm 11.35	55.48 \pm 9.69	50.87 \pm 9.35
Disease course (years)	/	6.41 \pm 8.88	7.27 \pm 5.11
ESR (mm/h)	/	34.7 \pm 24.88	56.12 \pm 40.36*
CRP (mg/L)	/	2.21 \pm 2.76	12.16 \pm 20.36*

HC: health controls; RA: rheumatoid arthritis; OA: osteoarthritis; ESR: erythrocyte sedimentation rate; CRP: C-reactive protein. * $p < 0.05$.

neutrophils [10] and also vascular dysfunction [11]. However, studies regarding AIM2 inflammasome on arthritis were still limited, especially investigations on clinical patients have not been reported, which leads to the AIM2 inflammasome in the pathogenesis of RA is not well demonstrated.

In this study, we investigate the differential expression partial of the AIM2 pathway associated proteins, including AIM2, ASC, caspase-1, and IL-1 β , from their features in plasma and synovium of OA and RA from mRNA and protein aspects. RA-fibroblast-like synoviocytes (RA-FLS) is critical to the pathogenesis of RA as it may develop a uniquely aggressive phenotype that increases invasiveness into the extracellular matrix and further exacerbates joint damage [12]. Therefore, in this study, we also attempt to observe si-AIM2's role in the viability of RA-FLS.

2. Materials and Methods

2.1. Patients' Serum for Enzyme Linked Immunosorbent Assay (ELISA). We enrolled 49 patients diagnosed with RA [13] and 25 patients diagnosed with OA [14] with comprehensive medical records from the Rheumatology Department in the Integrated Traditional Chinese and Western Medicine Hospital, Southern Medical University, China, between October 2017 and December 2018. Exclusion criteria included other autoimmune diseases, acute inflammation, fever, thyroid disease, diabetes, and severe liver and kidney diseases. Twenty health volunteers were enrolled as health controls (HC). Patients' sera were collected for ELISA assays of AIM2, ASC, caspase-1, and IL-1 β (R&D Systems, USA). The ELx808TM absorbance microplate reader was used to measure the absorbance values at 450 nm. Concentrations of proteins in the samples were calculated using the standard curve for each protein. The general information of the patients recruited for this study is given in Table 1. All subjects provided written informed consent for participation in the study as approved by the ethical committee of each institutional review board.

2.2. Patients' Synovium for Immunohistochemical (IHC) Staining. Arthroscopic surgery was performed on 41 RA and 26 OA patients for therapeutic purposes, and the patients' general information is shown in Table 2. Regular streptavidin biotin-based immunoperoxidase staining for AIM2, ASC, caspase-1, and IL-1 β was performed to formalin fixed, paraffin-embedded pathology keen synovium speci-

TABLE 2: General information of patients recruited for IHC in this study.

General information	RA ($n = 41$)	OA ($n = 26$)
Gender (male/female)	6/35	6/20
Age (y/o)	51.60 \pm 2.42	60.62 \pm 2.30
Disease course (years)	6.54 \pm 0.89	6.42 \pm 1.43
ESR (mm/h)	79.68 \pm 6.90	38.38 \pm 6.64***
CRP (mg/L)	30.26 \pm 5.44	7.015 \pm 4.22**

TABLE 3: General information of patients recruited for RT-qPCR in this study.

General information	RA ($n = 10$)	OA ($n = 9$)
Male to female	2 : 8	5 : 4
Age (years)	54.2 \pm 8.65	66.6 \pm 8.61**
ESR (mm/h)	86.5 \pm 50.5	37.8 \pm 29.3**
CRP (mg/L)	19.1 \pm 13.63	5.13 \pm 7.19*

mens. The H score was then applied to quantify the staining intensity [15].

RA: rheumatoid arthritis; OA: osteoarthritis; ESR: erythrocyte sedimentation rate; CRP: C-reactive protein. ** $p < 0.01$, *** $p < 0.001$.

2.3. Patients' Synovium for Quantitative Real-Time Polymerase Chain Reaction (qPCR). Synovium specimens taken from 10 RA patients and 9 OA patients were obtained via knee arthroscopy, and the patients' general information is given in Table 3. Specimens were soaked in TRIzol® Reagent (Thermo Scientific, USA) after removing adipose tissue in an aseptic environment and were then stored in a -20°C refrigerator in preparation for qPCR of the mRNA AIM2, ASC, caspase-1, and IL-1 β . qPCR was then done to evaluate the relative expression of the mRNAs of AIM2, ASC, caspase-1, and IL-1 β in FLS after transferring AIM2 siRNA. The primers used in the amplification of the target mRNAs are listed in Table 4.

RA: rheumatoid arthritis; OA: osteoarthritis; ESR: erythrocyte sedimentation rate; CRP: C-reactive protein. * $p < 0.05$, ** $p < 0.01$.

2.4. Immunofluorescent Staining for AIM2. In regard to immunofluorescent staining, both groups of RA and OA patients were blocked with normal goat serum in 0.01 M phosphate-buffered saline for 1 hour. The primary rabbit

TABLE 4: qPCR primers used in this study.

Primer name	Sense primer/sequence	Antisense primer
AIM2	AGCAAGATATTATCGGCACAGTG	GTTTCAGCGGGACATTAACCTT
ASC	CCTACTGTTCTTTCTGTGGAAG	CGAGGTCGTACGCCATCAC
CASPASE-1	TTTCCGCAAGGTTGATTTTCA	GGCATCTGCGCTCTACCATC
IL-1 β	TTCGACACATGGGATAACGAGG	TTTTTGCTGTGAGTCCCGGAG
GAPDH	ACAAC TTTGGTATCGTGGAAGG	GCCATCACGCCACAGTTTC

anti-rat AIM2 antibody (1:200) was incubated overnight at 4°C together with mouse antihuman vimentin (1:400). The following day, the sections were incubated for 60 minutes at 37°C with FITC-conjugated goat and anti-mouse antibodies (1:1000) as well as anti-rabbit antibodies (1:1000). The nuclei of cells were stained with DAPI. Observations were done under fluorescence microscopy for which the corresponding results were recorded.

2.5. AIM2 siRNA Preparation and Transfection. AIM2 siRNA were produced by the Ribobio Company, China. RA-FLS at 50–70% confluency were transfected with siRNAs (20 nM) as previously described [16]. The following siRNA sequences were used: untargeted control siRNA (5'-GCGCUAUCCAGCUUACGUAUU-3') and AIM2 siRNA (5'-GAGCTCTTCCACCTTTCA-3').

2.6. Isolation and Culture of Fibroblast-Like Synoviocytes (FLS). FLS were derived from synovial tissue specimens that were harvested from patients using microarthroscopy. They were then isolated using enzyme digestion, which was subsequently cultured in Dulbecco's Modified Essential Medium (DMEM) containing 10% fetal bovine serum (FBS, Invitrogen) and antibiotics (penicillin and streptomycin) at 37°C with 5% CO₂. The cells cultured between passages 4 and 9 were used in this study. The cells were frozen with a cell-freezing medium and stored in a -80°C freezer until they were needed.

2.7. Cell Counting Kit-8 (CCK-8) Assay. RA-FLS were seeded in 96-well plates (1 × 10⁴ cells/well) and treated with siRNA for 24, 48, and 72 hours, respectively. Cell viability was determined using Cell Counting Kit-8 (CCK-8, Dojindo Molecular Technology, Japan) according to the manufacturer's protocol. Finally, the optical density was monitored at 450 nm by a Multiskan Spectrum Microplate Reader (Thermo, USA).

2.8. Flow Cytometry in the Evaluation of Apoptosis. Flow cytometry was performed to evaluate the effects of siRNA AIM2 on FLS apoptosis. Accordingly, 48 hours after FLS was treated by siRNA AIM2, of 6-well plates in both NC and siRNA AIM2 group; the cells were collected (approximately 3 × 10⁵/well), washed twice with PBS, and resuspended in a 500 μ l 1 × binding buffer. They were then mixed with 5 μ l of Annexin-V-fluorescein isothiocyanate (FITC) and 5 μ l of propidium iodide (PI) and were detected by a flow cytometer (BD LSRFortessa™, USA). The scatter diagram demonstrated a distribution as follows: Q3: healthy

cells (FITC-/PI-), Q2: apoptotic cells at an advanced stage (FITC+/PI+), and Q4: apoptotic cells at an early stage (FITC+/PI-). The apoptosis rate is equal to the ratio of apoptotic cells to the total cells in Q4 plus the ratio of apoptotic cells to the total cells in Q2. Each experiment was conducted three times [17].

2.9. Transwell Test. For the Matrigel invasion assay, cells at the logarithmic growth phase were digested, collected, resuspended, and diluted into a concentration of 3 × 10⁴/ml in a serum-free medium. The cell suspension (200 μ l) was added to the upper chamber and coated with Matrigel (BD Bioscience) diluted with DMEM media (1:3), while 500 μ l DMEM media containing 10% FBS was added to the lower chamber. Following incubation for 12 h at 37°C, the cells in the upper membrane were discarded, and cells on the lower membrane were fixed using 4% Paraformaldehyde for 25 min and stained with 0.1% crystal violet (Beyotime, USA) for 10 min. Next, migrated RA-FLS five random fields were counted.

2.10. Automated Electrophoresis Western Blot Analysis. FLS were seeded at 1 – 2 × 10⁵ cells per well in 6-well plates and incubated for adherence. The medium in the wells was replaced with fresh medium containing metformin (5 mM) or saline for 48 h. After aspiration of the medium, the cell monolayers were rinsed with 1 ml ice-cold PBS and lysed in 80 μ l of lysis buffer (20 mM Tris-HCl pH 7.5, 150 mM NaCl, 1 mM EDTA, 1 mM EGTA, 1% (v/v) TritonX100, 2.5 mM sodium pyrophosphate, and 1 mM β -glycerophosphate), which were then supplemented with fresh 1 mM Na₃VO₄ and 1 mM dithiothreitol containing a 1 X protease inhibitor cocktail (Roche Molecular Biochemicals, Basel, Switzerland). The lysates were precleared by centrifugation at 18000 g for 15 min at 4°C. The supernatants were then collected, and the protein concentrations were measured using a Bradford assay (Thermofisher, Massachusetts, USA). Next, the lysates were adjusted to 5 mg/ml protein concentration. Capillary electrophoresis Western blot analysis was carried out using the manufacturer's reagents provided in the user manual (ProteinSimple WES, San Francisco, USA). Briefly, 5.6 μ l of the cell lysate was mixed with 1.4 μ l of the fluorescent master mix and heated at 95°C for 5 min. The samples, blocking reagent, wash buffer, antibody of tubulin (1:100 R&D Systems) and AIM2 (1:50 R&D Systems), secondary antibody, and chemiluminescent substrate were dispensed into the microplates. Then, electrophoretic separation and immunodetection were automatically performed using the default settings. The data was analyzed using the built-in

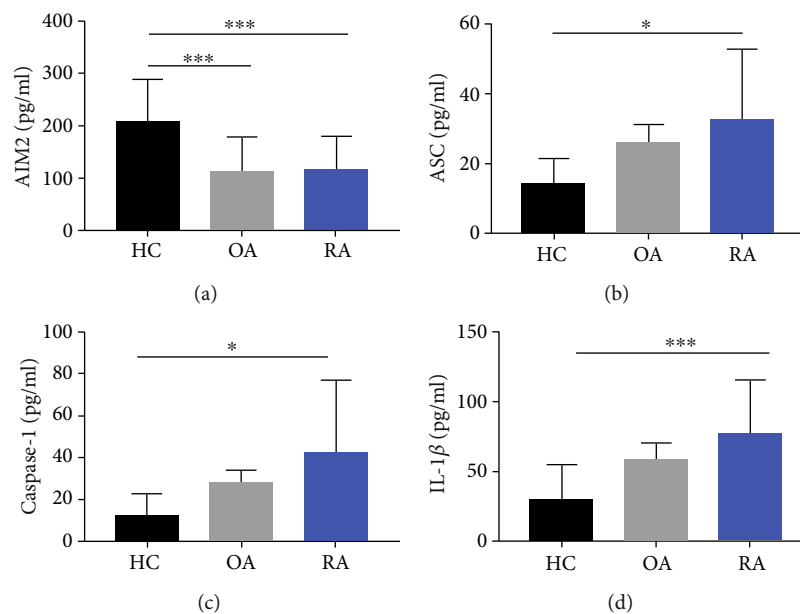


FIGURE 1: The differences in AIM2 pathway-related molecules in sera among HCs, OA, and RA patients. The HCs expressed obviously higher level of AIM2 than OA and RA patients (a), and ASC, caspase-1, and IL-1 β expressed obviously higher in RA patients than HCs (b-d). No statistical differences of these molecules between OA and RA (a-d). * $p < 0.05$, *** $p < 0.001$, and **** $p < 0.0001$.

Compass software for SW 4.0. The truncated and full-length AIM2 and tubulin intensities (area under the curve) were normalized to that of the tubulin peak (control). In most of the figures, electropherograms are represented as pseudo-blot, which were generated using the Compass software.

2.11. Statistical Analysis. The statistical analysis was conducted using the GraphPad Prism 7.0 software. All data were denoted as mean \pm SD. Differences between two groups were evaluated for statistical significance using Student's t -test. Kruskal-Wallis and Dunn's multiple comparison post hoc tests were used to evaluate the differences among three or more groups. Correlations were evaluated using Spearman's Rank correlation test, where $p \leq 0.05$ was considered as statistically significant.

3. Results

3.1. No Significant Difference of AIM2 Levels in Sera between OA and RA. Through ELISA, no differences in the AIM2 expression were observed between the sera of OA and RA; however, the HCs expressed obviously higher level of AIM2 than OA and RA patients (Figure 1(a)). The downstream molecules in AIM2 inflammasome pathway including ASC, caspase-1, and IL-1 β expressed obviously higher in RA patients than HCs. Although there were tendency of increasing expression from OA to RA, no statistical significance was observed (Figures 1(b)–1(d)).

3.2. AIM2 Was Expressed More in RA Synovium than in That of OA. The relative expression levels of mRNA AIM2 as well as the AIM2 pathway-related proteins including ASC and IL-

1 β were higher in the local synovium of RA than that of OA. Moreover, the relative expression of caspase-1 was higher in RA than in OA without statistical significance (Figure 2(a)).

Through the H scores in the synovium of RA, AIM2, and the AIM2 pathway-related proteins like ASC, caspase-1, and IL-1 β were more expressed than that of OA (Figure 2(b)). AIM2, ASC, caspase-1, and IL-1 β were positively correlated to the clinical features of RA, as indicated by the ESR and CRP levels (Figure 3).

By performing IHC staining, AIM2 and AIM2 pathway-related proteins were detected in the nucleus and cytoplasm, which are seen in most types of cells including macrophages, lymphocytes, and FLS. As FLS produce cytokines that perpetuate inflammation and proteases that contribute to cartilage destruction, it plays a critical role in the pathogenesis of RA [18]. Hence, this study focuses on the AIM2 pathway in FLS. It was confirmed that AIM2 could be expressed in the cytoplasm of FLS (Figure 4(a)), and AIM2 and its mRNA are relatively higher in RA-FLS than in OA (Figures 4(b) and 4(c)).

3.3. AIM2 siRNA Inhibited Proliferation but Not Migration and Apoptosis of RA-FLS. As we designed siRNAs for AIM2, its efficacy demonstrated its successful silencing of the mRNA AIM2 expression along with downstream molecules including ASC, caspase-1, and IL-1 β (Figure 5(a)). Western blot confirmed the successful silencing of the AIM2 expression by si-AIM2 (Figure 4(b)). By utilizing CCK-8 assay, AIM2 siRNA was found to inhibit the proliferation of RA-FLS (Figure 5(c)). However, no significant difference in the apoptotic rate or number of migrated cells was observed among the normal control and si-AIM2 groups (Figures 5(d) and 5(e)).

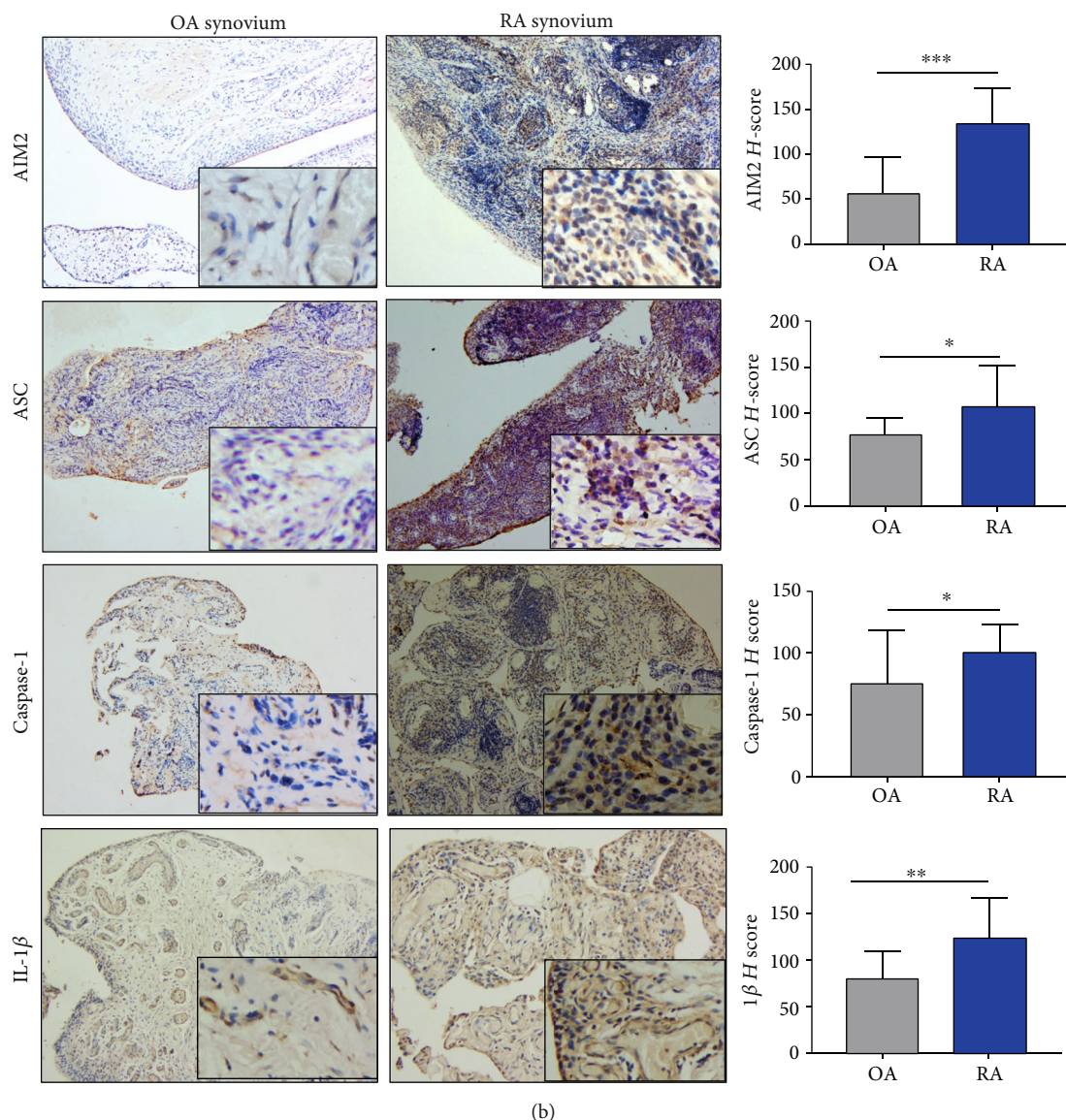
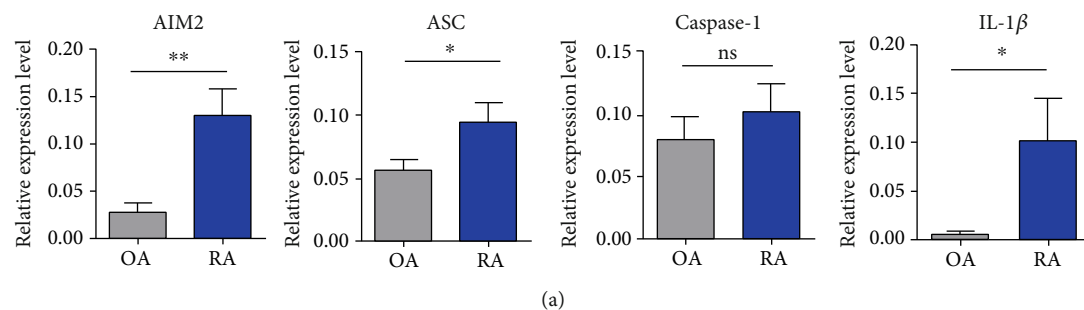


FIGURE 2: The differences in AIM2 pathway-related molecules in synovium among OA and RA. mRNA AIM2 and AIM2 pathway-related proteins including ASC and IL-1 β were expressed higher in RA than in OA; caspase-1 was higher in RA than in OA without statistical significance (a). H score for the synovium of RA, AIM2, and AIM2 pathway-related proteins including ASC, caspase-1, and IL-1 β was more expressed than that of OA (b). * $p < 0.05$, ** $p < 0.01$, and *** $p < 0.0001$.

4. Discussion

As one of the most commonly encountered autoimmune diseases, both innate and adaptive immune responses participate in the pathogenesis of RA [19]. AIM2 has been mostly

studied in cells of the immune system or within the context of infection; however, its role in other tissues remains to be investigated. AIM2 acts as an important component of inflammasome that senses potentially dangerous cytoplasmic DNA, leading to the activation of the ASC pyroptosome,

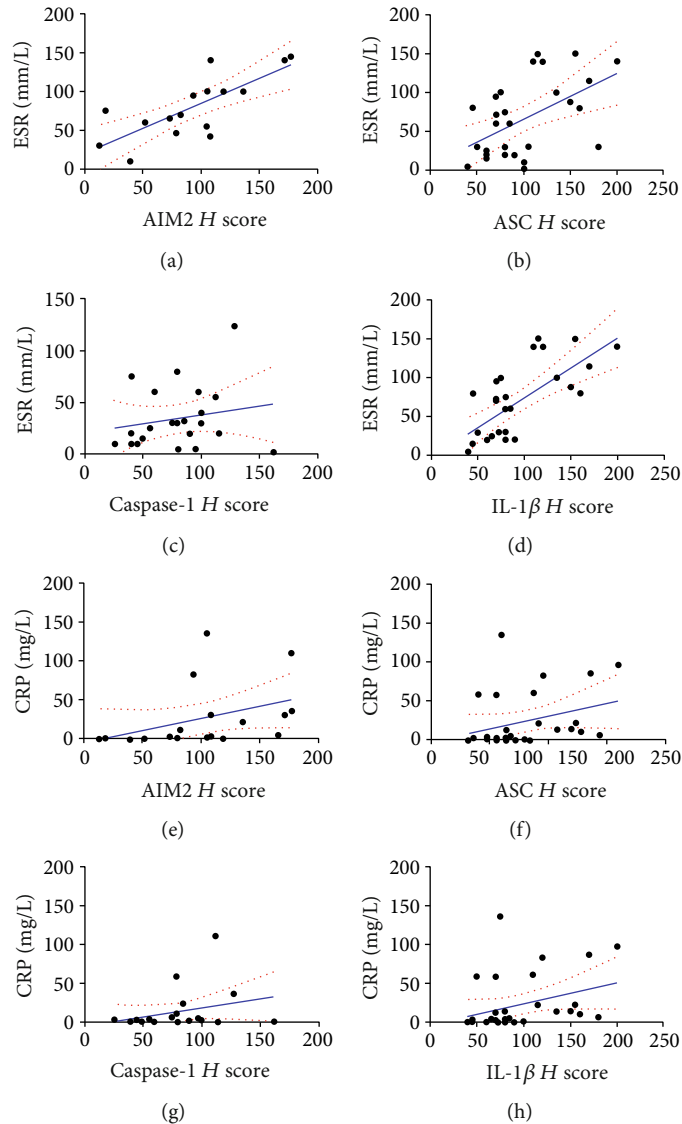


FIGURE 3: *H* scores of AIM2, ASC, and IL-1 β were positively correlated with ESR and CRP. AIM2 demonstrated a positive correlation with ESR ($r = 0.74$, $p = 0.001$, 95% CI: 0.38-0.9) and CRP ($r = 0.65$, $p = 0.003$, 95% CI: 0.25-0.86) (a, e). The positive correlations between ASC and ESR ($r = 0.5$, $p = 0.005$, 95% CI: 0.16-0.74) as well as CRP ($r = 0.42$, $p = 0.02$, 95% CI: 0.05-0.69) were detected (b, f). The positive correlations between IL-1 β and ESR ($r = 0.62$, $p = 0.0004$, 95% CI: 0.31-0.81) and CRP ($r = 0.41$, $p = 0.02$, 95% CI: 0.05-0.67) were detected. The correlations between CASPSE-1 and ESR as well as CRP were not statistically significant ($p > 0.05$) (c, d).

caspase-1, and processing of IL-1 β and IL-18 [20]. A plethora of MtDNA and damaged DNA have been observed in the synovial fluid of RA patients [21]. Although the role of AIM2 has been investigated in the context of DNase deficiency mice, the role of the AIM2 pathway in the pathogenesis of RA patients has rarely been investigated. Besides the distinct pathological differences, OA patients also have slightly increased inflammatory status and pannus-like tissue in affected synovium [22], which make them qualified to be the controls for study of RA. Therefore, this study compared the AIM2 pathway-associated proteins including AIM2, ASC, caspase-1, and IL-1 β in the sera and synovium of RA and OA.

Accordingly, it was found that AIM2, ASC, caspase-1, and IL-1 β were without a significant difference between OA and RA in plasma; however, upregulation was observed in

affected joints in the RA synovium than that of OA. Although AIM2 is mostly expressed in the cytoplasm, it may also be detected in serum [23]. We first analyzed the serum levels of AIM2 among HC, OA, and RA patients. However, the plasma levels of AIM2 inflammasome-associated molecules such as ASC, caspase-1, and IL-1 β among the OA and RA patients have no significant difference, although expressed higher in RA than HC, which is reasonable according to the knowledge that they participates in inflammation process [24]. A meta-analysis reported that a high level of expression of AIM2 in peripheral blood mononuclear cells (PBMC) was observed in RA patients [25]. It is surprisingly to observe the decreased levels of AIM2 in RA than HC in our study. Recently, Mendez-Frausto et al. [26] observed that AIM2 was reduced at a systemic level in patients with RA, and the monocytes of RA patients were found to be prone to releasing

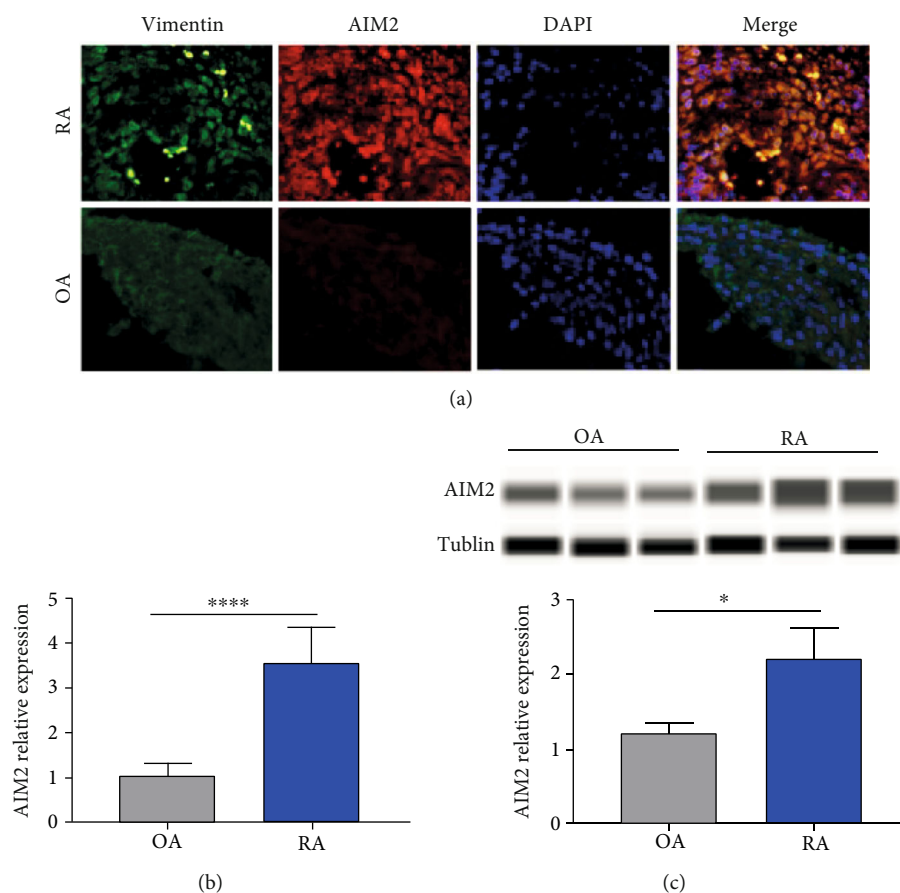


FIGURE 4: AIM2 is expressed more in RA-FLS than in OA. AIM2 expressed in the cytoplasm of FLS, which is higher in RA-FLS than in OA-FLS ((a) vimentin was labelled as green, AIM2 as red, and nuclei as blue by immunofluorescent staining). The relative expression of AIM2 mRNA and protein levels was higher in RA-FLS than in OA (b, c). * $p < 0.05$ and **** $p < 0.0001$.

IL-1 β in the absence of AIM2 inflammasome signals. These findings were in accordance with our results of ELISA; however, reasons regarding the decreased levels of AIM2 according to disease activity in serum remain unclear. Next, the mRNA and protein levels of AIM2 and its downstream proteins including ASC, caspase-1, and IL-1 β in RA were higher in RA than that in OA synovium. The results are consistent with previous investigations [27–29]. However, our data is the first study that investigates the expression of AIM2 inflammasomes in the synovium of inflamed joints from clinical patients. Studies showed that OA and RA pannus have similar qualitative metabolic characteristics and proinflammatory cytokine response; however, OA synovial tissue and pannus had lower production of proteoglycans, type II collagen, and proinflammation cytokines than RA [30, 31]. AIM2 in RA patients' synovium was elevated compared to a less severe form of OA inflammatory. Furthermore, the expression of AIM2 inflammasome-related molecules were observed positively correlated with the ESR and CRP, which confers obvious statistical significance. Thus, we speculate that AIM2 pathway contributes to the inflammatory pathogenesis of RA.

AIM2 plays a different role and acts via different signaling pathways under different circumstances according to studies regarding cancer that have been previously published.

The AIM2 pathway serves a putative role in tumorigenic reversion and may control cell proliferation [32, 33]. AIM2 expression suppressed the proliferation and tumorigenicity of human breast cancer cells, and AIM2 gene therapy inhibited mammary tumor growth in an orthotopic tumor model. However, AIM2 promotes cell growth in non-small-cell lung cancer [32]. AIM2 expression greatly suppressed nuclear factor-kappa B transcriptional activity and desensitized tumor necrosis factor-alpha (TNF- α) mediated nuclear factor-kappa B activation [34]. Inspired by the role of AIM2 in cancer research, we focused our study on FLS, which mimics the cancer cell biobehaviours of proliferation and invasion and is currently regarded as a crucial effector in the pathogenesis of RA. In IHC staining, we can observe multiple cells including FLS could be stained positively with AIM2 and immunofluorescent staining confirmed the expression of AIM2 in FLS. Then, qPCR and automated electrophoresis Western blot analysis showed RA-FLS express higher level of AIM2 than that of OA. In recent decades of research, the role of FLS in pathogenesis of rheumatoid arthritis has been arising more and more attention and regarded as key effector cells [35]. The synovium in RA transforms from a quiescent relatively acellular structure to a hyperplastic, invasive tissue teeming with immunocompetent cells, to form pannus, which contributes to destructing joint

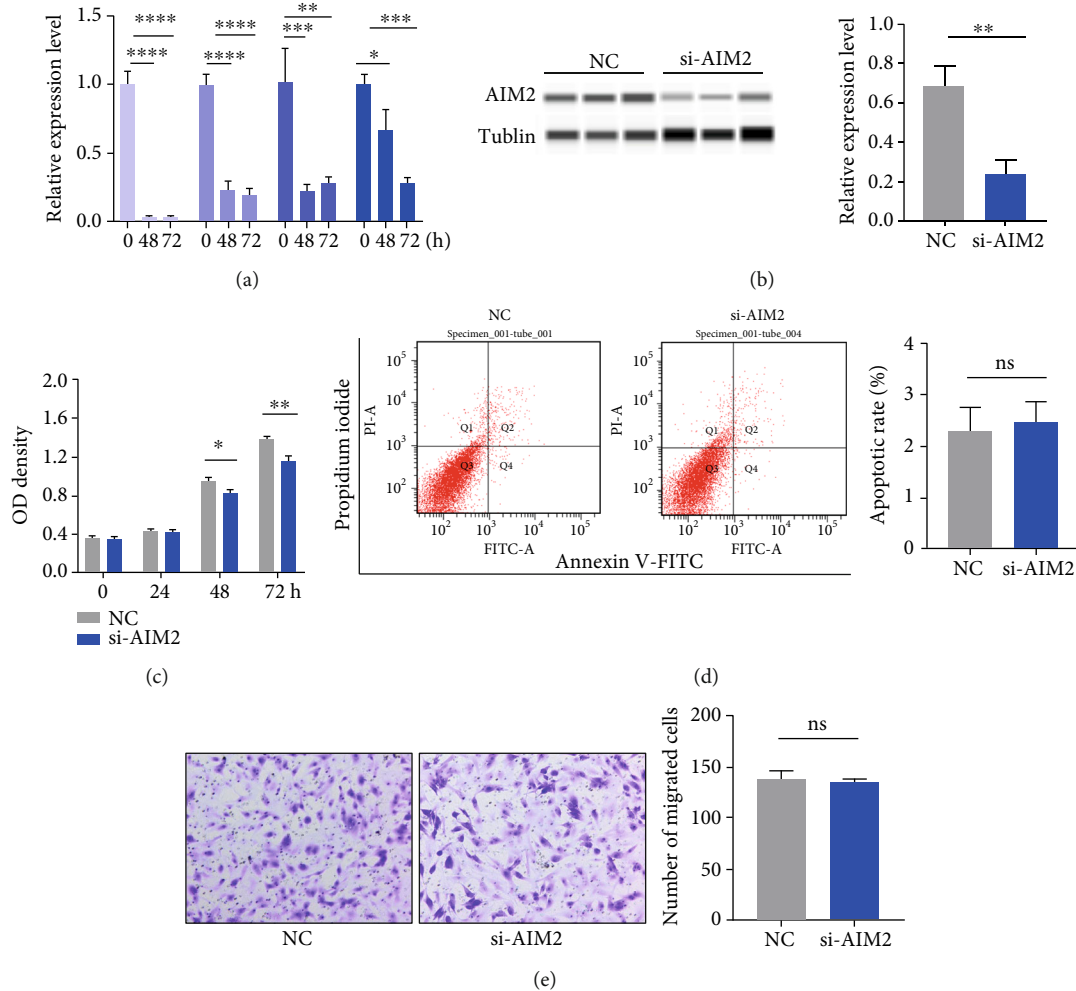


FIGURE 5: Proliferation, apoptosis, and migration assay of RA-FLS after si-AIM2 transfection. AIM2 and its downstream proteins including ASC, caspase-1, and IL-1 β were successfully silenced after 24 h of transfection (a). Western blot confirmed the successful silencing of the AIM2 expression by si-AIM2 (b). The proliferation of RA-FLS was inhibited after 48 h of transfection (c). There were no significant differences between the NC and si-AIM2 groups in apoptosis and migration assay (d, e). * $p < 0.05$, ** $p < 0.01$, *** $p < 0.001$, and **** $p < 0.0001$.

cartilage through their production of inflammatory cytokines [18]. Thus, we focus on whether AIM2 plays a role in viability of RA-FLS. The results demonstrated that the proliferation of FLS was inhibited when AIM2 was silenced in FLS by siRNA. However, the apoptosis and migration were unaffected.

In summary, based on the study of AIM2 pathway, we acknowledged its unregulated change in RA, which is more obvious in local affected joints. Furthermore, we learned AIM2 is upregulated in FLS, and suppress its expression leads to inhibiting effect on FLS proliferation, which suggest AIM2 a promising therapeutic target in RA. The corresponding underlying mechanisms of the results obtained in this study require further investigation.

Data Availability

The data used to support the findings of this study are available from the corresponding author upon request.

Ethical Approval

This study was approved by the Ethics Committee of Integrated Traditional Chinese and Western Medicine Hospital, Southern Medical University (approval No. NFZXIYEC-2017-002).

Conflicts of Interest

None declared.

Authors' Contributions

YC designed this study, analyzed the data, and wrote the manuscript. FJQ conducted the most assays, contributed equally to this work, and listed as first co-author. ESC, BJY, FFZ, and YY collected the clinical samples including plasma and synovium needed in this study. XFZ prepared the ethical

approval for the study. CHX participated and designed the study and reviewed the manuscript.

Acknowledgments

This work was funded by the National Natural Science of China (NSFC) (Project No. 81673723) and Scientific Research Project of Guangdong Province Traditional Chinese Medicine Bureau (Project No. 20201229).

References

- [1] E. Calabresi, F. Petrelli, A. F. Bonifacio, I. Puxeddu, and A. Alunno, "One year in review 2018: pathogenesis of rheumatoid arthritis," *Clinical and Experimental Rheumatology*, vol. 36, no. 2, pp. 175–184, 2018.
- [2] T. D. Mahajan and T. R. Mikuls, "Recent advances in the treatment of rheumatoid arthritis," *Current Opinion in Rheumatology*, vol. 30, no. 3, pp. 231–237, 2018.
- [3] The RACI consortium, the GARNET consortium, Y. Okada et al., "Genetics of rheumatoid arthritis contributes to biology and drug discovery," *Nature*, vol. 506, no. 7488, pp. 376–381, 2014.
- [4] S. Smith and C. Jefferies, "Role of DNA/RNA sensors and contribution to autoimmunity," *Cytokine & Growth Factor Reviews*, vol. 25, no. 6, pp. 745–757, 2014.
- [5] W. C. Li, D. L. Bai, Y. Xu et al., "Identification of differentially expressed genes in synovial tissue of rheumatoid arthritis and osteoarthritis in patients," *Journal of Cellular Biochemistry*, vol. 120, no. 3, pp. 4533–4544, 2018.
- [6] V. Hornung, A. Ablasser, M. Charrel-Dennis et al., "AIM2 recognizes cytosolic dsDNA and forms a caspase-1-activating inflammasome with ASC," *Nature*, vol. 458, no. 7237, pp. 514–518, 2009.
- [7] S. Huang, Z. Song, L. Jiang et al., "Absent in melanoma 2 (AIM2) expressed in human dental pulp mediates IL-1 β secretion in response to cytoplasmic DNA," *Inflammation*, vol. 38, no. 2, pp. 566–575, 2015.
- [8] V. A. Rathinam, Z. Jiang, S. N. Waggoner et al., "The AIM2 inflammasome is essential for host defense against cytosolic bacteria and DNA viruses," *Nature Immunology*, vol. 11, no. 5, pp. 395–402, 2010.
- [9] S. M. Man, R. Karki, and T. D. Kanneganti, "AIM2 inflammasome in infection, cancer, and autoimmunity: role in DNA sensing, inflammation, and innate immunity," *European Journal of Immunology*, vol. 46, no. 2, pp. 269–280, 2016.
- [10] M. Bakele, M. Joos, S. Burdi et al., "Localization and functionality of the inflammasome in neutrophils," *The Journal of Biological Chemistry*, vol. 289, no. 8, pp. 5320–5329, 2014.
- [11] J. Williams, "Characterisation of vascular dysfunction in a murine model of rheumatoid arthritis[Ph.D. Thesis]," Cardiff University, Cardiff, 2017.
- [12] P. G. de Oliveira, M. Farinon, E. Sanchez-Lopez, S. Miyamoto, and M. Guma, "Fibroblast-like synoviocytes glucose metabolism as a therapeutic target in rheumatoid arthritis," *Frontiers in Immunology*, vol. 10, p. 1743, 2019.
- [13] K. Kaarela, M. J. Kauppi, and K. E. S. Lehtinen, "The value of the ACR 1987 criteria in very early rheumatoid arthritis," *Scandinavian Journal of Rheumatology*, vol. 24, no. 5, pp. 279–281, 1995.
- [14] W. Zhang, M. Doherty, G. Peat et al., "EULAR evidence-based recommendations for the diagnosis of knee osteoarthritis," *Annals of the Rheumatic Diseases*, vol. 69, no. 3, pp. 483–489, 2010.
- [15] W. E. Pierceall, M. Wolfe, J. Suschak et al., "Strategies for H-score normalization of preanalytical technical variables with potential utility to immunohistochemical-based biomarker quantitation in therapeutic response diagnostics," *Analytical Cellular Pathology*, vol. 34, no. 3, pp. 168 pages, 2011.
- [16] Y. Dombrowski, M. Peric, S. Koglin et al., "Cytosolic DNA triggers inflammasome activation in keratinocytes in psoriatic lesions," *Science Translational Medicine*, vol. 3, no. 82, 2011.
- [17] P. S. Rabinovitch, M. Kubbies, Y. C. Chen, D. Schindler, and H. Hoehn, "BrdU—Hoechst flow cytometry: a unique tool for quantitative cell cycle analysis," *Experimental Cell Research*, vol. 174, no. 2, pp. 309–318, 1988.
- [18] M. F. Bustamante, R. Garcia-Carbonell, K. D. Whisenant, and M. Guma, "Fibroblast-like synoviocyte metabolism in the pathogenesis of rheumatoid arthritis," *Arthritis Research & Therapy*, vol. 19, no. 1, 2017.
- [19] F. Coutant and P. Miossec, "Evolving concepts of the pathogenesis of rheumatoid arthritis with focus on the early and late stages," *Current Opinion in Rheumatology*, vol. 32, no. 1, pp. 57–63, 2020.
- [20] T. Fernandes-Alnemri, J. W. Yu, P. Datta, J. Wu, and E. S. Alnemri, "AIM2 activates the inflammasome and cell death in response to cytoplasmic DNA," *Nature*, vol. 458, no. 7237, pp. 509–513, 2009.
- [21] S. Hajizadeh, J. DeGroot, J. M. TeKoppele, A. Tarkowski, and L. V. Collins, "Extracellular mitochondrial DNA and oxidatively damaged DNA in synovial fluid of patients with rheumatoid arthritis," *Arthritis Research & Therapy*, vol. 5, no. 5, pp. R234–R240, 2003.
- [22] C.-C. Yang, C.-Y. Lin, H.-S. Wang, and S.-R. Lyu, "Matrix metalloproteases and tissue inhibitors of metalloproteinases in medial plica and pannus-like tissue contribute to knee osteoarthritis progression," *PLoS One*, vol. 8, no. 11, article e79662, 2013.
- [23] J. Lugrin and F. Martinon, "The AIM2 inflammasome: sensor of pathogens and cellular perturbations," *Immunological Reviews*, vol. 281, no. 1, pp. 99–114, 2018.
- [24] V. A. K. Rathinam and F. K. Chan, "Inflammasome, inflammation, and tissue homeostasis," *Trends in Molecular Medicine*, vol. 24, no. 3, pp. 304–318, 2018.
- [25] S. Afroz, J. Giddaluru, S. Vishwakarma, S. Naz, A. A. Khan, and N. Khan, "A comprehensive gene expression meta-analysis identifies novel immune signatures in rheumatoid arthritis patients," *Frontiers in Immunology*, vol. 8, p. 74, 2017.
- [26] G. Méndez-Frausto, M. N. Medina-Rosales, E. E. Uresti-Rivera et al., "Expression and activity of AIM2-inflammasome in rheumatoid arthritis patients," *Immunobiology*, vol. 225, no. 2, article 151880, 2020.
- [27] Z. Yang, J. Cao, C. Yu, Q. Yang, Y. Zhang, and L. Han, "Caspase-1 mediated interleukin-18 activation in neutrophils promotes the activity of rheumatoid arthritis in a NLRP3 inflammasome independent manner," *Joint, Bone, Spine*, vol. 83, no. 3, pp. 282–289, 2016.
- [28] R. Cascão, J. Polido-Pereira, H. Canhão et al., "Caspase-1 is active since the early phase of rheumatoid arthritis," *Clinical and Experimental Rheumatology*, vol. 30, no. 1, p. 144, 2012.
- [29] A. Eljaafari, M. L. Tartelin, H. Aissaoui et al., "Bone marrow-derived and synovium-derived mesenchymal cells promote Th17 cell expansion and activation through caspase 1

- activation: contribution to the chronicity of rheumatoid arthritis,” *Arthritis Rheum*, vol. 64, no. 7, pp. 2147–2157, 2012.
- [30] J. Furuzawa-Carballeda, P. M. Macip-Rodriguez, and A. R. Cabral, “Osteoarthritis and rheumatoid arthritis pannus have similar qualitative metabolic characteristics and pro-inflammatory cytokine response,” *Clinical & Experimental Rheumatology*, vol. 26, no. 4, pp. 554–560, 2008.
- [31] C. Guo, R. Fu, S. Wang et al., “NLRP3 inflammasome activation contributes to the pathogenesis of rheumatoid arthritis,” *Clinical and Experimental Immunology*, vol. 194, no. 2, pp. 231–243, 2018.
- [32] M. Zhang, C. Jin, Y. Yang et al., “AIM2 promotes non-small-cell lung cancer cell growth through inflammasome-dependent pathway,” *Journal of Cellular Physiology*, vol. 234, no. 11, pp. 20161–20173, 2019.
- [33] J. Chen, Z. Wang, and S. Yu, “aiM2 regulates viability and apoptosis in human colorectal cancer cells via the Pi3K/akt pathway,” *OncoTargets and Therapy*, vol. 10, pp. 811–817, 2017.
- [34] I. F. Chen, F. Ou-Yang, J. Y. Hung et al., “AIM2 suppresses human breast cancer cell proliferation in vitro and mammary tumor growth in a mouse model,” *Molecular Cancer Therapeutics*, vol. 5, no. 1, pp. 1–7, 2006.
- [35] B. Bartok and G. S. Firestein, “Fibroblast-like synoviocytes: key effector cells in rheumatoid arthritis,” *Immunological Reviews*, vol. 233, no. 1, pp. 233–255, 2010.

Research Article

Molecularly Distinct NLRP3 Inducers Mediate Diverse Ratios of Interleukin-1 β and Interleukin-18 from Human Monocytes

Kristine Midtbö ^{1,2} Daniel Eklund ^{1,2} Eva Särndahl ^{1,2} and Alexander Persson ^{1,2}

¹School of Medical Sciences, Faculty of Medicine and Health, Örebro University, SE-701 82 Örebro, Sweden

²Inflammatory Response and Infection Susceptibility Centre (iRiSC), Faculty of Medicine and Health, Örebro University, SE-701 82 Örebro, Sweden

Correspondence should be addressed to Kristine Midtbö; kristine.midtbo@oru.se

Received 8 July 2020; Revised 10 September 2020; Accepted 29 September 2020; Published 22 October 2020

Academic Editor: Young-Su Yi

Copyright © 2020 Kristine Midtbö et al. This is an open access article distributed under the Creative Commons Attribution License, which permits unrestricted use, distribution, and reproduction in any medium, provided the original work is properly cited.

Inflammasomes cleave and activate interleukin- (IL-) 1 β and IL-18 which have both shared and unique biological functions. IL-1 β is an important mediator of the acute phase response to infections and tissue damage, whereas IL-18 takes part in activation and tailoring of the adaptive immune response. While IL-1 β has served as the prototypic indicator of inflammasome activation, few studies have compared the potential differences in IL-1 β and IL-18 production during inflammasome activation. Since these cytokines partake in different immune pathways, the involvement of inflammasome activity in different conditions needs to be described beyond IL-1 β production alone. To address a potential heterogeneity in inflammasome functionality, ATP, chitosan, or silica oxide (SiO₂) were used to induce NLRP3 inflammasome activation in THP-1 cells and the subsequent outcomes were quantified. Despite using doses of the inflammasome inducers yielding similar release of IL-1 β , SiO₂-stimulated cells showed a lower concentration of released IL-18 compared to ATP and chitosan. Hence, the cells stimulated with SiO₂ responded with a distinctly different IL-18 : IL-1 β ratio. The difference in the IL-18 : IL-1 β ratio for SiO₂ was constant over different doses. While all downstream responses were strictly dependent on a functional NLRP3 inflammasome, the differences did not depend on the level of gene expression, caspase-1 activity, or pyroptosis. We suggest that the NLRP3 inflammasome response should be considered a dynamic process, which can be described by taking the ratio between IL-1 β and IL-18 into account and moving away from an on/off perspective of inflammasome activation.

1. Introduction

IL-1 β and IL-18 are crucial for mounting a potent pro-inflammatory response and directing subsequent immune responses. Activation of interleukin- (IL-) 1 β and IL-18 into their biologically active forms require the formation of a multiprotein complex called inflammasome [1]. Today, several inflammasomes have been described, with the nomenclature depending on the main Nod-like receptor (NLR) involved. Upon activation, the NLRs oligomerize to form the core of the inflammasome complex by recruiting the adaptor protein apoptosis-associated speck-like protein containing a CARD (ASC). ASC in turn recruits and activates the serine protease caspase-1 that is the effector caspase responsible for the bioactivation of IL-1 β , IL-18, and gasdermin D (GSDMD) [2, 3].

Due to the inflammatory potency in the cytokines regulated by inflammasomes, activation of the inflammasome is under strict regulation and requires two distinct signals. Signal one upregulates inflammasome components and the pro-form of IL-1 β [3], while the second signal can then activate a specific NLR, initiating the formation of the inflammasome complex. Whereas many NLRs such as AIM2 and NLRC4 initiate inflammasome formation as a response to specific agonists, the NLRP3 inflammasome can be activated by a broad range of stimuli related to both pathogens, cellular stress and tissue damage. The NLRP3 inflammasome is by far the most studied inflammasome, and the vast array of potential inducers renders it unlikely that the NLRP3 receptor directly interacts with the agonists [4, 5]. Among the characterized inflammasome inducers are adenosine tri-

phosphate (ATP), a nucleotide and well-known danger signal which activates NLRP3 through K^+ efflux after binding to the ATP receptor P2X7 [6–9]. Chitosan, a family of linear polysaccharides found in fungal cell walls, is believed to activate the NLRP3 by lysosomal disruption [10], K^+ efflux, and/or through induction of reactive oxygen species [11, 12]. Inorganic silica oxide crystals (SiO_2) have been reported to activate the NLRP3 inflammasome through lysosome disruption, induction of mitochondrial damage [13, 14], or alternatively through the scavenger receptor SR-B1 [15].

Production of IL-1 β is often used as the proxy for describing inflammasome activation. However, using this benchmark indicates that inflammasome activation is a static mechanism, and the possibility of different signaling pathways inducing different effects on the functional aspects following inflammasome activation are generally not discussed. Active IL-1 β and IL-18 share several functions as proinflammatory cytokines, but they also have unique properties resulting in distinct immunological profiles. IL-1 β is a pyrogen that induces fever, which is a property that IL-18 lack [16, 17]. Other features of IL-1 β include neutrophil mobilization, acute phase protein production, Th17 differentiation, and enhanced antigen presentation and glycolytic rate in Th17 cells and macrophages [16–20]. On the other hand, IL-18 promotes Th1 or Th2 differentiation, depending on the cytokine environment [21], and induces IFN- γ production from Th1 cells and NK-cells as well as IL-13 and IL-4 from basophils and mast cells [22].

IL-1 β and IL-18 also contribute to the pathogenesis of many diseases, but they play different roles. Since IL-1 β promotes Th17 differentiation, IL-1 β can be related to many Th17-driven diseases, including rheumatoid arthritis, multiple sclerosis, and psoriasis [23–25]. IL-1 β also take part in the pathogenesis of gout, osteoarthritis, inflammatory bowel disease, pericarditis, macrophage activating syndrome, chronic obstructive pulmonary disease (COPD) [26–31], and chronic systemic inflammatory conditions, like cryopyrin-associated periodic syndrome (CAPS), adult-onset Still's disease, and familial Mediterranean fever (FMF) [26, 32, 33]. On the other hand, IL-18 is strongly related to IFN- γ and Th1/Th2 diseases, like systemic lupus erythematosus, Crohn's disease, and graft versus host rejection [16, 31, 34, 35]. IL-18 is also a key player in allergy, atherosclerosis, dermatitis, acute renal ischemia, hepatitis, and heart failure [31, 36–41]. However, even if IL-1 β or IL-18 may play a dominant role, both often contribute to the disease but play separate roles at different stages of diseases. Knockout studies in a mouse model of CAPS showed that loss of the IL-1 β or IL-18 receptor was differently beneficial in young and old mice [42]. Additionally, FMF have shown to be correlated to elevated levels of IL-18, while IL-1 β play a dominant role during inflammatory flare ups that are treated with IL-1 β inhibition [43, 44]. Several approved therapies target the IL-1 receptor (IL-1R) or free circulating IL-1 β , including the IL-1R antagonist anakinra (Kineret®). This have been proven to be successful in many cases but since targeting IL-1 β does not inhibit the effect of IL-18, it is not surprising that certain conditions are unaffected by the treatment [45], and recently, efforts have been made to investigate the effectiveness of instead

blocking IL-18 in certain inflammatory diseases [41, 46, 47]. Since IL-1 β and IL-18 contribute diversely to different diseases, it is unlikely that inflammasome activation is a static on/off process. Consequently, when studying inflammasome functionality, the activity may need to be described beyond IL-1 β production. This study was therefore designed to describe the outcome of NLRP3 inflammasome activation and the functional effects of diverse inflammasome inducers.

2. Materials and Methods

2.1. Cell Culture. THP-1 cells were cultured in RPMI medium 1640 (Gibco, Thermo Fisher Scientific, Waltham, MA cat. nr:31870-025) supplemented with 10% fetal bovine serum (FBS), Hepes (10 mM), sodium pyruvate (1 mM), GlutaMax (2 mM), glucose (2.5 g/L), and penicillin-streptomycin (PEST, 100 U/mL) all from Gibco (Thermo Fisher Scientific). The THP-1 cell lines used are THP-1 null cells (thp-null), THP-1 defNLRP3 cells (rhp-dnlp), THP-1 defASC cells (thp-dasc), THP-1 defCASP1 (thp-dcasp1), and THP-1 Xblue™-MD2-CD14 cells (thp-mcdsp) which were all acquired from InvivoGen (San Diego, CA). The THP-1 cells were kept undifferentiated as a model of human monocytes.

2.2. Isolation of Primary Human Monocytes. Human CD14⁺ cells were isolated from healthy volunteers. PBMCs were separated by density gradient centrifugation on Lymphoprep (Axis-Shield, Oslo, Norway), and the CD14⁺ cells were isolated by magnetic sorting using CD14 MACS microbeads (Miltenyi Biotech, Bergisch Gladbach, Germany) according to the manufacturer's protocol. The cells were cultured in DMEM medium (Lonza BioWhittaker, Thermo Fisher Scientific cat. nr: 11635220) supplemented with 10% human AB serum (pooled from five healthy volunteers), L-glutamine (5 mM), sodium pyruvate (5 mM), and glucose (2.5 g/L) (Gibco, Thermo Fisher Scientific).

2.3. Experimental Setup. THP-1 cells were seeded into 96- or 24-well plates and primed with lipopolysaccharide- (LPS-) B5 (E. coli serotype 055:K59(B5)H-, 100 ng/mL, or concentrations indicated in Figure 1(d)) for 10 minutes to induce instant priming, followed by additional stimulation with ATP (5 mM), chitosan (30 μ g/mL), or SiO_2 (30 μ g/mL) all from InvivoGen, for 24 h.

Isolated primary human monocytes were primed with 10 ng/mL LPS prior to stimulation with 10 nM ATP, 10 ng/mL chitosan, or 10 ng/mL SiO_2 .

2.4. Cytokine Measurement. The concentrations of cytokines were measured with enzyme-linked immunosorbent assay (ELISA) for IL-1 β (BioLegend, San Diego, CA) and IL-18 (R&D Systems, Minneapolis, MN) according to the manufacturer's instruction.

2.5. SEAP Reporter Assay. NF- κ B activity was measured indirectly by the SEAP activity from a NF- κ B responsive SEAP reporter gene in the reporter THP-1 xBlue™ cells. The accumulation of SEAP in the culture medium 24 h after stimulation was detected with the QUANTI-Blue™ (InvivoGen) according to the manufacturer's instructions. The OD was

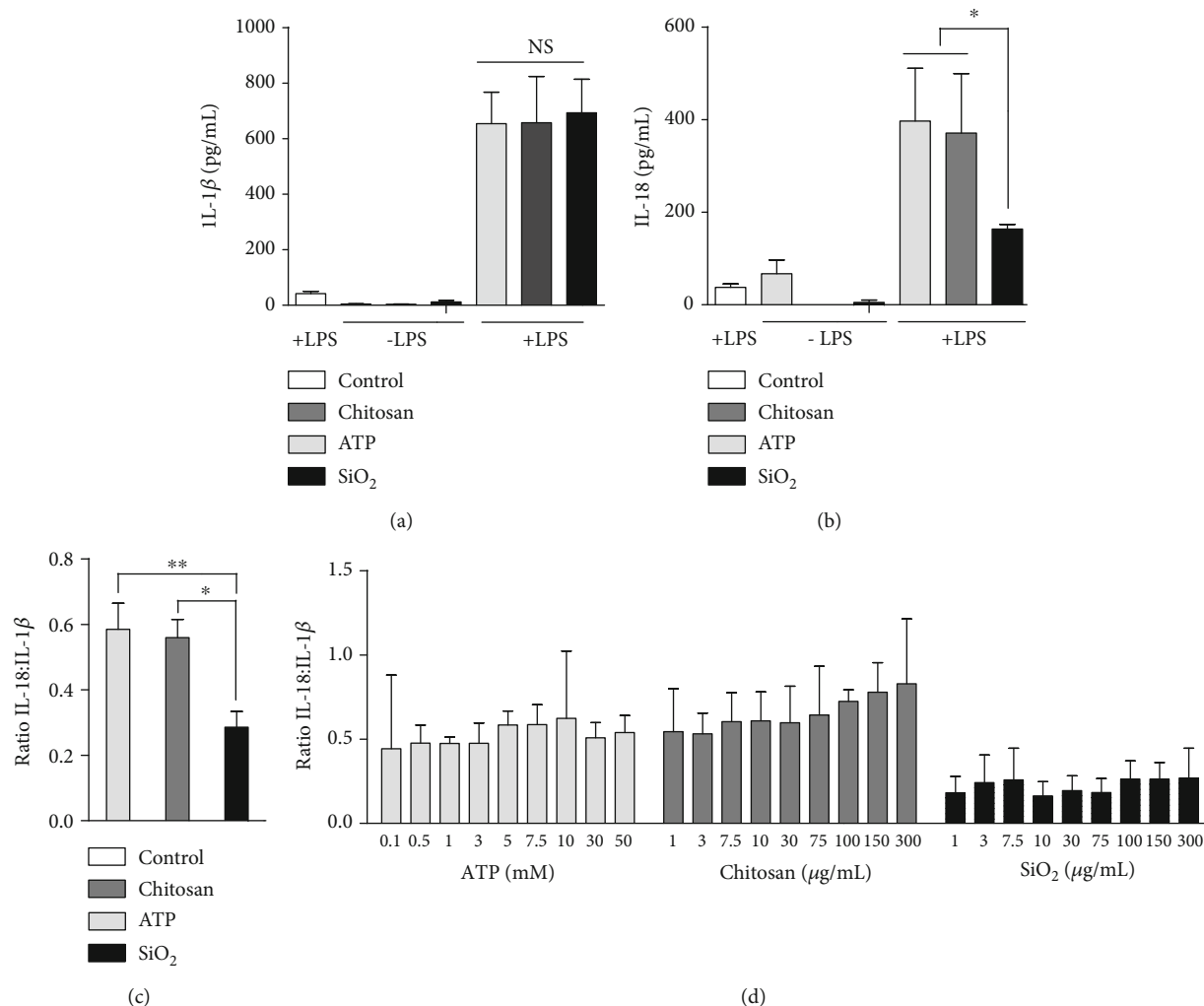


FIGURE 1: ATP, chitosan, and SiO₂ induce diverse IL-18 : IL-1 β ratio in THP-1 cells. The concentration of released IL-1 β (a) and IL-18 (b) in nonprimed (-LPS) and LPS-primed (+LPS, 100 ng/mL) cells, 24 h post stimulation were detected after stimulation with 5 mM ATP, 30 μ g/mL chitosan, or 30 μ g/mL SiO₂. The ratio between IL-1 β and IL-18 was calculated for each experiment (c) and after stimulation with increasing doses of ATP (mM), chitosan (μ g/mL), or SiO₂ (μ g/mL) (d). Controls were left untreated (-LPS) or treated with LPS alone (+LPS). Data are shown as mean \pm SD from three-six individual experiments. NS: non significant, * p < 0.05; ** p < 0.01.

measured at 635 nm with Cytation 3 imaging plate reader (BioTek, Winooski, VT).

2.6. FLICA Assay. Activation of caspase-1 was detected with the fluorescent probe FAM-YVAD-FMK (FLICA) from Immunochemistry Technologies (Bloomington, MN cat.nr: OKSA11275), that binds irreversibly to active caspase-1. The cells were stained for 1 h and washed two times in PBS prior to analysis. The percentage of positive cells was measured by flow cytometry, (Accuri™ C6, BD, Franklin Lakes, NJ).

2.7. Lactate Dehydrogenase Assay. Cellular rupture was detected using the Pierce® lactate dehydrogenase (LDH) cytotoxicity assay kit (Thermo Scientific) according to the manufacturer's instructions. Data are presented as percentage LDH calculated from a positive control (100% lysed cells).

2.8. Western Blotting. Cells used for Western blotting were stimulated in FBS-free media. Cells were lysed in RIPA lysis buffer (Merck Millipore, Burlington, MA), and the protein concentrations were measured using the Micro BCA™ Protein Assay (Thermo Scientific). The proteins were separated in 8-16% stain-free TGX gels (Bio-Rad, Hercules, CA), transferred to PVDF membranes (iBlot® 2 PVDF regular stacks, Invitrogen, Carlsbad, CA), and analysed by immunoblotting. The primary antibodies used were cleaved IL-1 β (1:1000 Cell Signaling Technologies, Danvers, MA. cat.nr:12242), IL-18 (1:1000 Abcam, Cambridge, UK. cat.nr: EPR19954-188), and caspase-1 p20 (1:750 Adipogen Life Sciences, cat.nr:AG-20B-0048-C100). Secondary antibodies used were goat anti mouse (1:5000 Abcam cat.nr: Ab6789), rabbit anti goat (1:2000 Dako, Agilent. Santa Clara, CA. cat.nr: P0160), and goat anti-rabbit (1:3000 Invitrogen cat.nr: A11034). Membranes were washed in TBST buffer and analysed with ChemiDoc™ MP Imaging System (Bio-Rad).

2.9. Extraction of mRNA, Reverse Transcription, and qPCR. Cells were lysed in RLT lysis buffer (Qiagen, Hilden, Germany) and drawn through a 22 G needle to homogenize the sample. Total RNA was extracted and purified with the QIAamp RNeasy Mini kit (Qiagen). RNA was quantified using NanoDrop 2000 (Thermo Fisher Scientific), and a High-Capacity cDNA Transcription kit (Thermo Fisher Scientific) was used for the reverse transcription reactions (900 ng of total RNA per 60 μ L reaction) on a LifePro Thermal Cycler (Bioer, Hangzhou, China). Quantitative real-time PCR was performed using TaqMan assays in QuantStudio 7 Flex PCR (Applied Biosystems, Thermo Fisher Scientific). The TaqMan assays used were *IL1B* (Hs01555410), *IL18* (Hs01038788_m1), *NLRP3* (Hs00918082_m1), *ASC/PYCARD* (Hs01547324_gH), *CASP1* (Hs00354836_m1), *CASP8* (Hs01018151_m1), *HPRT1* (Hs02800695_m1), and *TBP* (Hs00427620_m1), (all from Thermo Fisher Scientific). A comparative quantification was used, where the quantity of each experimental sample was determined using a standard curve as calibrator samples. Calibrator was prepared from human peripheral blood mononuclear cell (PBMC) cultures stimulated for 48 h with 1 μ g/mL LPS known to express the genes of interest in high abundance. A six-point serially fourfold diluted standard curve was developed from the calibrator by plotting the threshold cycles versus the dilution factor and the data fitted to a straight line, while confirming that the correlation coefficient (R²) for the line was 0.99 or greater. This plot was then used for extrapolating relative expression level information for the same gene of interest in unknown experimental samples. The relative quantity for the gene of interest was normalized to that of a reference gene in the same sample, and then, the normalized numbers was compared between samples. The reference genes used for normalization, *HPRT1* and *TBP*, were selected from four candidate genes using NormFinder R package (MOMA, Aarhus University Hospital, Denmark), where the geometric mean of said genes were used. RNA from stimulated PBMCs was extracted using QIAamp RNA Blood Mini Kit (Qiagen, Hilden, Germany) and converted into cDNA using the above protocols. 384-well plates were prepared using a PIRO Pipetting Robot (Dornier, Lindau, Germany). Cycle threshold (CT) cut-off value was set to 35 cycles. An acceptable coefficient of variation (CV) between duplicates was set to <15%. Water was used as the negative control.

2.10. Statistics. Statistical analyses were performed using GraphPad Prism 5. *p* values were assessed using two-tailed Student's *t*-tests and two-way analysis of variance (ANOVA) followed by Bonferroni's posttest. In the figures, **p* < 0.05, ***p* < 0.01, and ****p* < 0.001. All data shown are mean \pm SD for a minimum of three independent experiments.

3. Results

3.1. IL-1 β and IL-18 Release Is Mediated by Inflammasome Inducers ATP, Chitosan, or SiO₂. To confirm NLRP3 inflammasome activation by ATP, chitosan, and SiO₂, respectively, and their dependency on a priming signal, cells were primed with two doses of LPS. Cells stimulated with 1 μ g/mL LPS alone showed elevated levels of IL-1 β , uncharacteristic of a

true priming signal and only minor changes in IL-1 β and IL-18 production upon stimulation with ATP, chitosan, or SiO₂. However, 100 ng/mL LPS induced only low concentrations of IL-1 β and led to significant synergistic effect upon addition of inflammasome inducers (supplementary figure 1). Henceforth, all experiments performed on THP-1 cells were primed with 100 ng/mL LPS. To investigate potential differences in the response following inflammasome activation, concentrations of the inducers were titrated to doses resulting in similar IL-1 β levels released 24 h after stimulation (supplementary Figure 2. Stimulation of primed cells with 5 mM ATP, 30 μ g/mL chitosan, or 30 μ g/mL SiO₂ induced a significantly increased amount of IL-1 β compared to primed controls but showed no significant difference in the concentration of released IL-1 β when compared to each other (Figure 1(a)). However, stimulation with SiO₂ generated significantly lower levels of IL-18 compared to ATP and chitosan (Figure 1(b)). In terms of ratios, the IL-18 : IL-1 β ratio for ATP and chitosan was 1:0.6 in contrast to 1:0.2 for SiO₂ (Figure 1(c)). The divergent ratio of SiO₂ remained constant over a broad range of doses, indicating that the ratio is not sensitive to the amount of inducer (Figure 1(d)).

3.2. Gene Expression of Inflammasome Components in ATP-, Chitosan-, or SiO₂-Stimulated Cells. To elucidate whether the differences in IL-18 : IL-1 β ratio could be explained by changes in expression levels of inflammasome components and cytokines, gene expression levels of *IL1B*, *IL18*, *NLRP3*, *PYCARD* and *CASP1* were analysed. None of the inducers showed any effect on *IL1B* and *IL18* mRNA expression in LPS-primed cells (Figures 2(a) and 2(b)). Chitosan alone increased the *CASP1* expression (Figure 2(c)). No significant change was seen for *NLRP3* or the potential noncanonical route of activation through *CASP8*. Furthermore, the inducers showed no own effect on NF- κ B activation in unprimed cells. However, chitosan showed a synergistic increase in LPS-primed cells, as measured by utilizing the reporter gene SEAP in a modified THP-1 cell line (Figure 2(d)).

3.3. Activation of Caspase-1 and Induction of Cell Lysis by Diverse Inducers. To further investigate if observed differences in the IL-18 : IL-1 β ratio could be attributed to differences in caspase-1 activation, FLICA staining was used to quantify caspase-1 activity, and the presence of pro- and cleaved caspase-1 was detected by Western blot. Chitosan and SiO₂ but not ATP resulted in an increased percentage of FLICA-positive cells compared to primed controls, 24 h after stimulation (Figure 3(a)). No difference in the protein expression of pro-caspase-1 could be seen compared to the control for any of the inducers (data not shown), and any tendency of differentiating the expression of pro-IL-1 β and cleaved caspase-1 p20 fragment was statistically nonsignificant (Figures 3(c) and 3(d)). Furthermore, an LDH assay was used to examine the percentage of cell lysis 24 h after stimulation with the inducers. Chitosan and SiO₂ stimulation resulted in increased LDH release compared to the primed control (Figure 3(b)). The only significant difference between the inducers with regard to both LDH release and FLICA staining was found between ATP and SiO₂. The LDH results

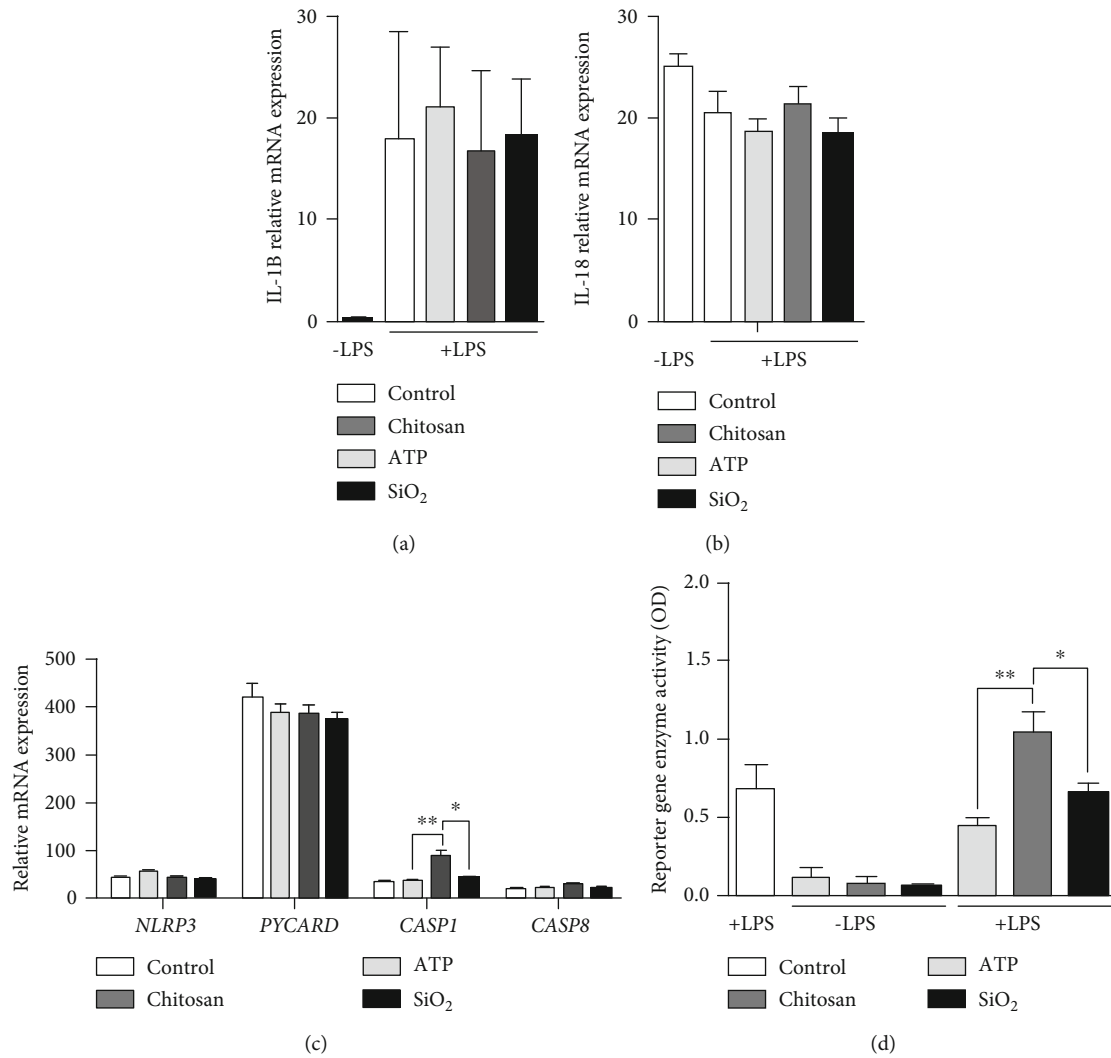


FIGURE 2: Gene expression of inflammasome components and cytokines do not correlate with the IL-18 : IL-1 β ratio. The relative mRNA expression of IL1B (a), IL18 (b), and the NLRP3 inflammasome components (c) NLRP3, ASC, and CASP1 as well as CASP8 were measured 24h after cells primed with LPS were stimulated with ATP, chitosan, or SiO₂ using qPCR. NF- κ B activation was detected indirectly by measuring the activation of the reporter gene SEAP (d). Controls were treated with LPS alone. Data are shown as mean \pm SD from six individual experiments. * p < 0.05; ** p < 0.01.

were validated by annexin V and 7AAD staining detected by flow cytometry (data not shown).

3.4. Release of Cytokines in Inflammasome-Deficient Cells by Diverse Inducers. The relevance of the NLRP3 inflammasome components for the response to the inducers were investigated using THP-1 knockout cells, lacking functional NLRP3, ASC, or caspase-1. Absence of NLRP3, ASC, and caspase-1, respectively, completely attenuated the release of IL-1 β and IL-18 (Figures 4(a) and 4(b)). While the inducers stimulated the release of other cytokines, not directly regulated by the inflammasome, (supplementary table I), this release was attenuated in inflammasome-deficient cells for several of the cytokines (supplementary figure 3), showing a primary dependency on inflammasome activation for subsequent responses.

3.5. IL-18 : IL-1 β Ratios in Primary Monocytes. Lastly, in order to investigate whether the results found in the THP-1 cell line is reflected in primary human cells, monocytes were isolated from healthy volunteers, primed with LPS and stimulated with ATP, chitosan, or SiO₂. As with the THP-1 cells, the doses of inducers were titrated to achieve the same concentration of released IL-1 β (supplementary Figure 2). However, a lower dose of LPS was required for priming primary human monocytes compared to THP-1 cells. At this dose, a synergistic effect by the inflammasome inducers was observed without risking the activation of the noncanonical pathway of inflammasome activation as previously reported by Gaidt et al. [48]. However, unlike the THP-1 cells, the concentrations of released IL-18 were higher than for IL-1 β for all inducers. Although not significant, monocytes responded with a similar pattern, as seen in THP-1 cells, with regard to IL-18 : IL-1 β ratios (Figures 5(a) and 5(b)).

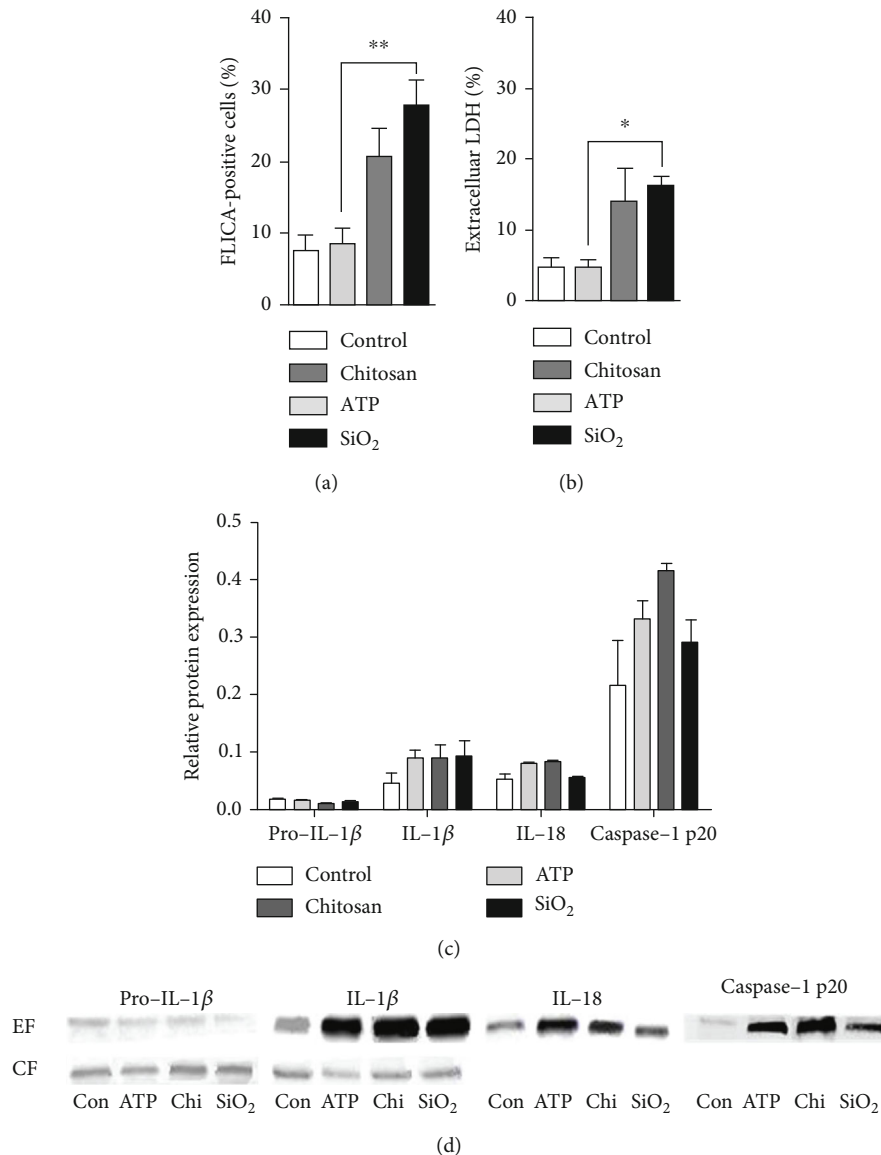


FIGURE 3: Caspase-1 activity and cell lysis do not correlate with the IL-1 β : IL-18 ratio. Caspase-1 activity was measured by flow cytometry using the FLICA probe (a), while LDH assay was used as a measure of cell rupture (b). Pro-IL-1 β , cleaved IL-1 β , IL-18, and caspase-1 p20 were detected in the extracellular fraction (EF) or cellular lysate as the cellular fraction (CF) by Western blot. The blot density was normalized against the total protein load to calculate the fraction (c). Representative blots are shown in (d). Measurement took place 24 h after stimulation, and controls were treated with LPS alone. Data are shown as mean \pm SD from six individual experiments. * $p < 0.05$; ** $p < 0.01$.

4. Discussion

NLRP3 inflammasome can be activated by numerous inducers and several pathways leading to inflammasome activation have been described. In this study, the differences in functional outcome of three diverse inflammasome inducers, ATP, chitosan, and SiO₂, with respect to their ability to activate the inflammasome to produce IL-1 β and IL-18 were investigated. Despite inducing the same level of IL-1 β release, the studied inducers showed a diverse ability to induce the production of IL-18. This diverse IL-18 : IL-1 β ratio remained throughout a broad span of doses. While all three inducers showed a strict dependency on priming with LPS and a functional NLRP3 inflammasome, differences could

not be attributed to caspase-1 activity, induction of gene expression, or their ability to induce cell death. Furthermore, these inducers exerted diverse effects on other inflammatory cytokines in an NLRP3-dependent fashion. This strengthens the idea that inflammasome activity is highly context-dependent and flexible process that cannot be regarded as an on/off process.

In this study, SiO₂ stimulation resulted in a lower release of IL-18 compared to ATP and chitosan, which also resulted in a different IL-18 : IL-1 β ratio. Since IL-1 β and IL-18 have both shared and unique biological properties, the ratio between them may impact the overall immunological profile, including Th1 or Th17 differentiation [16]. The inducers used in this study represent the broad range of different

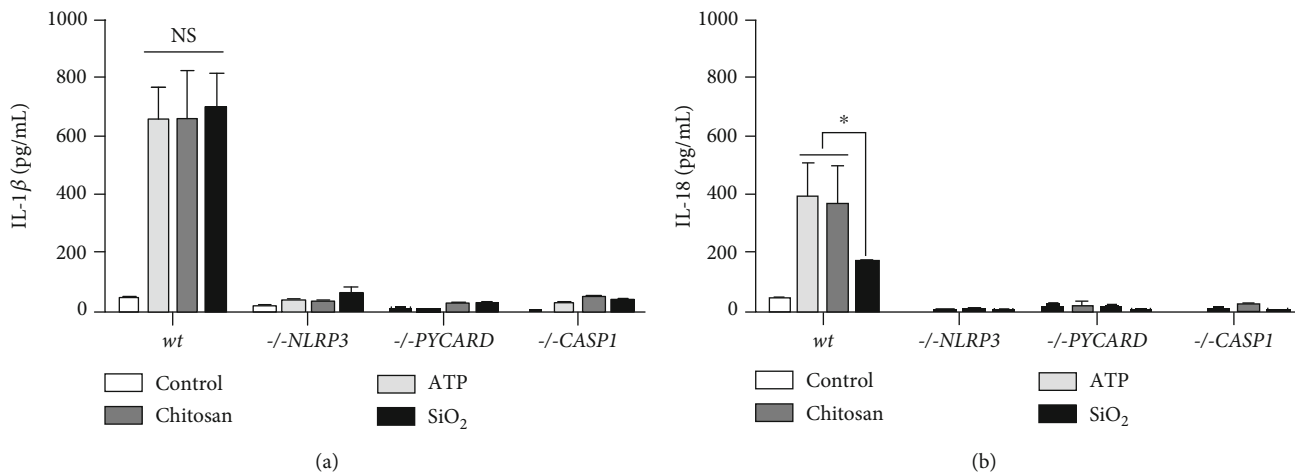


FIGURE 4: Release of IL-1 β and IL-18, induced by ATP, chitosan, or SiO₂ is strictly NLRP3 inflammasome dependent. The concentrations of released IL-1 β (a) and IL-18 (b) were measured from LPS-primed THP-1 monocytes with functional NLRP3 inflammasome (wt) and inflammasome-deficient THP-1 cells, lacking either functional NLRP3 (-/-NLRP3), ASC (-/-PYCARD), or caspase-1 (-/-CASPI1) following stimulation with ATP, chitosan, or SiO₂. Controls were treated with LPS alone. Data are shown as mean \pm SD from six individual experiments. NS: nonsignificant. * $p < 0.05$.

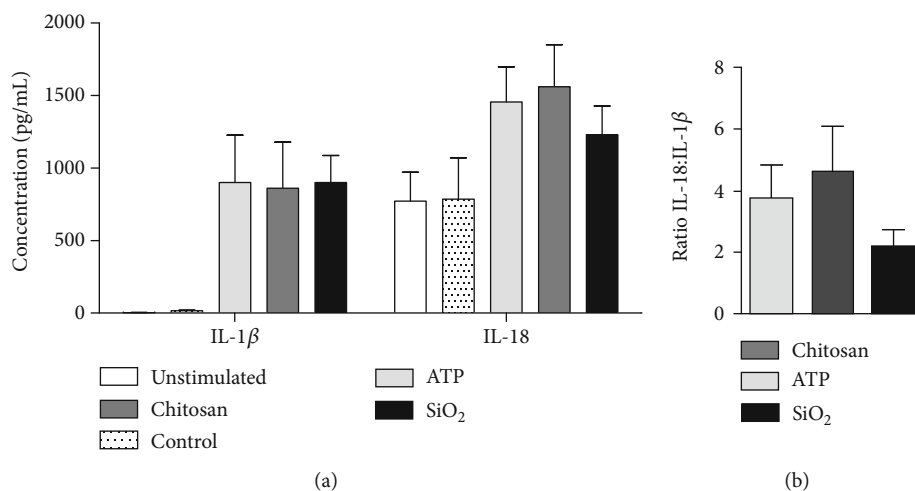


FIGURE 5: ATP, chitosan, and SiO₂ induce release of IL-1 β and IL-18 in primary monocytes. Primary human monocytes were isolated from peripheral blood from healthy volunteers. The release of IL-1 β and IL-18 was measured after stimulation with 10 nM ATP, 10 ng/mL chitosan, or 10 ng/mL SiO₂ from LPS-primed cells (10 ng/mL) (a). The IL-18 : IL-1 β ratios were calculated (b). Data are shown as mean \pm SD from six individual experiments.

stimuli that the NLRP3 inflammasome can respond to ATP is a DAMP involved in autoinflammatory diseases that arise during sterile inflammatory conditions, including CAPS and FMF, conditions involving both IL-1 β and IL-18 [49, 50]. Meanwhile, PAMP-induced inflammation may result in Th1, Th2, or Th17 differentiation, depending on the type of pathogen. Fungal chitosan is a PAMP, and clearance of fungi requires activation of Th1 and Th17 and therefore relies on both IL-1 β and IL-18 for efficient clearance [16, 51, 52]. SiO₂ on the other hand induces inflammation as a result of environmental exposure and its low IL-18 : IL-1 β ratio can also be viewed as an IL-1 β dominant inflammation. SiO₂ and other particle exposure are known to be correlated with an increased risk of systemic autoinflammatory diseases,

cardiovascular events, and lung disease, such as COPD, which are also strongly related to IL-1 β [53–56], and that can benefit from IL-1 β blocking treatment [57].

Furthermore, the importance of ratios between polarizing cytokines in cell differentiation and the immunological response have been suggested by Zielinski et.al [18], but the relevance of the ratio between IL-1 β and IL-18 have not been studied. The diverse ratios also show that the NLRP3 inflammasome activity is not static and can give a dynamic response, depending on the inducers. This flexibility of the NLRP3 inflammasome has previously been implicated by Schmidt and Lenz [58] and Bezbradica et al. [59], who demonstrate that the NLRP3 inflammasome show a greater response when stimulated with exogenous PAMPs than

endogenous DAMPs. In the current study, several attempts were made to elucidate a mechanism that could explain the difference in IL-18 : IL-1 β ratio for SiO₂, but no sufficient models were found. Nonetheless, differential regulation of *IL1B* and *IL18* mRNA expressions could be excluded as a mechanism, since the inducers did not affect the mRNA expression. Only LPS affected the *IL1B* expression, with a 100-fold increase compared to untreated controls, while *IL18* was constitutively expressed, as shown previously by Puren et al. [60] and Zhu and Kanneganti [61]. Likewise, mRNA expression of the inflammasome components also failed to explain why SiO₂ gives a diverse ratio, as both chitosan and SiO₂ show a lower *PYCARD* mRNA expression and chitosan alone affect the *CASP1* expression. Besides *NLRP3*, *PYCARD*, and *CASP1*, the mRNA expression of *CASP8* was also examined as caspase-8 has been previously shown to assist in inflammasome activation [48, 62] but its role here cannot be confirmed.

Additionally to IL-1 β and IL-18, the release of other cytokines, not directly regulated by the inflammasome, were measured and are summarized in supplementary table I. Stimulation with the inducers resulted in an increased release of several cytokines compared to primed control, of which chitosan significantly affected IL-6 and TNF compared to ATP and SiO₂ stimulation. The released IL-6 and TNF is likely a secondary response to the inducers, mediated indirectly by IL-1 β or IL-18 as the release did not occur in the THP-1 knockout cells deficient of *NLRP3* and caspase-1 (supplementary figure 3). However, this secondary response could not clearly be correlated to the IL-18 : IL-1 β ratio. Furthermore, the difference in IL-18 : IL-1 β ratio could not be attributed to the caspase-1 activity as chitosan and SiO₂, but not ATP, showed a higher percentage of cells positive for FLICA 24h after stimulation, when compared to LPS-primed controls. A difference in time kinetics between the three inducers may lead to a bias in FLICA-positive cells at 24h. However, the ratios described in this paper are derived from the accumulated production and release of inflammasome-activated cytokines at 24h in order to dilute the effect of inflammasome time kinetics. Next, as induction of cell death and the subsequent unspecific membrane leakage may affect the amounts of cytokines available for extracellular detection, extracellular LDH was used to measure cell lysis. ATP induced the release of IL-1 β without an increase of cell lysis compared to the controls. It is therefore likely that ATP induces GSDMD pores while escaping a pyroptotic fate, which have been demonstrated as a possible alternative to pyroptosis [48, 63]. Furthermore, the percentage of lysed cells did not reach over 30% after stimulation with chitosan and SiO₂ which means that the majority of the cells are still intact after 24h. However, since chitosan and SiO₂ both increased the percentage of lysed cells, the difference in the IL-18 : IL-1 β ratio cannot be explained by pyroptosis.

5. Conclusions

Taken together, our data suggest that the different inflammasome inducers lead to a diverse functional outcome that goes

beyond the direct production of the hallmark cytokine IL-1 β , irrespective of gene expression, cell lysis, and caspase-1 activity. The differential regulation of IL-1 β and IL-18 cleavage in human cells need further elucidation, and given the fact that the *NLRP3* inflammasome reacts to such a vast array of molecules and have been implicated in numerous, clinically distant diseases, a more holistic approach to studying inflammasome activation under different conditions is warranted. In conclusion, this study shows that the *NLRP3* inflammasome is capable of directly tailoring the specific response to a particular stimulus. By taking into account the ratio between IL-1 β and IL-18, it is possible to increase our understanding of how different inflammasome inducers affect inflammasome functionality and thus the subsequent immune responses.

Data Availability

The data used and analyzed in this paper can be obtained from the corresponding authors with reasonable requests.

Conflicts of Interest

The authors declare that there is no conflict of interest regarding the publication of this paper.

Acknowledgments

We sincerely thank Kaya Tuerxun for the technical support and Anton Ondracek for his assistance. We also want to thank Dr. Isak Demirel and Dr. Caroline Kardeby for the scientific discussions. This work was supported by the Swedish Knowledge Foundation (Synergi15, ref. no.: 20160044) and Örebro University (strategic grants, ref. nos.: ORU 2.2.1-4060/2013 and ORU 2018/01219).

Supplementary Materials

Supplementary Figure 1. Different doses of LPS affects the release of inflammasome cytokines. The concentration of released IL-1 β and IL-18 were detected 24h after stimulation of THP-1 cells with ATP, chitosan, and SiO₂. Cells were primed with (a) 1 μ g/mL or (b) 100 ng/mL LPS prior to stimulation. The concentration cytokines were normalized against the mean of the control (primed with LPS). Data are shown as mean \pm SD from six individual experiments. Supplementary Figure 2. Dose response of the inflammasome inducers ATP, chitosan, and SiO₂. Undifferentiated THP-1 cells were primed with LPS and stimulated with increasing doses of (a) ATP (mM), (b) chitosan (μ g/mL), or (c) SiO₂ (μ g/mL). Isolated primary monocytes were primed with LPS and stimulated with increasing doses of (d) ATP (M), (e) chitosan (g/mL), or (f) SiO₂ (g/mL). The concentration of released IL-1 β was measured 24h after stimulation. The selected doses are marked with arrows. Data are shown as mean \pm SD from three individual experiments. Supplementary Figure 3. Lack of inflammasome components affect inflammasome-independent cytokines. THP-1 monocytes with functional *NLRP3* inflammasome (wt) and inflammasome-deficient THP-1 cells, lacking either functional *NLRP3*, *ASC*, or caspase-1 proteins,

were primed with LPS and stimulated with ATP, chitosan, or SiO₂ for 24 h. Controls were treated with LPS alone. The concentration of released (a) IL-6, and (c) TNF were measured. The relative expression of (b) IL-6, and (d) TNF shown is compared to reference genes TBP and HPRT1. Data are shown as mean ± SD from six individual experiments. Supplementary Table I. Release of noninflammasome-related cytokine and chemokines. Human inflammatory panel 1 (BioLegend), a multiplex bead-based flow cytometry detection, was used according to the manufacturer's instructions to detect the concentrations of selected cytokines and chemokines from LPS-primed THP-1 cells following stimulation with ATP, chitosan, or SiO₂ for 24 h. Some cytokines could not be detected (ND) within the range of the kit. Data are shown as mean from six individual experiments. (*Supplementary Materials*)

References

- [1] F. Martinon, K. Burns, and J. Tschopp, "The inflammasome: a molecular platform triggering activation of inflammatory caspases and processing of proIL- β ," *Molecular Cell*, vol. 10, no. 2, pp. 417–426, 2002.
- [2] M. S. Dick, L. Sborgi, S. Rühl, S. Hiller, and P. Broz, "ASC filament formation serves as a signal amplification mechanism for inflammasomes," *Nature Communications*, vol. 7, no. 1, article 11929, 2016.
- [3] D. E. Place and T.-D. Kanneganti, "Recent advances in inflammasome biology," *Current Opinion in Immunology*, vol. 50, pp. 32–38, 2018.
- [4] S. Kesavardhana and T.-D. Kanneganti, "Mechanisms governing inflammasome activation, assembly and pyroptosis induction," *International Immunology*, vol. 29, no. 5, pp. 201–210, 2017.
- [5] Y. He, H. Hara, and G. Núñez, "Mechanism and regulation of NLRP3 inflammasome activation," *Trends in Biochemical Sciences*, vol. 41, no. 12, pp. 1012–1021, 2016.
- [6] C. B. A. Grahames, A. D. Michel, I. P. Chessell, and P. P. A. Humphrey, "Pharmacological characterization of ATP- and LPS-induced IL-1 β release in human monocytes," *British Journal of Pharmacology*, vol. 127, no. 8, pp. 1915–1921, 1999.
- [7] D. G. Perregaux, P. McNiff, R. Laliberte, M. Conklyn, and C. A. Gabel, "ATP acts as an agonist to promote stimulus-induced secretion of IL-1 beta and IL-18 in human blood," *The Journal of Immunology*, vol. 165, no. 8, pp. 4615–4623, 2000.
- [8] D. Perregaux and C. A. Gabel, "Interleukin-1 beta maturation and release in response to ATP and nigericin. Evidence that potassium depletion mediated by these agents is a necessary and common feature of their activity," *The Journal of Biological Chemistry*, vol. 269, no. 21, pp. 15195–15203, 1994.
- [9] R. Muñoz-Planillo, P. Kuffa, G. Martínez-Colón, B. L. Smith, T. M. Rajendiran, and G. Núñez, "K⁺ efflux is the common trigger of NLRP3 inflammasome activation by bacterial toxins and particulate matter," *Immunity*, vol. 38, no. 6, pp. 1142–1153, 2013.
- [10] D. Fong, P. Grégoire-Gélinas, A. P. Cheng et al., "Lysosomal rupture induced by structurally distinct chitosans either promotes a type 1 IFN response or activates the inflammasome in macrophages," *Biomaterials*, vol. 129, pp. 127–138, 2017.
- [11] C. L. Bueter, C. K. Lee, J. P. Wang, G. R. Ostroff, C. A. Specht, and S. M. Levitz, "Spectrum and mechanisms of inflammasome activation by chitosan," *The Journal of Immunology*, vol. 192, no. 12, pp. 5943–5951, 2014.
- [12] C. L. Bueter, C. K. Lee, V. A. K. Rathinam et al., "Chitosan but not chitin activates the inflammasome by a mechanism dependent upon phagocytosis," *The Journal of Biological Chemistry*, vol. 286, no. 41, pp. 35447–35455, 2011.
- [13] D. M. Gómez, S. Urcuqui-Inchima, and J. C. Hernandez, "Silica nanoparticles induce NLRP3 inflammasome activation in human primary immune cells," *Innate Immunity*, vol. 23, no. 8, pp. 697–708, 2017.
- [14] T. Kusaka, M. Nakayama, K. Nakamura, M. Ishimiya, E. Furusawa, and K. Ogasawara, "Effect of silica particle size on macrophage inflammatory responses," *PLoS One*, vol. 9, no. 3, article e92634, 2014.
- [15] M. Tsugita, N. Morimoto, M. Tashiro, K. Kinoshita, and M. Nakayama, "SR-B1 is a silica receptor that mediates canonical inflammasome activation," *Cell Reports*, vol. 18, no. 5, pp. 1298–1311, 2017.
- [16] C. L. Evavold and J. C. Kagan, "How inflammasomes inform adaptive immunity," *Journal of Molecular Biology*, vol. 430, no. 2, pp. 217–237, 2018.
- [17] C. A. Dinarello, "The biological properties of interleukin-1," *European Cytokine Network*, vol. 5, no. 6, pp. 517–531, 1994.
- [18] C. E. Zielinski, F. Mele, D. Aschenbrenner et al., "Pathogen-induced human TH17 cells produce IFN- γ or IL-10 and are regulated by IL-1 β ," *Nature*, vol. 484, no. 7395, pp. 514–518, 2012.
- [19] O. M. Finucane, J. Sugrue, A. Rubio-Araiz, M.-V. Guillot-Sestier, and M. A. Lynch, "The NLRP3 inflammasome modulates glycolysis by increasing PFKFB3 in an IL-1 β -dependent manner in macrophages," *Scientific Reports*, vol. 9, no. 1, article 4034, 2019.
- [20] K. Deason, T. D. Troutman, A. Jain et al., "BCAP links IL-1R to the PI3K-mTOR pathway and regulates pathogenic Th17 cell differentiation," *The Journal of Experimental Medicine*, vol. 215, no. 9, pp. 2413–2428, 2018.
- [21] K. Nakanishi, T. Yoshimoto, H. Tsutsui, and H. Okamura, "Interleukin-18 is a unique cytokine that stimulates both Th1 and Th2 responses depending on its cytokine milieu," *Cytokine & Growth Factor Reviews*, vol. 12, no. 1, pp. 53–72, 2001.
- [22] K. Nakanishi, "Unique action of Interleukin-18 on T cells and other immune cells," *Frontiers in Immunology*, vol. 9, p. 763, 2018.
- [23] Y. H. Lee and S.-C. Bae, "Associations between interleukin-1 and IL-1 receptor antagonist polymorphisms and susceptibility to rheumatoid arthritis: a meta-analysis," *Cellular and Molecular Biology*, vol. 61, no. 8, pp. 105–111, 2015.
- [24] S. M. Burm, L. A. N. Peferoen, E. A. Zuiderwijk-Sick et al., "Expression of IL-1 β in rhesus EAE and MS lesions is mainly induced in the CNS itself," *Journal of Neuroinflammation*, vol. 13, no. 1, p. 138, 2016.
- [25] Y. Cai, F. Xue, C. Quan et al., "A critical role of the IL-1 β -IL-1R signaling pathway in skin inflammation and psoriasis pathogenesis," *The Journal of Investigative Dermatology*, vol. 139, no. 1, pp. 146–156, 2019.
- [26] C. A. Dinarello, "Interleukin-1 in the pathogenesis and treatment of inflammatory diseases," *Blood*, vol. 117, no. 14, pp. 3720–3732, 2011.
- [27] S. Dionne, I. D. D'Agata, J. Hiscott, T. Vanounou, and E. G. Seidman, "Colonic explant production of IL-1 and its receptor antagonist is imbalanced in inflammatory bowel disease (IBD)," *Clinical and Experimental Immunology*, vol. 112, no. 3, pp. 435–442, 1998.
- [28] Z.-K. Xie, Q.-P. Huang, J. Huang, and Z.-F. Xie, "Association between the IL1B, IL1RN polymorphisms and COPD risk: a

- meta-analysis,” *Scientific Reports*, vol. 4, no. 1, article 6202, 2015.
- [29] K. J. Baines, J.-J. Fu, V. M. McDonald, and P. G. Gibson, “Airway gene expression of IL-1 pathway mediators predicts exacerbation risk in obstructive airway disease,” *International Journal of Chronic Obstructive Pulmonary Disease*, vol. 12, pp. 541–550, 2017.
- [30] L. Cantarini, G. Lopalco, C. Selmi et al., “Autoimmunity and autoinflammation as the yin and yang of idiopathic recurrent acute pericarditis,” *Autoimmunity Reviews*, vol. 14, no. 2, pp. 90–97, 2015.
- [31] C. A. Dinarello, “Overview of the IL-1 family in innate inflammation and acquired immunity,” *Immunological Reviews*, vol. 281, no. 1, pp. 8–27, 2018.
- [32] S. Tarte and T.-D. Kanneganti, “Inflammasomes in the pathophysiology of autoinflammatory syndromes,” *Journal of Leukocyte Biology*, vol. 107, no. 3, pp. 379–391, 2020.
- [33] T. A. Dowds, J. Masumoto, L. Zhu, N. Inohara, and G. Núñez, “Cryopyrin-induced interleukin 1 β secretion in monocytic cells: enhanced activity of disease-associated mutants and requirement for ASC,” *The Journal of Biological Chemistry*, vol. 279, no. 21, pp. 21924–21928, 2004.
- [34] T. T. Pizarro, M. H. Michie, M. Bentz et al., “IL-18, a novel immunoregulatory cytokine, is up-regulated in Crohn’s disease: expression and localization in intestinal mucosal cells,” *Journal of Immunology*, vol. 162, no. 11, pp. 6829–6835, 1999.
- [35] N. Calvani, H. B. Richards, M. Tucci, G. Pannarale, and F. Silvestris, “Up-regulation of IL-18 and predominance of a Th1 immune response is a hallmark of lupus nephritis,” *Clinical and Experimental Immunology*, vol. 138, no. 1, pp. 171–178, 2004.
- [36] H. Konishi, H. Tsutsui, T. Murakami et al., “IL-18 contributes to the spontaneous development of atopic dermatitis-like inflammatory skin lesion independently of IgE/stat 6 under specific pathogen-free conditions,” *Proceedings of the National Academy of Sciences of the United States of America*, vol. 99, no. 17, pp. 11340–11345, 2002.
- [37] T. Tanaka, H. Tsutsui, T. Yoshimoto et al., “Interleukin-18 is elevated in the sera from patients with atopic dermatitis and from atopic dermatitis model mice, NC/Nga,” *International Archives of Allergy and Immunology*, vol. 125, no. 3, pp. 236–240, 2001.
- [38] H. Tanaka, N. Miyazaki, K. Oashi et al., “IL-18 might reflect disease activity in mild and moderate asthma exacerbation,” *The Journal of Allergy and Clinical Immunology*, vol. 107, no. 2, pp. 331–336, 2001.
- [39] T. Yoshimoto, H. Tsutsui, K. Tominaga et al., “IL-18, although anti-allergic when administered with IL-12, stimulates IL-4 and histamine release by basophils,” *Proceedings of the National Academy of Sciences of the United States of America*, vol. 96, no. 24, pp. 13962–13966, 1999.
- [40] Y. Ishikawa, T. Yoshimoto, and K. Nakanishi, “Contribution of IL-18-induced innate T cell activation to airway inflammation with mucus hypersecretion and airway hyperresponsiveness,” *International Immunology*, vol. 18, no. 6, pp. 847–855, 2006.
- [41] K. Yasuda, K. Nakanishi, and H. Tsutsui, “Interleukin-18 in health and disease,” *International Journal of Molecular Sciences*, vol. 20, no. 3, p. 649, 2019.
- [42] S. D. Brydges, L. Broderick, M. D. McGeough, C. A. Pena, J. L. Mueller, and H. M. Hoffman, “Divergence of IL-1, IL-18, and cell death in NLRP3 inflammasomopathies,” *The Journal of Clinical Investigation*, vol. 123, no. 11, pp. 4695–4705, 2013.
- [43] S. Haznedaroglu, M. A. Oztürk, B. Sancak et al., “Serum interleukin 17 and interleukin 18 levels in familial Mediterranean fever,” *Clinical and Experimental Rheumatology*, vol. 23, 4 Suppl 38, pp. S77–S80, 2005.
- [44] H. Babaoglu, O. Varan, H. Kucuk et al., “On demand use of anakinra for attacks of familial Mediterranean fever (FMF),” *Clinical Rheumatology*, vol. 38, no. 2, pp. 577–581, 2019.
- [45] G. Cavalli and C. A. Dinarello, “Anakinra therapy for non-cancer inflammatory diseases,” *Frontiers in Pharmacology*, vol. 9, article 1157, 2018.
- [46] C. A. Dinarello and G. Kaplanski, “Interleukin-18 treatment options for inflammatory diseases,” *Expert Review of Clinical Immunology*, vol. 1, no. 4, 2014.
- [47] G. Fenini, E. Contassot, and L. E. French, “Potential of IL-1, IL-18 and Inflammasome inhibition for the treatment of inflammatory skin diseases,” *Frontiers in Pharmacology*, vol. 8, p. 278, 2017.
- [48] M. M. Gaidt, T. S. Ebert, D. Chauhan et al., “Human monocytes engage an alternative inflammasome pathway,” *Immunity*, vol. 44, no. 4, pp. 833–846, 2016.
- [49] E. Sag, Y. Bilginer, and S. Ozen, “Autoinflammatory diseases with periodic fevers,” *Current Rheumatology Reports*, vol. 19, no. 7, p. 41, 2017.
- [50] J. Palomo, D. Dietrich, P. Martin, G. Palmer, and C. Gabay, “The interleukin (IL)-1 cytokine family—balance between agonists and antagonists in inflammatory diseases,” *Cytokine*, vol. 76, no. 1, pp. 25–37, 2015.
- [51] F. L. van de Veerdonk and M. G. Netea, “T-cell subsets and antifungal host defenses,” *Current Fungal Infection Reports*, vol. 4, no. 4, pp. 238–243, 2010.
- [52] S. Patel and A. Goyal, “Chitin and chitinase: role in pathogenicity, allergenicity and health,” *International Journal of Biological Macromolecules*, vol. 97, pp. 331–338, 2017.
- [53] L. Andersson, I. L. Bryngelsson, A. Hedbrant et al., “Respiratory health and inflammatory markers - exposure to respirable dust and quartz and chemical binders in Swedish iron foundries,” *PLoS One*, vol. 14, no. 11, article e0224668, 2019.
- [54] H. Westberg, A. Hedbrant, A. Persson et al., “Inflammatory and coagulatory markers and exposure to different size fractions of particle mass, number and surface area air concentrations in Swedish iron foundries, in particular respirable quartz,” *International Archives of Occupational and Environmental Health*, vol. 92, no. 8, pp. 1087–1098, 2019.
- [55] C. J. Johnston, K. E. Driscoll, J. N. Finkelstein et al., “Pulmonary chemokine and mutagenic responses in rats after sub-chronic inhalation of amorphous and crystalline silica,” *Toxicological Sciences*, vol. 56, no. 2, pp. 405–413, 2000.
- [56] A. Torres, B. Dalzon, V. Collin-Faure, and T. Rabilloud, “Repeated vs. acute exposure of RAW264.7 mouse macrophages to silica nanoparticles: a bioaccumulation and functional change study,” *Nanomaterials*, vol. 10, no. 2, p. 215, 2020.
- [57] G. Cavalli, F. Fallanca, C. A. Dinarello, and L. Dagna, “Treating pulmonary silicosis by blocking interleukin 1,” *American Journal of Respiratory and Critical Care Medicine*, vol. 191, no. 5, pp. 596–598, 2015.
- [58] R. L. Schmidt and L. L. Lenz, “Distinct licensing of IL-18 and IL-1 β secretion in response to NLRP3 inflammasome activation,” *PLoS One*, vol. 7, no. 9, article e45186, 2012.
- [59] J. S. Bezradica, R. C. Coll, and K. Schroder, “Sterile signals generate weaker and delayed macrophage NLRP3 inflammasome

responses relative to microbial signals,” *Cellular & Molecular Immunology*, vol. 14, no. 1, pp. 118–126, 2017.

- [60] A. J. Puren, G. Fantuzzi, and C. A. Dinarello, “Gene expression, synthesis, and secretion of interleukin 18 and interleukin 1beta are differentially regulated in human blood mononuclear cells and mouse spleen cells,” *Proceedings of the National Academy of Sciences of the United States of America*, vol. 96, no. 5, pp. 2256–2261, 1999.
- [61] Q. Zhu and T.-D. Kanneganti, “Cutting edge: distinct regulatory mechanisms control proinflammatory cytokines IL-18 and IL-1 β ,” *Journal of Immunology*, vol. 198, no. 11, pp. 4210–4215, 2017.
- [62] C. M. Cahill and J. T. Rogers, “Interleukin (IL) 1 β induction of IL-6 is mediated by a novel phosphatidylinositol 3-kinase-dependent AKT/I κ B kinase α pathway targeting activator protein-1,” *The Journal of Biological Chemistry*, vol. 283, no. 38, pp. 25900–25912, 2008.
- [63] L. DiPeso, D. X. Ji, R. E. Vance, and J. V. Price, “Cell death and cell lysis are separable events during pyroptosis,” *Cell Death Discovery*, vol. 3, no. 1, article 17070, 2017.

Review Article

The Role of Inflammation in the Pathogenesis of Preeclampsia

Michał Michalczyk,¹ Aleksander Celewicz,¹ Marta Celewicz,² Paula Woźniakowska-Gondek,¹ and Rafał Rzepka ¹

¹Department of Gynecology and Obstetrics, Collegium Medicum, University of Zielona Góra, Zielona Góra, Poland

²Department of Obstetrics and Gynecology, Pomeranian Medical University, Szczecin, Poland

Correspondence should be addressed to Rafał Rzepka; rafalrz123@gmail.com

Received 28 May 2020; Revised 12 July 2020; Accepted 22 September 2020; Published 5 October 2020

Academic Editor: Young-Su Yi

Copyright © 2020 Michał Michalczyk et al. This is an open access article distributed under the Creative Commons Attribution License, which permits unrestricted use, distribution, and reproduction in any medium, provided the original work is properly cited.

Preeclampsia (PE) affects 5-8% of pregnant women, and it is the major cause of perinatal morbidity and mortality. It is defined as arterial hypertension in women after 20 weeks of gestation which cooccurs with proteinuria (300 mg/d) or as arterial hypertension which is accompanied by one of the following: renal failure, liver dysfunction, hematological or neurological abnormalities, intrauterine growth restriction, or uteroplacental insufficiency. Currently, pathophysiology of preeclampsia poses a considerable challenge for perinatology. Preeclampsia is characterized by excessive and progressive activation of the immune system along with an increase in proinflammatory cytokines and antiangiogenic factors in fetoplacental unit as well as in vascular endothelium in pregnant women. A single, major underlying mechanism of preeclampsia is yet to be identified. This paper discusses the current understanding of the mechanisms which underlie the development of the condition. Some significant factors responsible for PE development include oxidative stress, abnormal concentration and activity in mononuclear phagocytic system, altered levels of angiogenic and antiangiogenic factors, and impaired inflammatory response triggered by inflammasomes. Detailed understanding of pathophysiology of inflammatory process in PE can largely contribute to new, targeted anti-inflammatory therapies that may improve perinatal outcomes in PE patients.

1. Introduction

Preeclampsia (PE) affects 5-8% of pregnant women, and it constitutes the major cause of perinatal morbidity and mortality [1]. The International Society for the Study of Hypertension in Pregnancy (ISSHP) defines PE as a combination of arterial hypertension and proteinuria (300 mg/d) present after 20 weeks of gestation or as arterial hypertension which is accompanied by one of the following: renal failure, liver dysfunction, hematological or neurological abnormalities, intrauterine growth restriction (IUGR), or uteroplacental insufficiency [2]. Nowadays, pathophysiology of preeclampsia poses an actual challenge for perinatology [3]. The causes of the condition can be ascribed to excessive maternal systemic inflammatory response to pregnancy. The response is elicited by the activation of innate and adaptive immune systems [4, 5] to the degree which is determined by both environmental and genetic factors [6–11].

In normal pregnancy, the maternal spiral arteries are invaded by extravillous trophoblast cells (EVT) leading to gradual replacement of vascular endothelium. The process is referred to as spiral artery remodeling [12], and when impaired, it leads to placental ischemia and ischemia-reperfusion injury as a result [13]. Failure to sufficient vascular remodeling results in pathological narrowing of spiral arteries and placental blood flow reduction [14], which, as a consequence, leads to tissue ischemia, damaged vascular endothelium, microangiopathic thrombosis, oxidative stress, and inflammatory response [15]. The degree of impairment to trophoblast invasion is also affected by the severity of arterial hypertension in patients with PE [16].

Inflammasomes are high in molecular weight, multimeric, and self-organizing protein complexes of the innate immune system which do not only play a significant role in inflammatory response activation and the release of IL-1 β and IL-18 but also function like a finely tuned alarm in

cellular apoptosis regulation by triggering and enhancing systems in response to stress and/or cellular infections. Following the inflammasome signaling activation, inflammatory processes can potentially promote the development and secretion of proinflammatory cytokines including danger signaling and pyroptotic cell death, i.e., quick inflammation-induced apoptosis.

Contrary to immunosuppression which occurs in normal pregnancy, preeclamptic pregnancy is characterized by excessive immune activation. Th1 cells, NK cells, and self-reactive B cells stimulate the inflammatory response through cytokines activity, which results in an inappropriate trophoblast invasion and impaired spiral artery remodeling in early pregnancy [17, 18]. Uteroplacental underperfusion is therefore the cause of placental ischemia which triggers oxidative-inflammation cascade and increases production of antiangiogenic factors: soluble fms-like tyrosine kinase 1 (sFlt-1) and soluble endoglin (sEng) [19–21].

Preeclampsia is characterized by excessive and progressively increased immune activation with a rise in proinflammatory cytokines and antiangiogenic factors both in the intrauterine environment and maternal endothelium [22], which is the cause of placental dysfunction and maternal systemic complications [23, 24].

2. Activation of Response Inflammatory as One of the Causes of PE

The exchange of nutrient and oxygen between maternal and fetal circulatory systems is the crucial role of the placenta. The fetal/maternal exchange takes place at the chorionic villi cellular membrane and intervillous space filled with maternal blood. For normal placental functioning, it is of key importance for placentation to coincide with spiral artery remodeling by extravillous trophoblast [25]. A vital role here is played by reactive oxygen species (ROS) as signaling pathways necessary for proper placentation in normal pregnancy. Moreover, low oxygen level in early pregnancy is also a significant factor which stimulates placental angiogenesis [26, 27].

In the first trimester of gestation, the fetus develops in low oxygen concentration, which promotes trophoblast cells proliferation. During placentation in the first weeks of gestation, the uterine arteries undergo a distinctive transformation to become vessels of high volume and low resistance capacity. This specific and unique process results in elevated intervillous oxygen level during the first trimester, which entails a significant enhancement to oxygen exchange at the maternal-fetal interface to satisfy the needs of the developing fetus [13, 28, 29]. Additionally, impaired trophoblast invasion causing temporary ischemia with subsequent reperfusion creates contributory conditions for oxidative stress, which appears to lead to consequent endothelial damage and inflammatory activation [30–32]. Such a pathological condition induces systemic inflammatory response by activation of endothelial cells and other cell types, a release of proinflammatory cytokines, and cellular debris shed by syncytiotrophoblast (STB) [33, 34]. A large number of studies have already determined that maternal immune malfunction, particularly within innate immunity compartment,

which also contributes to the activation of the immune response involved in pathogenesis of PE. What plays a significant role here are the changes to mononuclear phagocyte system [35]. Macrophages are vital for tissue homeostasis; they regulate inflammatory process and are key regulators of tissue repair.

Systemic inflammatory response is characteristic of all pregnancies; however, in pregnancies complicated with PE inflammatory response reaches extreme intensity [36]. This is expressed by abnormally upregulated immune reactions to the activation of innate immune system and other proinflammatory factors [17]. Consequently, inappropriate trophoblast invasion in myometrium and insufficient spiral arteries remodeling result in placental ischemia. Furthermore, the ensuing oxidative stress is enhanced by excessive release of placental factors: syncytiotrophoblast-derived extracellular vesicles (SEDVs), sFlt-1, and vascular endothelial growth factor (VEGF) that enter maternal circulation, which also contribute to arterial hypertension [37, 38]. These angiogenic factors are also potent mediators of inflammatory response, and they augment inflammation symptoms in PE patients [39]. Cytotrophoblast secreting interleukins 1 β , 2, 4, 6, 8, 10, 12, and 18, transforming growth factor β 1 (TGF β 1), IFN- γ -inducible protein 10/IP-10, tumor necrosis factor (TNF- α), interferon γ (IFN- γ), monocyte chemoattractant protein-1 (MCP-1), intercellular adhesion molecule-1 (ICAM-1), and vascular cell adhesion molecule-1 (VCAM-1) also contributes to PE development [17, 40–43]. Certain cytokines (IL-1 β and IL-18) also affect maternal vascular endothelium and cause its dysfunction [43]. Moreover, by direct or indirect activation of other inflammatory pathways, these cytokines can exacerbate clinical symptoms of PE. The factors which augment the inflammatory response in syncytiotrophoblast also include cholesterol and uric acid [44]. Molecular mechanisms regulating human placental inflammatory response involve the so-called inflammasomes which activate protease, caspase-1 (K1), leading to proinflammatory cytokines IL-1 β and IL-18 activation and secretion of interferon γ , and finally IL-6 [45]. Given that as yet no effective PE therapy has been developed and delivery of the placenta remains the only definitive treatment, thorough investigation of molecular pathways accountable for the cause and severity of the condition seems to be a promising way to design PE prevention and/or treatment methods.

3. Oxidative Stress as the Cause of Inflammatory Response in PE

Activation of the oxidative stress is the condition that must be met for the physiological pregnancy to develop [46]. Oxidative stress involves an imbalance between reactive oxygen species and tissue antioxidant defense system [47–49].

Nitric oxide (NO) regulates vascular tone in order to increase uterine blood flow, and it modulates vasodilation which depends on the endothelial functioning and is also regulated by pregnancy-induced estrogen increase. Nitric oxide is released from endothelial cells, and its two-way activity includes relaxation of blood vessel walls and blood anticoagulation. Endothelial nitric oxide synthase isoform (eNOS)

affects endothelium by reducing vascular wall tension, and it inhibits platelet and leukocyte adhesion to the vascular endothelium, which plays a key role in attenuation of inflammatory response. On the other hand, the inflammation-induced inducible nitric oxide synthase (iNOS) generates excessive amounts of NO. This inflammation-related endothelial dysfunction is considered one of potential causes of PE [50, 51].

The most significant elements of defense against ROS include enzymatic antioxidants: superoxide dismutase (SOD), glutathione peroxidase (GPx), and catalase (CAT). Antioxidant defense system also involves vitamin C, E, α tocopherol, β -carotene, ubiquinone, carotenoids, and glutathione [52]. In the first trimester of gestation, placental tissue is characterized by low content and activity of enzymatic antioxidants such as CAT, GPx, Cu/Zn, and Mn-SOD, which makes trophoblasts particularly susceptible to oxidative damage [53]. Thus, at the beginning of the first trimester, when the intervillous blood oxygen level increases approx. 3-fold due to maternal blood flow to the placenta, reactive oxygen levels are observed to increase rapidly [54, 55].

The major role that ROS plays in PE pathogenesis concentrates on stimulating the secretion of proinflammatory cytokines, chemokines, and cellular debris from apoptotic changes to syncytiotrophoblast [56]. Oxidative stress is also accountable for the activation of NLRP3 inflammasome, caspase-1, and, consequently, IL-1 β release [56, 57]. PE can be characterized as an inflammatory response to placental ischemia and its subsequent reperfusion [53]. Reperfusion-induced placental damage coincides with pathological inflammatory response, which leads to aggravated systemic inflammatory responses and tissue damage by ROS. Scientific evidence clearly indicates that reduced placental blood flow caused by pathological trophoblastic invasion and abnormal angiogenesis induces placental oxidative stress which results in vascular inflammation and endothelial dysfunction [58]. Increased cellular exposition to ROS causes protein carboxylation, lipid peroxidation, and DNA oxidation. These changes are typically found in preeclamptic placentas. When intracellular ROS production is on the increase, interaction between NO and ROS results in formation of peroxynitrite (ONOO⁻) which, in turn, causes eNOS inactivation. In the face of the loss of enzymatic activity, tissue homeostasis is compromised, and oxidative damage to the placenta occurs thereby inducing inflammatory response and a release of large amounts of SEDVs. Activation of the inflammatory response triggered by oxidative stress plays a key role in the etiology of PE [58].

4. Monocytes and Macrophages as the Cause of Inflammatory Response in PE

Normal functioning of the mononuclear phagocytic system is the crucial element of human innate immunity. Scientific data suggest that a disruption to the immune response in preeclamptic pregnancy is caused by disturbance to phagocytic system activity [35]. Monocytes fall into three major groups: classical, intermediate, and nonclassical. Tissue macrophages can be divided into proinflammatory (M1) and anti-

inflammatory (M2). Monocyte differentiation is controlled by cytokines [35]. It has not been decisively determined yet which monocyte subset is most predisposed to differentiate to M1 or M2 macrophages, and whether identical monocytes can undergo tissue-dependent differentiation to M1 and/or M2. Whether selective exhaustion of a selected monocyte subset affects the tissue composition of macrophage population is yet to be determined too.

What mechanisms specifically underlie monocytes activation in pregnancy remain unknown. Syncytiotrophoblast is considered to play the critical role in the process [59, 60]. Quantitative and qualitative profiles of circulating monocytes reflect the severity of preeclamptic pregnancy. The monocyte count and monocyte/lymphocyte ratio have been demonstrated to be higher in preeclamptic women than in normal pregnancies [61, 62]. In preeclamptic pregnancies, reduced levels of anti-inflammatory (classical) monocytes and significantly elevated levels of proinflammatory (intermediate and nonclassical) monocytes are observed in comparison with normal pregnancies [63–65]. Ma et al. analyzed proinflammatory cytokines in blood serum of pregnant women with PE and estimated the percentage of monocytes positive for M1 and M2 markers. CD14+CD11c+CD163-(M1) monocytes in PE women were found to be significantly higher, which correlated with elevated levels of proinflammatory mediators: IL-1 β , IL-6, and MCP-1 [66]. As nonclassical subpopulation becomes more dominant and numerous, the systemic inflammatory response is augmented in preeclamptic patients. The inflammatory response enhancement is caused by extracellular factors and cytokines which activate monocytes [67]. In the future, monocyte count and flow cytometry monocyte phenotyping may play a significant role in predicting disease progression in PE.

Proper decidual balance between pro- and anti-inflammatory macrophages is vital for normal pregnancy development. The increase in nonclassical macrophages subpopulation can affect tissue macrophages system in the endometrium and can be accountable for disturbed placentation in preeclamptic pregnancy [67]. Macrophage polarization into M2 macrophages, physiologically occurring in the second trimester, is believed to be inhibited in preeclamptic pregnancies [21]. Consequently, there is no suppression to M1 macrophages activity, which increases the production of proinflammatory cytokines IFN- γ , TNF- α , and IL-6 and decreases IL-4 and IL-10 levels [21, 68].

The shift in macrophage differentiation from M2 to M1 is ascribed to high levels of proinflammatory and low levels of anti-inflammatory cytokines in preeclamptic placental tissue [69, 70]. Apart from cytokines, what has an impact on macrophage differentiation is the so-called cell axis. A large number of studies have reported that it is the placental mesenchymal stem cells that play a key role in macrophage differentiation into one of the subpopulations, M1 or M2. They are also capable of selective activation of macrophages [71, 72]. Wang et al. determined an important function of hyaluronate in normal pregnancy development. High hyaluronate levels were found to stimulate macrophage polarization to M2 subtype and regulate cytokine production (i.e., IL-10) by decidual macrophages [73].

5. Inflammasomes as the Cause of Inflammatory Response in PE

Inflammasomes are cytosolic multiprotein complexes composed of pattern recognition receptor (PRR), apoptosis-associated speck-like protein containing a caspase recruitment domain (ASC), and proinflammatory caspase-1 [74]. The inflammasome recognition receptor is responsible for the response to microbe-derived (viral, bacterial) pathogens: pathogen-associated molecular pattern (PAMP), the body's own cells affected by stress: stress-associated molecular pattern (SAMP), and the cells from damaged tissue: damage-associated molecular pattern (DAMP) [75, 76]. The activated receptor leads to the consequent inflammasome self-oligomerization and caspase-1 activation [77]. This initiates low-level inflammatory response causing IL-1 β and IL-18 release [78–80] and pyroptotic cell death (inflammation-induced apoptosis) [81, 82]. Originally, inflammasomes were considered specific to innate immunity response [83]; however, recent analyses have reported that they are also engaged in the promotion of adaptive immunity [84, 85]. Cellular potential for inflammatory signaling is largely dependent on PRR expression on the cell surface. Two major classes of PRR families include Toll-like receptors (TLRs) and Nod-like receptors (NLRs) [86].

TLRs are transmembrane receptors which recognize PAMPs and DAMPs outside of the cell and in intracellular endosomes. To date, ten TLRs have been identified and described. Each of these receptors is stimulated by their specific ligands thereby triggering signaling cascades in response to infection caused by Gram (+)/Gram (-) bacteria or RNA viruses [87, 88].

NLRs belong to the cytosolic PRRs and constitute a system of intracellular sensors of DAMPs or PAMPs. The inflammatory response activated by NLRs is thus stimulated and sustained by endogenous “danger” signals. Numerous NLRs and NLR-dependent inflammasomes have been identified so far, and these include pyrin domain-containing proteins (NLRP1, NLRP3), NLR-family caspase activators, caspase activation and recruitment domain (CARD), domain-containing protein-4 (NLRC4), and apoptosis-associated speck-like protein containing a CARD (ASC) [89].

Since inflammasome components are expressed on placental cells, recent studies report that inflammasomes are actively involved in inflammatory response related to placental dysfunction in PE. Mulla et al. [90] and Xie et al. [88] proved that NLRP3 activation in trophoblasts and peripheral blood plays an important role in the pathogenesis of PE. Moreover, enhanced expression of NLRP1 and NLRP3 has been demonstrated in peripheral monocytes from preeclamptic women [91, 92]. Additionally, women with PE demonstrate an elevated level of total cholesterol and uric acid which both belong to host-derived damage-associated molecular patterns (DAMPs)—endogenous alarmins [93, 94]. This, in turn, can lead to the NLRP3 inflammasome activation in syncytiotrophoblasts. The NLRP3 inflammasome is the most widely investigated and therefore the best-characterized of all the inflammasomes. It is distinguished by its two major features: its activation can be triggered by

a variety of unrelated factors (including PAMPs, DAMPs, and alarmins) [95, 96], and it is highly expressed on the cells of innate immune system (macrophages, neutrophils, and dendritic cells) in many tissues [97, 98]. The NLRP3 inflammasome activation can be described as a two-signal model. The first so-called priming signal is initiated by inflammatory stimuli which affect transmembrane PRRs (TLRs) and activate the NF- κ B pathway, leading to upregulation of pro-IL-1 β and NLRP3 protein levels [99]. The second signal involves simultaneous signaling pathways after PAMP or DAMP recognition: they initiate assembly of the NLRP3 inflammasome complex and activate procaspase-1 into its cleaved form, which results in the release of IL-1 β and IL-18 (Figure 1) [75].

Several molecular mechanisms are triggered by NLRP3 activation, and these, among others, include potassium ion efflux, lysosomal rupture, mitochondrial dysfunction, calcium influx, and decrease of intracellular cAMP [100–102]. A well-established mechanism of NLRP3 inflammasome activation is a decrease in the intracellular potassium concentration. It confirms the assumption that numerous microbiological and endogenous signals can activate inflammasomes by reducing the level of cytosolic potassium [103]. However, signaling pathways of inflammasome activation which are independent of changes to cytosolic potassium concentration have also been described [104]. The NLRP3 inflammasome can also be activated in a caspase-11-mediated noncanonical pathway. The signaling pathway was first described in mice infected with *Escherichia coli*, *Citrobacter rodentium*, and *Vibrio cholerae* (caspase-11 homologs in humans are caspase-4 and caspase-5) [105–107]. Similarly to the canonical pathway results, noncanonical activation pathway leads to caspase-1 cleavage resulting in IL-1 β and IL-18 release. However, caspase-11 sensing and binding with LPS are typical to the noncanonical pathway only [108]. Active caspase-11 also cleaves gasdermin D (GSDMD), which allows the N-terminal domain of GSDMD to form pores in the plasma membrane thereby triggering pyroptosis, proinflammatory form of cell death, linked to caspase-11 activation, and the release of IL-1 β and IL-18 [109, 110]. Inflammasomes play one of the critical roles in the process of the host protection against pathogens, and they are actively involved in the immunoregulation, which is of key importance for the systemic homeostasis [111]. Therefore, any pathological interference in inflammasomes activation may augment placental inflammatory response thereby inducing clinical and laboratory symptoms related to PE.

6. Conclusions

Over the recent years, our understanding of the pathophysiological background of PE has been enriched considerably. Preeclampsia involves a chronic activation of maternal immune system which is demonstrated by elevated proinflammatory cytokine levels and simultaneously reduced influence of immunoregulatory factors. The imbalance is promoted by prolonged inflammatory response in pregnancies complicated with PE. To date, a single and conclusive mechanism underlying preeclampsia has not been identified

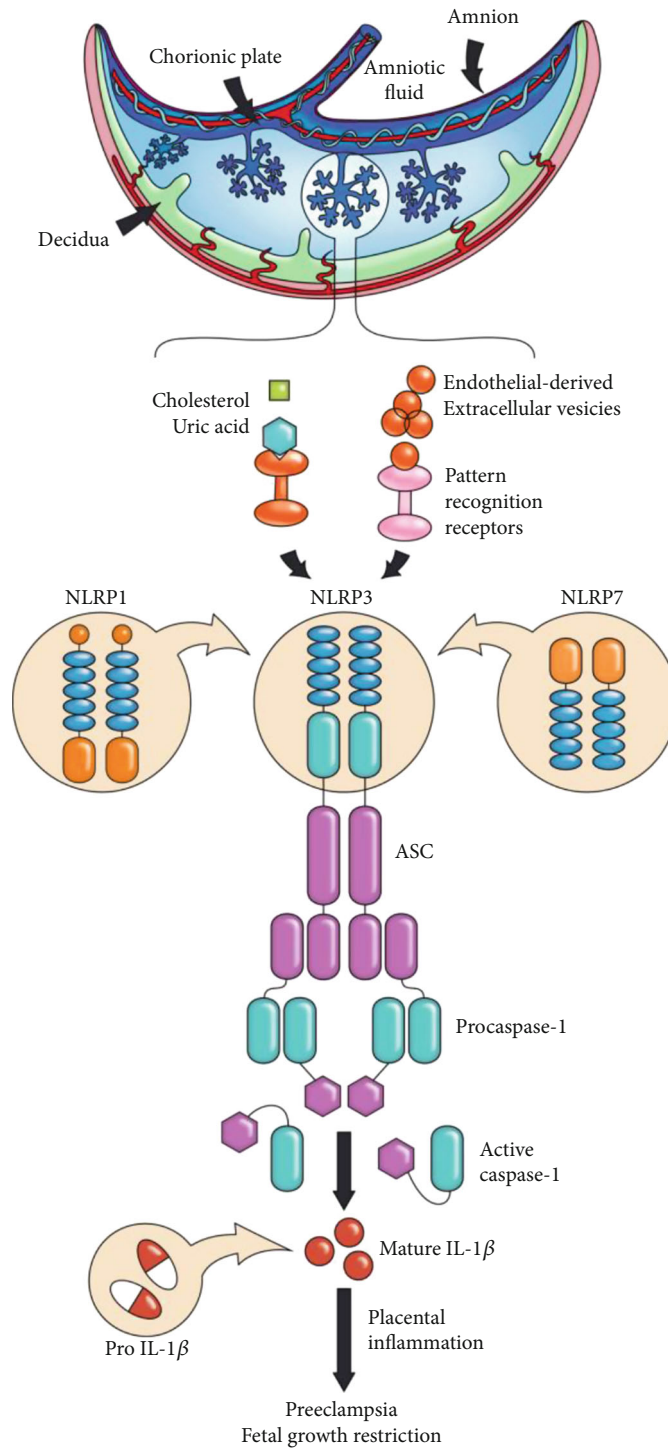


FIGURE 1: Inflammasomes in placental inflammation. Endothelial-derived extracellular vesicles and/or alarmins (e.g., cholesterol or uric acid) can activate the NLRP3, NLRP1, and NLRP7 inflammasomes in the placenta, leading to the processing and release of active caspase-1 and mature IL-1 β . The resulting inflammation may lead to placental diseases such as preeclampsia and fetal growth restriction.

yet. The analyses to determine the cause of the immune imbalance leading to enhanced systemic inflammatory response which occurs in PE appear to be an intriguing aim for further research which may contribute to the identification of new targets for PE therapies. More thorough understanding of the pathophysiology of inflammatory

process in preeclampsia can largely contribute to the design of new, targeted anti-inflammatory therapies. The examples of such potential include the use of highly selective NLRP-3—inflammasome inhibitor MCC950. This diarylsulfonylurea-containing compound blocks the release of proinflammatory IL-1 β by preventing oligomerization

of the inflammasome adaptor protein ASC. Flow cytometry monocyte phenotyping could also be applied in therapies for PE. Finally, bearing in mind the oxidative stress underlying the inflammatory response activation in PE, antioxidant therapy could also provide a promising solution. In conclusion, the findings of further research into the subject will have a key impact on the development of a targeted therapy which can improve the perinatal outcomes in women affected with preeclampsia.

Data Availability

No data were used to support this study.

Disclosure

The data being presented in the journal has not been published elsewhere in whole. The authors agree to publish the work in the Mediators of Inflammation.

Conflicts of Interest

The authors declare that there is no conflict of interests regarding the publication of this paper.

References

- [1] J. Espinoza, A. Vidaeff, C. M. Pettker, and H. Simhan, "Gestational hypertension and preeclampsia," *Obstetrics & Gynecology*, vol. 133, no. 1, pp. 1–3, 2019.
- [2] B. Mol, C. T. Roberts, S. Thangaratinam, L. A. Magee, C. de Groot, and G. J. Hofmeyr, "Pre-eclampsia," *The Lancet*, vol. 387, no. 10022, pp. 999–1011, 2016.
- [3] A. L. Tranquilli, G. Dekker, L. Magee et al., "The classification, diagnosis and management of the hypertensive disorders of pregnancy: a revised statement from the ISSHP," *Pregnancy hypertension*, vol. 4, no. 2, pp. 97–104, 2014.
- [4] C. W. Redman, G. P. Sacks, and I. L. Sargent, "Preeclampsia: an excessive maternal inflammatory response to pregnancy," *American Journal of Obstetrics and Gynecology*, vol. 180, no. 2, pp. 499–506, 1999.
- [5] S. Saito, A. Shiozaki, A. Nakashima, M. Sakai, and Y. Sasaki, "The role of the immune system in preeclampsia," *Molecular Aspects of Medicine*, vol. 28, no. 2, pp. 192–209, 2007.
- [6] A. Ohkuchi, R. Iwasaki, H. Suzuki et al., "Normal and high-normal blood pressures, but not body mass index, are risk factors for the subsequent occurrence of both preeclampsia and gestational hypertension: a retrospective cohort study," *Hypertension research: official journal of the Japanese Society of Hypertension*, vol. 29, no. 3, pp. 161–167, 2006.
- [7] T. H. de Lima, N. Sass, R. Mattar et al., "Cytokine gene polymorphisms in preeclampsia and eclampsia," *Hypertension research: official journal of the Japanese Society of Hypertension*, vol. 32, no. 7, pp. 565–569, 2009.
- [8] A. Molvarec, L. Kalabay, Z. Derzsy et al., "Preeclampsia is associated with decreased serum alpha (2)-HS glycoprotein (fetuin-A) concentration," *Hypertension research: official journal of the Japanese Society of Hypertension*, vol. 32, no. 8, pp. 665–669, 2009.
- [9] A. Molvarec, Z. Derzsy, J. Kocsis et al., "Circulating anti-heat-shock-protein antibodies in normal pregnancy and preeclampsia," *Cell Stress & Chaperones*, vol. 14, no. 5, pp. 491–498, 2009.
- [10] P. Aggarwal, V. Jain, and V. Jha, "Endothelial nitric oxide synthase, angiotensin-converting enzyme and angiotensinogen gene polymorphisms in hypertensive disorders of pregnancy," *Hypertension Research*, vol. 33, no. 5, pp. 473–477, 2010.
- [11] A. Molvarec, L. Tamási, G. Losonczy, K. Madách, Z. Prohászka, and J. Rigó Jr., "Circulating heat shock protein 70 (HSPA1A) in normal and pathological pregnancies," *Cell Stress & Chaperones*, vol. 15, no. 3, pp. 237–247, 2010.
- [12] R. J. Skow, E. C. King, C. D. Steinback, and M. H. Davenport, "The influence of prenatal exercise and pre-eclampsia on maternal vascular function," *Clinical science (London, England: 1979)*, vol. 131, no. 17, pp. 2223–2240, 2017.
- [13] T. Chaiworapongsa, P. Chaemsaihong, L. Yeo, and R. Romero, "Pre-eclampsia part I: current understanding of its pathophysiology. Nature reviews," *Nephrology*, vol. 10, no. 8, pp. 466–480, 2014.
- [14] S. M. Lee, R. Romero, Y. J. Lee, I. S. Park, C.-W. Park, and B. H. Yoon, "Systemic inflammatory stimulation by micro-particles derived from hypoxic trophoblast as a model for inflammatory response in preeclampsia," *American Journal of Obstetrics and Gynecology*, vol. 207, no. 4, pp. 337.e1–337.e8, 2012.
- [15] C. S. Roland, J. Hu, C. E. Ren et al., "Morphological changes of placental syncytium and their implications for the pathogenesis of preeclampsia," *Cellular and Molecular Life Sciences: CMLS*, vol. 73, no. 2, pp. 365–376, 2016.
- [16] R. Madazli, E. Budak, Z. Calay, and M. F. Aksu, "Correlation between placental bed biopsy findings, vascular cell adhesion molecule and fibronectin levels in pre-eclampsia," *BJOG: an international journal of obstetrics and gynaecology*, vol. 107, no. 4, pp. 514–518, 2000.
- [17] D. C. Cornelius, "Preeclampsia: From Inflammation to Immunoregulation," *Clinical medicine insights: Blood disorders*, vol. 11, article 1179545X17752325, 2018.
- [18] V. R. Ribeiro, M. Romao-Veiga, G. G. Romagnoli et al., "Association between cytokine profile and transcription factors produced by T-cell subsets in early- and late-onset preeclampsia," *Immunology*, vol. 152, no. 1, pp. 163–173, 2017.
- [19] A. Umapathy, L. W. Chamley, and J. L. James, "Reconciling the distinct roles of angiogenic/anti-angiogenic factors in the placenta and maternal circulation of normal and pathological pregnancies," *Angiogenesis*, vol. 23, no. 2, pp. 105–117, 2020.
- [20] F. R. Helmo, A. Lopes, A. Carneiro et al., "Angiogenic and antiangiogenic factors in preeclampsia," *Pathology, Research and Practice*, vol. 214, no. 1, pp. 7–14, 2018.
- [21] I. L. Sargent, A. M. Borzychowski, and C. W. Redman, "Immunoregulation in normal pregnancy and pre-eclampsia: an overview," *Reproductive Biomedicine Online*, vol. 13, no. 5, pp. 680–686, 2006.
- [22] W. A. Bennett, S. Lagoo-Deenadayalan, J. A. Stopple et al., "Cytokine expression by first-trimester human chorionic villi," *American journal of reproductive immunology*, vol. 40, no. 5, pp. 309–318, 1998.
- [23] G. Gadonski, B. B. LaMarca, E. Sullivan, W. Bennett, D. Chandler, and J. P. Granger, "Hypertension produced by reductions in uterine perfusion in the pregnant rat: role of interleukin 6," *Hypertension*, vol. 48, no. 4, pp. 711–716, 2006.

- [24] M. Baumann, S. Becker, H. J. Krüger, H. Vogler, T. Maurer, and H. P. Beck-Bornholdt, "Flow cytometric determination of the time of metastasis during fractionated radiation therapy of the rat rhabdomyosarcoma R1H," *International Journal of Radiation Biology*, vol. 58, no. 2, pp. 361–369, 2009.
- [25] G. J. Burton and E. Jauniaux, "Placental oxidative stress: from miscarriage to preeclampsia," *Journal of the Society for Gynecologic Investigation*, vol. 11, no. 6, pp. 342–352, 2016.
- [26] M. G. Elliot, "Oxidative stress and the evolutionary origins of preeclampsia," *Journal of Reproductive Immunology*, vol. 114, pp. 75–80, 2016.
- [27] R. D. Pereira, N. E. De Long, R. C. Wang, F. T. Yazdi, A. C. Holloway, and S. Raha, "Angiogenesis in the placenta: the role of reactive oxygen species signaling," *Bio Med research international*, vol. 2015, article 814543, pp. 1–12, 2015.
- [28] E. Jauniaux, L. Poston, and G. J. Burton, "Placental-related diseases of pregnancy: involvement of oxidative stress and implications in human evolution," *Human Reproduction Update*, vol. 12, no. 6, pp. 747–755, 2006.
- [29] W. Stevens, T. Shih, D. Incerti et al., "Short-term costs of preeclampsia to the United States health care system," *American journal of obstetrics and gynecology*, vol. 217, no. 3, pp. 237–248.e16, 2017.
- [30] L. Myatt and R. P. Webster, "Vascular biology of preeclampsia," *Journal of thrombosis and haemostasis: JTH*, vol. 7, no. 3, pp. 375–384, 2009.
- [31] S. R. Hansson, Å. Nääv, and L. Erlandsson, "Oxidative stress in preeclampsia and the role of free fetal hemoglobin," *Frontiers in Physiology*, vol. 5, p. 516, 2015.
- [32] H. W. Yung, D. Atkinson, T. Champion-Smith, M. Olovsson, D. S. Charnock-Jones, and G. J. Burton, "Differential activation of placental unfolded protein response pathways implies heterogeneity in causation of early- and late-onset preeclampsia," *The Journal of Pathology*, vol. 234, no. 2, pp. 262–276, 2014.
- [33] L. C. Sánchez-Aranguren, C. E. Prada, C. E. Riaño-Medina, and M. Lopez, "Endothelial dysfunction and preeclampsia: role of oxidative stress," *Frontiers in Physiology*, vol. 5, p. 372, 2014.
- [34] A. K. Smáráson, I. L. Sargent, P. M. Starkey, and C. W. Redman, "The effect of placental syncytiotrophoblast microvillous membranes from normal and pre-eclamptic women on the growth of endothelial cells in vitro," *British Journal of Obstetrics and Gynaecology*, vol. 100, no. 10, pp. 943–949, 1993.
- [35] P. Vishnyakova, A. Elchaninov, T. Fatkhudinov, and G. Sukhikh, "Role of the monocyte-macrophage system in normal pregnancy and preeclampsia," *International Journal of Molecular Sciences*, vol. 20, no. 15, p. 3695, 2019.
- [36] C. W. Redman and I. L. Sargent, "Immunology of preeclampsia," *American journal of reproductive immunology*, vol. 63, no. 6, pp. 534–543, 2010.
- [37] A. M. Borzychowski, I. L. Sargent, and C. W. Redman, "Inflammation and pre-eclampsia," *Seminars in Fetal & Neonatal Medicine*, vol. 11, no. 5, pp. 309–316, 2006.
- [38] I. L. Sargent, A. M. Borzychowski, and C. W. Redman, "NK cells and human pregnancy—an inflammatory view," *Trends in Immunology*, vol. 27, no. 9, pp. 399–404, 2006.
- [39] L. H. Tangerås, G. S. Stødle, G. D. Olsen et al., "Functional Toll-like receptors in primary first-trimester trophoblasts," *Journal of Reproductive Immunology*, vol. 106, pp. 89–99, 2014.
- [40] I. Roth, D. B. Corry, R. M. Locksley, J. S. Abrams, M. J. Litton, and S. J. Fisher, "Human placental cytotrophoblasts produce the immunosuppressive cytokine interleukin 10," *The Journal of Experimental Medicine*, vol. 184, no. 2, pp. 539–548, 1996.
- [41] B. D. LaMarca, M. J. Ryan, J. S. Gilbert, S. R. Murphy, and J. P. Granger, "Inflammatory cytokines in the pathophysiology of hypertension during preeclampsia," *Current Hypertension Reports*, vol. 9, no. 6, pp. 480–485, 2007.
- [42] A. Szarka, J. Rigó Jr., L. Lázár, G. Beko, and A. Molvarec, "Circulating cytokines, chemokines and adhesion molecules in normal pregnancy and preeclampsia determined by multiplex suspension array," *BMC Immunology*, vol. 11, no. 1, p. 59, 2010.
- [43] C. Rusterholz, S. Hahn, and W. Holzgreve, "Role of placentally produced inflammatory and regulatory cytokines in pregnancy and the etiology of preeclampsia," *Seminars in Immunopathology*, vol. 29, no. 2, pp. 151–162, 2007.
- [44] G. S. Stødle, G. B. Silva, L. H. Tangerås et al., "Placental inflammation in pre-eclampsia by nod-like receptor protein (NLRP)3 inflammasome activation in trophoblasts," *Clinical and Experimental Immunology*, vol. 193, no. 1, pp. 84–94, 2018.
- [45] N. Gomez-Lopez, K. Motomura, D. Miller, V. Garcia-Flores, J. Galaz, and R. Romero, "Inflammasomes: their role in normal and complicated pregnancies," *Journal of immunology*, vol. 203, no. 11, pp. 2757–2769, 2019.
- [46] X. Yang, L. Guo, H. Li, X. Chen, and X. Tong, "Analysis of the original causes of placental oxidative stress in normal pregnancy and pre-eclampsia: a hypothesis," *The Journal of Maternal-Fetal & Neonatal Medicine*, vol. 25, no. 7, pp. 884–888, 2011.
- [47] K. Matsubara, Y. Matsubara, S. Hyodo, T. Katayama, and M. Ito, "Role of nitric oxide and reactive oxygen species in the pathogenesis of preeclampsia," *The Journal of Obstetrics and Gynaecology Research*, vol. 36, no. 2, pp. 239–247, 2010.
- [48] N. Sinha and P. K. Dabla, "Oxidative stress and antioxidants in hypertension—a current review," *Current Hypertension Reviews*, vol. 11, no. 2, pp. 132–142, 2015.
- [49] B. Kalyanaraman, "Teaching the basics of redox biology to medical and graduate students: oxidants, antioxidants and disease mechanisms," *Redox Biology*, vol. 1, no. 1, pp. 244–257, 2013.
- [50] K. Matsubara, T. Higaki, Y. Matsubara, and A. Nawa, "Nitric oxide and reactive oxygen species in the pathogenesis of preeclampsia," *International Journal of Molecular Sciences*, vol. 16, no. 3, pp. 4600–4614, 2015.
- [51] U. Förstermann, N. Xia, and H. Li, "Roles of vascular oxidative stress and nitric oxide in the pathogenesis of atherosclerosis," *Circulation Research*, vol. 120, no. 4, pp. 713–735, 2017.
- [52] E. Birben, U. M. Sahiner, C. Sackesen, S. Erzurum, and O. Kalayci, "Oxidative stress and antioxidant defense," *World Allergy Organization Journal*, vol. 5, no. 1, pp. 9–19, 2012.
- [53] L. Poston, N. Igosheva, H. D. Mistry et al., "Role of oxidative stress and antioxidant supplementation in pregnancy disorders," *The American Journal of Clinical Nutrition*, vol. 94, suppl_6, pp. 1980S–1985S, 2011.
- [54] E. Jauniaux, A. L. Watson, J. Hempstock, Y. P. Bao, J. N. Skepper, and G. J. Burton, "Onset of maternal arterial blood flow and placental oxidative stress. A possible factor in human early pregnancy failure," *The American Journal of Pathology*, vol. 157, no. 6, pp. 2111–2122, 2000.

- [55] M. H. Schoots, S. J. Gordijn, S. A. Scherjon, H. van Goor, and J. L. Hillebrands, "Oxidative stress in placental pathology," *Placenta*, vol. 69, pp. 153–161, 2018.
- [56] P. R. Nunes, M. Peracoli, M. Romao-Veiga et al., "Hydrogen peroxide-mediated oxidative stress induces inflammasome activation in term human placental explants," *Pregnancy hypertension*, vol. 14, pp. 29–36, 2018.
- [57] D. I. Chiarello, C. Abad, D. Rojas et al., "Oxidative stress: normal pregnancy versus preeclampsia," *Biochimica et biophysica acta. Molecular basis of disease*, vol. 1866, no. 2, article 165354, 2020.
- [58] R. Aouache, L. Biquard, D. Vaiman, and F. Miralles, "Oxidative stress in preeclampsia and placental diseases," *International Journal of Molecular Sciences*, vol. 19, no. 5, p. 1496, 2018.
- [59] O. Nonn, J. Güttler, D. Forstner et al., "Placental CX3CL1 is deregulated by angiotensin II and contributes to a pro-inflammatory trophoblast-monocyte interaction," *International Journal of Molecular Sciences*, vol. 20, no. 3, p. 641, 2019.
- [60] M. Siwetz, M. Sundl, D. Kolb et al., "Placental fractalkine mediates adhesion of THP-1 monocytes to villous trophoblast," *Histochemistry and Cell Biology*, vol. 143, no. 6, pp. 565–574, 2015.
- [61] J. Wang, Q. W. Zhu, X. Y. Cheng et al., "Assessment efficacy of neutrophil-lymphocyte ratio and monocyte-lymphocyte ratio in preeclampsia," *Journal of Reproductive Immunology*, vol. 132, pp. 29–34, 2019.
- [62] M. E. Brien, I. Boufaied, D. D. Soglio, E. Rey, L. Leduc, and S. Girard, "Distinct inflammatory profile in preeclampsia and postpartum preeclampsia reveal unique mechanisms," *Biology of Reproduction*, vol. 100, no. 1, pp. 187–194, 2019.
- [63] T. I. Alahakoon, H. Medbury, H. Williams, N. Fewings, X. M. Wang, and V. W. Lee, "Characterization of fetal monocytes in preeclampsia and fetal growth restriction," *Journal of Perinatal Medicine*, vol. 47, no. 4, pp. 434–438, 2019.
- [64] T. I. Alahakoon, H. Medbury, H. Williams, N. Fewings, X. M. Wang, and V. W. Lee, "Distribution of monocyte subsets and polarization in preeclampsia and intrauterine fetal growth restriction," *The Journal of Obstetrics and Gynaecology Research*, vol. 44, no. 12, pp. 2135–2148, 2018.
- [65] G. Jabalie, M. Ahmadi, L. Koushaeian et al., "Metabolic syndrome mediates proinflammatory responses of inflammatory cells in preeclampsia," *American journal of reproductive immunology*, vol. 81, no. 3, article e13086, 2019.
- [66] Y. Ma, Y. Ye, J. Zhang, C. C. Ruan, and P. J. Gao, "Immune imbalance is associated with the development of preeclampsia," *Medicine*, vol. 98, no. 14, article e15080, 2019.
- [67] K. P. Conrad, M. B. Rabaglino, and E. D. Post Uiterweer, "Emerging role for dysregulated decidualization in the genesis of preeclampsia," *Placenta*, vol. 60, pp. 119–129, 2017.
- [68] M. B. Pinheiro, K. B. Gomes, and L. M. Duse, "Fibrinolytic system in preeclampsia," *Clinica chimica acta; international journal of clinical chemistry*, vol. 416, pp. 67–71, 2013.
- [69] J. Xu, Y. Gu, J. Sun, H. Zhu, D. F. Lewis, and Y. Wang, "Reduced CD200 expression is associated with altered Th1/Th2 cytokine production in placental trophoblasts from preeclampsia," *American journal of reproductive immunology*, vol. 79, no. 1, 2018.
- [70] R. Aggarwal, A. K. Jain, P. Mittal, M. Kohli, P. Jwanjal, and G. Rath, "Association of pro- and anti-inflammatory cytokines in preeclampsia," *Journal of Clinical Laboratory Analysis*, vol. 33, no. 4, article e22834, 2019.
- [71] M. H. Abumaree, S. Al Harthy, A. M. Al Subayyil et al., "Decidua basalis mesenchymal stem cells favor inflammatory M1 macrophage differentiation in vitro," *Cell*, vol. 8, no. 2, p. 173, 2019.
- [72] M. H. Abumaree, M. A. Al Jumah, B. Kalionis et al., "Human placental mesenchymal stem cells (pMSCs) play a role as immune suppressive cells by shifting macrophage differentiation from inflammatory M1 to anti-inflammatory M2 macrophages," *Stem Cell Reviews and Reports*, vol. 9, no. 5, pp. 620–641, 2013.
- [73] S. Wang, F. Sun, M. Han et al., "Trophoblast-derived hyaluronan promotes the regulatory phenotype of decidual macrophages," *Reproduction (Cambridge, England)*, vol. 157, no. 2, pp. 189–198, 2019.
- [74] F. Martinon, K. Burns, and J. Tschopp, "The Inflammasome," *Molecular Cell*, vol. 10, no. 2, pp. 417–426, 2002.
- [75] K. V. Swanson, M. Deng, and J. P. Ting, "The NLRP3 inflammasome: molecular activation and regulation to therapeutics. Nature reviews," *Immunology*, vol. 19, no. 8, pp. 477–489, 2019.
- [76] Y. Wang, A. L. Sedlacek, S. Pawaria, H. Xu, M. J. Scott, and R. J. Binder, "Cutting edge: the heat shock protein gp 96 activates Inflammasome-signaling platforms in APCs," *Journal of immunology*, vol. 201, no. 8, pp. 2209–2214, 2018.
- [77] E. Latz, T. S. Xiao, and A. Stutz, "Activation and regulation of the inflammasomes. Nature reviews," *Immunology*, vol. 13, no. 6, pp. 397–411, 2013.
- [78] N. A. Thornberry, H. G. Bull, J. R. Calaycay et al., "A novel heterodimeric cysteine protease is required for interleukin-1 beta processing in monocytes," *Nature*, vol. 356, no. 6372, pp. 768–774, 1992.
- [79] R. A. Black, S. R. Kronheim, J. E. Merriam, C. J. March, and T. P. Hopp, "A pre-aspartate-specific protease from human leukocytes that cleaves pro-interleukin-1 beta," *The Journal of Biological Chemistry*, vol. 264, no. 10, pp. 5323–5326, 1989.
- [80] P. J. Sansonetti, A. Phalipon, J. Arondel et al., "Caspase-1 activation of IL-1beta and IL-18 are essential for Shigella flexneri-induced inflammation," *Immunity*, vol. 12, no. 5, pp. 581–590, 2000.
- [81] B. T. Cookson and M. A. Brennan, "Pro-inflammatory programmed cell death," *Trends in Microbiology*, vol. 9, no. 3, pp. 113–114, 2001.
- [82] E. A. Miao, J. V. Rajan, and A. Aderem, "Caspase-1-induced pyroptotic cell death," *Immunological Reviews*, vol. 243, no. 1, pp. 206–214, 2011.
- [83] F. Martinon, V. Pétrilli, A. Mayor, A. Tardivel, and J. Tschopp, "Gout-associated uric acid crystals activate the NALP3 inflammasome," *Nature*, vol. 440, no. 7081, pp. 237–241, 2006.
- [84] G. Doitsh, N. L. Galloway, X. Geng et al., "Corrigendum: cell death by pyroptosis drives CD4 T-cell depletion in HIV-1 infection," *Nature*, vol. 544, no. 7648, p. 124, 2017.
- [85] E. Stewart, J. A. Triccas, and N. Petrovsky, "Adjuvant strategies for more effective tuberculosis vaccine immunity," *Microorganisms*, vol. 7, no. 8, p. 255, 2019.
- [86] P. Broz and V. M. Dixit, "Inflammasomes: mechanism of assembly, regulation and signalling. Nature reviews," *Immunology*, vol. 16, no. 7, pp. 407–420, 2016.

- [87] J. V. Ilekis, E. Tsilou, S. Fisher et al., "Placental origins of adverse pregnancy outcomes: potential molecular targets: an Executive Workshop Summary of the Eunice Kennedy Shriver National Institute of Child Health and Human Development," *American Journal of Obstetrics and Gynecology*, vol. 215, no. 1, pp. S1–S46, 2016.
- [88] F. Xie, Y. Hu, S. E. Turvey et al., "Toll-like receptors 2 and 4 and the cryopyrin inflammasome in normal pregnancy and pre-eclampsia," *BJOG: an international journal of obstetrics and gynaecology*, vol. 117, no. 1, pp. 99–108, 2010.
- [89] A. Lu, V. G. Magupalli, J. Ruan et al., "Unified polymerization mechanism for the assembly of ASC-dependent inflammasomes," *Cell*, vol. 156, no. 6, pp. 1193–1206, 2014.
- [90] M. J. Mulla, K. Myrtolli, J. Potter et al., "Uric acid induces trophoblast IL-1 β production via the inflammasome: implications for the pathogenesis of preeclampsia," *American journal of reproductive immunology*, vol. 65, no. 6, pp. 542–548, 2011.
- [91] M. Romão-Veiga, M. L. Matias, V. R. Ribeiro et al., "Induction of systemic inflammation by hyaluronan and hsp 70 in women with pre-eclampsia," *Cytokine*, vol. 105, pp. 23–31, 2018.
- [92] M. L. Matias, V. J. Gomes, M. Romao-Veiga et al., "Silibinin downregulates the NF- κ B pathway and NLRP1/NLRP3 inflammasomes in monocytes from pregnant women with preeclampsia," *Molecules*, vol. 24, no. 8, p. 1548, 2019.
- [93] J. L. Dziki, G. Hussey, and S. F. Badylak, "Alarmins of the extracellular space," *Seminars in Immunology*, vol. 38, pp. 33–39, 2018.
- [94] M. E. Bianchi, "DAMPs, PAMPs and alarmins: all we need to know about danger," *Journal of Leukocyte Biology*, vol. 81, no. 1, pp. 1–5, 2007.
- [95] P. Duewell, H. Kono, K. J. Rayner et al., "NLRP3 inflammasomes are required for atherogenesis and activated by cholesterol crystals," *Nature*, vol. 464, no. 7293, pp. 1357–1361, 2010.
- [96] L. Freeman, H. Guo, C. N. David, W. J. Brickey, S. Jha, and J. P. Ting, "NLR members NLRC4 and NLRP3 mediate sterile inflammasome activation in microglia and astrocytes," *The Journal of Experimental Medicine*, vol. 214, no. 5, pp. 1351–1370, 2017.
- [97] M. Kool, V. Pétrilli, T. De Smedt et al., "Cutting edge: alum adjuvant stimulates inflammatory dendritic cells through activation of the NALP3 inflammasome," *Journal of immunology*, vol. 181, no. 6, pp. 3755–3759, 2008.
- [98] E. L. Goldberg, J. L. Asher, R. D. Molony et al., " β -Hydroxybutyrate deactivates neutrophil NLRP3 inflammasome to relieve gout flares," *Cell Reports*, vol. 18, no. 9, pp. 2077–2087, 2017.
- [99] F. G. Bauernfeind, G. Horvath, A. Stutz et al., "Cutting edge: NF- κ B activating pattern recognition and cytokine receptors license NLRP3 inflammasome activation by regulating NLRP3 expression," *Journal of immunology*, vol. 183, no. 2, pp. 787–791, 2009.
- [100] V. Pétrilli, S. Papin, C. Dostert, A. Mayor, F. Martinon, and J. Tschopp, "Activation of the NALP3 inflammasome is triggered by low intracellular potassium concentration," *Cell Death and Differentiation*, vol. 14, no. 9, pp. 1583–1589, 2007.
- [101] L. Gov, C. A. Schneider, T. S. Lima, W. Pandori, and M. B. Lodoen, "NLRP3 and potassium efflux drive rapid IL-1 β release from primary human monocytes during *Toxoplasma gondii* infection," *Journal of immunology*, vol. 199, no. 8, pp. 2855–2864, 2017.
- [102] T. Murakami, J. Ockinger, J. Yu et al., "Critical role for calcium mobilization in activation of the NLRP3 inflammasome," *Proceedings of the National Academy of Sciences of the United States of America*, vol. 109, no. 28, pp. 11282–11287, 2012.
- [103] R. Muñoz-Planillo, P. Kuffa, G. Martínez-Colón, B. L. Smith, T. M. Rajendiran, and G. Núñez, "K⁺ efflux is the common trigger of NLRP3 inflammasome activation by bacterial toxins and particulate matter," *Immunity*, vol. 38, no. 6, pp. 1142–1153, 2013.
- [104] C. J. Groß, R. Mishra, K. S. Schneider et al., "K⁺ efflux-independent NLRP3 inflammasome activation by small molecules targeting mitochondria," *Immunity*, vol. 45, no. 4, pp. 761–773, 2016.
- [105] J. Shi, Y. Zhao, Y. Wang et al., "Inflammatory caspases are innate immune receptors for intracellular LPS," *Nature*, vol. 514, no. 7521, pp. 187–192, 2014.
- [106] E. Viganò, C. E. Diamond, R. Spreafico, A. Balachander, R. M. Sobota, and A. Mortellaro, "Human caspase-4 and caspase-5 regulate the one-step non-canonical inflammasome activation in monocytes," *Nature Communications*, vol. 6, no. 1, p. 8761, 2015.
- [107] N. Kayagaki, S. Warming, M. Lamkanfi et al., "Non-canonical inflammasome activation targets caspase-11," *Nature*, vol. 479, no. 7371, pp. 117–121, 2011.
- [108] N. Kayagaki, M. T. Wong, I. B. Stowe et al., "Noncanonical inflammasome activation by intracellular LPS independent of TLR4," *Science*, vol. 341, no. 6151, pp. 1246–1249, 2013.
- [109] J. Shi, Y. Zhao, K. Wang et al., "Cleavage of GSDMD by inflammatory caspases determines pyroptotic cell death," *Nature*, vol. 526, no. 7575, pp. 660–665, 2015.
- [110] N. Kayagaki, I. B. Stowe, B. L. Lee et al., "Caspase-11 cleaves gasdermin D for non-canonical inflammasome signalling," *Nature*, vol. 526, no. 7575, pp. 666–671, 2015.
- [111] T. Strowig, J. Henao-Mejia, E. Elinav, and R. Flavell, "Inflammasomes in health and disease," *Nature*, vol. 481, no. 7381, pp. 278–286, 2012.

Research Article

P2Y₂ Receptor Induces *L. amazonensis* Infection Control in a Mechanism Dependent on Caspase-1 Activation and IL-1 β Secretion

Maria Luiza Thorstenberg,¹ Monique Daiane Andrade Martins,¹ Vanessa Figliuolo,¹ Claudia Lucia Martins Silva,² Luiz Eduardo Baggio Savio,¹ and Robson Coutinho-Silva¹ 

¹Laboratório de Imunofisiologia, Instituto de Biofísica Carlos Chagas Filho, Universidade Federal do Rio de Janeiro, Rio de Janeiro, Brazil

²Laboratório de Farmacologia Bioquímica e Molecular, Instituto de Ciências Biomédicas, Universidade Federal do Rio de Janeiro, Brazil

Correspondence should be addressed to Robson Coutinho-Silva; rcsilva@biof.ufrj.br

Received 26 June 2020; Accepted 7 September 2020; Published 1 October 2020

Academic Editor: Tae Jin lee

Copyright © 2020 Maria Luiza Thorstenberg et al. This is an open access article distributed under the Creative Commons Attribution License, which permits unrestricted use, distribution, and reproduction in any medium, provided the original work is properly cited.

Leishmaniasis is a neglected tropical disease caused by an intracellular parasite of the genus *Leishmania*. Damage-associated molecular patterns (DAMPs) such as UTP and ATP are released from infected cells and, once in the extracellular medium, activate P2 purinergic receptors. P2Y₂ and P2X7 receptors cooperate to control *Leishmania amazonensis* infection. NLRP3 inflammasome activation and IL-1 β release resulting from P2X7 activation are important for outcomes of *L. amazonensis* infection. The cytokine IL-1 β is required for the control of intracellular parasites. In the present study, we investigated the involvement of the P2Y₂ receptor in the activation of NLRP3 inflammasome elements (caspase-1 and 11) and IL-1 β secretion during *L. amazonensis* infection in peritoneal macrophages as well as in a murine model of cutaneous leishmaniasis. We found that 2-thio-UTP (a selective P2Y₂ agonist) reduced parasite load in *L. amazonensis*-infected murine macrophages and in the footpads and lymph nodes of infected mice. The antiparasitic effects triggered by P2Y₂ activation were not observed when cells were pretreated with a caspase-1 inhibitor (Z-YVAD-FMK) or in macrophages from caspase-1/11 knockout mice (CASP-1,11^{-/-}). We also found that UTP treatment induced IL-1 β secretion in wild-type (WT) infected macrophages but not in cells from CASP-1,11^{-/-} mice, suggesting that caspase-1 activation by UTP triggers IL-1 β secretion in *L. amazonensis*-infected macrophages. Infected cells pretreated with IL-1R antagonist did not show reduced parasitic load after UTP and ATP treatment. Our *in vivo* experiments also showed that intralesional UTP treatment reduced both parasite load (in the footpads and popliteal lymph nodes) and lesion size in wild-type (WT) and CASP-11^{-/-} but not in CASP-1,11^{-/-} mice. Taken together, our findings suggest that P2Y₂R activation induces CASP-1 activation and IL-1 β secretion during *L. amazonensis* infection. IL-1 β /IL-1R signaling is crucial for P2Y₂R-mediated protective immune response in an experimental model of cutaneous leishmaniasis.

1. Introduction

Leishmaniasis is a vector-borne disease caused by flagellated protozoans of the genus *Leishmania*. This disease represents a spectrum of neglected tropical diseases that are endemic in 98 countries worldwide [1]. The clinical manifestations range from cutaneous or mucocutaneous lesions to lethal visceral pathology. Cutaneous leishmaniasis, whose symp-

tomys range from local ulcers to mucosal tissue destruction, can be caused by *L. amazonensis*, *L. major*, *L. braziliensis*, and *L. guaynensis* [2].

In humans, *Leishmania* promastigotes are injected into the dermis (i.e., through the bite of an infected sandfly) and establish infection in phagocytic cells [3]. The recognition of pathogen-associated molecular patterns (PAMPs) by phagocytes leads to the release of damage-associated

molecular patterns (DAMPs) such as the extracellular nucleotides ATP (eATP) and UTP (eUTP) that are involved in the killing of intracellular pathogens through the activation of P2 receptors ([4, 5]. P2 purinergic/pyrimidinergic receptors can be subdivided into metabotropic G-protein-coupled P2Y (P2Y_{1,2,4,6,11-14}) and ionotropic P2X receptors (P2X₁₋₇) [6]. The following agonists activate P2 receptors: P2X and P2Y₁₁-ATP; P2Y_{2,4}-ATP and -UTP; P2Y₁, P2Y₁₂, and P2Y₁₃-ADP; P2Y₆-UDP; and P2Y₁₄-UDP-glucose [7]. P2Y receptors (P2YR) can be constitutively expressed or regulated under pathological conditions [8]. Metabotropic G-coupled-proteins such as calcium-sensing receptor and P2YR were reported to be implicated in NLRP3 inflammasome activation in inflammatory models [9–13].

Evidence supports the involvement of the noncanonical NLRP3 inflammasome assembly in the elimination of *L. amazonensis* infection by P2X7R triggering, acting as an important platform to improve host leishmanicidal mechanisms. Nevertheless, the mechanisms involved in the activation of this inflammasome in leishmaniasis remain elusive [14, 15]. ATP/P2X7R signaling during *L. amazonensis* infection has been partially elucidated during the last decade; it is assumed to be the most potent canonical activator of the NLRP3 inflammasome [16] and more recently in non-canonical activation of NLRP3 inflammasome assembly [14, 17, 18]. We previously demonstrated that the antiparasite immune response attributed to the P2YR agonist UTP involves paracrine activation of the P2X7 receptor (P2X7R) and PAXX-1 channels in macrophages from mice infected with *L. amazonensis* [19]; UTP induces production and release of reactive oxygen species (ROS), nitrite oxide (NO) [20, 21], and leukotriene B₄ (LTB₄) [19] that is assumed to be crucial for parasite death. In addition to these inflammatory mediators, IL-1 β mediates the control of intracellular parasite infections [4] [22]. In the present study, we investigated caspase-1/IL-1 β axis activation in the protective immune response induced by P2Y₂ receptor activation in an experimental model of cutaneous leishmaniasis.

2. Materials and Methods

2.1. Chemicals. UTP (uridine triphosphate), ATP (adenosine triphosphate), Dulbecco's modified Eagle's medium (DMEM), and 199 medium were purchased from Sigma-Aldrich (St. Louis, MO, USA); 2-thio-UTP and FMK-Z-YVAD were from Tocris (Bristol, UK).

2.2. Mice. The experiments, maintenance, and care of mice were carried out according to the guidelines of the Brazilian College of Animal Experimentation (COBEA). We used wild-type BALB/c and C57BL/6 (Jackson Laboratory, USA), as well as CASP-1,11 and CASP-11 knockout mice (CASP-1,11^{-/-} and CASP-11^{-/-} against the C57BL/6 background) (Genentech Laboratory, South San Francisco, CA, USA). CASP-1,11^{-/-} and CASP-11^{-/-} mice were maintained at the Laboratory of Transgenic Animals of the Federal University of Rio de Janeiro (UFRJ, RJ, Brazil). The mice were housed in a temperature-controlled room (22°C) with a light/dark cycle (12 h). Food and water were provided *ad libitum*. The

animal experimentation protocols used in this study were approved by the Ethics Committee on the Use of Animals (CEUA) from the IBCCF, UFRJ, document no. 077/15.

2.3. Parasite Culture. We used *L. amazonensis* (MHOM/BR/Josefa) strain in both *in vitro* and *in vivo* experiments. Amastigotes isolated from mouse lesions (from BALB/c mice) were allowed to transform into axenic promastigote forms by growth at 24°C, for 7 days, in 199 medium supplemented with 10% heat-inactivated fetal bovine serum (FBS; Gibco BRL, 2% male human urine, 1% L-glutamine and 0.25% hemin). Promastigotes in the late stationary phase of growth until the tenth passage were used to preserve parasite virulence.

2.4. Cell Culture and Infection. Resident macrophages were harvested from the peritoneal cavity by washes with cold phosphate buffer saline (PBS). Cells were directly seeded on culture plates (in DMEM-supplemented medium, at 37°C, with 5% CO₂) for 1 h and washed gently with PBS (twice) to remove nonadherent cells. The cells were cultured for 24 h in DMEM supplemented (10% FBS and 100 units penicillin/streptomycin) at 37°C (and 5% CO₂) and infected for 4 h or 1 h with *L. amazonensis* promastigotes (MOI ratio 10:1, Leishmania: macrophage) at 37°C. The noninternalized parasites were removed by extensive washing with sterile PBS. Then, infected cells were maintained in an incubator at 37°C and 5% CO₂ until the moment of stimulation.

2.5. In Vitro Stimulus and Inhibitor Treatments. Infected macrophages (48 h after infection) were treated with 10 μ M Z-YVAD-FMK, 2 μ M Z-LEVD-FMK, or IL-1Ra (100 ng/mL) for 30 minutes before stimulation with UTP (100 μ M) or ATP (50, 100, or 500 μ M) for an additional 30 minutes at 37°C and 5% CO₂. Then, cell monolayers were washed with PBS and maintained in DMEM supplemented (10% FBS and 100 units penicillin/streptomycin) at 37°C (and 5% CO₂) for 24 h, when infection index and cytokine production were measured.

2.6. Macrophage Infection Index. Intracellular parasite loads were analyzed as previously described [19]. Briefly, cells were infected and treated with nucleotides and were fixed onto slides, stained using a panoptic stain (Laborclin®, PR, Brazil), and counted using a Primo Star light microscope (Zeiss, Germany), with a 40x objective (100x for representative pictures). Images were acquired using a Bx51 camera (Olympus, Tokyo Japan) operated using the Cell[^]F software. We calculated the "infection index," representing the overall infection load, based on the count of about 100 cells in a total of five fields to obtain the number of infected macrophages and the average number of parasites per macrophage. Individual amastigotes were clearly visible in the cytoplasm of infected macrophages. The results were expressed as the infection index II = (%infected macrophages) \times (amastigotes/infected macrophage)/100.

2.7. Murine Model of Infection and In Vivo Treatments. Female BALB/c mice, wild-type (WT), CASP-1,11^{-/-}, and CASP-11^{-/-} C57BL/6 (8–12 weeks old) were infected in the

dermis of the footpad by intradermal injection of 10^6 *L. amazonensis* promastigotes in PBS. Intralesional treatment with 20 μ L of 10 μ M 2-thio-UTP, 1 mM UTP (pH = 7.4), or vehicle (for 3 weeks, twice a week) started 7 days postinfection (d.p.i.). Lesion growth was calculated by evaluation of the “swelling” (thickness of the infected footpad – thickness of the uninfected footpad from the same mouse), using a traditional caliper (Mitutoyo®). Forty-eight hours after the final injection (26 d.p.i.), the animals were euthanized, and the infected footpad and popliteal lymph nodes were removed and dissociated (in M199-supplemented culture medium) for parasitic load determination.

2.8. Parasite Number in Mouse Tissues. The parasite load of *L. amazonensis* in infected tissues was determined using a limiting dilution assay, as previously described [19, 23]. Mice were euthanized in a CO₂ chamber, followed by cervical dislocation. The footpads and lymph nodes were collected and weighed, and cells from the whole footpad and draining lymph nodes were dissociated using a cell strainer 40 μ m (BD®) in PBS. Large pieces of tissue debris were removed by centrifugation at 150 g; cells were separated by centrifugation at 2,000 g for 10 min and resuspended in supplemented M199. Samples were cultured in 96-well flat-bottom microtiter plates (BD®, USA) at 26–28°C. After a minimum of 7 days, wells were examined using phase-contrast microscopy in an inverted microscope (NIKON TMS, JP) and scored as “positive” or “negative” for the presence of parasites. Wells were scored “positive” when at least one parasite was observed per well.

2.9. Cytokine Levels. Measuring IL-1 β released in cell supernatants, peritoneal macrophages from WT, and CASP-1,11^{-/-} mice were plated in 96-well plates (2.0×10^5) and infected with promastigotes of *L. amazonensis* (MOI 10:1) as described in Section 2.4. Then, cells were treated with 100 μ M UTP or 3 mM ATP for 30 min. Cells were washed after 30 min and maintained at 37°C for an additional 4 h, and the supernatants were collected for further analyses. Enzyme-linked immunosorbent assays (ELISA) were performed using commercial kits, as instructed by the manufacturer (R&D Systems, Minneapolis, MN, USA). We also measured cytokine production in footpads from WT, CASP-1,11^{-/-}, and CASP-11^{-/-} mice. Briefly, the infected footpads were collected and processed as described above. IL-1 β and IL-1 α levels were measured using ELISA with commercial kits, as instructed by the manufacturer (R&D Systems, Minneapolis, MN, USA). Protein concentrations were determined using the bicinchoninic acid method (Thermo Fisher, BCA protein assay kit, Rockford, IL, USA), and cytokine levels in tissue were corrected for by the total amount of protein.

2.10. Statistical Analysis. Statistical analyses were performed using the Student’s *t*-test to compare two groups. For more than two groups, data were analyzed using the one-way analysis of variance (ANOVA) followed by Tukey’s multiple comparison post hoc test, using the Prism 5.0 software (GraphPad Software, La Jolla, CA, USA). Differences

between experimental groups were considered statistically significant when $P < 0.05$.

3. Results

3.1. P2Y₂R Contributes to *L. amazonensis* Infection Control. We recently reported that UTP-intralesional treatment elicited a Th₁ immune response in an experimental model of cutaneous leishmaniasis [21], suggesting the involvement of P2Y₂R. Here, we evaluated whether the intralesional treatment with a selective P2Y₂R agonist (2-thio-UTP) would promote *L. amazonensis* control in BALB/c mice. As shown in Figure 1(a), tissues were harvested for analysis at 26 d.p.i. We found that 2-thio-UTP treatment reduced the parasitic load in the footpads (Figure 1(b)) and draining lymph nodes (Figure 1(c)), as well as the number of leukocytes in the draining lymph nodes of infected mice (Figure 1(d)) when compared to those of control mice. We also investigated the antiparasitic effect attributed to 2-thio-UTP (range 0.025–1 μ M) and UTP (range 1–100 μ M) in infected macrophages. We found that all concentrations of UTP significantly reduced the infection index in both BALB/c (Figure 1(f)) and C57BL/6 WT macrophages (Figure 1(h)). Antiparasitic effects of 2-thio-UTP treatment were observed at concentrations ranging from 0.05 to 1 μ M in both BALB/c (Figure 1(g)) and C57BL/6 WT macrophages (Figure 1(i)). These results suggest that P2Y₂R activation contributes to the control of *L. amazonensis* infection.

3.2. Caspase-1 Is Required to P2Y₂R-Mediated *L. amazonensis* Control in Macrophages. Previously, we showed that antiparasitic effects attributed by UTP and ATP involve P2X₇R and PANX-1 channels in infected macrophages [19]. We also reported that antiparasitic immune responses triggered by the ATP/P2X₇R/PANX-1 axis require NLRP3 inflammasome activation in macrophages infected with *L. amazonensis* [14]. Here, we determined whether CASP-1 activation (an essential component of the NLRP3 inflammasome) participates in infection control mediated by eUTP. We found that the antileishmanial effects of UTP were absent in infected macrophages from mice genetically deficient for CASP-1,11 enzymes (CASP-1,11^{-/-} mice) (Figures 2(b)–2(f)). When we blocked CASP-1 with Z-YVAD-FMK (CASP-1 inhibitor), the antiparasitic effects attributed to UTP treatment were abrogated (Figures 3(b)–3(f)). By contrast, the antiparasitic effects of UTP were significant in macrophages from CASP-11^{-/-} mice and in WT macrophages treated with Z-LEVD-FMK (CASP-11 inhibitor) (Supplementary Figure 1). These findings suggest that the activity of CASP-1 but not CASP-11 is relevant to *L. amazonensis* control mediated by the P2Y₂ receptor.

3.3. P2Y₂R Stimulation Promotes IL-1 β Secretion from *L. amazonensis*-Infected Macrophages. IL-1 β is an important proinflammatory cytokine produced in response to several pathogens, and its secretion is induced by inflammasome activation in a P2X₇-dependent manner during *L. amazonensis* infection [24]. Therefore, we determined whether activation of the inflammasome via UTP/P2Y₂R would result in

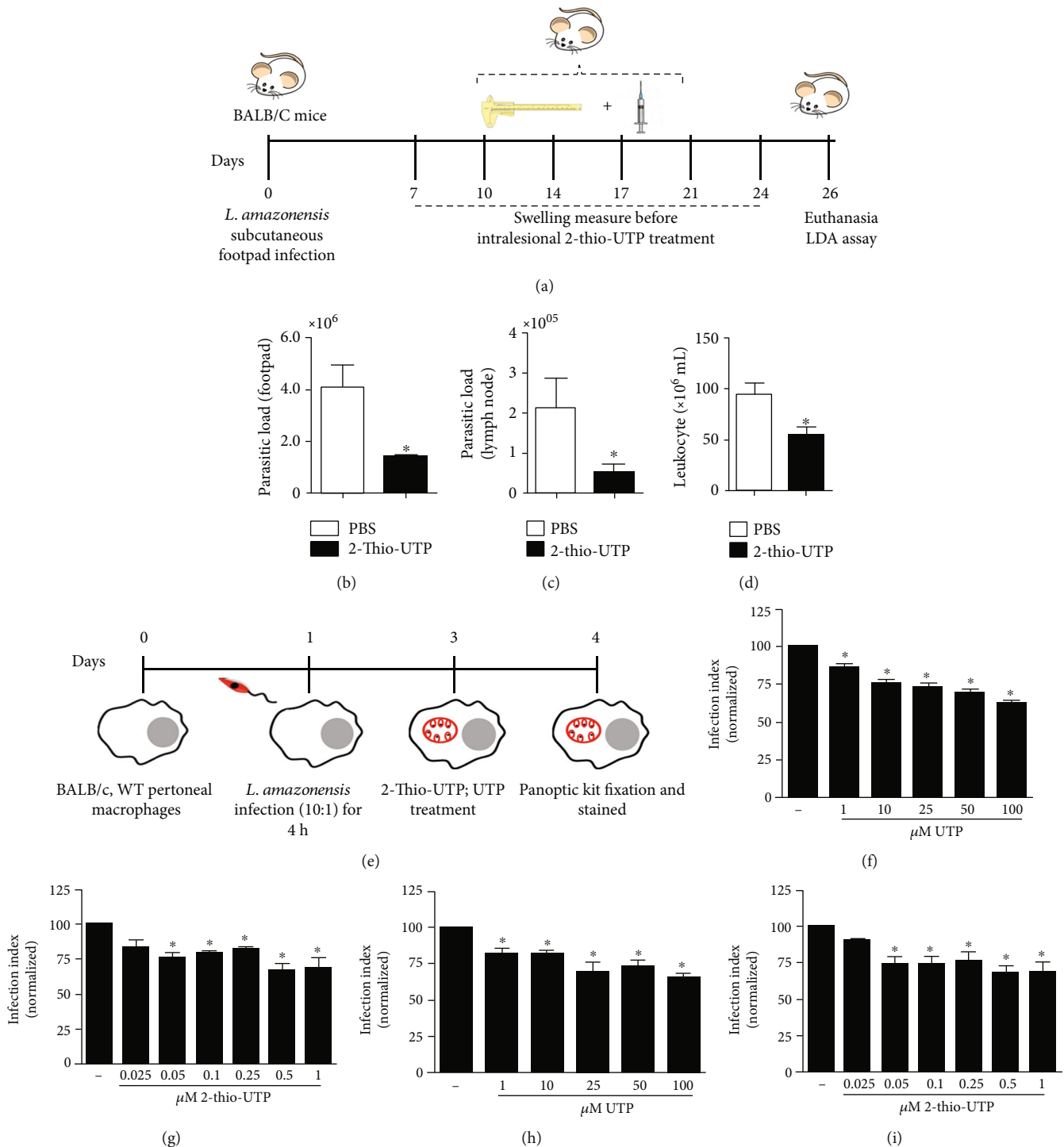


FIGURE 1: P2Y₂R selective agonist 2-thio-UTP improves host resistance against *L. amazonensis*. (a) Schematics showing the animal model of *in vivo* experiments. BALB/c mice ($n = 6/\text{group}$) were subcutaneously injected in the footpad with 10^6 promastigotes (*L. amazonensis* at stationary phase). From 7 days postinfection (d.p.i.), mice were treated with 10 μM 2-thio-UTP in 20 μL PBS and injected into the infected footpad twice a week for 3 weeks (six doses). (b–d) Animals were euthanized 26 d.p.i., and the footpads and popliteal lymph nodes were removed and used for further analysis. (b) Parasitic loads in the footpads and lymph nodes (c) were determined using a limiting dilution assay (LDA). (d) Leukocyte numbers from popliteal lymph nodes. (e) Schematics showing the design of *in vitro* experiments. BALB/c (f, g) and C57Bl/6 (WT) (h, i) macrophages infected for 48 h were treated for 30 min with UTP (1–100 μM UTP) (f–h) or 2-thio-UTP (0.025–1 μM) (g–i). After 30 h, cells were fixed, stained with the panoptic kit, and observed with light microscopy. The effect of treatments on infection was quantified by determining the “infection index” (% of infection \times number of amastigotes/total number of cells)/100; normalized to the untreated), by direct counting under the light microscope. Data represent mean \pm SEM of three independent experiments performed in triplicate, with pools of cells from four animals each experiment. * $P < 0.05$ relative to the untreated group (one-way analysis of variance followed by Tukey’s test).

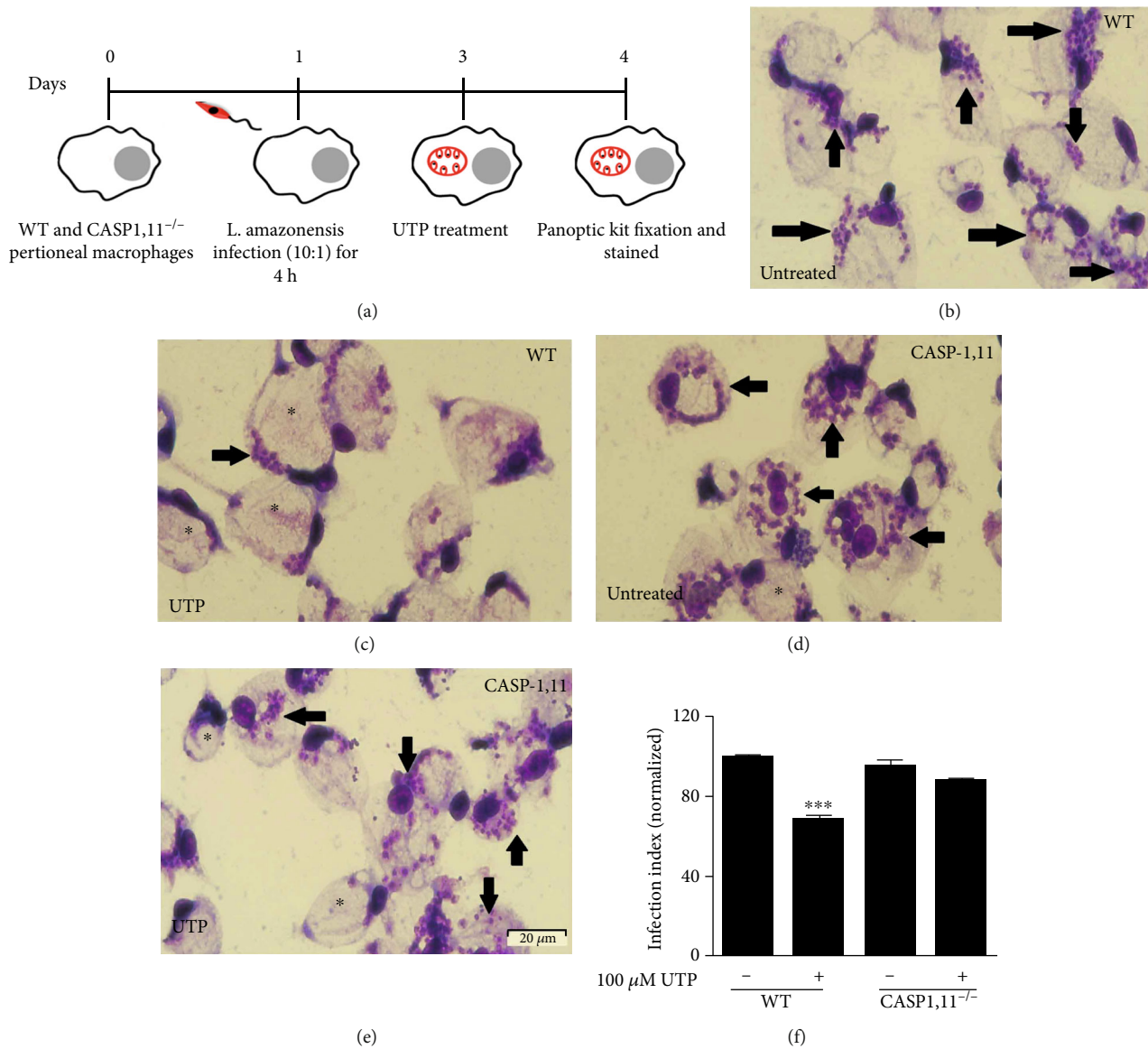


FIGURE 2: Control of *L. amazonensis* infection by UTP requires CASP-1,11. (a) Schematics showing the infection and treatments. Representative images of infected peritoneal macrophages from WT (b, c) and CASP-1,11^{-/-} (d, e) treated with UTP (100 μM) (d, e) for 30 min or left untreated (b, c). The antiparasitic effect of UTP treatment was evaluated through the “infection index” (f). Data represent mean ± SEM of three independent experiments performed in triplicate, with pools of 3–4 animals in each experiment. ***P < 0.0001 relative to the untreated group (one-way analysis of variance followed by Tukey’s test).

the secretion of IL-1β by *L. amazonensis*-infected cells. We found that UTP treatment induced IL-1β secretion in WT-infected macrophages but not in macrophages from CASP-1/11^{-/-} mice (Figure 4(a)), suggesting that activation of the canonical NLRP3 inflammasome by eUTP triggers IL-1β secretion in *L. amazonensis*-infected macrophages in a caspase-1-dependent fashion. Treatment with UTP or ATP did not reduce the parasitic load in infected macrophages pretreated with IL-1R antagonist (Figures 4(b)–4(i)), suggesting that IL-1R signaling is essential to *L. amazonensis* control mediated by P2X and P2Y receptors.

3.4. Treatment with UTP Promotes the Control of In Vivo *L. amazonensis* Infection through Caspase-1 Activation and IL-

1β Production. To confirm the importance of the CASP-1 activation by UTP/P2Y₂ activation, we evaluated the requirement of CASP-1 in the protection elicited by UTP treatment during *L. amazonensis* infection *in vivo*. We injected UTP at intervals of 3–4 days, from 7 days postinfection in the footpads of WT, CASP-1,11^{-/-}, and CASP-11^{-/-} mice infected with 10⁶ promastigotes of *L. amazonensis*. Mice were euthanized 26 days postinfection, and lesion development (swelling) was measured during the development of leishmaniasis (Figure 5(a)). As depicted in Figure 5(b), WT mice treated with UTP showed significantly smaller lesion sizes and lower parasite loads (the final one both in the footpads and lymph nodes) than in control mice (Figures 5(b), 5(e), and 5(f)).

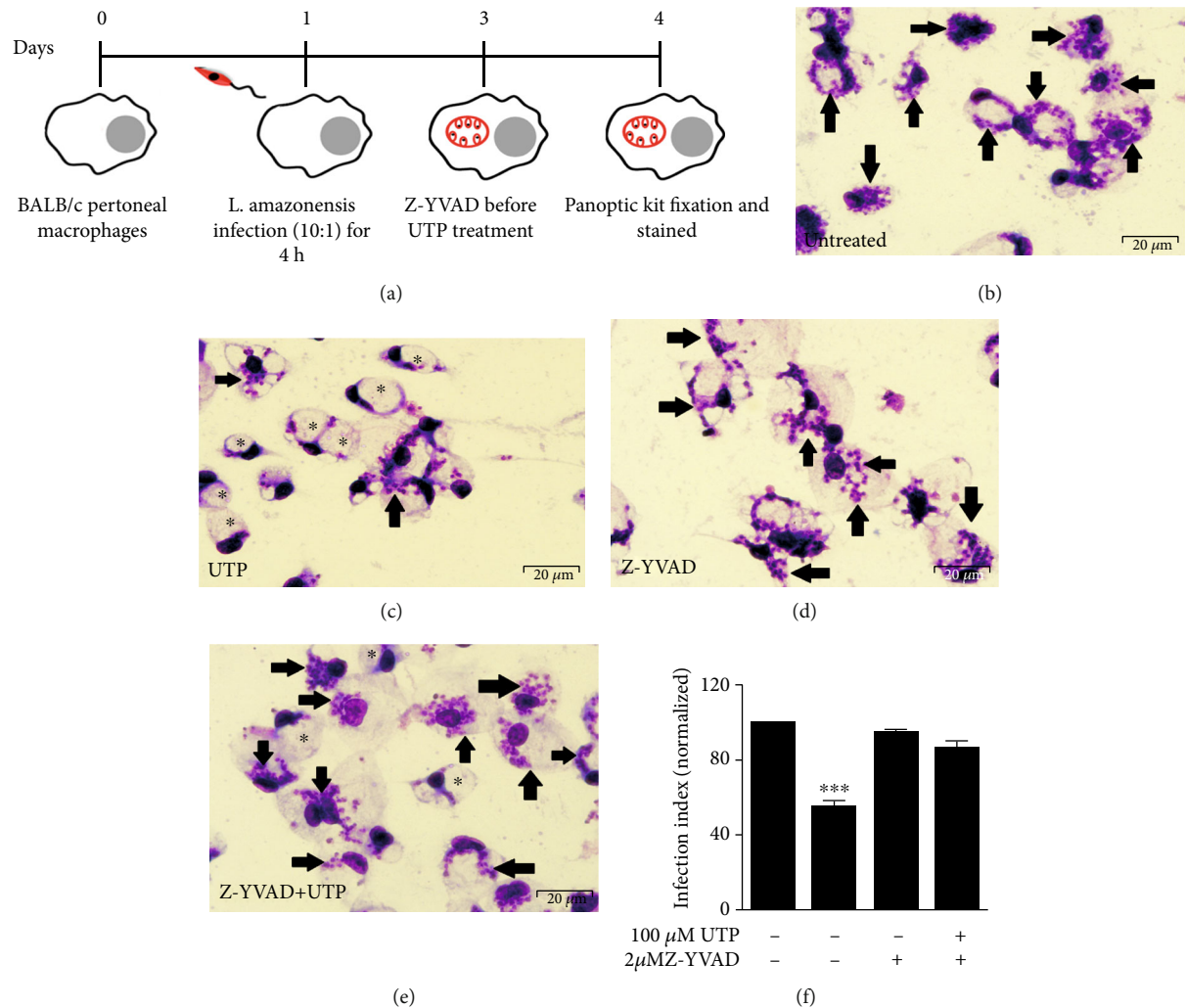


FIGURE 3: The antiparasitic effect by P2Y₂R requires CASP-1 activity. (a) Schematics showing the infection and treatments. Infected peritoneal macrophages from BALB/c were treated with UTP (100 μ M) (c, e) for 30 min or left untreated (b) following Z-YVAD-FMK (2 μ M) (d, e). The antiparasitic effect of UTP treatment was evaluated through the “infection index” (f). Data represent mean \pm SEM of three independent experiments performed in triplicate, with pools of 3–4 animals in each experiment. *** P < 0.0001 relative to the untreated group (one-way analysis of variance followed by Tukey’s test).

However, these protective effects were absent in CASP-1,11^{-/-} mice, where UTP treatment did not reduce either lesion size or parasite load (Figures 5(c), 5(e), and 5(f)). UTP treatment in CASP-11^{-/-} infected mice did not significantly decrease lesion size but rather induced a significant reduction in parasite load (Figures 5(d), 5(e), and 5(f)). Of note, both knockouts showed increased parasite loads when compared to infected WT mice (Figures 5(e) and 5(f)), as previously reported [15].

We also evaluated whether CASP-1 and CASP-11 were relevant to the production of IL-1 β and IL-1 α in mice treated with UTP. The footpads from infected WT and CASP-11^{-/-} mice treated with UTP showed higher levels of IL-1 β , as compared to the control footpads (Figure 5(g)). However, no increase in IL-1 β was found in the footpads of UTP-treated CASP-1,11^{-/-} mice (Figure 5(g)), suggesting that CASP-1 is involved in UTP-induced IL-1 β production. Levels of IL-1 α did not differ in the footpads from WT,

CASP-1,11^{-/-}, and CASP-11^{-/-} mice after UTP treatment (Figure 5(h)).

4. Discussion

Cutaneous leishmaniasis affects millions of people worldwide. Nevertheless, the host defense mechanisms that are modulated to control parasite replication and treat the disease are not thoroughly characterized, and several aspects of the disease remain poorly understood [25]. We previously reported the involvement of purinergic receptors, including P2Y₂R and P2X7R, in the control of *L. amazonensis* infection *in vitro* and *in vivo* [4, 19]. These receptors induce the activation of several microbicidal mechanisms in host cells during infection (i.e., NO, ROS, LTB₄ production) [20, 21, 26, 27]. Here, we identified a protective mechanism triggered by P2Y₂R, using incubation with either a specific agonist for P2Y₂R, 2-thio UTP, or low concentrations of UTP (100 μ M) or ATP

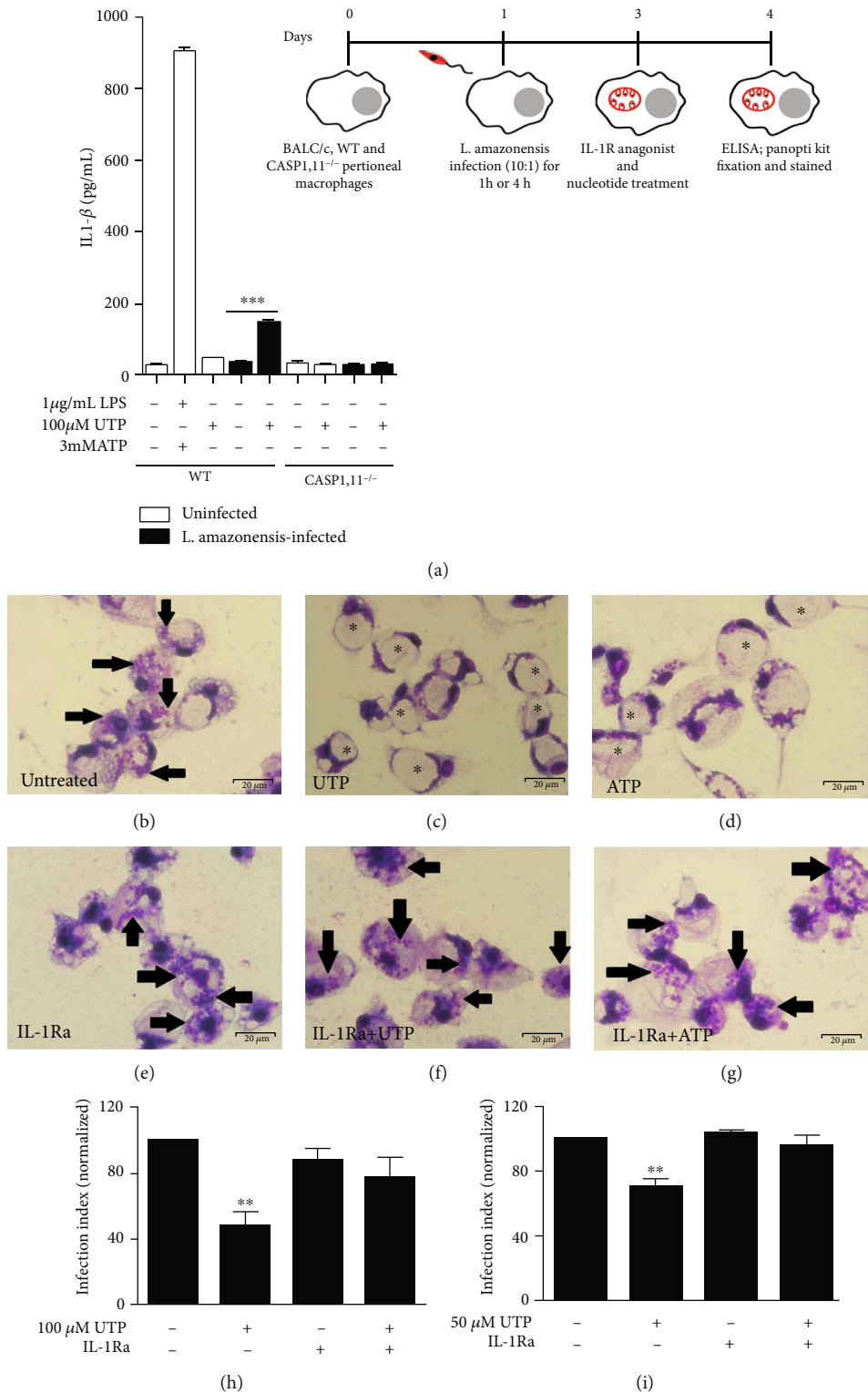


FIGURE 4: Control of *L. amazonensis* infection by UTP and ATP involves IL-1R signaling. (a) Peritoneal macrophages from WT and CASP1,11^{-/-} mice were infected with *L. amazonensis* promastigotes for 1 h and treated with UTP for 30 min. Cell culture supernatants were harvested 4 h later. Uninfected cells were primed with LPS (1 μ g/mL) for 2 h followed by ATP (3 mM), as the second signal (a positive control). IL-1 β was measured 6 h later in the positive control group. (b–d) BALB/c-infected macrophages untreated (e–g) or treated with IL-1Ra (100 ng/mL) for 30 min prior (c, f) UTP and (d, g) ATP pulse for 30 min. Twenty-four hours after nucleotide treatment, cells were fixed and stained using the panoptic kit to measure parasitic load using the “infection index” (h, i). Data are mean \pm SEM of three independent experiments performed in triplicate, with pools of 3–4 animals in each experiment. ****P* < 0.0001 and ***P* < 0.005 relative to the untreated group (one-way analysis of variance followed by Tukey’s test).

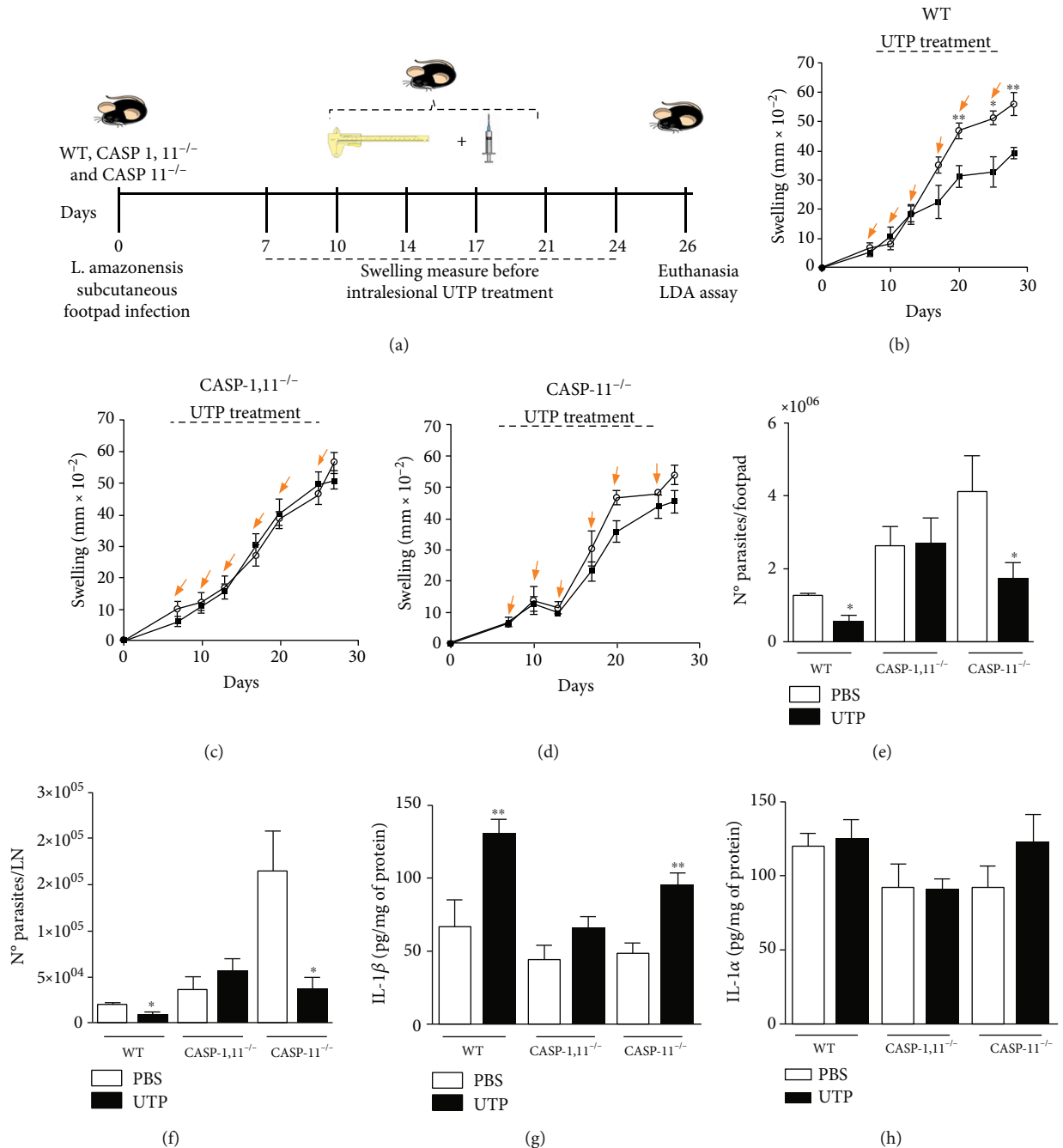


FIGURE 5: CASP-1 activity is necessary for the protective effects of UTP during *in vivo* infection with *L. amazonensis*. (a) Schematics showing the experimental approach of *in vivo* experiments. WT, CASP-1,11^{-/-}, and CASP-1,11^{-/-} mice ($n = 5$ and 6 /group) were infected with 10^6 *L. amazonensis*; following 7 d.p.i., we started the intrasoleal treatment with 1 mM UTP into the infected footpad twice a week for 3 weeks (six doses). (b–d) Swelling (thickness) was measured using a traditional Mitutoyo® caliper, and the lesion size was determined by the thickness of the infected footpad – thickness of the uninfected footpad from the same mouse. (e–h) Animals were euthanized 26 d.p.i. when the footpad and popliteal lymph nodes were excised and used to quantify parasite load and cytokine production. (e) Parasite loads in the footpads (f) and in popliteal lymph nodes from WT and CASP-1,11^{-/-} mice by limiting dilution assay (LDA). (g) IL-1 β and (h) IL-1 α production into the footpad was measured by ELISA. Data represent mean \pm SEM values, $n = 5 - 6$ mice per group. ** $P < 0.01$ and * $P < 0.05$ in comparison to the untreated group (one-way analysis of variance followed by Tukey's test).

(50 μ M) during *in vitro* infection with *L. amazonensis*. Parasite elimination upon P2Y₂R activation *in vitro* and *in vivo* depends on caspase-1 activation and IL-1R signaling.

The role of P2X7R in the IL-1 β maturation via NLRP3 inflammasome assembly in both infectious and inflamma-

tory disorders is currently accepted [16, 28, 29]. Jin et al. [10] also proposed a P2Y₂R-mediated inflammasome activation pathway [10]. Interestingly, inflammasome assembly and signaling are closely associated with the physiopathology of leishmaniasis [30–32]. We and others have shown that the

NLRP3 inflammasome is protective and contributes to restricting *L. amazonensis* parasite replication in macrophages as well as *in vivo* [30, 33, 34]. The canonical NLRP3 inflammasome promotes IL-1 β and IL-18 activation through the engagement of NLRP3, ASC, and caspase-1 activation. In addition to these components, the noncanonical NLRP3 inflammasome requires a caspase-11 expression for proper caspase-1 activation [35].

Despite the apparent importance of the inflammasome for disease outcomes, the mechanisms by which NLRP3 inflammasome is activated during *Leishmania* infection remain poorly understood. ROS production via dectin-1 and P2X7R activation appears to be involved in NLRP3 inflammasome activation [14, 34]. The mechanisms of NLRP3 inflammasome activation required for IL-1 β generation during infection by *Leishmania* have been recently elucidated. IL-1 β from a non-canonical NLRP3 source was implicated in the elimination of pathogens [36, 37] including *L. amazonensis* [14]. In support of this finding, caspase-11 was shown to be activated in response to the cytosolic delivery of *Leishmania* LPG in macrophages [30]. Previous *in vitro* studies from our group reported that ATP/P2X7 axis was critical for *L. amazonensis* control in a mechanism dependent on IL-1R signaling by non-canonical NLRP3 inflammasome activation [14, 24]. In these settings, *L. amazonensis* elimination by P2X7R activation was followed by LTB₄ release and subsequent activation of the NLRP3 complex and IL-1 β release, requiring the activation of both CASP-1 and CASP-11 [4, 14]. NLRP3 activation by LTB₄ depended on ROS induction [38]. Likewise, P2X7R activation triggered ROS production and the host immune response in several intracellular pathogen diseases, including *Toxoplasma gondii*, *Chlamydia* spp., and *Plasmodium chabaudi* infections [39–41].

P2X7R was also necessary for antiparasitic responses attributed to UTP/P2Y₂R in *L. amazonensis* infection [19]. The elimination of *L. amazonensis in vitro* triggered by P2Y₂R involves P2X7-dependent LTB₄ secretion, in a mechanism requiring pannexin-1. P2X7R expression was also required for *in vivo* control of *L. amazonensis* by UTP, supporting the notion of a collaborative effect among P2 receptors to improve the antiparasitic immune response in leishmaniasis [19]. In the present study, we showed, through *in vitro* and *in vivo* studies, that CASP-1 and IL-1R signaling, but not CASP-11, were necessary to boost host immune responses induced by P2Y₂R, contributing to protection against *L. amazonensis*.

Antileishmanial effects triggered by P2Y₂R involve two steps. The first one is mediated by ATP release with an autocrine/paracrine effect on P2X7R [19]. The second reveals a pathway of IL-1 β induction triggered by P2Y₂R (activated by low ATP concentrations). Corroborating our results, P2Y₂R signaling triggered inflammasome activation in several inflammatory models [9, 13], and caspase-1-mediated secretion of IL-1 β after activation of NLRP3 [9] and NLCR4 inflammasomes [42] after P2Y₂R activation have been reported.

In the present study, we showed that P2Y₂R induced lower levels of extracellular IL-1 β when compared to P2X7R engagement by exogenous ATP, even though the

technique used to measure extracellular nucleotides did not directly reflect their concentration around cells. These findings suggest that the P2X7R-dependent pathway triggered by P2Y₂R could be activated to a lesser extent than that of P2X7R activation triggered by exogenous ATP. P2X7 receptor activation and its effect on immune cells vary according to ATP levels. P2X7 receptor stimulation with low ATP (100 μ M) leads to the formation of a cation-selective channel. Its activation by high levels of ATP triggers the formation of a nonselective pore [43, 44]. The latter scenario is usually related to pronounced ROS production, inflammasome activation, and IL-1 β release in various systems [45]. High ATP levels can activate the P2X7R that acts as the second signal for noncanonical NLRP3 inflammasome activation during *L. amazonensis* infection. Chaves et al. [14] demonstrated activation of the noncanonical NLRP3 and IL-1 β release after P2X7R activation *in vitro* after incubation of infected macrophages with exogenous ATP (500 μ M) [14]. In this context, P2X7R activation by high exogenous ATP concentrations during infection with *L. amazonensis* might lead to higher levels of extracellular LTB₄, which in turn would favor ROS production and triggering of the noncanonical NLRP3 inflammasome assembly. Our data suggest that P2Y₂ receptor activation is not able to induce P2X7 receptor activation at a level that triggers activation of the non-canonical NLRP3 inflammasome assembly. Nevertheless, the exact inflammasome-related pathways triggered under these conditions are unknown and require further studies.

Our *in vivo* results showed that, while lack of CASP-1/11 abrogated IL-1 β induction and reduction in parasite load after activation of P2Y₂R, mice deficient in CASP-11 preserved an antileishmanial response after treatment with UTP. These findings suggest that, during *in vivo* infection by *L. amazonensis*, caspase-1 is the main source of IL-1 β and is responsible for controlling the parasitic infection. This pathway is further enhanced by P2Y₂R signaling. Even though P2X7R activation appears to enhance IL-1 β production through the noncanonical NLRP3 *in vitro* [14], its participation in the control of *in vivo* infection by *L. amazonensis* has not been addressed. It needs to be studied in depth before reaching further conclusions. Taken together, these data suggest that not only P2X7R but also P2Y₂R, a G-protein-coupled receptor, is involved in the activation of IL-1 β production/release in immune cells during infection with *L. amazonensis*. IL-1R activation, in turn, controls *L. amazonensis* infection. These results suggest that DAMPs boost the immune response against *L. amazonensis* infection via P2 receptors.

5. Conclusion

P2Y₂R activation by UTP/ATP induced CASP-1 activation and IL-1 β secretion in the context of *L. amazonensis* infection. IL-1 β /IL-1R signaling was crucial to P2Y₂R-mediated protective immune responses in an experimental model of cutaneous leishmaniasis. These findings suggest that P2Y₂R may be a possible therapeutic target to treat *L. amazonensis* infection by potentiating IL-1 β /IL-1R signaling and controlling parasite replication.

Data Availability

The file data used to support the findings of this study are available from the corresponding author upon request.

Conflicts of Interest

The authors declare no competing or financial interests.

Acknowledgments

The authors wish to thank Priscilla Braga, Fabiane Cristina Rodrigues, and Barbara Gabrielle Araujo for technical assistance. This work was supported by grants from Conselho Nacional de Desenvolvimento Científico e Tecnológico (CNPq) and Fundação de Amparo à Pesquisa do Estado do Rio de Janeiro (FAPERJ, Brazil—E-26/010.002985/2014, E-26/203.027/2 015, E-26/202.774/2018, and E-26/202.701/2019).

Supplementary Materials

Supplementary Figure 1: infected peritoneal macrophages from BALB/c (A) were pretreated with Z-YVAD-FMK (2 μ M) for 30 minutes and then with 100 μ M UTP for another 30 minutes. Peritoneal macrophages from WT or CASP-11^{-/-} were infected and after 48 h treated or not with UTP (100 μ M) for 30 minutes (B). Twenty-four hours later, cells were fixed and stained with panoptic stain, and glass coverslips on slides were evaluated using the “infection index” by a direct count under light microscopy. Data represent mean \pm SEM of three independent experiments performed in triplicate, with pools of 3–4 animals in each experiment. *** $P < 0.0001$ relative to the untreated group (one-way analysis of variance followed by Tukey’s test). (Supplementary Materials)

References

- [1] S. Burza, S. L. Croft, and M. Boelaert, “Leishmaniasis,” *The Lancet*, vol. 392, no. 10151, pp. 951–970, 2018.
- [2] J. Alvar, I. D. Vélez, C. Bern et al., “Leishmaniasis worldwide and global estimates of its incidence,” *PLoS One*, vol. 7, no. 5, article e35671, 2012.
- [3] D. Sacks and N. Noben-Trauth, “The immunology of susceptibility and resistance to *Leishmania major* in mice,” *Nature Reviews. Immunology*, vol. 2, no. 11, pp. 845–858, 2002.
- [4] M. M. Chaves, C. Marques-da-Silva, A. P. Monteiro, C. Canetti, and R. Coutinho-Silva, “Leukotriene B4 modulates P2X7 receptor-mediated *Leishmania amazonensis* elimination in murine macrophages,” *Journal of Immunology*, vol. 192, no. 10, pp. 4765–4773, 2014.
- [5] L. E. B. Savio and R. Coutinho-Silva, “Immunomodulatory effects of P2X7 receptor in intracellular parasite infections,” *Current Opinion in Pharmacology*, vol. 47, pp. 53–58, 2019.
- [6] V. Ralevic and G. Burnstock, “Receptors for purines and pyrimidines,” *Pharmacological Reviews*, vol. 50, pp. 413–492, 1998.
- [7] K. A. Jacobson, E. G. Delicado, C. Gachet et al., “Update of P2Y receptor pharmacology: IUPHAR Review 27,” *British Journal of Pharmacology*, vol. 177, no. 11, pp. 2413–2433, 2020.
- [8] D. Le Duc, A. Schulz, V. Lede et al., “P2Y receptors in immune response and inflammation,” in *Advances in Immunology*, pp. 85–121, Elsevier, 2017.
- [9] L. Baron, A. Gombault, M. Fanny et al., “The NLRP3 inflammasome is activated by nanoparticles through ATP, ADP and adenosine,” *Cell Death & Disease*, vol. 6, p. 1629, 2015.
- [10] H. Jin, Y. S. Ko, and H. J. Kim, “P2Y2R-mediated inflammasome activation is involved in tumor progression in breast cancer cells and in radiotherapy-resistant breast cancer,” *International Journal of Oncology*, vol. 53, pp. 1953–1966, 2018.
- [11] G. S. Lee, N. Subramanian, A. I. Kim et al., “The calcium-sensing receptor regulates the NLRP3 inflammasome through Ca²⁺ and cAMP,” *Nature*, vol. 492, no. 7427, pp. 123–127, 2012.
- [12] M. Rossol, M. Pierer, N. Raulien et al., “Extracellular Ca²⁺ is a danger signal activating the NLRP3 inflammasome through G protein-coupled calcium sensing receptors,” *Nature Communications*, vol. 3, no. 1, p. 1329, 2012.
- [13] T. Suzuki, K. Kohyama, K. Moriyama et al., “Extracellular ADP augments microglial inflammasome and NF-kappa B activation via the P2Y12 receptor,” *European Journal of Immunology*, vol. 50, no. 2, pp. 205–219, 2019.
- [14] M. M. Chaves, D. A. Sinflorio, M. L. Thorstenberg et al., “Non-canonical NLRP3 inflammasome activation and IL-1 β signaling are necessary to *L. amazonensis* control mediated by P2X7 receptor and leukotriene B₄,” *PLoS Pathogens*, vol. 15, article e1007887, 2019.
- [15] D. S. Lima-Junior, D. L. Costa, V. Carregaro et al., “Inflammasome-derived IL-1 β production induces nitric oxide-mediated resistance to *Leishmania*,” *Nature Medicine*, vol. 19, no. 7, pp. 909–915, 2013.
- [16] P. Pelegrin and A. Surprenant, “Pannexin-1 mediates large pore formation and interleukin-1 β release by the ATP-gated P2X7 receptor,” *The EMBO Journal*, vol. 25, no. 21, pp. 5071–5082, 2006.
- [17] S. Ruhl and P. Broz, “Caspase-11 activates a canonical NLRP3 inflammasome by promoting K(+) efflux,” *European Journal of Immunology*, vol. 45, no. 10, pp. 2927–2936, 2015.
- [18] D. Yang, Y. He, R. Munoz-Planillo, Q. Liu, and G. Nunez, “Caspase-11 requires the pannexin-1 channel and the purinergic P2X7 pore to mediate pyroptosis and endotoxic shock,” *Immunity*, vol. 43, no. 5, pp. 923–932, 2015.
- [19] M. L. Thorstenberg, M. V. Rangel Ferreira, N. Amorim et al., “Purinergic cooperation between P2Y2 and P2X7 receptors promote cutaneous leishmaniasis control: involvement of pannexin-1 and leukotrienes,” *Frontiers in Immunology*, vol. 9, p. 1531, 2018.
- [20] C. Marques-da-Silva, M. M. Chaves, S. P. Chaves et al., “Infection with *Leishmania amazonensis* upregulates purinergic receptor expression and induces host-cell susceptibility to UTP-mediated apoptosis,” *Cellular Microbiology*, vol. 13, no. 9, pp. 1410–1428, 2011.
- [21] C. Marques-da-Silva, M. M. Chaves, M. L. Thorstenberg et al., “Intralesional uridine-5'-triphosphate (UTP) treatment induced resistance to *Leishmania amazonensis* infection by boosting Th1 immune responses and reactive oxygen species production,” *Purinergic Signal*, vol. 14, no. 2, pp. 201–211, 2018.
- [22] A. C. A. Moreira-Souza, C. L. C. Almeida-da-Silva, T. P. Rangel et al., “The P2X7 receptor mediates *Toxoplasma gondii* control

- in macrophages through canonical NLRP3 inflammasome activation and reactive oxygen species production,” *Frontiers in Immunology*, vol. 8, article 1257, 2017.
- [23] R. G. Titus, M. Marchand, T. Boon, and J. A. Louis, “A limiting dilution assay for quantifying *Leishmania major* in tissues of infected mice,” *Parasite Immunology*, vol. 7, no. 5, pp. 545–555, 1985.
- [24] M. M. Chaves, C. Canetti, and R. Coutinho-Silva, “Crosstalk between purinergic receptors and lipid mediators in leishmaniasis,” *Parasites & Vectors*, vol. 9, no. 1, p. 489, 2016.
- [25] P. Scott and F. O. Novais, “Cutaneous leishmaniasis: immune responses in protection and pathogenesis,” *Nature Reviews Immunology*, vol. 16, no. 9, pp. 581–592, 2016.
- [26] S. P. Chaves, E. C. Torres-Santos, C. Marques et al., “Modulation of P2X7 purinergic receptor in macrophages by *Leishmania amazonensis* and its role in parasite elimination,” *Microbes and Infection*, vol. 11, no. 10–11, pp. 842–849, 2009.
- [27] V. R. Figliuolo, S. P. Chaves, L. E. B. Savio et al., “The role of the P2X7 receptor in murine cutaneous leishmaniasis: aspects of inflammation and parasite control,” *Purinergic Signal*, vol. 13, no. 2, pp. 143–152, 2017.
- [28] Y. Marinho, C. Marques-da-Silva, P. T. Santana et al., “MSU crystals induce sterile IL-1 β secretion via P2X7 receptor activation and HMGB1 release,” *Biochimica et Biophysica Acta (BBA) - General Subjects*, vol. 1864, article 129461, 2020.
- [29] L. E. B. Savio, M. P. de Andrade, C. G. da Silva, and R. Coutinho-Silva, “The P2X7 receptor in inflammatory diseases: angel or demon?,” *Frontiers in Pharmacology*, vol. 9, p. 52, 2018.
- [30] R. V. H. de Carvalho, W. A. Andrade, D. S. Lima-Junior et al., “*Leishmania* lipophosphoglycan triggers caspase-11 and the non-canonical activation of the NLRP3 inflammasome,” *Cell Reports*, vol. 26, no. 2, pp. 429–437.e5, 2019.
- [31] D. S. Zamboni and D. S. Lima-Junior, “Inflammasomes in host response to protozoan parasites,” *Immunological Reviews*, vol. 265, no. 1, pp. 156–171, 2015.
- [32] D. S. Zamboni and D. L. Sacks, “Inflammasomes and Leishmaniasis: in good times or bad, in sickness or in health,” *Current Opinion in Microbiology*, vol. 52, pp. 70–76, 2019.
- [33] R. V. H. de Carvalho, A. L. N. Silva, L. L. Santos, W. A. Andrade, K. S. G. de Sa, and D. S. Zamboni, “Macrophage priming is dispensable for NLRP3 inflammasome activation and restriction of *Leishmania amazonensis* replication,” *Journal of Leukocyte Biology*, vol. 106, no. 3, pp. 631–640, 2019.
- [34] D. S. Lima-Junior, T. W. P. Mineo, V. L. G. Calich, and D. S. Zamboni, “Dectin-1 activation during *Leishmania amazonensis* phagocytosis prompts Syk-dependent reactive oxygen species production to trigger inflammasome assembly and restriction of parasite replication,” *Journal of Immunology*, vol. 199, no. 6, pp. 2055–2068, 2017.
- [35] C. Pellegrini, L. Antonioli, G. Lopez-Castejon, C. Blandizzi, and M. Fornai, “Canonical and non-canonical activation of NLRP3 inflammasome at the crossroad between immune tolerance and intestinal inflammation,” *Front Immunology*, vol. 8, article 36, 2017.
- [36] V. R. Figliuolo, S. P. Chaves, L. E. B. Savio et al., “Toll or interleukin-1 receptor (TIR) domain-containing adaptor inducing interferon- β (TRIF)-mediated caspase-11 protease production integrates toll-like receptor 4 (TLR4) protein- and Nlrp3 inflammasome-mediated host defense against enteropathogens,” *The Journal of Biological Chemistry*, vol. 287, no. 41, pp. 34474–34483, 2012.
- [37] N. Kayagaki, M. T. Wong, I. B. Stowe et al., “Noncanonical inflammasome activation by intracellular LPS independent of TLR4,” *Science*, vol. 341, no. 6151, pp. 1246–1249, 2013.
- [38] F. A. Amaral, V. V. Costa, L. D. Tavares et al., “NLRP3 inflammasome-mediated neutrophil recruitment and hypernociception depend on leukotriene B (4) in a murine model of gout,” *Arthritis and Rheumatism*, vol. 64, no. 2, pp. 474–484, 2012.
- [39] G. Corrêa, C. M. da Silva, A. C. de Abreu Moreira-Souza, R. C. Vommaro, and R. Coutinho-Silva, “Activation of the P2X7 receptor triggers the elimination of *Toxoplasma gondii* tachyzoites from infected macrophages,” *Microbes and Infection*, vol. 12, no. 6, pp. 497–504, 2010.
- [40] R. Coutinho-Silva, L. Stahl, M. N. Raymond et al., “Inhibition of chlamydial infectious activity due to P2X7R-dependent phospholipase D activation,” *Immunity*, vol. 19, no. 3, pp. 403–412, 2003.
- [41] A. C. A. Moreira-Souza, Y. Marinho, G. Correa et al., “Pyrimidinergic receptor activation controls *Toxoplasma gondii* infection in macrophages,” *PLoS One*, vol. 10, no. 7, article e0133502, 2015.
- [42] H. Jin and H. J. Kim, “NLRC4, ASC and caspase-1 are inflammasome components that are mediated by P2Y2R activation in breast cancer cells,” *International Journal of Molecular Sciences*, vol. 21, no. 9, p. 3337, 2020.
- [43] R. Coutinho-Silva, L. A. Alves, W. Savino, and P. M. Persechini, “A cation non-selective channel induced by extracellular ATP in macrophages and phagocytic cells of the thymic reticulum,” *Biochimica et Biophysica Acta*, vol. 1278, no. 1, pp. 125–130, 1996.
- [44] R. Coutinho-Silva and P. M. Persechini, “P2Z purinoceptor-associated pores induced by extracellular ATP in macrophages and J774 cells,” *American Journal of Physiology*, vol. 273, pp. C1793–C1800, 1997.
- [45] S. C. Hung, C. H. Choi, N. Said-Sadier et al., “P2X4 assembles with P2X7 and pannexin-1 in gingival epithelial cells and modulates ATP-induced reactive oxygen species production and inflammasome activation,” *PLoS One*, vol. 8, no. 7, article e70210, 2013.

Review Article

Molecular Mechanisms Contributing Bacterial Infections to the Incidence of Various Types of Cancer

Salah A. Sheweita ^{1,2} and Awad S. Alsamghan ³

¹Department of Biotechnology, Institute of Graduate Studies and Research, Alexandria University, Alexandria 21526, Egypt

²Department of Clinical Biochemistry, Faculty of Medicine, King Khalid University, Abha, Saudi Arabia

³Department of Family and Community Medicine, Faculty of Medicine, King Khalid University, Abha, Saudi Arabia

Correspondence should be addressed to Salah A. Sheweita; ssheweita@yahoo.com

Received 10 March 2020; Revised 11 June 2020; Accepted 17 June 2020; Published 8 July 2020

Guest Editor: Young-Su Yi

Copyright © 2020 Salah A. Sheweita and Awad S. Alsamghan. This is an open access article distributed under the Creative Commons Attribution License, which permits unrestricted use, distribution, and reproduction in any medium, provided the original work is properly cited.

Cancer causes a major health concern worldwide due to high incidence and mortality rates. To accomplish this purpose, the Scopus, PubMed, and Web of Science databases were searched using the keywords bacteria and cancer. Most of published research addressed several different factors that induced cancer, such as toxins, medications, smoking, and obesity. Nonetheless, few studies are dealing with cancer induction via bacterial infection. In addition, mechanisms of cancer induction via bacterial infections are not well understood. Therefore, in this review, we will shed light on different bacteria that induced cancer via different molecular mechanisms. Among the bacterial infection that induced cancer, *Helicobacter pylori* was the first recognized bacteria which caused gastric cancer and might be also linked to extragastric cancer in humans. *H. pylori* has been associated with adenocarcinoma in the distal stomach by its ability to cause severe inflammations. It has been found that inflammations induced cancer via different mechanisms including induction of cell proliferation and production of high levels of free radicals. Recently, free radicals were found to induce and cause various types of cancer. *Salmonella typhi* has been found to be associated with gallbladder carcinoma (GBC). Also, intercellular infection of lungs with *Chlamydia pneumoniae* was found to contribute as one of the ethological factors of lung cancer. Moreover, infection of the urinary tract with *Staphylococcus aureus*, *Klebsiella* spp., and *Proteus mirabilis* has been found to cause bladder cancer. These microorganisms produce a high level of N-nitrosamines which are metabolically activated leading to the generation of alkylating agents that damage DNA and other macromolecules. It is concluded that a certain bacterium is linked with induction of a specific type of cancer via different molecular and biochemical mechanisms as discussed in the text in details. This infection could potentially affect human health in different ways. In addition, it is important to know the possible factors involved in cancer induction for better treatment of cancer patients.

1. Introduction

Genetic, environmental, and dietary factors are identified as the main factors of cancer induction, and their interaction leads to carcinogenesis. Environmental factors such as tobacco smoke and occupational exposure to hazardous chemicals account for 90% of all cancers. The majority of the exogenous compounds are chemical carcinogens which undergo metabolic activation to form metabolites which interact with cellular macromolecules and initiate carcinogenesis by causing damage to the DNA, hence are called

exogenous genotoxic carcinogens. These carcinogens consist of a wide variety of compounds, which differ in their chemical structure but possess a common ability to form chemical bonds with DNA, resulting in the generation of “DNA adducts.” The formation of these DNA adducts is recognized as the initial step in chemical carcinogenesis [1, 2]. In addition, the initial stage of gene mutilation is also based on endogenous mechanisms that cause mutations or even gene deletions. Very common endogenous mediators are free radicals or reactive oxygen species (ROS), which cause oxidative damage to DNA and cause different mutations (Figure 1)

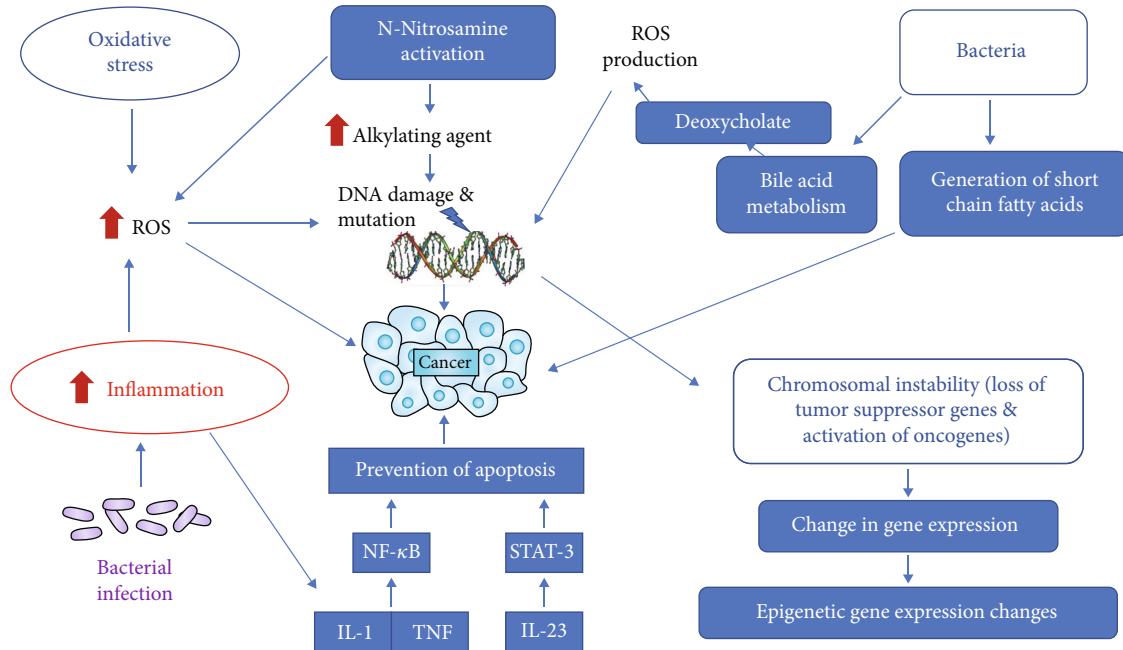


FIGURE 1: Different molecular mechanisms of carcinogenesis induced by bacterial infection and oxidative stress.

[3, 4]. Recent studies have shown a causative relationship between bacterial infection and the onset of cancer in organs such as lungs, colon, and cervix, which are constantly exposed to bacteria (Figure 1) [5]. The harmony of cells and the control of its growth and proliferation are regulated by a well-synchronized signalling pathway. Any alteration or deregulation of these pathways triggers carcinogenesis. During bacterial infection, various bacteria target and trigger these signalling pathways. Therefore, in this review, we have focused on the role of some bacteria in the incidence of cancer since a number of bacteria have been associated with cancer via triggering signalling pathways. *Helicobacter pylori*, *Salmonella typhi*, *Streptococcus bevis*, and *Chlamydia pneumonia* cause stomach, gallbladder, colorectal, and lung cancers, respectively, through different mechanisms.

1.1. *Salmonella typhi* Induced Gallbladder Cancer. *Salmonella typhi* is a rod-shaped gram-negative bacterium of the Enterobacteriaceae family, which is well known to cause typhoid or enteric fever. These bacteria colonize in the gallbladder causing asymptomatic chronic infection [6]. Epidemiological studies from *S. typhi* endemic regions have shown that most of the chronically infected carriers developed gall cholelithiasis, a primary predisposing reason for the onset of gallbladder cancer (GBC). Typhoid toxins produced by *S. typhi* have a carcinogenic potential which damages the DNA and alters the cell cycle in the infected cells. Apart from this, the extracellular polymeric substances (EPS) produced in the biofilm of *S. typhi* are the key factor for persistent infection and cholecystitis leading to exposure of the epithelium to carcinogenic toxins produced by *S. typhi* [6]. Until the 1990s, in Chile, under the backdrop of a typhoid epidemic, a high prevalence of gallbladder cancer incidence was observed, which was mainly attributed to its association with *Salmonella enterica* serovar typhi (*S. typhi*) Vi antibodies. How-

ever, the exact mechanism underlying this association is still under investigation [7]. Another study in India claimed chronic *Salmonella enterica* serovar typhi infection to be a significant risk factor for the development of gallbladder cancer, although no direct association and mechanism have been explained yet [8].

1.1.1. Molecular Mechanism Underlying Induction of Gallbladder Cancer. The role of *Salmonella typhi* in altering the genomic sequence of tumor protein p53 (TP53) and amplification of protooncogene c-MYC results in malignant transformation from predisposed mice gallbladder organoids and fibroblasts (Table 1 and Figure 1). *Salmonella typhi* effectors released during an infection contribute to the autoactivation of protein kinase which is triggered by mitogen (MAPK) and the Akt pathways (Table 1). This process is pathognomonic in initiating as well as sustaining malignant transformation, which is a consistent observation in gallbladder cancer patients in India. Hence, the role of *Salmonella typhi* predisposed epithelium of gallbladder to toxic metabolites was established [8]. Another mechanism is primarily attributable to the production by *S. typhi* of genotoxic substances (cytotoxic distending toxin B (CdtB)), which is the functional unit of cytotoxic distending toxin (CDT) and cytotoxic necrotizing factor 1 (CNF1). The CdtB works by targeting the DNA in the human host cells while CNF1 inhibits the activity of cytokines leading to inflammation and cell cycle inhibition [9] (Table 1 and Figure 1). Moreover, CNF1 also affects the transcription termination process in prokaryotes by altering the Rho proteins [9]. *S. typhi* changed the protein expressions of CdtB and CNF1 leading ultimately to cancer of the gallbladder.

The function of the gallbladder is to store bile, which consists of bile salts and acids. Various mechanisms have been suggested in which altered bile salt metabolism produces

TABLE 1: Types of cancer induction and mechanisms of carcinogenesis induced by different microbiota.

Cancer	Bacteria inducing cancer	Mechanisms of carcinogenesis	References
Gallbladder cancer	<i>Salmonella typhi</i>	Changes in the sequence of p53 gene; activation of protein kinase; cytolethal distending toxin B (CdtB); biliary deoxycholate; cholic acid derivatives; 5-alpha,6-alpha-epoxide cholesterol; upregulation of the PI3K pathway	[8, 10–13]
Lung cancer	<i>Chlamydia pneumoniae</i>	Alteration in apoptosis and/or cell programming signalling; overexpression of miRNA-328; by stimulating lung-resident $\gamma\delta$ T cells; development of Myd88-dependent IL-1b and IL-23; generation of reactive oxygen species; increased secretion of cytokines, IL-8, IL-10, and TNF	[5, 19–24]
Colorectal cancer	<i>Streptococcus bovis</i> , <i>Helicobacter pylori</i> , <i>Bacteroides fragilis</i> , <i>Enterococcus faecalis</i> , <i>Clostridium septicum</i> , <i>Fusobacterium spp.</i> , and <i>Escherichia coli</i>	Secretion of <i>Bacteroides fragilis</i> toxin; activation of NF- μ B; expression of IL-17A, and TNF- α ; β -catenin expression, induction of IL-17R, NF- κ B, and Stat3 signals; induction of the gene expression of colibactin (clbB) and <i>Bacteroides fragilis</i> toxin (BFT), increased colonial interleukin-17, and colonic epithelial DNA damage	[69, 72–75]
Breast cancer	<i>Methylobacterium radiotolerans</i> , <i>Sphingomonas yanoikuyae</i>	Microbiota secretes bioactive metabolites including estrogens, short-chain fatty acids, amino acid metabolites, or secondary bile acids; dysbiosis	[78, 79]
Bladder cancer	<i>Staphylococcus albus hemolytic</i> , <i>Staphylococcus aureus</i> , <i>Klebsiella spp.</i> , <i>Proteus mirabilis</i> , and <i>E. coli</i>	Formation of N-nitrosamines; DNA methylation; reactive chemical species	[83–87]

carcinogenic compounds from long-term *S. typhi* carriers. Bacterial enzymes which were present in *S. typhi* work primarily on bile acids to generate high concentrations of toxic metabolites and secondary bile acids (Figure 1). These toxic metabolites lead to the pathology of the epithelium of the gallbladder. A glycosidase enzyme, β -glucuronidase, deconjugates the conjugated primary bile salts resulting in the production of high concentrations of toxic metabolites which have carcinogenic effects [9] (Table 1). These metabolites bind to DNA in human epithelial cells, exerting its mitogenic action [10, 11]. It has also been shown that high concentrations of biliary deoxycholate, a secondary bile acid, are present at elevated levels in patients with gallbladder carcinoma [9]. Another mechanism suggested that *S. typhi* mutagenicity is due to its cholesterol interaction, which ultimately forms the structural basis of the gallstones. These bacteria not only transform the bile salts into secondary forms of bile but also convert cholesterol itself into carcinogenic compounds like 5-alpha,6-alpha-epoxide cholesterol, leading to pathogenic changes in epithelial cells [12] (Table 1). Another study has shown that *S. typhi* bacteria are capable of metabolizing primary bile acids into mutagenic cholic acid derivative types in the presence of bile and cholesterol substrates that cause gall bladder cancer [11].

1.2. Chlamydia pneumoniae and Lung Cancer. Lung cancer is closely related to chronic inflammation, but it has not completely elucidated the causes of inflammation and the basic immune mediators. Chlamydia (formerly called Chlamydia) pneumoniae is a species of Chlamydia, an intracellular bacterium that infects the cells of the respiratory tract in humans. It is responsible for about 10% of community-

acquired pneumonia and 5% of sinusitis, pharyngitis, and bronchitis [13]. Chronic pneumocyte infection by *C. pneumoniae* predisposes for the development of lung cancer, which is a major public health concern due to its high incidence and mortality [13]. The existence of *C. pneumoniae* in 230 lung cancer cases has been found, and the lung cancer risk was increased by 1.6 in *C. pneumoniae*-infected patients [14]. In addition, in patients with bronchoscopy and lung cancer, an association between chronic *C. pneumoniae* infection and incidence of lung cancer was found [15]. It has been found that IgA antibodies were increased in lung cancer patients infected with *C. pneumoniae* [16]. In another study, increased *C. pneumoniae*-specific IgA levels in smokers with lung cancer were found [17].

1.2.1. Mechanism of Lung Cancer Induction. Post chlamydial infection, numerous proteins are released which are hypothesized to cause lung cancer by targeting either mitochondrial or cytoplasmic cellular activities. Their mechanism of action is by competitive inhibition where these targeting proteins and host proteins compete to bind with the substrate [5]. In a study done by Alshamsan et al., it was reported that out of 1112 proteins derived from *C. pneumoniae*, 183 and 513 proteins targeted the mitochondrial and cytoplasmic cellular processes of the host cells, respectively [18]. This leads to disturbance of normal cellular growth, resulting in an alteration in apoptosis or programmed cell death leading to the development of lung cancer. It is also assumed that these proteins are incorporated into the intracellular organelles leading to the formation of a host cell proteome. Various bioinformatics tools such as nuclear localization signal (NLS) mapper, HumMPLoc 2.0, ExpASY pI/Mw tool, and balanced subcellular

localization predictor (BaCeILO) showed that 47 of the 1112 bacterial proteins were responsible for nuclear targeting which altered the host replication and transcription [5].

Many evidences have showed that microRNA (miRNA) played an important role in the metastasis and progression of lung cancer. A miRNA, miR-328, targets H2AX (a histone protein) in the regulation of lung cancer cell apoptosis (Table 1). Overexpression of miRNA-328 is associated with lung cancer, whereas its downregulation was shown to decrease the incidence of lung cancer that is induced by *C. pneumoniae*. In addition, suppression of miRNA-328 causes increased caspase 3 activity and apoptosis in cancer cells, resulting in lesser tumor volume [19].

A diverse bacterial community is colonized in the lung mucosal tissue and is commonly linked to clinical outcomes in patients with lung cancer which triggers lung adenocarcinoma-related inflammation by stimulating lung-resident $\gamma\delta$ T cells [20]. It has been found that commensal bacteria stimulated the development of Myd88-dependent IL-1b and IL-23 from myeloid cells, inducing the proliferation and activation of Vg6+Vd1+ $\gamma\delta$ T cells containing IL-17 and other effector molecules to promote inflammation and proliferation of tumor cells (Figure 1) [20]. Local microbiota-immune crosstalk has been found to be correlated with the development of lung tumors, and molecular mediators that can serve as effective targets for lung cancer intervention have been identified (Table 1) [20]. Other mechanisms of bacterial infection causing lung cancer are the gene damage and the neoplastic transformation which are triggered by inflammatory mediators, nitric oxide (NO), and other reactive oxygen species (Figure 1) [21, 22]. An in vitro study has shown that chronic bacterial infection by *C. pneumoniae* causes increased secretion of cytokines, IL-8, IL-10, and TNF, in human alveolar macrophages and peripheral blood mononuclear cells (Table 1 and Figure 1) [23]. IL-8 is an angiogenic factor acting as a promotor of tumor growth of non-small-cell lung carcinomas in humans [24, 25]. Moreover, nitric oxide liberation is also increased in chlamydial infections which might induce an inflammatory response that leads to the development of lung cancer [26].

1.3. *Helicobacter pylori* and Gastric Cancer. *Helicobacter pylori* (*H. pylori*) is a gram-negative microaerophilic bacterium having a helical shape with an ability to penetrate the mucoid lining of the stomach causing infection. Although many patients infected with *H. pylori* may be asymptomatic, long-term complications include gastric ulcers, inflammation of the gastric lining leading to gastritis, and gastric carcinoma. Gastric carcinoma is a global health concern due to high morbidity and mortality. Though there are numerous predisposing risk factors such as family history, dietary habits (high salts and nitrates), alcohol, and smoking, *H. pylori* infection has one strongest association with gastric carcinoma [27]. Apart from environmental, dietary, and genetic factors which play a vital role in the development of most of the cancers, infection by *H. pylori* also causes cancer [28, 29]. The ability of the bacteria to enter the gastric cells and colonize for years allows it to interact with human cells and impart its harmful effects. These microbes release an onco-

protein, CagA, which affects the normal epithelial cell division in the gastric mucosa (Table 1) [30]. Other factors such as environmental, dietary (essential micronutrients), and gastrointestinal microflora also increase the carcinogenic potential of *H. pylori* [30]. In order to study the association between *H. pylori* and gastric carcinoma, epidemiological studies were carried out since 1991. Numerous studies on a large number of individuals were conducted, and reports were published [31–33]. These studies provided valuable insights and strongly encouraged subsequent studies. Later, in another study, it was demonstrated that *H. pylori* antibodies were highly prevalent in asymptomatic patients who developed gastric carcinoma [34, 35]. Nolen et al. reported an earlier onset of gastric carcinoma and a higher mortality rate in Alaska Native people as compared to the US population. This was attributed to the higher prevalence of *H. pylori* infection, antimicrobial resistance, and reinfection in people in Alaska Natives as compared to the US population [36]. A study in Japan on 213 gastric cancer patients showed 88.2% of patients having higher levels of *H. pylori* antibodies. This too suggests the role of *H. pylori* in various preceding stages such as acute gastritis, atrophic gastritis, intestinal cell metaplasia, and finally intestinal type of gastric carcinoma [37]. Another study by Frydman et al. showed a strong relationship between *H. pylori* infection and gastric cancer in younger gastric carcinoma patients [38].

1.3.1. Mechanisms of Induction of Gastric Carcinoma. Patients with a history of *H. pylori* infection underwent annual endoscopic observation after eradication and were screened for novel markers such as gastric epithelium released tissue, protein biomarkers, and other proteins associated with cellular metaplasia in dysplasia in carcinoma. Other markers such as CD44, a signalling molecule in cell proliferation and differentiation, and metalloproteinase, an immune response-mediated marker, were also assayed (Table 1) [39, 40]. Metaplastic intestinal cells are characterized by overexpression of gastrointestinal stem cell markers like PROM1 gene product, leucine-rich repeat-containing G-protein coupled receptor 5 (LGR5), and genes related to the metabolism of messenger RNA and nucleic acids [39].

Various mechanisms have explained the role of *H. pylori* in altering the chemical contents of gastric juice and changes in gastric mucosal cells which cause chronic inflammation and subsequent carcinogenesis [41]. Colonization of gastric mucosal cells by *H. pylori* results in an inflammatory response by host cells. This leads to infiltration of host cells by macrophages, polymorph, nuclear leukocytes, T lymphocytes, and B lymphocytes. Therefore, the pathogen, along with its induced cytokines, stimulates the accumulation and activation of inflammatory cells [42]. Infiltration of gastric mucosal cells by activated inflammatory cells and neutrophils following infection by *H. pylori* produces free oxygen radicals both in the pyloric and duodenal mucosa which upregulates the production of IL-8 resulting in a greater inflammatory response [43–46]. These free radicals, being highly reactive, cause damage to proteins and DNA resulting in mutations (Table 1) [47]. Data showing the role of free radicals in the onset of gastric carcinoma is lacking [48]. Post *H. pylori*

infection results in increased ammonia levels in the gastric mucosal cells of rats, which acted as promoters of gastric carcinoma by inducing N-methyl-N-nitro-N-nitroso guanidine (MNNG) [49]. Ascorbic acid, an antioxidant, reacts with nitroso compounds producing nitric oxide instead of harmful N-nitroso compounds [50]. Ascorbic acid concentration is lowered in the gastric juice following *H. pylori* infection, resulting in increased activity of free intermediate radicals. However, following eradication of *H. pylori*, increased gastric juice levels of vitamin C were observed [51–53]. As with most of the other microbes, the oncogenic activity in *H. pylori* is attributed to its proteins. Expression of cytotoxic mediators such as CagA and VacA by *H. pylori* causes activation or differentiation of gastric fibroblasts in rats which disrupt multiple cell signalling and proliferation pathways. Some major pathways include deregulation of Janus kinase/signal transducers, activation of nuclear factor kappa B (NF- κ B), and activation of transcription (JAK/STAT), which lead to inflammation and initiation of carcinogenic cascades (Table 1) [54]. Although the inflammatory process begins in the epithelial cells, it spreads to the surrounding activated fibroblast cells resulting in tumor progression, invasion, and metastasis. The expression of downstream targets of STAT3 and the epithelial-mesenchymal transition inducing transcription factor (EMT-TFs) are increased in activated fibroblasts (Figure 1) [54, 55].

AMP-activated alpha 1 catalytic subunit (PRKAA1) is one of the subunits of the mammalian 5'-AMP-activated protein kinase (AMPK). They play a crucial role in the maintenance of intracellular energy metabolism and hence are considered as a gastric carcinoma risk factor [56]. In NF- κ Bp50 knockdown rats, *H. pylori* infection upregulates the expression of p-NF- κ Bp50, NF- κ Bp50, and PRKAA1 expression, which promotes carcinogenesis. PRKAA1 knockdown in gastric cancer cells showed a significant decrease in cell invasion and migration. It also inhibited the expression of MMP-2 and activation of NF- κ B, whereas on the contrary, PRKAA1 involved in NF- κ Bp50 mediated gastric cancer cell invasion and migration indicated their role in gastric cell carcinogenesis [56]. *H. pylori*-induced inflammatory response of gastric cells leads to increased epithelial cell turnover by increasing its proliferation and apoptosis. Apart from *H. pylori*, other inflammatory markers such as TNF and interferon-gamma (INF- γ) also trigger apoptosis. Another marker identified as *H. pylori* activated peripheral blood mononuclear cells (PBMCs) upregulates the expression of Fas antigen in RGM-1 (Rat Gastric Mucosal Cell First) gastric cells. In the presence of Fas ligand, RGM-1 cells and PBMC medium showed immense and rapid cell proliferation and cell death (Table 1) [29, 57, 58].

Increased gastric mucosal cell turnover also increases the demand for a DNA repair system. Increased cell proliferation results in increased rates of mutation, hence requiring greater surveillance and rectification by DNA mismatch repair (MMR) [59]. Therefore, decreased MMR activity results in mutation. Microsatellite instability (MSI) is a marker of deficiency of DNA MMR activity (Figure 1). Mutations in hMSH3 and hMSH6 (DNA MMR gene), receptors of growth factors, and transforming growth factor β -RII are seen in

MSI-positive gastric carcinoma [60–62]. Other DNA MMR gene, hMLH1, and sometimes hMSH2 expression are completely lost [63–67]. These findings are enough to suggest that *H. pylori* causes deficient MMR in the gastric mucosal cells, resulting in the development of early stages of gastric carcinoma (Table 1).

1.4. Colorectal Cancer and Bacterial Infection. For more than 100 years ago, bacteria were first identified in human tumors. However, the classification of the tumor microbiome remained difficult due to its low abundance [68]. Each type of tumor has a distinct composition of microbiome [68]. The symbiotic relationships between resident microorganisms and the digestive tract contribute significantly to the maintenance of gut homeostasis [69]. Changes to the microbiota triggered by changes in the environment (e.g., infection, diet, and/or lifestyle) may, however, disrupt this symbiotic relationship and facilitate diseases such as inflammatory bowel diseases and cancer. Colorectal cancer is a complex mixture of tumor cells, nonneoplastic cells, and a significant number of microorganisms, and microbiota involvement in colorectal carcinogenesis is becoming increasingly apparent. Nevertheless, several changes in gut microbiota's bacterial composition have been documented in colorectal cancer, indicating a major role for dysbiosis in colorectal carcinogenesis [69]. Some bacterial species, such as *Streptococcus bovis*, *Helicobacter pylori*, *Bacteroides fragilis*, *Enterococcus faecalis*, *Clostridium septicum*, *Fusobacterium spp.*, and *Escherichia coli*, have been identified and suspected to play a role in colorectal carcinogenesis (Table 1) [69]. The potential interactions between bacterial microbiota and colorectal carcinogenesis such as genotoxicity and inflammation derived from bacteria have been found [69].

A microbial etiology for colorectal human cancer (hCRC) has been suggested and pursued for a long time [70]. Establishing how one or more members of the microbiota initiate and/or promote hCRC could stimulate the development of novel prevention approaches, since hCRC has a long time to go from initiation to presentation. It has also been proposed that various intestinal microbes may lead to a common pathway to tumorigenesis [70]. Over 90 percent of hCRC is sporadic, with a small proportion of inherited mutations. Germline mutations in the tumor suppressor gene of adenomatous polyposis coli (APC) are responsible for the family adenomatous polyposis (FAP) (Figure 1) [71]. In addition, at least 80 percent of intermittent hCRC shows adenomatous polyposis coli (APC) mutations as well.

1.4.1. Molecular Mechanism Underlying Induction of Colorectal Cancer. Enterotoxigenic *Bacteroides fragilis* (ETBF) is a commensal bacterium of the human intestine and a potent initiator of colitis through the secretion of *Bacteroides fragilis* toxin (BFT) [72] (Table 1). BFT induces the cleavage of E-cadherin in colon cells, which then leads to the activation of NF- μ B. Zerumbone, a key component of the plant *Zingiber zerumbet* (L.), has antibacterial and anti-inflammatory effects. Treatment with zerumbone significantly reduced expression of IL-17A, TNF- α , and KC in ETBF-infected mouse colonic tissues [72] (Table 1). Zerumbone-treated ETBF-infected

mice also showed a decline in colon NF- κ B signalling. Moreover, HT29/C1 colonic epithelial cells treated with BFT-induced BFT signalling and IL-8 secretion. However, an E-cadherin cleavage mediated by BFT was unaffected [72]. It has been found that ETBF colonization in mice did not change after treatment with zerumbone, whereas it decreased ETBF-induced colitis through inhibition of NF- κ B signalling [72]. ApcMin mice colonized with the enterotoxigenic human pathobiont *Bacteroides fragilis* (ETBF) as a model of colon tumorigenesis induced by microbes have been used [73]. *Bacteroides fragilis* toxin (BFT) activates a procarcinogenic, multistage inflammatory cascade in colonic epithelial cells (CECs) that includes IL-17R, NF- κ B, and Stat3 signals (Figure 1) [73]. While necessary, activation of Stat3 in CECs is not sufficient to cause tumorigenesis of the ETBF colon. Therefore, BFT induces a procarcinogenic signalling relay from the CEC to a Th17 mucosal response resulting in selective NF- κ B activation in distal colon CECs, which collectively activates distal colon tumorigenesis based on myeloid cells [73].

While β -catenin signalling is documented to be associated with inflammatory responses, and BFT is known to cleave E-cadherin associated with β -catenin, little is known about inflammation control in ETBF infection by β -catenin mediation [74]. After stimulation with BFT, expression of β -catenin in intestinal epithelial cells was reduced relatively early and then recovered relatively late after stimulation to normal levels. In comparison, phosphorylation of β -catenin occurred early in stimulation at high rates in BFT-exposed cells and decreased as time went by [74] (Table 1). Inactivation of β -catenin in BFT-stimulated cells has resulted in increased NF- κ B activity and interleukin-8 (IL-8) expression (Figure 1). In addition, glycogen synthase kinase 3 β inhibition was associated with increased β -catenin expression and attenuated NF- κ B activity and expression of IL-8 in BFT-exposed cells. These findings indicate negative control of β -catenin in BFT-stimulated intestinal epithelial cells as a consequence of acute inflammation in ETBF infection [74].

Colonic mucosa has been observed in patients with family adenomatous polyposis (FAP), who develop benign precursor lesions (polyps) early in life [75]. Patchy bacterial biofilms predominantly composed of *Escherichia coli* and *Bacteroides fragilis* were identified. Genes for colibactin (clbB) and *Bacteroides fragilis* toxin (BFT), which encode secreted oncotoxins, have been highly enriched in the colonic mucosa of patients with FAP compared to healthy people [75]. It has been found that a tumor colonized with *E. coli* (colibactin) and enterotoxigenic *B. fragilis* has demonstrated increased colonial interleukin-17 and colonic epithelial DNA damage with faster tumor initiation and increased mortality compared to mice with a bacterial strain alone (Table 1 and Figure 1). This study indicated an unlikely link between the early colon neoplasia and tumorigenic bacteria [75].

1.5. Breast Cancer and Bacterial Infection. The most common cancer among women is breast cancer [76]. Breast cancer is a major cause of death among women all over the world. Breast cancer has a lifetime effect on one in eight women. The number of newly diagnosed cases of invasive breast cancer in the US is estimated at 268,000 in 2019, while the newly diagnosed

cases in situ are estimated at about 62,930 [77]. Of these, 41,760 women are expected to die of breast cancer in the US in 2019 [77]. In developed countries, breast cancer survival for five years is over 80 percent thanks to screening services and the consequent early detection [78].

1.5.1. Molecular Mechanism Underlying Induction of Breast Cancer. Breast cancer is characterized by dysbiosis, an aberrant composition of the microbiome [79]. In this study, we address differences in the metabolism of breast cancer cells, as well as breast and gut microbiome composition in breast cancer. The role of the breast microbiome in breast cancer is unclear, but the gut microbiome does seem to play a part in the disease pathology. The gut microbiota secretes bioactive metabolites that modulate breast cancer (reactivated estrogens, short-chain fatty acids, amino acid metabolites, or secondary bile acids) (Figure 1) [79]. Such blood-borne microbial metabolites have been shown to modulate breast cancer behavior. These metabolites mimic human hormones, since they are formed in a “gland” (in this case, the microbiome) and are then transferred through the bloodstream to distant sites of action. These metabolites tend to be essential tumor microenvironmental constituents [79].

While there are proven risk factors for diet, age, and genetic predisposition, most breast cancers have unknown etiologies. The human microbiota is a group of microbes that inhabit the human body. Microbial imbalance, or microbial dysbiosis, has been involved in numerous human diseases including obesity, diabetes, and colon cancer [80]. In a qualitative breast microbiota DNA study, the bacterium *Methylobacterium radiotolerans* has been found to be relatively enriched in tumor tissue, while the *Sphingomonas yanokuyae* bacterium is relatively enriched in paired normal tissue (Table 1). In paired normal breast tissue, but not in tumor tissue, the relative abundances of these two bacterial species were inversely correlated, indicating that dysbiosis is associated with breast cancer. In addition, total bacterial DNA load was decreased in the tumor versus paired normal and healthy breast tissues. Interestingly, the bacterial DNA load was associated inversely with advanced disease, a result that may have broad implications in breast cancer diagnosis and staging. Microbial DNA is present in the breast and can affect the local immune system [80].

1.6. Bladder Cancer and Bacterial Infection. Numerous laboratory, clinical, and community-based epidemiological studies have been conducted to determine the connection between urinary tract bacterial infection and bladder carcinoma incidence. Increased risk of bladder cancer following bacterial urinary tract infection has been identified in patients with recurrent or chronic cystitis and paraplegic patients [81]. Bacteria that are present in the urine have the ability to reduce ingested nitrates into nitrite which transforms into a nitrosating agent in acidic or neutral pH. About 39 to 66% of patients hospitalized with bladder carcinoma tested positive for bacteriuria, thus indicating urinary tract infection (UTI) [82]. In another study, urine samples were collected from 76 bladder carcinoma patients, and bacterial counts were 10^3 CFU/ml in 60% of patients which was much

higher than female patients. Microbial urine profile revealed the presence of *Staphylococcus albus* hemolytic, *Staphylococcus aureus*, *Klebsiella* spp., *Proteus mirabilis*, and *E. coli* [83].

1.6.1. Mechanism of Induction of Bladder Cancer. These species are bacteria-producing nitrate and thus play an important role in the production of N-nitrosamines (Figure 1). These organisms have been shown *in vitro* to perform a nitrosation reaction between ingested or metabolically derived nitrates and secondary amines under physiological pH, leading to the formation of N-nitrosamines (Figure 1) [84]. The formation of endogenous N-nitrosamines leads to the initiation of neoplastic events in patients. Moreover, elevated levels of N-nitrosamines have been consistently detected in bladder carcinoma patients [85]. Bacteria-infected rats have shown also increased nitrosation of amine precursors leading to increased levels of N-nitrosamines [85]. The presence of these compounds in urine may therefore provide the origin of initiating events crucial to the development of bladder cancer (Table 1). However, in order to communicate their carcinogenic effects, these compounds need activation to produce the reactive chemical species that can alkylate constituents of tissue. DNA methylation has been identified exclusively in patients with bladder cancer in different tissues of the human population [86, 87].

1.7. Conclusion. It is concluded that various specific species of bacteria have the pathogenic ability to induce carcinogenesis. Although there are some common mechanisms like the release of free radicals that cause damage to DNA and other regulatory proteins, there are other complex molecular mechanisms showing the role of bacterial proteins in the activation of specific inflammatory proteins. Therefore, in this review, we have highlighted the role of bacteria in the induction of malignancy providing evidences of their mechanism. Strong evidence from the literature showed an association of *Salmonella typhi*, *Chlamydia pneumonia*, and *H. pylori* with gallbladder cancer, lung cancer, and gastric cancer, respectively. Therefore, it is increasingly apparent that dissection of the complex interplay between man and microbial flora is essential to understand the pathogenesis of many malignancies.

Conflicts of Interest

The authors declare that there is no conflict of interest regarding the publication of this article.

References

- [1] M. C. Poirier, R. M. Santella, and A. Weston, "Carcinogen macromolecular adducts and their measurement," *Carcinogenesis*, vol. 21, no. 3, pp. 353–359, 2000.
- [2] S. A. Sheweita, "Drug-metabolizing enzymes: mechanisms and functions," *Current Drug Metabolism*, vol. 1, no. 2, pp. 107–132, 2000, Review.
- [3] M. H. Mostafa, S. A. Sheweita, and P. J. O'Connor, "Relationship between Schistosomiasis and Bladder Cancer," *Clinical Microbiology Reviews*, vol. 12, no. 1, pp. 97–111, 1999.
- [4] S. A. Sheweita and A. K. Tilmisany, "Cancer and phase II drug-metabolizing enzymes," *Current Drug Metabolism*, vol. 4, no. 1, pp. 45–58, 2003.
- [5] S. Khan, A. Imran, A. A. Khan, M. Abul Kalam, and A. Alshamsan, "Systems biology approaches for the prediction of possible role of Chlamydia pneumoniae proteins in the etiology of lung cancer," *PLoS One*, vol. 11, no. 2, article e0148530, 2016.
- [6] E. G. Di Domenico, I. Cavallo, M. Pontone, L. Toma, and F. Ensoli, "Biofilm producing *Salmonella typhi*: chronic colonization and development of gallbladder cancer," *International Journal of Molecular Sciences*, vol. 18, no. 9, p. 1887, 2017.
- [7] J. Koshiol, A. Wozniak, P. Cook et al., "Salmonella enterica serovar typhi and gallbladder cancer: a case-control study and meta-analysis," *Cancer Medicine*, vol. 5, no. 11, pp. 3310–3335, 2016.
- [8] T. Scanu, R. M. Spaapen, J. M. Bakker et al., "Salmonella Manipulation of Host Signaling Pathways Provokes Cellular Transformation Associated with Gallbladder Carcinoma," *Cell Host & Microbe*, vol. 17, no. 6, pp. 763–774, 2015.
- [9] A. Sharma, K. L. Sharma, A. Gupta, A. Yadav, and A. Kumar, "Gallbladder cancer epidemiology, pathogenesis and molecular genetics: Recent update," *World Journal of Gastroenterology*, vol. 23, no. 22, pp. 3978–3998, 2017.
- [10] Q. Shi, G. R. Haenen, L. Maas et al., "Inflammation-associated extracellular β -glucuronidase alters cellular responses to the chemical carcinogen benzo [a]pyrene," *Archives of Toxicology*, vol. 90, no. 9, pp. 2261–2273, 2016.
- [11] C. D. Klaassen and J. Y. Cui, "Review: mechanisms of how the intestinal microbiota alters the effects of drugs and bile acids," *Drug Metabolism and Disposition*, vol. 43, no. 10, pp. 1505–1521, 2015.
- [12] A. Sevanian and A. R. Peterson, "Cholesterol epoxide is a direct-acting mutagen," *Proceedings of the National Academy of Sciences of the United States of America*, vol. 81, no. 13, pp. 4198–4202, 1984.
- [13] J.-C. J. Tsay, B. G. Wu, M. H. Badri et al., "Airway microbiota is associated with upregulation of the PI3K pathway in lung cancer," *American Journal of Respiratory and Critical Care Medicine*, vol. 198, no. 9, pp. 1188–1198, 2018.
- [14] A. L. Laurila, T. Anttila, E. Läärä et al., "Serological evidence of an association between Chlamydia pneumoniae infection and lung cancer," *International Journal of Cancer*, vol. 74, no. 1, pp. 31–34, 1997.
- [15] E. Brandén, J. Gnarpe, G. Hillerdal et al., "Detection of Chlamydia pneumoniae on cytospin preparations from bronchoalveolar lavage in COPD patients and in lung tissue from advanced emphysema," *International Journal of Chronic Obstructive Pulmonary Disease*, vol. 2, no. 4, pp. 643–650, 2007.
- [16] H. Koyi, E. Branden, J. Gnarpe, H. Gnarpe, and B. Steen, "An association between chronic infection with *Chlamydia pneumoniae* and lung cancer. A prospective 2-year study," *APMIS*, vol. 109, no. 9, pp. 572–580, 2001.
- [17] M. Paldanius, A. Bloigu, M. Leinonen, and P. Saikku, "Measurement of chlamydia pneumoniae-specific immunoglobulin A (IgA) antibodies by the microimmunofluorescence (MIF) method: comparison of seven fluorescein-labeled anti-human IgA conjugates in an in-house MIF test using one commercial MIF and one enzyme immunoassay kit," *Clinical Diagnostic Laboratory Immunology*, vol. 10, no. 1, pp. 8–12, 2003.

- [18] A. Alshamsan, S. Khan, A. Imran, I. A. Aljuffali, and K. Alsaleh, "Prediction of Chlamydia pneumoniae protein localization in host mitochondria and cytoplasm and possible involvements in lung cancer etiology: a computational approach," *Saudi Pharmaceutical Journal*, vol. 25, no. 8, pp. 1151–1157, 2017.
- [19] M. Shen, L. Cai, K. Jiang, W. Xu, Y. Chen, and Z. Xu, "The therapeutic role of inhibition of miR-328 on pulmonary carcinoma induced by chlamydia pneumoniae through targeting histone H2AX," *Cancer Biomarkers*, vol. 1, pp. 1–8, 2018.
- [20] C. Jin, G. K. Lagoudas, C. Zhao et al., "Commensal microbiota promote lung cancer development via $\gamma\delta$ T cells," *Cell*, vol. 176, no. 5, pp. 998–1013.e16, 2019.
- [21] N. Parikh, R. L. Shuck, M. Gagea, L. Shen, and L. A. Donehower, "Enhanced inflammation and attenuated tumor suppressor pathways are associated with oncogene-induced lung tumors in aged mice," *Aging Cell*, vol. 17, no. 1, article e12691, 2018.
- [22] G. A. de Oliveira, R. Y. S. Cheng, L. A. Ridnour et al., "Inducible nitric oxide synthase in the carcinogenesis of gastrointestinal cancers," *Antioxidants & Redox Signaling*, vol. 26, no. 18, pp. 1059–1077, 2017.
- [23] J. Rupp, L. Pfeleiderer, C. Jugert et al., "Chlamydia pneumoniae hides inside apoptotic neutrophils to silently infect and propagate in macrophages," *PLoS One*, vol. 4, no. 6, article e6020, 2009.
- [24] R. K. Singh, M. Gutman, R. Radinsky, C. D. Bucana, and I. J. Fidler, "Expression of interleukin 8 correlates with the metastatic potential of human melanoma cells in nude mice," *Cancer Research*, vol. 54, no. 12, pp. 3242–3247, 1994.
- [25] M. N. Khan, B. Wang, J. Wei et al., "CXCR1/2 antagonism with CXCL8/Interleukin-8 analogue CXCL8(3-72)K11R/G31P restricts lung cancer growth by inhibiting tumor cell proliferation and suppressing angiogenesis," *Oncotarget*, vol. 6, no. 25, pp. 21315–21327, 2015.
- [26] J. M. Mayer, M. L. Woods, Z. Vavrin, and J. B. Hibbs Jr., "Gamma interferon induced nitric oxide production reduces Chlamydia trachomatis infectivity in McCoy cells," *Infection and Immunity*, vol. 61, no. 2, pp. 491–497, 1993.
- [27] Y. J. Choi and N. Kim, "Gastric cancer and family history," *The Korean Journal of Internal Medicine*, vol. 31, no. 6, pp. 1042–1053, 2016.
- [28] Y. H. Park and N. Kim, "Review of atrophic gastritis and intestinal metaplasia as a premalignant lesion of gastric cancer," *Journal of Cancer Prevention*, vol. 20, no. 1, pp. 25–40, 2015.
- [29] T. A. Sebrell, M. Hashimi, B. Sidar et al., "A novel gastric spheroid co-culture model reveals chemokine-dependent recruitment of human dendritic cells to the gastric epithelium," *Cellular and Molecular Gastroenterology and Hepatology*, vol. 8, no. 1, pp. 157–171.e3, 2019.
- [30] M. Amieva and R. M. Peek Jr., "Pathobiology of Helicobacter pylori -Induced Gastric Cancer," *Gastroenterology*, vol. 150, no. 1, pp. 64–78, 2016.
- [31] A. Takahashi-Kanemitsu, C. T. Knight, and M. Hatakeyama, "Molecular anatomy and pathogenic actions of Helicobacter pylori CagA that underpin gastric carcinogenesis," *Cellular & Molecular Immunology*, vol. 17, no. 1, pp. 50–63, 2020.
- [32] J. Y. Park, D. Forman, L. A. Waskito, Y. Yamaoka, and J. E. Crabtree, "Epidemiology of Helicobacter pylori and CagA-Positive infections and global variations in gastric cancer," *Toxins*, vol. 10, no. 4, p. 163, 2018.
- [33] A. Sokic-Milutinovic, T. Alempijevic, and T. Milosavljevic, "Role of Helicobacter pylori infection in gastric carcinogenesis: current knowledge and future directions," *World Journal of Gastroenterology*, vol. 21, no. 41, pp. 11654–11672, 2015.
- [34] M. McClain, A. C. Beckett, and T. L. Cover, "Helicobacter pylori vacuolating toxin and gastric cancer," *Toxins*, vol. 9, no. 10, p. 316, 2017.
- [35] J. Khatoon, R. P. Rai, and K. N. Prasad, "Role of Helicobacter pylori in gastric cancer: updates," *World Journal of Gastrointestinal Oncology*, vol. 8, no. 2, pp. 147–158, 2016.
- [36] L. D. Nolen, S. M. Vindigni, J. Parsonnet et al., "Combating Gastric Cancer in Alaska Native People: An Expert and Community Symposium," *Gastroenterology*, vol. 158, no. 5, pp. 1197–1201, 2020.
- [37] O. Toyoshima, T. Nishizawa, M. Arita et al., "Helicobacter pylori infection in subjects negative for high titer serum antibody," *World Journal of Gastroenterology*, vol. 24, no. 13, pp. 1419–1428, 2018.
- [38] G. H. Frydman, N. Davis, P. L. Beck, and J. G. Fox, "Helicobacter pylori Eradication in patients with immune Thrombocytopenic purpura: a review and the role of biogeography," *Helicobacter*, vol. 20, no. 4, pp. 239–251, 2015.
- [39] S. E. Morales-Guerrero, C. I. Rivas-Ortiz, S. Ponce de León-Rosales et al., "Translation of gastric disease progression at gene level expression," *Journal of Cancer*, vol. 11, no. 2, pp. 520–532, 2020.
- [40] J. Matsuzaki, H. Tsugawa, and H. Suzuki, "Precision medicine approaches to prevent gastric cancer," *Gut and Liver*, pp. 1–9, 2020.
- [41] H. Mei and H. Tu, "Vitamin C and Helicobacter pylori infection: current knowledge and future prospects," *Frontiers in Physiology*, vol. 9, 2018.
- [42] A. M. O'Hara, A. Bhattacharyya, J. Bai et al., "Tumor necrosis factor (TNF)- α -induced IL-8 expression in gastric epithelial cells: Role of reactive oxygen species and AP endonuclease-1/redox factor (Ref)-1," *Cytokine*, vol. 46, no. 3, pp. 359–369, 2009.
- [43] G. R. Davies, C. E. Collins, N. Banatvala et al., "A direct relationship between infective load of Helicobacter pylori and oxygen free radical production in antral mucosal biopsies," *Gut*, vol. 34, Supplement 1, pp. 73–79, 1993.
- [44] A. P. Gobert and K. T. Wilson, "Polyamine- and NADPH-dependent generation of ROS during Helicobacter pylori infection: A blessing in disguise," *Free Radical Biology & Medicine*, vol. 105, pp. 16–27, 2017.
- [45] O. Handa, Y. Naito, and T. Yoshikawa, "Redox biology and gastric carcinogenesis: the role of Helicobacter pylori," *Redox Report*, vol. 16, no. 1, pp. 1–7, 2013.
- [46] S. Kyung, J. W. Lim, and H. Kim, " α -Lipoic acid inhibits IL-8 expression by activating Nrf 2 signaling in Helicobacter pylori-infected gastric epithelial cells," *Nutrients*, vol. 11, no. 10, p. 2524, 2019.
- [47] D. Kidane, W. J. Chae, J. Czochoch et al., "Interplay between DNA repair and inflammation, and the link to cancer," *Critical Reviews in Biochemistry and Molecular Biology*, vol. 49, no. 2, pp. 116–139, 2013.
- [48] S. A. Sheweita and M. H. Mostafa, "N-Nitrosamines and their effects on the level of glutathione, glutathione reductase and glutathione S-transferase activities in the liver of male mice," *Cancer Letters*, vol. 99, no. 1, pp. 29–34, 1996.

- [49] M. Tsujii, S. Kawano, S. Tsuji et al., “Ammonia: a possible promoter in *Helicobacter pylori* -related gastric carcinogenesis,” *Cancer Letters*, vol. 65, no. 1, pp. 15–18, 1992.
- [50] C. P. M. S. Oliveira, P. Kassab, F. P. Lopasso et al., “Protective effect of ascorbic acid in experimental gastric cancer: reduction of oxidative stress,” *World Journal of Gastroenterology*, vol. 9, no. 3, pp. 446–448, 2003.
- [51] M. Jarosz, J. Dzieniszewski, E. Dabrowska-Ufniarz, M. Wartanowicz, S. Ziemlanski, and P. I. Reed, “Effects of high dose vitamin C treatment on *Helicobacter pylori* infection and total vitamin C concentration in gastric juice,” *European Journal of Cancer Prevention*, vol. 7, no. 6, pp. 449–454, 1998.
- [52] M. Epplen, X. O. Shu, Y. B. Xiang et al., “Fruit and vegetable consumption and risk of distal gastric cancer in the Shanghai Women’s and Men’s Health studies,” *American Journal of Epidemiology*, vol. 172, no. 4, pp. 397–406, 2010.
- [53] Z. W. Zhang, S. E. Patchett, D. Perrett, P. H. Katelaris, P. Domizio, and M. J. G. Farthing, “The relation between gastric vitamin C concentrations, mucosal histology, and CagA seropositivity in the human stomach,” *Gut*, vol. 43, no. 3, pp. 322–326, 1998.
- [54] G. Krzysiek-Maczka, A. Targosz, U. Szczyrk, M. Strzalka, T. Brzozowski, and A. Ptak-Belowska, “Involvement of epithelial-mesenchymal transition-inducing transcription factors in the mechanism of *Helicobacter pylori*-induced fibroblasts activation,” *Journal of Physiology and Pharmacology*, vol. 70, no. 5, 2019.
- [55] F. Teresa, N. Serra, G. Capra et al., “*Helicobacter pylori* and Epstein–Barr Virus Infection in Gastric Diseases: Correlation with IL-10 and IL1RN Polymorphism,” *Journal of Oncology*, vol. 2019, Article ID 1785132, 8 pages, 2019.
- [56] Y. Zhang, X. Zhou, Q. Zhang, Y. Zhang, X. Wang, and L. Cheng, “Involvement of NF- κ B signaling pathway in the regulation of PRKAA1-mediated tumorigenesis in gastric cancer,” *Artificial Cells, Nanomedicine, and Biotechnology*, vol. 47, no. 1, pp. 3677–3686, 2019.
- [57] J. E. Crabtree, “Role of cytokines in pathogenesis of *Helicobacter pylori*-induced mucosal damage,” *Digestive Diseases and Sciences*, vol. 43, 9 Supplement, pp. 46S–55S, 1998.
- [58] J. Houghton, L. S. Macera-Bloch, L. Harrison, K. H. Kim, and R. M. Korah, “Tumor necrosis factor alpha and interleukin 1 β up-regulate gastric mucosal fas antigen expression in *Helicobacter pylori* infection,” *Infection and Immunity*, vol. 68, no. 3, pp. 1189–1195, 2000.
- [59] T. A. Kunkel and D. A. Erie, “Eukaryotic Mismatch Repair in Relation to DNA Replication,” *Annual Review of Genetics*, vol. 49, no. 1, pp. 291–313, 2015.
- [60] M. Romano, V. Ricci, A. di Popolo et al., “*Helicobacter pylori* upregulates expression of epidermal growth factor-related peptides, but inhibits their proliferative effect in MKN 28 gastric mucosal cells,” *The Journal of Clinical Investigation*, vol. 101, no. 8, pp. 1604–1613, 1998.
- [61] M. Ratti, A. Lampis, J. C. Hahne, R. Passalacqua, and N. Valeri, “Microsatellite instability in gastric cancer: molecular bases, clinical perspectives, and new treatment approaches,” *Cellular and Molecular Life Sciences*, vol. 75, no. 22, pp. 4151–4162, 2018.
- [62] G. Calin, G. N. Ranzani, D. Amadori et al., “Somatic frameshift mutations in the Bloom syndrome BLM gene are frequent in sporadic gastric carcinomas with microsatellite mutator phenotype,” *BMC Genetics*, vol. 2, no. 1, p. 14, 2001.
- [63] K. Sakata, G. Tamura, Y. Endoh, K. Ohmura, S. Ogata, and T. Motoyama, “Hypermethylation of the *hMLH1* gene promoter in solitary and multiple gastric cancers with microsatellite instability,” *British Journal of Cancer*, vol. 86, no. 4, pp. 564–567, 2002.
- [64] S. Richman, “Deficient mismatch repair: read all about it (review),” *International Journal of Oncology*, vol. 47, no. 4, pp. 1189–1202, 2015.
- [65] P. Ye, Y. Shi, and A. Li, “Association between hMLH1 promoter methylation and risk of gastric cancer: a meta-analysis,” *Frontiers in Physiology*, vol. 9, p. 368, 2018.
- [66] N. H. Haron, E. A. Mohamad Hanif, M. R. Abdul Manaf et al., “Microsatellite instability and altered expressions of MLH1 and MSH2 in gastric cancer,” *Asian Pacific Journal of Cancer Prevention*, vol. 20, no. 2, pp. 509–517, 2019.
- [67] J. C. Santos and M. L. Ribeiro, “Epigenetic regulation of DNA repair machinery in *Helicobacter pylori*-induced gastric carcinogenesis,” *World Journal of Gastroenterology*, vol. 21, no. 30, pp. 9021–9037, 2015.
- [68] D. Nejman, I. Livyatan, G. Fuks et al., “The human tumor microbiome is composed of tumor type-specific intracellular bacteria,” *Science*, vol. 368, no. 6494, pp. 973–980, 2020.
- [69] J. Gagnière, J. Raisch, J. Veziat et al., “Gut microbiota imbalance and colorectal cancer,” *World Journal of Gastroenterology*, vol. 22, no. 2, pp. 501–518, 2016.
- [70] C. L. Sears and W. S. Garrett, “Microbes, microbiota, and colon cancer,” *Cell Host & Microbe*, vol. 15, no. 3, pp. 317–328, 2014.
- [71] K. W. Kinzler and B. Vogelstein, “Lessons from hereditary colorectal cancer,” *Cell*, vol. 87, no. 2, pp. 159–170, 1996.
- [72] S. Hwang, M. Jo, J. E. Hong et al., “Zerumbone suppresses enterotoxigenic *Bacteroides fragilis* infection-induced colonic inflammation through inhibition of NF- κ B,” *International Journal of Molecular Sciences*, vol. 20, no. 18, p. 4560, 2019.
- [73] L. Chung, E. Thiele Orberg, A. L. Geis et al., “*Bacteroides fragilis* Toxin Coordinates a Pro-carcinogenic Inflammatory Cascade via Targeting of Colonic Epithelial Cells,” *Cell Host & Microbe*, vol. 23, no. 2, pp. 203–214.e5, 2018.
- [74] J. I. Jeon, S. H. Ko, and J. M. Kim, “Intestinal epithelial cells exposed to *Bacteroides fragilis* enterotoxin regulate NF- κ B activation and inflammatory responses through β -catenin expression,” *Infection and Immunity*, vol. 87, no. 11, 2019e00312-19.
- [75] C. M. Dejea, P. Fathi, J. M. Craig et al., “Patients with familial adenomatous polyposis harbor colonic biofilms containing tumorigenic bacteria,” *Science*, vol. 359, no. 6375, pp. 592–597, 2018.
- [76] E. Senkus, S. Kyriakides, S. Ohno et al., “Primary breast cancer: ESMO Clinical Practice Guidelines for diagnosis, treatment and follow-up[†],” *Annals of Oncology*, vol. 26, pp. v8–v30, 2015.
- [77] “U.S. Breast Cancer Statisticshttps,” 2017, March 2019, <http://breastcancer.org>, http://breastcancer.org/symptoms/understand_bc/statistics.
- [78] A. Bleyer and H. G. Welch, “Effect of three decades of screening mammography on breast-cancer incidence,” *The New England Journal of Medicine*, vol. 367, no. 21, pp. 1998–2005, 2012.
- [79] E. Mikó, T. Kovács, E. Sebő et al., “Microbiome—microbial metabolome—cancer cell interactions in breast cancer—familiar, but unexplored,” *Cell*, vol. 8, no. 4, pp. 293–302, 2019.

- [80] C. Xuan, J. M. Shamonki, A. Chung et al., "Microbial dysbiosis is associated with human breast cancer," *PLoS One*, vol. 9, no. 1, article e83744, 2014.
- [81] A. F. Kantor, P. Hartge, R. N. Hoover, A. S. Narayana, J. W. Sullivan, and J. F. Fraumeni Jr., "Urinary tract infection and risk of bladder cancer," *American Journal of Epidemiology*, vol. 119, no. 4, pp. 510–515, 1984.
- [82] J. S. Lehman, Z. Farid, J. H. Smith, S. Bassily, and N. A. El-Masry, "Urinary schistosomiasis in Egypt: clinical, radiological, bacteriological and parasitological correlations," *Transactions of the Royal Society of Tropical Medicine and Hygiene*, vol. 67, no. 3, pp. 384–399, 1973.
- [83] R. M. Hicks, M. M. Ismail, C. L. Walters, P. T. Beecham, M. F. Rabie, and M. A. el Alamy, "Association of bacteriuria and urinary nitrosamine formation with *Schistosoma haematobium* infection in the Qalyub area of Egypt," *Transactions of the Royal Society of Tropical Medicine and Hygiene*, vol. 76, no. 4, pp. 519–527, 1982.
- [84] S. Calmels, H. Ohshima, and H. Bartsch, "Nitrosamine formation by denitrifying and non-denitrifying bacteria: implication of nitrite reductase and nitrate reductase in nitrosation catalysis," *Journal of General Microbiology*, vol. 134, no. 1, pp. 221–226, 1988.
- [85] A. R. Tricker, D. J. Stickler, J. C. Chawla, and R. Preussmann, "Increased urinary nitrosamine excretion in paraplegic patients," *Carcinogenesis*, vol. 12, no. 5, pp. 943–946, 1991.
- [86] D. Umbenhauer, C. P. Wild, R. Montesano et al., "O6-Methyldeoxyguanosine in oesophageal DNA among individuals at high risk of oesophageal cancer," *International Journal of Cancer*, vol. 36, no. 6, pp. 661–665, 1985.
- [87] S. H. Kroft and R. Oyasu, "Urinary bladder cancer: mechanisms of development and progression," *Laboratory Investigation*, vol. 71, no. 2, pp. 158–174, 1994.

Research Article

Amelioration of Coagulation Disorders and Inflammation by Hydrogen-Rich Solution Reduces Intestinal Ischemia/Reperfusion Injury in Rats through NF- κ B/NLRP3 Pathway

Ling Yang ¹, Yan Guo ¹, Xin Fan ¹, Ye Chen ², Bo Yang ¹, Ke-Xuan Liu ³,
and Jun Zhou ¹

¹Department of Anesthesiology, The Affiliated Hospital of Southwest Medical University, Luzhou, China

²Department of Traditional Chinese Medicine, The Affiliated Hospital of Southwest Medical University, Luzhou, China

³Department of Anesthesiology, Nanfang Hospital, Southern Medical University, Guangzhou, China

Correspondence should be addressed to Jun Zhou; scjunzhou@gmail.com

Received 28 March 2020; Accepted 28 May 2020; Published 10 June 2020

Guest Editor: Tae Jin lee

Copyright © 2020 Ling Yang et al. This is an open access article distributed under the Creative Commons Attribution License, which permits unrestricted use, distribution, and reproduction in any medium, provided the original work is properly cited.

Intestinal ischemia/reperfusion (I/R) injury often causes inflammatory responses and coagulation disorders, which is further promoting the deterioration of the disease. Hydrogen has anti-inflammatory, antioxidative, and antiapoptotic properties against various diseases. However, the effect of hydrogen on coagulation dysfunction after intestinal I/R and the underlying mechanism remains unclear. The purpose of this study was to explore whether hydrogen-rich solution (HRS) could attenuate coagulation disorders and inflammation to improve intestinal injury and poor survival following intestinal I/R. The rat model of intestinal I/R injury was established by clamping the superior mesenteric artery for 90 min and reperfusion for 2 h. HRS (10 or 20 mL/kg) or 20 mL/kg 0.9% normal saline was intravenously injected at 10 min before reperfusion, respectively. The samples were harvested at 2 h after reperfusion for further analyses. Moreover, the survival rate was observed for 24 h. The results showed that HRS improved the survival rate and alleviated serum diamine oxidase activities, intestinal injury, edema, and apoptosis. Interestingly, HRS markedly improved intestinal I/R-mediated coagulation disorders as evidenced by abnormal conventional indicators of coagulation and thromboelastography. Additionally, HRS attenuated inflammatory responses and the elevated tissue factor (TF) and inhibited nuclear factor kappa beta (NF- κ B) and nucleotide binding and oligomerization domain-like receptor family pyrin domain-containing 3 (NLRP3) inflammasome activation in peripheral blood mononuclear cells. Moreover, inflammatory factors and myeloperoxidase were closely associated with TF level. This study thus emphasized upon the amelioration of coagulation disorders and inflammation by HRS as a mechanism to improve intestinal I/R-induced intestinal injury and poor survival, which might be partially related to inhibition of NF- κ B/NLRP3 pathway.

1. Introduction

Intestinal ischemia/reperfusion (I/R) injury is a pathophysiological process related to various clinical acute and severe diseases, such as mesenteric arterial thrombosis, hemorrhagic shock, and severe burns. It has the characteristics of high morbidity and high mortality [1–3]. Intestinal I/R injury potentially leads to a compromised mucosal barrier and increases intestinal permeability and translocation of intestinal bacteria. It also can release a great number of inflamma-

tory mediators and cytokines into the blood, causing multiple organ failure [3–7].

Inflammatory cytokines are the major mediators involved in coagulation activation. When the inflammatory response is out of control, the coagulation function is bound to be affected [8, 9]. The body's normal coagulation function is coordinated and maintained by the coagulation system, anticoagulation system, and fibrinolytic system. The coagulation disorder could occur when these three regulatory systems are out of balance. It exists in various diseases

involving inflammatory reactions, such as sepsis, I/R, severe burns, and traumatic shock. The process often manifests as bleeding tendency, thrombosis, hemorrhagic-thrombotic syndrome, and so on. Intestinal I/R could irritate the body with infectious factors, which could also cause abnormal blood coagulation [10, 11].

Hydrogen (H_2) is the oldest and simplest molecule in our Universe. It can protect a variety of organ injuries as well due to its antioxidation, anti-inflammatory, and antiapoptotic effects [12, 13]. Interestingly, H_2 has a remarkable therapeutic effect on various diseases, including organ ischemia-reperfusion injury and sepsis [14–17]. Previous studies reported that hydrogen-rich solution (HRS) might have a protective effect on intestinal I/R injury, while its molecular mechanism has still remained elusive [18, 19]. More importantly, to date, the effects of HRS on coagulation dysfunction after intestinal I/R injury and the underlying mechanism remained obscure.

Hence, the purpose of this study was to explore whether hydrogen-rich solution (HRS) could attenuate coagulation disorders and inflammation to improve intestinal injury and poor survival following intestinal I/R.

2. Materials and Methods

2.1. Animals and Experimental Protocol. Adult healthy male Sprague Dawley (SD) rats (body weight, 220–250 g) were provided by the Experimental Animal Center of the Southwest Medical University (Luzhou, China). The animals were maintained under the environmental conditions of $(23 \pm 2)^\circ\text{C}$, 12 h:12 h light-dark cycle, with normal diet, and free access to drinking water. The rats were acclimated for 1 week in the environment before the experiments. The experimental protocols and animal care were approved by the Animal Ethics Committee of the Affiliated Hospital of Southwest Medical University (No. 20180306042). In addition, animal care and handling were performed in accordance with the National Institutes of Health guidelines.

One hundred and fifty-six rats were randomly divided into four groups ($n = 39$ per group): sham-operated group (SHAM), I/R group (I/R), I/R plus hydrogen-rich saline (10 mL/kg, HRS1); and I/R plus hydrogen-rich saline (20 mL/kg, HRS2). In each group, 15 rats were selected and were observed until 24 h after intestinal I/R for survival analysis; 8 rats were chosen, and the samples (blood and intestine) were harvested for morphological evaluation, intestinal edema, and coagulation-related indicators at 2 h after I/R. In addition, due to the limited blood volume of the rats, another 8 rats in each group had to be selected to obtain blood samples (7 mL) for subsequent analysis (inflammation and TF). Finally, blood samples (6 mL) were collected from the 8 remaining rats in each group for thromboelastography and platelet count.

2.2. I/R Model and HRS Treatment. Intestinal I/R injury model was established as described previously [4, 6]. Briefly, the rats were fasted for 12 h, with free access to drinking water before surgery. The rats were anesthetized by intraperitoneal injection of 1% sodium pentobarbital (30 mg/kg), and

the abdomen was opened along the midline of the abdomen to separate the superior mesenteric artery (SMA). Except for the SHAM group, a noninvasive microarterial clamp was used to clip the SMA for 90 min and reperfusion for 2 h in the other groups. In the SHAM group, only the SMA was isolated, and no clamping was performed. Moreover, rats in the HRS1 group and HRS2 group were injected with HRS (concentration: ≥ 0.6 mmol/L, ≥ 0.6 ppm) 10 or 20 mL/kg (Hydrovita Biotechnology Co, Beijing, China) at 10 min before reperfusion through the tail vein, respectively [19, 20]. The rats in the SHAM group and I/R group were injected with 20 mL/kg 0.9% normal saline. The incision was infiltrated with 0.125% ropivacaine to alleviate postoperative pain.

2.3. Collection of Specimens. The rats were sacrificed at 2 h after reperfusion with an overdose of sodium pentobarbital (100 mg/kg, intraperitoneal), and blood was taken through the abdominal aorta, 2 cm of small intestine tissue was taken 5 cm from the end of the ileum. The part of the intestinal segment (1 cm) was fixed with 4% paraformaldehyde for morphological analysis; another 1 cm of intestine tissue was for measuring intestinal edema.

2.4. Small Bowel Morphology. The paraffin-embedded tissues were stained with hematoxylin-eosin (H&E). Two pathologists, who were blinded to the study groups, observed the small intestine tissue under a light microscope ($\times 200$, Olympus, Tokyo, Japan). For each slice, 5 fields were randomly selected, and Chiu's scoring method was used to assess the degree of intestinal injury [21].

2.5. Assessment of Edema in Intestine. The severity of intestinal edema was evaluated by the wet/dry (W/D) weight ratio method [22]. In brief, intestinal segments were harvested, and the surfaces of them were wiped, then the wet weight (W) was measured. Furthermore, the tissues were placed in an 80°C oven to dry for 24 hours, and the dry weight (D) was obtained. The W/D weight ratio was then calculated.

2.6. TUNEL Assay of Intestine. The terminal deoxynucleotidyl transferase-mediated dUDP-biotin nick end labeling (TUNEL) method with a commercial assay kit (Roche, Indianapolis, IN, USA) was used to detect the apoptosis in intestine. The slices of intestinal tissue were deparaffinized and treated with TUNEL solution as previously described [6]. The total number of cells and positive cells per visual field were calculated. The apoptotic index = $100 \times \text{TUNEL positive cells}/\text{total cells}\%$.

2.7. Detection of Coagulation-Related Indicators. Blood samples (3 mL) were centrifuged at 3000 rpm for 10 min, and related indicators of coagulation function, such as prothrombin time (PT), activated partial thromboplastin time (APTT), thrombin time (TT), fibrinogen (FIB), fibrinogen degradation product (FDP), D-dimer (D-Di), and prothrombin time-international standardization ratio (PT-INR), were detected by an automatic coagulometer (Stago, Paris, France).

2.8. Thromboelastography and Platelet Count. Briefly, thromboelastography (TEG) was performed with TEG 5000 Hemostasis System (Hemoscope Corporation, Niles, IL, USA) by adding 20 μ L of 0.2 M calcium chloride and 340 μ L of citrated whole blood to kaolin. The reaction time (R), clotting time (K), coagulation angle (α -Angle), and maximal amplitude (MA) were recorded [23]. An additional 3 mL of blood was tested for platelet count by an automatic hematology analyzer, BC-6800, Mindray (Shenzhen, China).

2.9. Detection of Serum Inflammatory Markers, DAO, and Tissue Factor. A total of 7 mL blood was taken through the abdominal aorta, of which 4.5 mL blood samples were maintained at room temperature for 2 h, centrifuged at 1000 rpm for 20 min, and the supernatant was used to detect the levels of tissue factor (TF); tumor necrosis factor- α (TNF- α); interleukin-1 β (IL-1 β), interleukin-6 (IL-6), and interleukin-10 (IL-10); and the activities of diamine oxidase (DAO) and myeloperoxidase (MPO) in serum. The enzyme-linked immunosorbent assay (ELISA) kits were utilized according to the manufacturer's instructions [(TF, TNF- α and IL-6; Cloud-Clone Corp[®], Wuhan, China); (IL-1 β and IL-10; R&D Systems, Inc, Minneapolis, MN, USA); (DAO and MPO; Nanjing Jiancheng Bioengineering Institute, China)]. The results were expressed as pg/mL and U/mL, respectively.

2.10. Western Blotting Analysis. The remaining 2.5 mL blood samples were processed according to the animal mononuclear cell separation method, and peripheral blood mononuclear cell layers were extracted. Then, the mononuclear cell layer was added with cell fission extraction protein, and the protein concentration was determined by bicinchoninic acid (BCA) assay. For each group of samples, 40 μ g of protein was loaded, electrophoresed on a 10% sodium dodecyl sulfate-polyacrylamide gel electrophoresis (SDS-PAGE) gel, and then, the protein was transferred onto a polyvinylidene fluoride (PVDF) membrane (Amersham Biosciences, NJ, USA) and blocked with 5% milk for 2 h at room temperature. Subsequently, the membrane was incubated overnight at 4°C with primary antibodies for phospho-NF- κ B p65 (1:200; Abcam, USA), NF- κ B p65 (1:500; Cell Signaling Technology, Inc., Danvers, MA), NLRP3 (1:300), Caspase 1 (1:500), and β -actin (1:300) (Santa Cruz Biotechnology, Inc., CA, USA). It was then washed thrice with Tris-buffered saline with Tween 20 (TBST) and incubated with an anti-rabbit IgG (1:5000; Beyotime Biotechnology, Shanghai, China) or anti-mouse IgG (1:2500; Santa Cruz Biotechnology, Inc., CA, USA) secondary antibody for 1 h at 37°C. Finally, exposure and development were performed with ECL luminescent reagent, visualized with a protein imaging system, and protein bands were analyzed with Image J software (version 1.31; National Institutes of Health, Bethesda, ML, USA).

2.11. Survival Rate. The rats in all groups were observed continuously for 24 hours via video (SMART, Barcelona, Spain) to evaluate survival rate. All rats were allowed food and water *ad libitum*.

2.12. Statistical Analysis. Data was presented as mean \pm standard deviation (SD) and analyzed using the GraphPad

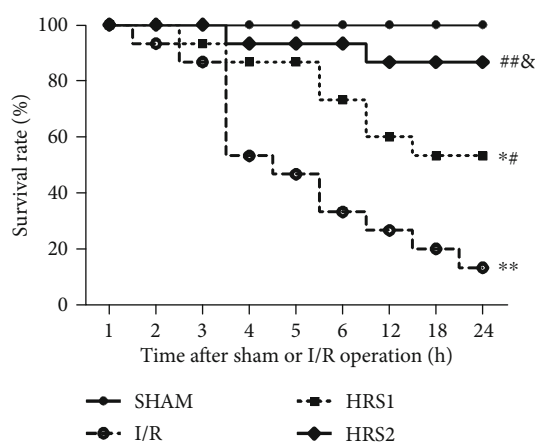


FIGURE 1: HRS improved the survival of rats after intestinal I/R. Rats subjected to intestinal ischemia for 90 minutes by occluding the superior mesenteric artery (SMA) were received normal saline (vehicle) or HRS (10 or 20 mL/kg of body weight) via the tail vein at 10 min before reperfusion and were observed for 24 hours. Data are presented as the survival percentage of animals. The survival rate is estimated and compared by the Kaplan-Meier method and the log-rank test ($n = 15/\text{group}$). * $P < 0.05$, ** $P < 0.01$ vs. SHAM group; # $P < 0.05$, ## $P < 0.01$ vs. I/R group; & $P < 0.05$ vs. HRS1 group.

Prism 6 program (GraphPad Software Inc., San Diego, Calif, USA). Survival studies were analyzed using the Kaplan-Meier method followed by a log-rank test. The survival rates were expressed as a percentage and tested by the Fisher exact probability method. For all other data, one-way analysis of variance (ANOVA) with the Bonferroni post hoc test was used to compare differences. Correlation between different variables was assessed by Pearson coefficient [17]. $P < 0.05$ was considered to be statistically significant.

3. Results

3.1. HRS Improved the Survival of Rats after Intestinal I/R. As illustrated in Figure 1, the survival rate at 24 h was significantly reduced in rats subjected to an intestinal I/R event (13.33%, 2 of 15 rats) compared to sham controls (100%, 15 of 15 rats; $P < 0.01$). However, HRS treatment significantly increased the 24-h survival of rats to 53.33% (8 of 15 rats) in the HRS1 group and 86.67% (13 of 15 rats) in the HRS2 group, respectively ($P < 0.05$ or $P < 0.01$). Moreover, 24-h survival of rats in the HRS2 group was higher than that in the HRS1 group ($P < 0.05$). The results showed that HRS could improve the survival of intestinal I/R rats in a dose-dependent manner.

3.2. HRS Reduced Small Intestinal Injury, Edema and Serum DAO Activity. As shown in Figure 2, the results of H&E staining showed that the histopathological structure of intestinal mucosa was normal in the SHAM group, the villi and glands were neat, and Chiu's score was significantly lower than that in the I/R group ($P < 0.01$). However, the epithelial cell shedding was observed in small intestinal mucosa of rats in the I/R group, and Chiu's score was higher. Chiu's score in the HRS1 group or HRS2 group was noticeably lower than that

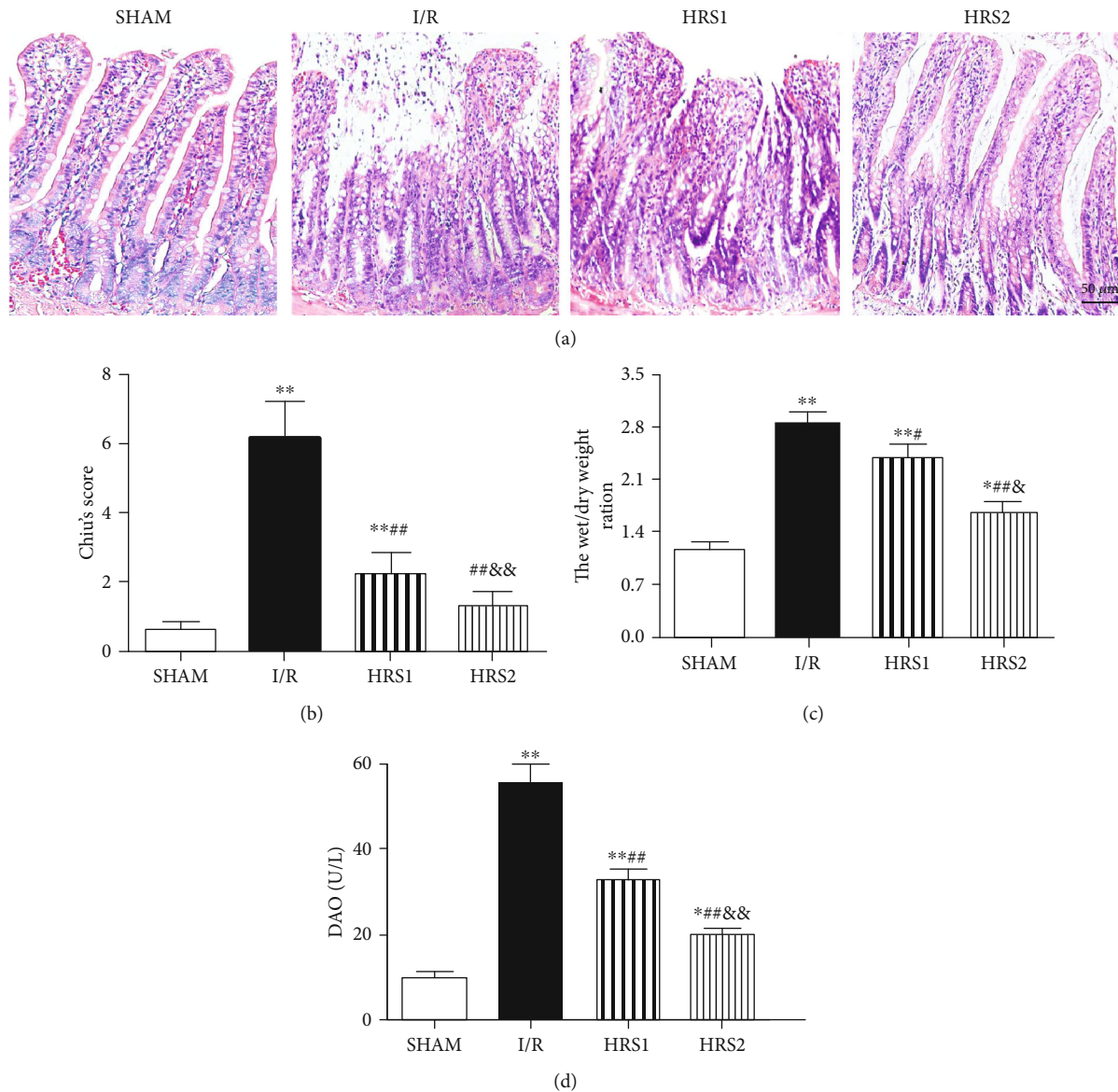


FIGURE 2: HRS alleviated the histopathological damage in the intestine. (a) Representative images were shown for the pathological changes of intestinal mucosal tissues (hematoxylin and eosin staining, original magnification $\times 200$). (b) The histopathological score of intestine (Chiu's score). (c) The *W/D* weight ratio. (d) Serum DAO activities. The data were represented as mean \pm SD ($n = 8/\text{group}$). * $P < 0.05$, ** $P < 0.01$ vs. SHAM group; # $P < 0.05$, ## $P < 0.01$ vs. I/R group; &# $P < 0.05$, &&# $P < 0.01$ vs. HRS1 group. Scale bar = 50 μm .

in the I/R group ($P < 0.05$ or $P < 0.01$). There was no significant difference between the HRS1 group and HRS2 group (Figures 2(a) and 2(b)). In addition, compared with those of the SHAM group, the *W/D* ratio of intestine and serum DAO activities in the I/R, HRS1, and HRS2 groups were all significantly higher ($P < 0.05$ or $P < 0.01$). However, the *W/D* ratio and DAO activities in the HRS groups were significantly lower than those in the I/R group. There was significant difference between the HRS1 group and HRS2 group ($P < 0.05$ or $P < 0.01$) (Figures 2(c) and 2(d)).

3.3. HRS Attenuated Apoptosis of Intestine. As shown in Figure 3, few TUNEL-positive cells were detected in the SHAM group, the apoptotic index was significantly higher in the I/R group than that in the sham group ($P < 0.01$).

Compared with the I/R group, the apoptotic index was significantly lower in the HRS1 and HRS2 groups ($P < 0.01$). The apoptotic index showed no significantly statistical difference in the HRS1 and HRS2 groups (Figure 3).

3.4. HRS Improved Coagulation Disorders. Compared with the SHAM group, the levels of PT, APTT, TT, FDP, D-Di, and PT-INR in the I/R group were increased, while the FIB level was decreased ($P < 0.01$). After HRS treatment, the levels of PT, APTT, TT, FDP, D-Di, and PT-INR were attenuated, whereas the FIB level was elevated ($P < 0.05$ or $P < 0.01$). The above-mentioned factors also showed significantly statistical difference in the HRS1 and HRS2 groups ($P < 0.05$ or $P < 0.01$) (Figure 4).

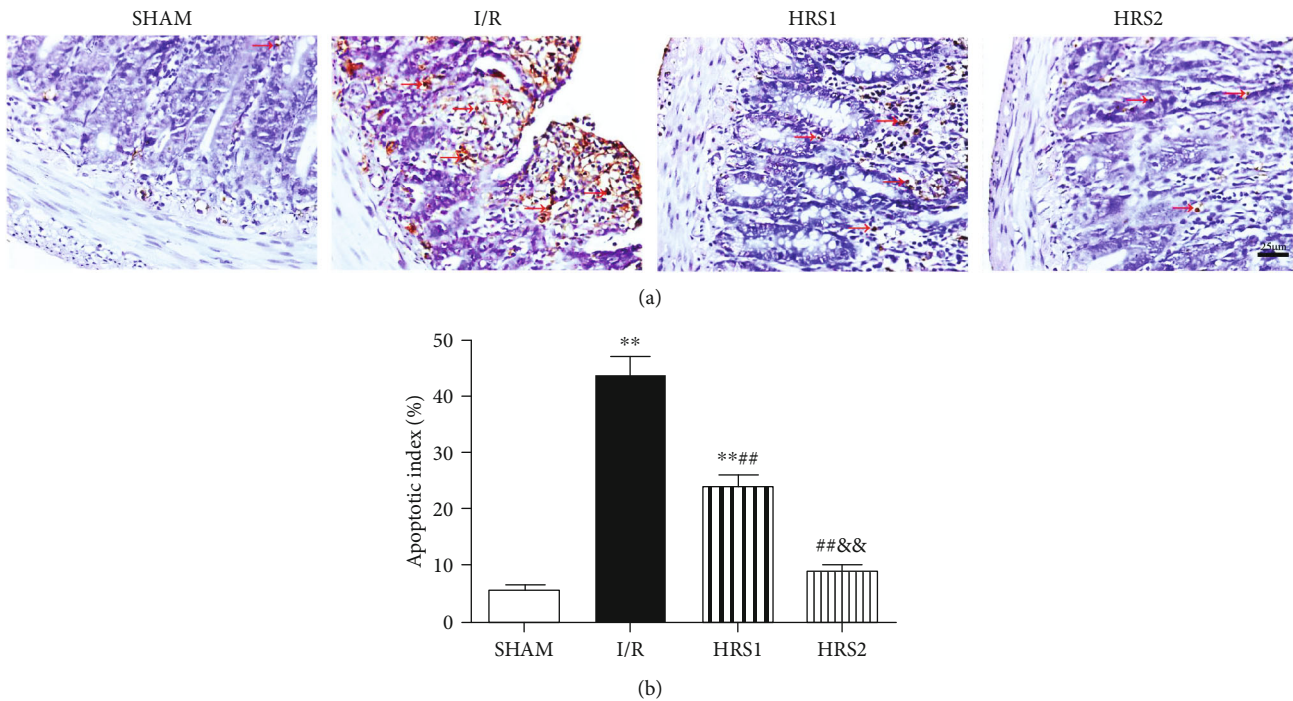


FIGURE 3: HRS attenuated apoptosis in intestinal tissues. (a) Representative images for intestinal apoptotic cells (original magnification $\times 400$). TUNEL-positive cells with dark brown nuclei indicated apoptosis (red arrows). (b) The quantitative analysis of apoptotic index among different groups. The data were represented as mean \pm SD ($n = 8$ /group). ** $P < 0.01$ vs. SHAM group; ## $P < 0.01$ vs. I/R group; && $P < 0.01$ vs. HRS1 group. Scale bar = $25 \mu\text{m}$.

3.5. Effects of HRS on Thromboelastography and Platelet Count. Herein, R and K values were increased after intestinal I/R injury, while α -angle and MA values were decreased ($P < 0.01$). Compared with I/R group, R and K values were reduced, whereas α -angle and MA values were remarkably increased in the HRS1 and HRS2 groups ($P < 0.05$ or $P < 0.01$). In addition, the above-mentioned factors also showed significantly statistical difference in the HRS1 and HRS2 groups ($P < 0.05$ or $P < 0.01$). However, there was no significant difference in platelet count among all groups ($P > 0.05$) (Figure 5).

3.6. Effect of HRS on Serum TNF- α , IL-6, IL-1 β , IL-10, MPO, and TF Levels. Compared with the SHAM group, the levels of TNF- α , IL-6, IL-1 β , MPO, and TF in the serum of rats in the I/R group were elevated, while the levels of IL-10 were reduced ($P < 0.01$). HRS treatment caused significant decrease in TNF- α , IL-6, IL-1 β , MPO, and TF and significant increase in IL-10 when compared to the I/R group ($P < 0.05$ or $P < 0.01$). The improvements of the above-mentioned factors were more obvious in the HRS2 group than those in the HRS1 group ($P < 0.05$ or $P < 0.01$) (Figure 6).

3.7. Correlation Analysis. To determine the relationship between tissue factor and inflammation or intestinal injury, we further analyzed the correlation between them. As illustrated in Figure 7, overall, TF was positively correlated with TNF- α ($r = 0.9007$, $P < 0.01$), IL-1 β ($r = 0.8467$, $P < 0.01$), IL-6 ($r = 0.8974$, $P < 0.01$), MPO ($r = 0.8552$, $P < 0.01$), and

Chiu's score ($r = 0.9399$, $P < 0.01$), while TF was negatively correlated with IL-10 ($r = -0.7915$, $P < 0.01$).

3.8. HRS Inhibited the NF- κ B and NLRP3 Pathway. NF- κ B and NLRP3 signaling pathways were involved in the inflammatory response to acute intestinal injury. To investigate the possible mechanism of HRS in improving intestinal I/R injury and coagulation function, we further studied the expressions of phospho-NF- κ B p65 (p-NF- κ B p65), NF- κ B p65, NLRP3, and Caspase 1 in peripheral blood mononuclear cells. It was disclosed that intestinal I/R injury could up-regulate the expressions of p-NF- κ B p65, NLRP3, and Caspase 1 as compared to the SHAM group ($P < 0.01$), while HRS could significantly down-regulate the corresponding expressions in a dose-dependent manner as compared to the I/R group ($P < 0.05$ or $P < 0.01$) (Figure 8).

4. Discussion

Intestinal I/R injury is associated with increases in luminal epithelial permeability and ingress of bacterial molecules (e.g., enterotoxin) or bacteria themselves which can result in systemic inflammatory responses, multiple organ failure, and even leading to death [1–3]. In the present study, Chiu's score, the W/D ratio of intestine, and serum DAO activities increased, indicating that intestinal I/R injury caused a great damage to the intestine, and the model was successfully established [4, 6, 22]. The present results also demonstrated that HRS could attenuate intestinal injury, as evidenced by

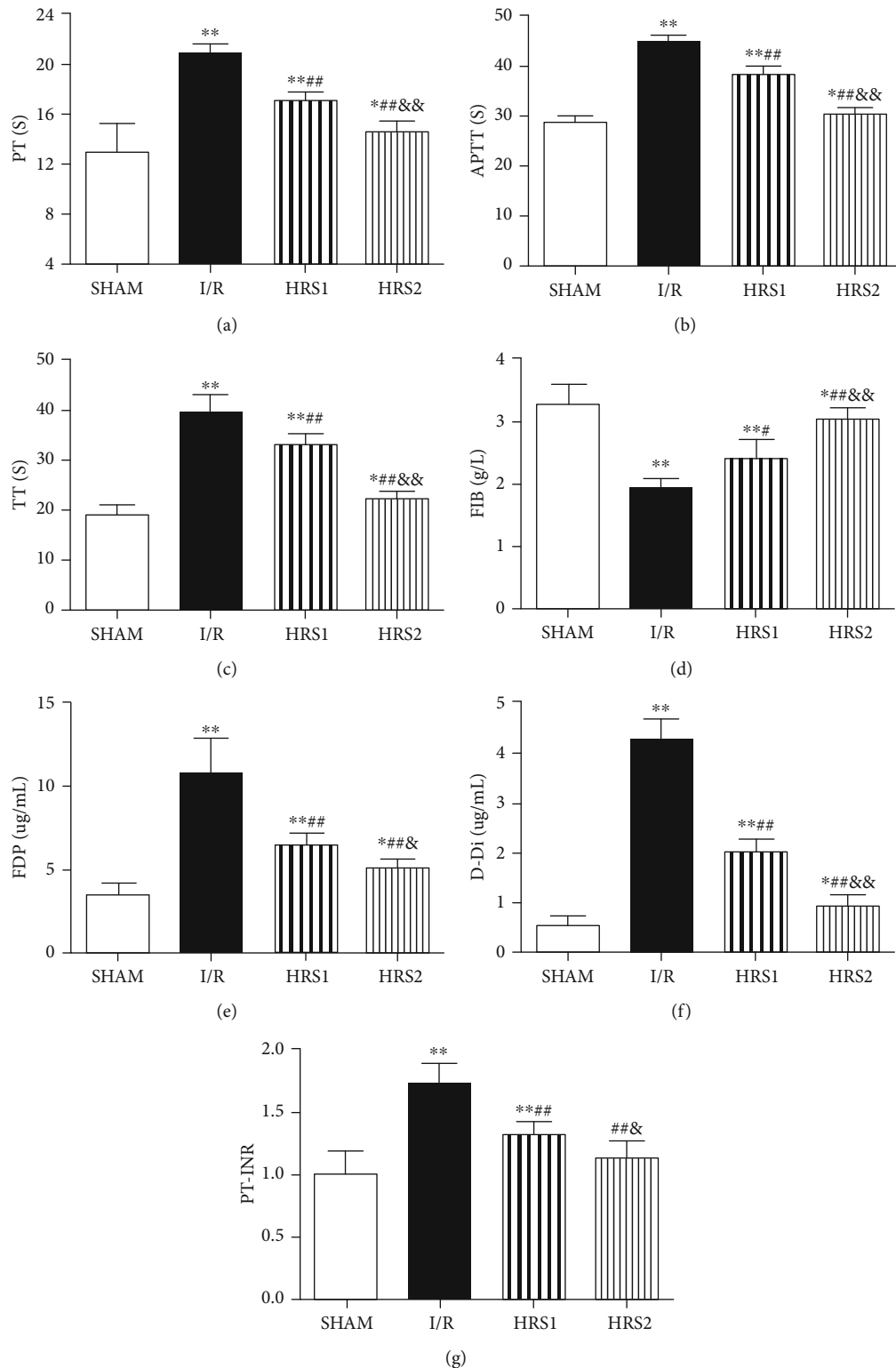


FIGURE 4: HRS improved coagulation disorders. (a) Prothrombin time (PT), (b) activated partial thrombin time (APTT), (c) thrombin time (TT), (d) fibrinogen (FIB), (e) fibrinogen degradation product (FDP), (f) d-dimer (D-Di), (g) prothrombin time-international standardization ratio (PT-INR). The data were represented as mean \pm SD ($n = 8/\text{group}$). * $P < 0.05$, ** $P < 0.01$ vs. SHAM group; # $P < 0.05$, ## $P < 0.01$ vs. I/R group; & $P < 0.05$, && $P < 0.01$ vs. HRS1 group.

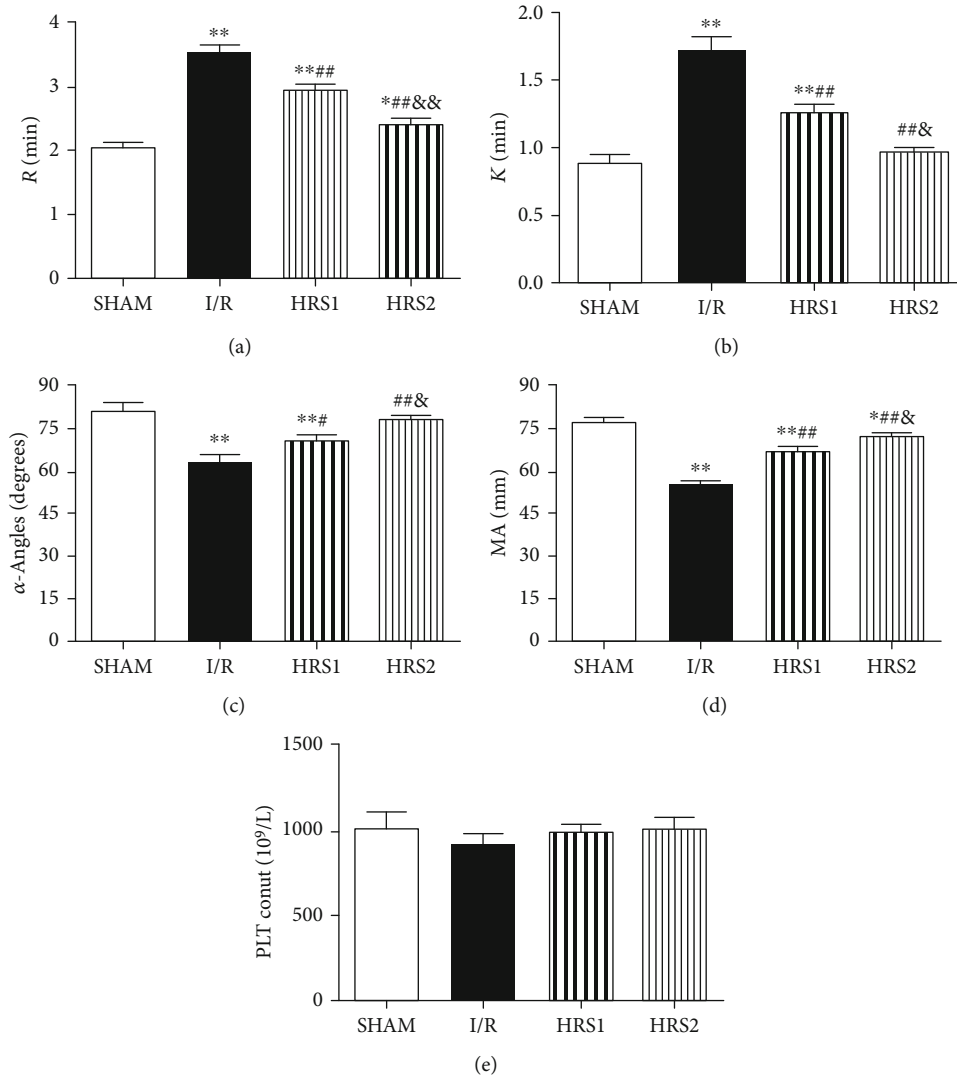


FIGURE 5: Effects of HRS on thromboelastography (TEG) and platelet count. (a–e) were R, K, α -Angles, MA, and PLT count, respectively. The data were represented as mean \pm SD ($n = 8/\text{group}$). * $P < 0.05$, ** $P < 0.01$ vs. SHAM group; # $P < 0.05$, ## $P < 0.01$ vs. I/R group; & $P < 0.05$, && $P < 0.01$ vs. HRS1 group.

the improved morphological changes and survival rate. Interestingly, an important finding was that HRS might significantly improve intestinal I/R-mediated coagulation disorders and inflammation, at least in part, by inhibition of activated NF- κ B/NLRP3 pathway.

Intestinal I/R injury may cause not only damage to organs and tissues, but also coagulation disorders. The coagulation function of it is regulated by the coagulation, anticoagulation, and fibrinolytic systems, which would affect each other and maintain a dynamic balance under physiological conditions [24]. If any of the three is abnormal and the balance is broken, bleeding or thrombosis may occur. PT and APTT reflect the activity of coagulation factors in the exogenous and endogenous coagulation pathways, respectively. If the coagulation factors are consumed, they may be significantly prolonged. FIB and TT are related to the final stage of coagulation, that is, fibrinogen becomes fibrin. FDP is a degradation product of fibrin or fibrinogen; D-dimer is an important landmark substance for forming thrombus

and dissolving fibrin. It can act as a marker for early diagnosis of acute mesenteric ischemia [25]. PT-INR is mainly used to evaluate the anticoagulant level of anticoagulant drugs (e.g., Warfarin). If it exceeds the upper limit, there is a risk of bleeding, and if it is lower than the lower limit, the anticoagulation may be insufficient [26]. The principle of thromboelastography is to detect and quantify dynamic changes of the viscoelastic properties of a blood sample during clotting under low shear stress [23]. During the interaction between inflammation and coagulation, inflammatory mediators may facilitate thrombus formation through at least three pathways at the same time, including up-regulation of procoagulant pathways, down-regulation of physiological anticoagulant mechanisms (antithrombin, protein C system, and tissue factor pathway inhibitor), and inhibition of fibrinolysis [8, 9].

The present study confirmed that after intestinal I/R injury, PT, APTT, and TT were prolonged and FDP and D-Di levels could be increased; besides, PT-INR was

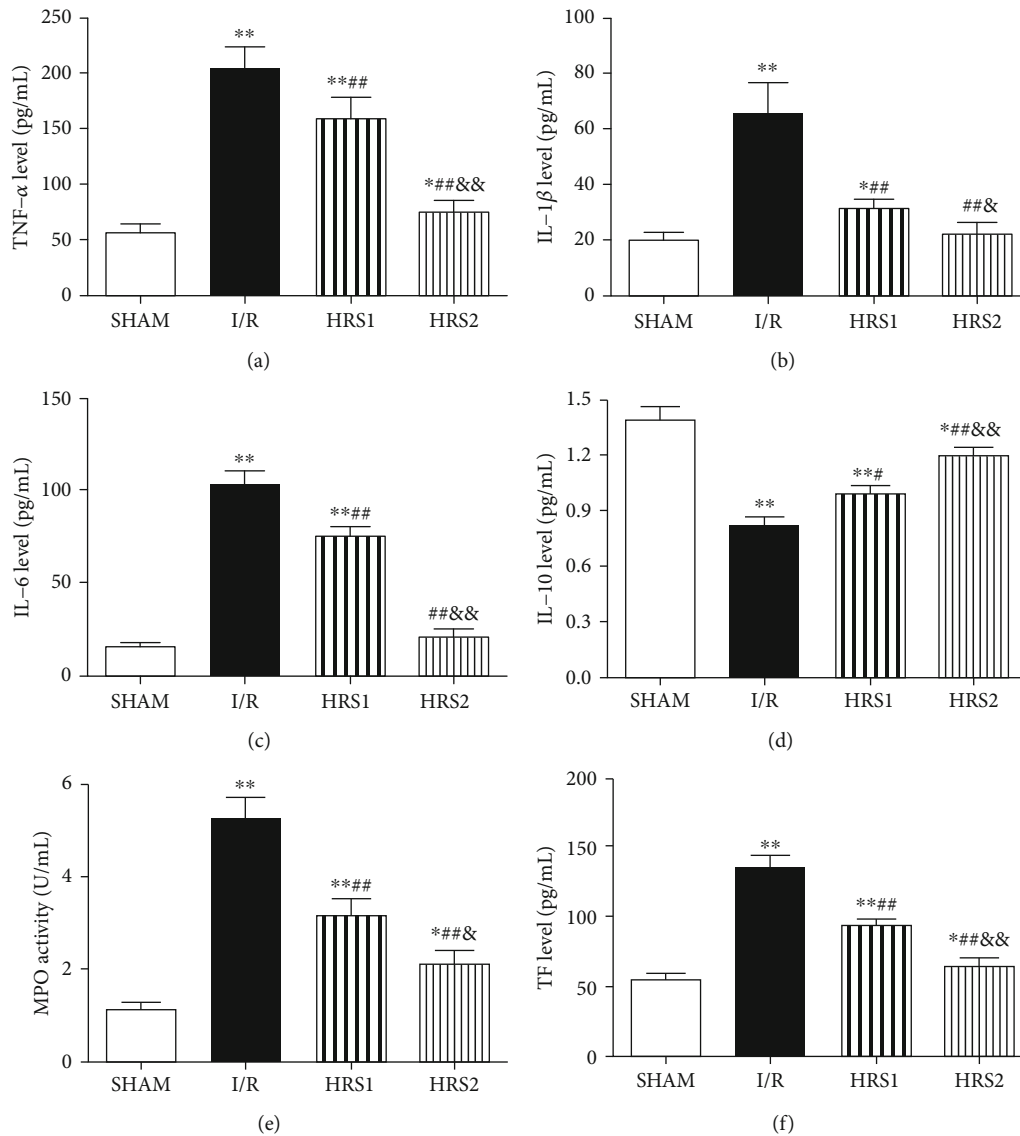


FIGURE 6: HRS reduced inflammatory stress and TF level. (a–f) were TNF- α , IL-1 β , IL-6, IL-10, MPO, and TF levels, respectively. The data were represented as mean \pm SD ($n = 8$ /group). * $P < 0.05$, ** $P < 0.01$ vs. SHAM group; # $P < 0.05$, ## $P < 0.01$ vs. I/R group; & $P < 0.05$, && $P < 0.01$ vs. HRS1 group.

elevated and FIB level was decreased. R and K values were additionally increased according to thromboelastography, while the α -angle and MA values were decreased. The above-mentioned findings suggested that the coagulation disorders occurred. The results were consistent with previous studies [10, 11]. Additionally, after intestinal I/R injury, the levels of TNF- α , IL-1 β , IL-6, and MPO in blood were noticeably increased, while the level of IL-10 was decreased dramatically.

TNF- α and IL-6 are classic proinflammatory factors in the inflammatory phase. MPO, as an inflammatory biomarker, can reflect leukocyte infiltration. The monocyte-macrophage system may synthesize and release TNF- α . When TF expression is up-regulated, it can activate proteinase-activated receptor 1 (PAR-1) on the surface of monocytes. TNF- α may activate the cytokine cascade and induce monocytes to express TF, thereby forming a vicious

cycle of inflammatory cascade and activation of the coagulation system [27]. Under stimulation of inflammatory factors, the expression of TF is significantly increased in endothelial cells and monocytes, activating the coagulation system through the exogenous coagulation pathway [28, 29]. Under mediation of calcium ions, activated coagulation factor FX and activated coagulation factor FV can form a complex and may generate a small amount of thrombin and simultaneously activate endogenous coagulation pathway, which can mediate the coagulation cascade and coagulation dysfunction [26]. In the activation of inflammatory response, TF assumes the task of connecting inflammation and coagulation. Inflammatory factors, such as TNF- α , IL-1 β , and IL-6, can stimulate monocytes to up-regulate TF express. A recent report has shown that TF is regarded to be the primary initiator of coagulation in severe infection. Local activation of coagulation can be prevented by inhibiting TF level in

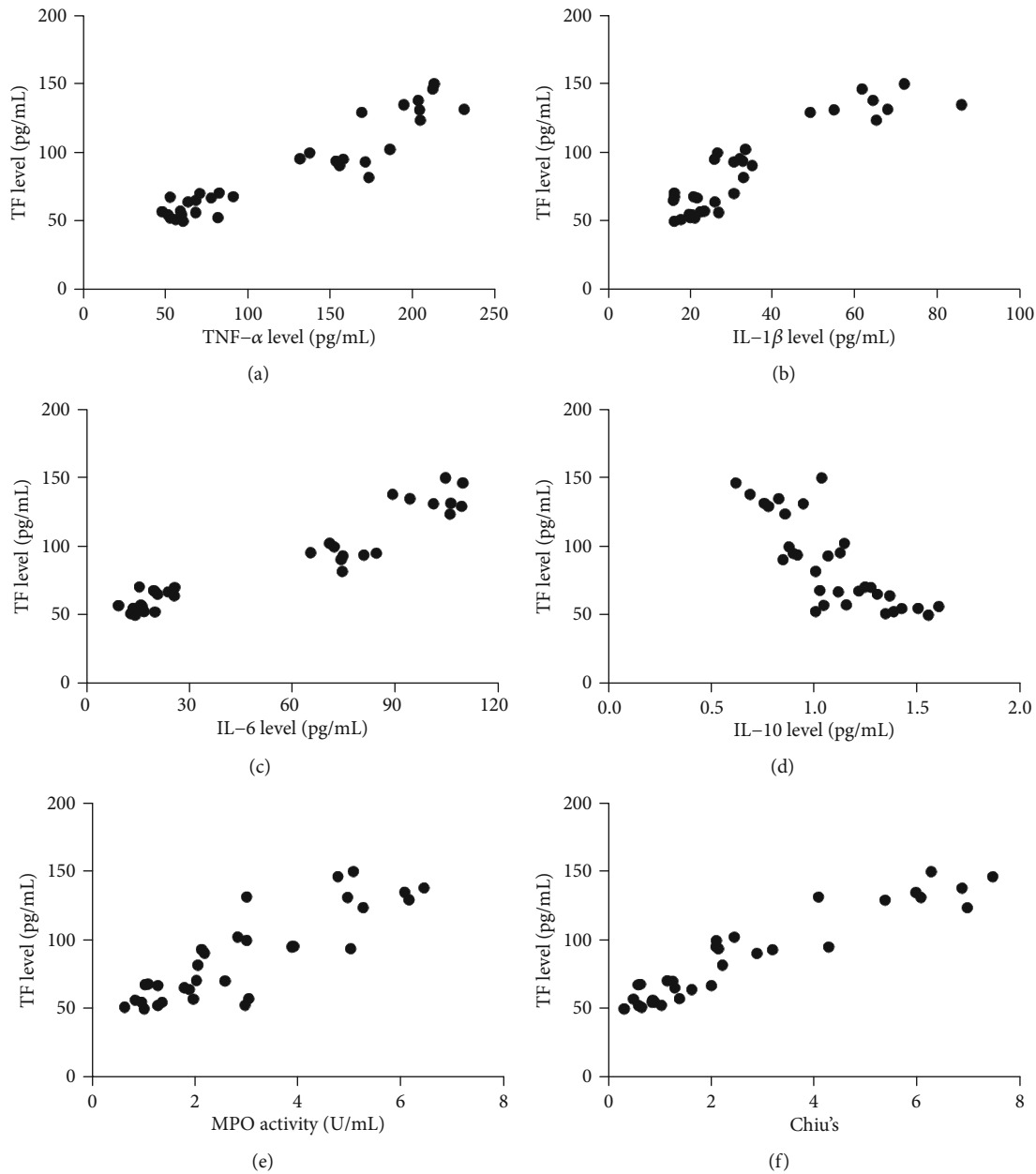


FIGURE 7: Correlation analysis. Correlations ($N = 32$) between TF level and TNF- α level (a), TF level and IL-1 β level (b), TF level and IL-6 level (c), TF level and IL-10 level (d), TF level and MPO activity (e), TF level and Chiu's score (f).

models of sepsis [30]. Interestingly, in our study, TF level was positively correlated with Chiu's score, which indicated that TF level could also be elevated by intestinal I/R. Previous study showed that the mentioned process was closely associated with the expression of TF in peripheral blood mononuclear cells [27, 29, 30]. TF level was also positively correlated with TNF- α , IL-1 β , IL-6, and MPO levels and was negatively correlated with IL-10, indicating that the TF level was closely associated with the inflammatory factors, which may cause coagulation disorders.

NF- κ B is one of the key pathways connecting inflammation and immunity, especially the modulation of proinflammatory factors [31]. Under pathological conditions, such as inflammation, hypoxia, and infection, NF- κ B will

break away from the binding of its inhibitory protein and enter the nucleus, resulting in a series of effects, such as participating in transcription of the TF gene [28]. Activation of the NF- κ B pathway can be mediated by toll-like receptors (TLRs), interleukin 1 receptor (IL-1R), tumor necrosis factor receptor (TNFR), and antigen receptors. Typical stimulating signal molecules are TNF- α , IL-6, IL-1 β , lipopolysaccharide (LPS), and bacterial cell wall [32]. In the rat model of intestinal I/R injury, the expression levels of p-NF- κ B p65, NLRP3, Caspase-1, and inflammatory factors were increased. It is hinted that NF- κ B/NLRP3 pathway might be involved in intestinal I/R injury. The NLRP3 inflammasome was also shown to mediate hepatic injury induced by intestinal I/R [4]. Therefore, it can be concluded

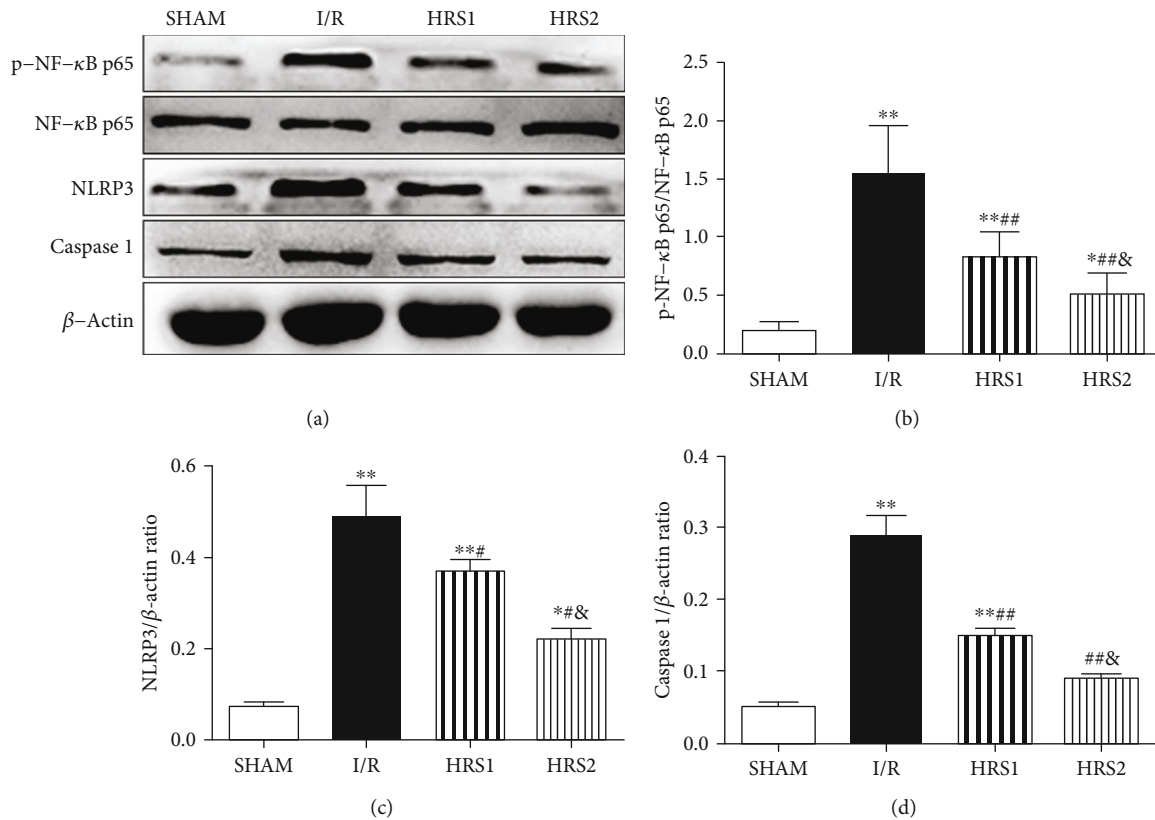


FIGURE 8: HRS inhibited NF- κ B and NLRP3 inflammasome activation. Western blot was used to detect the expression levels of phospho-NF- κ B p65, NF- κ B p65, NLRP3, and Caspase 1 proteins in PBMCs (a-d). The data were represented as mean \pm SD ($n = 8$ /group). * $P < 0.05$, ** $P < 0.01$ vs. SHAM group; # $P < 0.05$, ## $P < 0.01$ vs. I/R group; & $P < 0.05$ vs. HRS1 group.

that NF- κ B and NLRP3 inflammasome may be a therapeutic target for disease management [33, 34]. If it could inhibit the activation of the NF- κ B/NLRP3 pathway, it could not only attenuate the inflammatory response and protect the intestine but also inhibit the TF level and weaken coagulation disorders.

Molecular hydrogen was previously taken as an inert gas into account, while a research reported that it has antioxidant, anti-inflammatory, and antiapoptotic properties, with organ protection for a variety of acute and chronic diseases [12, 13]. In an animal model of intestinal I/R injury, H₂ can simultaneously reduce local intestinal damage and distant organs damage [12, 18, 19]. In addition, H₂ can inhibit the activation of NF- κ B and NLRP3 pathways, which has a certain therapeutic effect on other diseases. The present experiment revealed that Chiu's score after HRS treatment was reduced, and the coagulation function was improved. The PT, APTT, TT, FDP, D-Di, and PT-INR were significantly lower than those in the intestinal I/R group. FIB level, α -angle, and MA values were increased, while R and K values were decreased. Additionally, HRS significantly reversed the above-mentioned trend of inflammatory factors induced by intestinal I/R.

Platelets are often activated by trauma, infection, etc. and participate in anti-infection, hemostasis, and repair processes. The main mechanisms of thrombocytopenia in septic rats include bone marrow suppression and neonatal thrombocytopenia, immune-mediated platelet destruction,

and platelet depletion [35]. However, in the rat model of intestinal I/R injury, there were no statistically significant differences in platelet count among all groups, which was consistent with a previous study [36]. We speculated that the cause might be (at least in part) inflammatory exudation after intestinal I/R, which leads to blood concentration, abnormal distribution of platelets in the body, platelet aggregation, and increased attachment. A recent study demonstrated that hydrogen can inhibit platelet activation and reduce thrombus formation in a thrombosis model [37]. Coagulation disorders can be associated with several factors, including coagulation factors and platelets. In the present study, when platelet count was close to normal level, coagulation dysfunction occurred in rats, suggesting that multiple factors might be involved in coagulation dysfunction during intestinal I/R injury. Hydrogen improved coagulation dysfunction, which might be related to inhibiting inflammatory response. However, the degree of platelet activation during intestinal I/R injury, the level of consumption, and changes in its function still require to be further studied.

There could be some limitations in the current study. Firstly, regarding therapeutic effects of HRS in improving intestinal I/R-induced coagulation disorders, only the inflammatory response was observed. Therefore, further investigation is needed to explore the other functions of HRS as well as its role in other inflammatory conditions. Secondly, this study focused on the short-term effect of HRS on intestinal I/R-induced coagulation disorders and

poor survival, while the long-term impact of HRS is yet to explore. The survival rate might be changed in prolonged time in the I/R and HRS treatment groups, and the optimal therapeutic windows of HRS for improving coagulation disorders and survival rate are required further exploration. Finally, two different dosages of HRS were determined based on previous studies [17, 38], without exploring possible effects of HRS at additional dosage on coagulation disorders induced by intestinal I/R injury. The optimal dosage of HRS needs further investigation in future studies.

5. Conclusion

In summary, the present study confirmed that intestinal I/R could cause coagulation disorders and the activation of NF- κ B and NLRP3 inflammasome in rats. Interestingly, HRS could strikingly improve intestinal I/R-induced intestinal injury and poor survival, which might be partially related to ameliorating coagulation disorders and inflammation via inactivation of NF- κ B/NLRP3 Pathway. That is an important finding, indicating that HRS might have clinical potentials for critically ill patients associated with intestinal I/R to improve coagulation disorders and mortality.

Data Availability

The data used to support the findings of this study are included within the article.

Conflicts of Interest

The authors declare that they have no conflicts of interest.

Authors' Contributions

Ling Yang and Yan Guo contributed equally to this work. Jun Zhou and Ke-Xuan Liu conceived and designed the experiments. Ling Yang, Yan Guo, and Xin Fan performed the experiments. Ye Chen analyzed the data and Bo Yang wrote the manuscript. All authors read and approved the manuscript.

Acknowledgments

This study was supported by grants from the National Natural Science Foundation of China (Nos. 81873930 and 81301055) and partly by a project of Science and Technology Department of Sichuan Province (No. 20YYJC2019). We would like to thank Dr. Jian-Guo Feng and Dr. Jing Jia for their excellent technical supports.

References

- [1] I. H. Mallick, W. Yang, M. C. Winslet, and A. M. Seifalian, "Ischemia-reperfusion injury of the intestine and protective strategies against injury," *Digestive diseases and sciences*, vol. 49, no. 9, pp. 1359–1377, 2004.
- [2] J. Grootjans, K. Lenaerts, W. A. Buurman, C. H. C. Dejong, and J. P. M. Derikx, "Life and death at the mucosal-luminal interface: new perspectives on human intestinal ischemia-reperfusion," *World journal of gastroenterology*, vol. 22, no. 9, pp. 2760–2770, 2016.
- [3] D. Y. Zheng, M. Zhou, J. Jin et al., "Inhibition of P38 MAPK downregulates the expression of IL-1 β to protect lung from acute injury in intestinal ischemia reperfusion rats," *Mediators of inflammation*, vol. 2016, Article ID 9348037, 8 pages, 2016.
- [4] X. Fan, J. Du, M.-H. Wang et al., "Irisin contributes to the hepatoprotection of dexmedetomidine during intestinal ischemia/reperfusion," *Oxidative medicine and cellular longevity*, vol. 2019, Article ID 7857082, 15 pages, 2019.
- [5] Q. T. Meng, C. Cao, Y. Wu et al., "Ischemic post-conditioning attenuates acute lung injury induced by intestinal ischemia-reperfusion in mice: role of Nrf2," *Laboratory investigation*, vol. 96, no. 10, pp. 1087–1104, 2016.
- [6] J. Zhou, W. Q. Huang, C. Li et al., "Intestinal ischemia/reperfusion enhances microglial activation and induces cerebral injury and memory dysfunction in rats*," *Critical care medicine*, vol. 40, no. 8, pp. 2438–2448, 2012.
- [7] N. F. Cerqueira, C. A. Hussni, and W. B. Yoshida, "Pathophysiology of mesenteric ischemia/reperfusion: a review," *Acta Cirurgica Brasileira*, vol. 20, no. 4, pp. 336–343, 2005.
- [8] M. Levi, T. T. Keller, E. van Gorp, and H. ten Cate, "Infection and inflammation and the coagulation system," *Cardiovascular research*, vol. 60, no. 1, pp. 26–39, 2003.
- [9] M. Levi and T. van der Poll, "Inflammation and coagulation," *Critical care medicine*, vol. 38, 2 Suppl, pp. S26–S34, 2010.
- [10] I. G. Schoots, M. Levi, A. K. van Vliet, A. M. Maas, E. H. P. Roossink, and T. M. van Gulik, "Inhibition of coagulation and inflammation by activated protein C or antithrombin reduces intestinal ischemia/reperfusion injury in rats," *Critical care medicine*, vol. 32, no. 6, pp. 1375–1383, 2004.
- [11] I. G. Schoots, M. Levi, E. H. P. Roossink, P. B. Bijlsma, and T. M. van Gulik, "Local intravascular coagulation and fibrin deposition on intestinal ischemia-reperfusion in rats," *Surgery*, vol. 133, no. 4, pp. 411–419, 2003.
- [12] M. Shen, H. Zhang, C. Yu, F. Wang, and X. Sun, "A review of experimental studies of hydrogen as a new therapeutic agent in emergency and critical care medicine," *Medical gas research*, vol. 4, no. 1, p. 17, 2014.
- [13] L. Qian, Z. Wu, J. Cen, S. Pasca, and C. Tomuleasa, "Medical application of hydrogen in hematological diseases," *Oxidative medicine and cellular longevity*, vol. 2019, Article ID 3917393, 6 pages, 2019.
- [14] I. Ohsawa, M. Ishikawa, K. Takahashi et al., "Hydrogen acts as a therapeutic antioxidant by selectively reducing cytotoxic oxygen radicals," *Nature medicine*, vol. 13, no. 6, pp. 688–694, 2007.
- [15] B. Tao, L. Liu, N. Wang, D. Tong, W. Wang, and J. Zhang, "Hydrogen-rich saline attenuates lipopolysaccharide-induced heart dysfunction by restoring fatty acid oxidation in rats by mitigating c-Jun N-terminal kinase activation," *Shock*, vol. 44, no. 6, pp. 593–600, 2015.
- [16] J. Zhou, Y. Chen, G. Q. Huang et al., "Hydrogen-rich saline reverses oxidative stress, cognitive impairment, and mortality in rats submitted to sepsis by cecal ligation and puncture," *The Journal of surgical research*, vol. 178, no. 1, pp. 390–400, 2012.
- [17] R. Zou, M. H. Wang, Y. Chen et al., "Hydrogen-rich saline attenuates acute lung injury induced by limb ischemia/reperfusion via down-regulating chemerin and NLRP3 in rats," *Shock*, vol. 52, no. 1, pp. 134–141, 2019.

- [18] T. Shigeta, S. Sakamoto, X. K. Li et al., "Luminal injection of hydrogen-rich solution attenuates intestinal ischemia-reperfusion injury in rats," *Transplantation*, vol. 99, no. 3, pp. 500–507, 2015.
- [19] X. Zheng, X. Zheng, Y. Mao et al., "Hydrogen-rich saline protects against intestinal ischemia/reperfusion injury in rats," *Free radical research*, vol. 43, no. 5, pp. 478–484, 2009.
- [20] Y. Lu, C. F. Li, N. N. Ping et al., "Hydrogen-rich water alleviates cyclosporine A-induced nephrotoxicity via the Keap1/Nrf2 signaling pathway," *Journal of biochemical and molecular toxicology*, vol. 34, no. 5, 2020.
- [21] J. Du, X. Fan, B. Yang, Y. Chen, K. X. Liu, and J. Zhou, "Irisin pretreatment ameliorates intestinal ischemia/reperfusion injury in mice through activation of the Nrf2 pathway," *International immunopharmacology*, vol. 73, pp. 225–235, 2019.
- [22] B. Yang, Y. Chen, Y. H. Long et al., "Intestinal and limb ischemic preconditioning provides a combined protective effect in the late phase, but not in the early phase, against intestinal injury induced by intestinal ischemia-reperfusion in rats," *Shock*, vol. 49, no. 5, pp. 596–603, 2018.
- [23] F. J. Castellino, D. L. Donahue, R. M. Navari, V. A. Ploplis, and M. Walsh, "An accompanying genetic severe deficiency of tissue factor protects mice with a protein C deficiency from lethal endotoxemia," *Blood*, vol. 117, no. 1, pp. 283–289, 2011.
- [24] M. Levi and T. van der Poll, "Coagulation and sepsis," *Thrombosis research*, vol. 149, pp. 38–44, 2017.
- [25] H. Altinyollar, M. Boyabatli, and U. Berberoğlu, "D-dimer as a marker for early diagnosis of acute mesenteric ischemia," *Thrombosis research*, vol. 117, no. 4, pp. 463–467, 2006.
- [26] S. Palta, R. Saroa, and A. Palta, "Overview of the coagulation system," *Indian journal of anaesthesia*, vol. 58, no. 5, pp. 515–523, 2014.
- [27] B. Østerud, "Tissue factor expression in blood cells," *Thrombosis research*, vol. 125, pp. S31–S34, 2010.
- [28] M. Mussbacher, M. Salzmann, C. Brostjan et al., "Cell type-specific roles of NF- κ B linking inflammation and thrombosis," *Frontiers in immunology*, vol. 10, 2019.
- [29] H. Zelaya, A. S. Rothmeier, and W. Ruf, "Tissue factor at the crossroad of coagulation and cell signaling," *Journal of thrombosis and haemostasis*, vol. 16, no. 10, pp. 1941–1952, 2018.
- [30] T. van der Poll, "Tissue factor as an initiator of coagulation and inflammation in the lung," *Critical Care*, vol. 12, Suppl 6, p. S3, 2008.
- [31] K. Taniguchi and M. Karin, "NF- κ B, inflammation, immunity and cancer: coming of age," *Nature reviews Immunology*, vol. 18, no. 5, pp. 309–324, 2018.
- [32] K. Iwai, H. Fujita, and Y. Sasaki, "Linear ubiquitin chains: NF- κ B signalling, cell death and beyond," *Nature reviews Molecular cell biology*, vol. 15, no. 8, pp. 503–508, 2014.
- [33] R. He, Y. Li, C. Han, R. Lin, W. Qian, and X. Hou, "L-Fucose ameliorates DSS-induced acute colitis via inhibiting macrophage M1 polarization and inhibiting NLRP3 inflammasome and NF- κ B activation," *International immunopharmacology*, vol. 73, pp. 379–388, 2019.
- [34] W. Zhao, X. Huang, X. Han et al., "Resveratrol suppresses gut-derived NLRP3 inflammasome partly through stabilizing mast cells in a rat model," *Mediators of inflammation*, vol. 2018, Article ID 6158671, 10 pages, 2018.
- [35] A. Dewitte, S. Lepreux, J. Villeneuve et al., "Blood platelets and sepsis pathophysiology: a new therapeutic prospect in critical ill patients," *Annals of intensive care*, vol. 7, no. 1, p. 115, 2017.
- [36] K. Arakawa, I. Takeyoshi, M. Muraoka, K. Matsumoto, and Y. Morishita, "Measuring platelet aggregation to estimate small intestinal ischemia-reperfusion injury," *Journal of Surgical Research*, vol. 122, no. 2, pp. 195–200, 2004.
- [37] Y. Wang, Y. P. Wu, J. J. Han et al., "Inhibitory effects of hydrogen on in vitro platelet activation and in vivo prevention of thrombosis formation," *Life sciences*, vol. 233, p. 116700, 2019.
- [38] J. He, S. Xiong, J. Zhang et al., "Protective effects of hydrogen-rich saline on ulcerative colitis rat model," *Journal of Surgical Research*, vol. 185, no. 1, pp. 174–181, 2013.

Research Article

Intravenous Arginine Administration Downregulates NLRP3 Inflammasome Activity and Attenuates Acute Kidney Injury in Mice with Polymicrobial Sepsis

Sharon Angela Tanuseputero,¹ Ming-Tsan Lin,² Sung-Ling Yeh ² and Chiu-Li Yeh ^{1,3,4}

¹School of Nutrition and Health Sciences, College of Nutrition, Taipei Medical University, Taipei, Taiwan

²Department of Surgery, National Taiwan University Hospital and College of Medicine, National Taiwan University, Taipei, Taiwan

³Nutrition Research Center, Taipei Medical University Hospital, Taipei, Taiwan

⁴Research Center of Geriatric Nutrition, College of Nutrition, Taipei Medical University, Taipei, Taiwan

Correspondence should be addressed to Chiu-Li Yeh; clyeh@tmu.edu.tw

Received 26 February 2020; Revised 29 March 2020; Accepted 20 April 2020; Published 11 May 2020

Guest Editor: Young-Su Yi

Copyright © 2020 Sharon Angela Tanuseputero et al. This is an open access article distributed under the Creative Commons Attribution License, which permits unrestricted use, distribution, and reproduction in any medium, provided the original work is properly cited.

Acute kidney injury (AKI) is a major complication of sepsis. Nucleotide-binding domain-like receptor protein 3 (NLRP3) inflammasomes are multiprotein complexes that mediate septic AKI. L-arginine (Arg) is a conditionally essential amino acid in catabolic conditions and a substrate for nitric oxide (NO) production; however, its use in sepsis is controversial. This study investigated the effect of intravenous Arg supplementation on modulating NLRP3 inflammasome activity in relation to septic AKI. Mice were divided into normal control (NC), sham, sepsis saline (SS), and sepsis Arg (SA) groups. In order to investigate the role of NO, L-N6-(1-iminoethyl)-lysine hydrochloride (L-NIL), an inducible NO synthase inhibitor, was administered to the sepsis groups. Sepsis was induced using cecal ligation and puncture (CLP). The SS and SA groups received saline or Arg via tail vein 1 h after CLP. Mice were sacrificed at 6, 12, and 24 h after sepsis. The results showed that compared to the NC group, septic mice had higher plasma kidney function parameters and lower Arg levels. Also, renal NLRP3 inflammasome protein expression and tubular injury score increased. After Arg treatment, plasma Arg and NO levels increased, kidney function improved, and expressions of renal NLRP3 inflammasome-related proteins were downregulated. Changes in plasma NO and renal NLRP3 inflammasome-related protein expression were abrogated when L-NIL was given to the Arg sepsis groups. Arg plus L-NIL administration also attenuated kidney injury after CLP. The findings suggest that intravenous Arg supplementation immediately after sepsis restores plasma Arg levels and is beneficial for attenuating septic AKI, partly via NO-mediated NLRP3 inflammasome inhibition.

1. Introduction

Sepsis is a life-threatening organ dysfunction syndrome due to dysregulated host responses to infection [1]. Among others, the kidneys are one of the first organs to be affected by sepsis since the kidneys receive 20% of the blood flow output, processing 120~150 mL of plasma each minute, and thus have high exposure to secreted proinflammatory mediators [2]. It was reported that 40%~50% of septic patients develop acute kidney injury (AKI) and thereafter have 6~8-fold higher mortality compared to those without AKI [3]. The

pathophysiology of septic AKI is complex and multifactorial. Previous studies showed that deranged immune cell activation and proinflammatory cytokine production are the main causes of AKI. Insults from both infection and cell damages trigger persistent cycle of inflammatory response, in which innate immunity plays a major role [2, 4].

Inflammatory response occurs in almost all kinds of kidney diseases. Inflammasomes are protein complexes that form within activated immune cells and tissue-resident cells that lead to a series of inflammatory reactions [5]. NLRP3 is a member of the nucleotide-binding and oligomerization

domain- (NOD-) like receptor family and was described as the inflammasome sensor [6]. After recognition of infecting microbials and cellular damage in a two-step mechanism, NLRP3 will form an activated complex with apoptosis-associated speck-like protein (ASC) and procaspase-1 which will subsequently cleave into IL-1 β [7]. NLRP3 inflammasome responses to varieties of pathogens. The activation of NLRP3 inflammasome has been proved to contribute to the inflammatory response of sepsis-induced AKI, which causes an impaired kidney morphology, increased renal tubular cell apoptosis, and NLRP3-dependent proinflammatory cytokine (i.e., IL-1 β and IL-18) production [8–10].

Arginine (Arg) is a nonessential amino acid that serves as the precursor of various metabolites and is the sole substrate of nitric oxide (NO) [11]. *De novo* synthesis of Arg is regulated by the kidneys [12]. Regarding the notion that sepsis is an Arg-deficient state [13], Arg supplementation was proposed and shown to have favorable effects in critically ill surgical patients [14, 15]. Also, Arg enhanced the immune response and protein turnover and showed beneficial effects in a porcine model of endotoxemia [16]. A study performed by our laboratory showed that intravenous Arg administration attenuated sepsis-induced lung injury [17]. Since NO is an inhibitor of caspase-1 [18], availability of NO may inhibit NLRP3 inflammasome activation and subsequent IL-1 β and IL-18 production. We hypothesized that intravenous Arg administration may downregulate renal NLRP3 expression, possibly via NO signaling, and thus attenuate septic AKI. In order to clarify the role of NO in regulating the NLRP3 inflammasome associated with AKI, a specific inducible NO synthase (iNOS) inhibitor was administered in addition to Arg in a mouse model of polymicrobial sepsis in this study.

2. Materials and Methods

2.1. Animals. Male C57BL/6J mice (5 to 6 weeks old, weighing 20~25 g) were used in the experiment. All mice were subjected to acclimatization in a temperature ($21 \pm 2^\circ\text{C}$) and humidity controlled room (50%~55%) with a 12 h light-dark cycle in the Laboratory Animal Center at Taipei Medical University (TMU), Taipei, Taiwan. During the period of study, all mice were given standard chow diet and water *ad libitum*. Care of laboratory animals was in full compliance with the Guide for the Care and Use of Laboratory Animals (National Research Council, 1996). Experimental protocols were approved by the TMU's Animal Care and Use Committee.

2.2. Study Protocol. Mice were randomly assigned to a normal control (NC) group ($n = 6$), a sham group ($n = 6$), a septic saline (SS, $n = 24$) group, and a septic Arg (SA, $n = 24$) group. Polymicrobial peritonitis sepsis was induced by cecal ligation and puncture (CLP) as described previously [17]. Mice were anesthetized, a midline incision (1~1.5 cm) was made in the abdominal wall, and the cecum was identified. The cecum was exposed, and approximately 50% of the distal end of the cecum was ligated with 3-0 silk. Using a 23-gauge needle, it was punctured twice on the cecal end, gently compressed to extrude a small amount of feces, and then replaced back in

the abdomen. The incision was closed in two layers using 2-0 silk sutures. The animals were resuscitated with subcutaneous sterile saline (40 mL/kg body weight (BW)) after the CLP operation. Mice in the sham group were subjected to the same surgical procedure except for CLP. After surgery, animals were allowed free access to food and water. All CLP manipulations were performed by the same person to ensure consistency. One hour after CLP, mice were intravenously injected with a bolus (100 μL) of saline or Arg solution (300 mg/kg BW) via a tail vein. This dosage of Arg was previously proven to have beneficial effects in resolving inflammatory responses in a catabolic condition [19]. Mice were sacrificed at 6, 12, and 24 h after CLP to investigate the dynamic inflammatory responses. Mice were anesthetized with an intraperitoneal (IP) injection of Zoletil® (Virbac, Carros, France; 25 mg/kg BW) and Rompun (Bayer, Leverkusen, Germany; 10 mg/kg BW), and blood samples were collected by cardiac puncture. Blood samples from mice were collected into tubes containing heparin and were centrifuged at $1500 \times g$ at 4°C for 15 min to collect plasma which was stored in -80°C for further analysis. The upper half of a kidney was separated for histological analysis, while the remaining part was kept at -80°C for further analysis. To investigate the role of NO, L-N (6)-iminoethyl-lysine (L-NIL) (Sigma, St. Louis, MO, USA), an inducible (i) NOS inhibitor, was administered to mice in the septic saline (SSL, $n = 15$) and septic Arg (SAL, $n = 15$) groups. L-NIL (3 mg/kg BW) was given intraperitoneally at the end of CLP and at 6 h after sepsis induction [20]. Mice in the SSL and SAL groups were sacrificed at 6, 12, and 24 h to collect blood and kidney samples. Survival rates were expressed as the number of mice which survived until the designated sacrifice time point per total amount of mice.

2.3. Analysis of Plasma Amino Acid Concentrations. Plasma samples were prepared using a Waters AccQTag derivatization kit (Manchester, UK) and subjected to ultraperformance liquid chromatography (UPLC) separation using the ACQUITY UPLC system (Waters). A multiple reaction monitoring (MRM) analysis was performed using a Xevo TQ-XS (Waters) mass spectrometer. Data were analyzed using Waters MassLynx 4.2 software and quantified using TargetLynx.

2.4. Analysis of Plasma NO Concentrations. Plasma NO was measured using a Total Nitric Oxide and Nitrate/Nitrite Assay (R&D Systems, Minneapolis, MN, USA) according to the manufacturer's instructions. Briefly, the amount of NO was calculated based on the enzymatic conversion of nitrate to nitrite by nitrate reductase, followed by the Griess reaction which produces a chromophoric compound detectable at wavelengths of 540/570 nm. The difference in measurements of nitrite and nitrate was considered the concentration of NO.

2.5. Analysis of Plasma Biomarkers for Kidney Function and Injury. Plasma creatinine (Cr) and blood urea nitrogen (BUN) were sent for laboratory analysis in the National Laboratory Animal Center, Taipei, Taiwan. Values are expressed

in mg/dL. For measurement of plasma neutrophil gelatinase-associated lipocalin (NGAL), an indicator of AKI, 40 μ L of the obtained plasma was centrifuged at 11000 \times g for 10 min at 4°C. Supernatants were measured by Quantikine® enzyme-linked immunosorbent assay (ELISA) kits (R&D Systems) according to the manufacturer's instructions, and results are expressed in μ g/mL.

2.6. Analysis of Renal Lipid Peroxidation Levels. Lipid peroxidation was analyzed based on thiobarbituric acid-reactive substance (TBARS) levels. One half of kidney tissues (0.05~0.07 g) was homogenized in 250~350 μ L of T-PER™ tissue protein extraction reagent (Thermo, Rockford, IL, USA) and centrifuged to obtain lysates. Protein lysates were supplemented with 0.22% H₂SO₄, 0.67% thiobarbituric acid, and 10% phosphotungstic acid, boiled at 95°C, extracted with 1-butanol (Sigma), and centrifuged at 700 \times g for 15 min at 4°C. The upper layer was collected and analyzed fluorometrically at 555/515 nm. Values were expressed as μ M malondialdehyde (MDA)/ μ g protein.

2.7. Renal NLRP3 Inflammasome-Related Protein Expressions. Protein expressions of NLRP3 inflammasome-related species were analyzed by Western blotting. Briefly, kidney protein extracts were separated by 8%~15% sodium dodecyl sulfate polyacrylamide gel electrophoresis (SDS-PAGE), transferred to polyvinylidene difluoride membranes, blocked, and probed with primary antibodies such as anti-NLRP3, IL-1 β , ASC (Cell Signaling Technology, Danvers, MA), and caspase-1 (Abcam, Cambridge, UK) overnight at 4°C. After incubation with the secondary antibody, proteins were visualized in a chemiluminescent solution (Merck Millipore, Burlington, MA, USA) using the BioSpectrum Imaging System (UVP, Upland, CA, USA) and quantified using Image-Pro Plus software version 4.5 (Media Cybernetics, Silver Springs, MD, USA). Densities of target proteins were normalized against β -actin.

2.8. Kidney Histology. The middle segments of kidney tissues were collected and fixed with 4% paraformaldehyde. Series of 5 μ m thick sections stained with hematoxylin and eosin (H&E) were examined to determine the morphology of the kidneys. Digital images at 200 \times magnification per section were captured. Five fields per section were analyzed for morphological lesions. Images were assessed by Image-Pro Plus software, and a scoring system based on Kuruş et al. [21] was used as follows: 0 indicates no tubular injury; 1 indicates <10% of tubules injured; 2 indicates 10%~25% of tubules injured; 3 indicates 26%~50% of tubules injured; 4 indicates 51%~75% of tubules injured; and 5 indicates >75% of tubules injured.

2.9. Statistical Analysis. Data are presented as the mean \pm standard deviation (SD). Results were analyzed using GraphPad Prism 5 software (San Diego, CA, USA). Differences between groups were assessed using a one-way analysis of variance (ANOVA) followed by Tukey's post hoc test. Values were considered statistically significant at $P < 0.05$.

3. Results

3.1. BW Change and Survival Rates. There were no differences in initial BWs before the sham or CLP operation (data not shown). No difference in survival rates was observed between the two septic groups at 24 h after CLP (66% and 72% in both the SS and SA groups).

3.2. Changes in Plasma Amino Acid Levels. Arg concentrations had significantly decreased by 6 h and sustained the levels till the 24 h time point after sepsis compared to the NC and sham groups. Other amino acids, such as glutamine and citrulline, were also depleted in the septic groups at 6 h or the all time points. After Arg administration, levels of Arg had significantly increased at all time points, while glutamine exclusively increased at 6 and 12 h compared to the saline-treated groups. Citrulline and proline concentrations had significantly increased after 12 and/or 24 h post-CLP (Figure 1).

3.3. Plasma Biomarkers of Kidney Function. NGAL had significantly increased at 24 h of sepsis compared to levels in the NC and sham groups. Levels of Cr and BUN were higher in the sepsis groups than those in the NC and sham groups at 12 and 24 h. Levels of NGAL significantly dropped by 24 h, while Cr and BUN levels had decreased at 12 and 24 h in the Arg-treated sepsis group (SA group) when compared to the corresponding SS group (Table 1).

3.4. Plasma NO Levels with or without an iNOS Inhibitor. There were no differences in NO levels among the NC, sham, and sepsis groups at 6 or 12 h after CLP. Compared to the NC group, NO production in the septic groups had increased by 24 h. Arg-treated groups had higher NO levels than the saline groups at 12 and 24 h post-CLP (Figure 2(a)). In the sepsis groups treated with L-NIL, no differences in plasma NO concentrations were observed among the NC, sham, and sepsis groups at the various time points (Figure 2(b)).

3.5. Lipid Peroxide Levels in the Kidneys. TBARS values in the sepsis groups had significantly increased at 6 and 12 h after CLP compared to the NC group. After Arg treatment, TBARS values at 6 and 12 h post-CLP were significantly lower compared to the respective saline group (Figure 3(a)). In the sepsis groups treated with L-NIL, no differences in TBARS concentrations were observed between the saline- and Arg-treated sepsis groups (Figure 3(b)).

3.6. Kidney NLRP3 Inflammasome-Associated Protein Expression in Sepsis Groups. Compared to the NC and sham groups, protein levels of caspase-1 had increased by 12 h while NLRP3, ASC, and IL-1 β had increased by both 12 and 24 h after CLP. After Arg treatment, expressions of NLRP3 and ASC were significantly reduced at 12 and 24 h, while caspase-1 and IL-1 β exhibited reduced expression at 24 h (Figure 4).

3.7. Kidney NLRP3 Inflammasome-Associated Protein Expressions in Sepsis Groups with the iNOS Inhibitor. There were no differences in NLRP3, ASC, caspase-1, and IL-1 β protein levels between the saline- and Arg-treated groups at each time point (Figure 5).

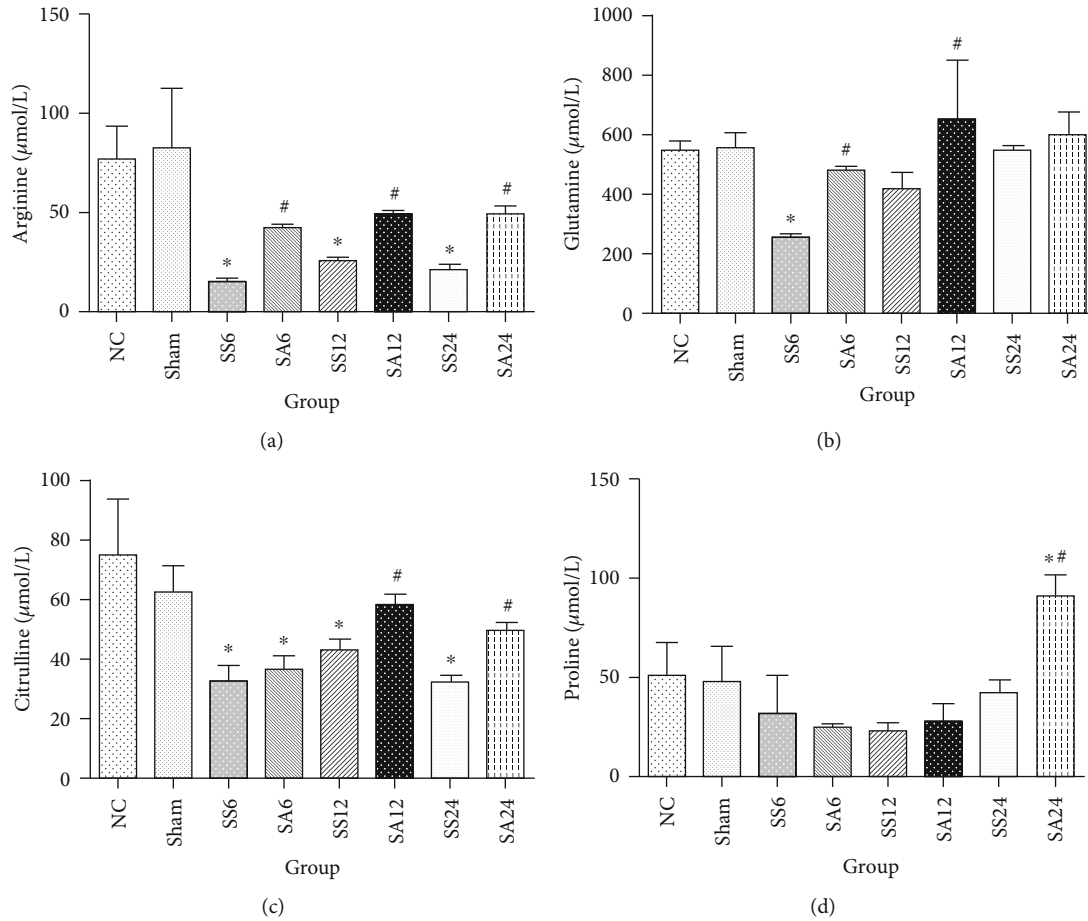


FIGURE 1: Plasma arginine, glutamine, citrulline, and proline concentrations of the normal and experimental groups. NC: normal control group; Sham: sham group; SS: sepsis group with saline injection sacrificed at 6, 12, and 24 h after cecal ligation and puncture (CLP); SA: sepsis group with arginine injection sacrificed at 6, 12, and 24 h after CLP. Results are presented as the mean \pm SD; $n = 6$ for each group. Differences between groups were analyzed with a one-way ANOVA with Tukey's post hoc test. *Significantly differs from the NC group; #significantly differs from the SS groups at the same time point ($P < 0.05$).

TABLE 1: Kidney injury marker levels and kidney function indicators.

	NGAL ($\mu\text{g/mL}$)	Creatinine (mg/dL)	BUN (mg/dL)
NC	0.11 \pm 0.01	0.17 \pm 0.02	33.90 \pm 1.31
Sham	0.47 \pm 0.36	0.20 \pm 0.04	36.60 \pm 1.51
SS6	7.92 \pm 3.29	0.17 \pm 0.05	34.03 \pm 2.19
SA6	8.07 \pm 0.93	0.13 \pm 0.02	38.38 \pm 5.85
SS12	7.59 \pm 0.97	0.67 \pm 0.07*	82.15 \pm 4.05*
SA12	14.03 \pm 4.19	0.35 \pm 0.09#	55.55 \pm 2.19#
SS24	53.51 \pm 27.78*	0.62 \pm 0.08*	115 \pm 19.46*
SA24	18.61 \pm 1.59#	0.42 \pm 0.10#	31.93 \pm 18.56#

The experimental groups consisted of NC: normal control group; Sham: sham group; SS: sepsis group with saline injection sacrificed at 6, 12, and 24 h after cecal ligation and puncture (CLP); SA: sepsis group with arginine injection sacrificed at 6, 12, and 24 h after CLP. BUN: blood urea nitrogen; NGAL: neutrophil gelatinase-associated lipocalin-2. Data were analyzed using a one-way ANOVA with Tukey's post hoc test and presented as the mean \pm SD. *Significantly differs from the NC group; #significantly differs from the SS groups at the same time point ($P < 0.05$).

3.8. *Kidney Histology of the Sepsis Groups with or without the iNOS Inhibitor.* Tubular injury was observed in the sepsis groups at 12 and 24 h, as indicated by vacuole formation and sloughing of tubular epithelial cells. In contrast, Arg-treated groups had significantly lower injury scores compared to the SS groups at 24 h (Figure 6(a)). Despite being treated with L-NIL, less tubular damage accompanied by a lower injury score was also observed in the Arg sepsis group at 24 h after CLP (Figure 6(b)).

4. Discussion

There is controversy surrounding the supplementation of Arg in the critically ill, especially in septic patients. An investigation by Bertolini et al. [22] found that mortality rates increased in the septic patients with Arg treatment. However, some clinical studies found that an infusion with Arg did not result in any adverse changes in hemodynamic parameters [23, 24]. Supplemental Arg by either an enteral or parenteral route is safe and may be beneficial to septic patients [23]. Sepsis is considered as an Arg-deficient state [13]. The drop in Arg availability in sepsis may be due to increased demand

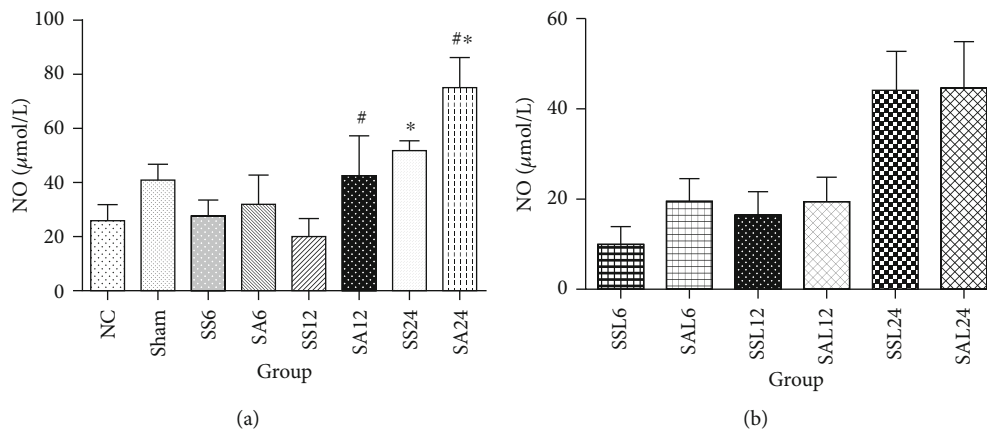


FIGURE 2: Plasma nitric oxide (NO) levels in (a) the normal and experimental groups. NC: normal control group; Sham: sham group; SS: sepsis group with saline injection sacrificed at 6, 12, and 24 h after cecal ligation and puncture (CLP); SA: sepsis group with arginine injection sacrificed at 6, 12, and 24 h after CLP. (b) Experimental groups with the inducible NO synthase (iNOS) inhibitor, L-N (6)-iminoethyl-lysine (L-NIL) administration. SSL: sepsis group with saline plus L-NIL, sacrificed at 6, 12, and 24 h after CLP; SAL: sepsis group with Arg plus L-NIL, sacrificed at 6, 12, and 24 h after CLP. Results are presented as the mean \pm SD; $n = 6$ for each group. Differences between groups were analyzed using a one-way ANOVA with Tukey's post hoc test. *Significantly differs from the NC group; #significantly differs from the SS groups at the same time point in (a).

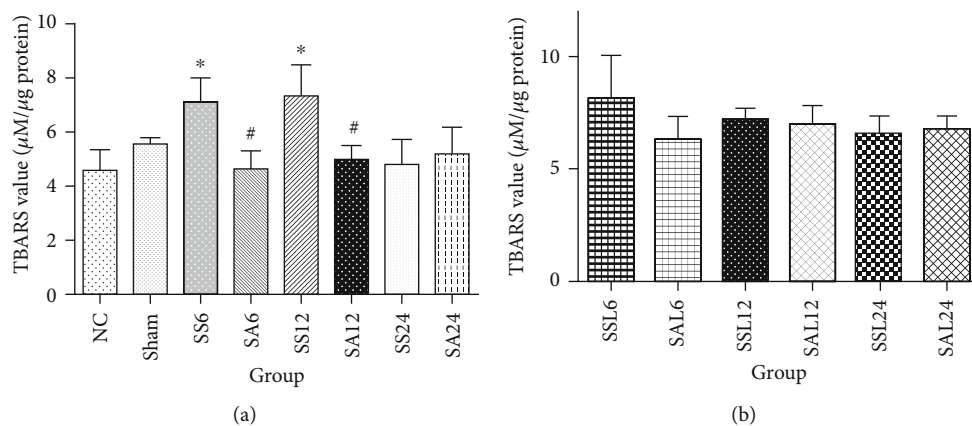


FIGURE 3: Renal thiobarbituric acid-reactive substance (TBARS) values in (a) the normal and experimental groups. NC: normal control group; Sham: sham group; SS: sepsis group with saline injection sacrificed at 6, 12, and 24 h after cecal ligation and puncture (CLP); SA: sepsis group with arginine injection sacrificed at 6, 12, and 24 h after CLP. (b) Experimental groups with the nitric oxide synthase (iNOS) inhibitor, L-N (6)-iminoethyl-lysine (L-NIL) administration. SSL: sepsis group with saline plus L-NIL, sacrificed at 6, 12, and 24 h after CLP; SAL: sepsis group with Arg plus L-NIL, sacrificed at 6, 12, and 24 h after CLP. Results are presented as the mean \pm SD; $n = 6$ for each group. Differences among groups were analyzed using a one-way ANOVA with Tukey's post hoc test. *Significantly differs from the NC group; #significantly differs from the SS groups at the same time point ($P < 0.05$) in (a).

of amino acid for protein synthesis [12] or the activation of myeloid-derived suppressor cells which may enhance the arginase activity [25]. In a rodent model of sepsis, arterial levels of Arg were reduced as early as 90 min after the onset of LPS induction [26]. Therefore, in this study, Arg was injected immediately after CLP induction to account for the expected decrease in plasma Arg. Findings from the current study showed that Arg administration enhanced NO production and downregulated NLRP3 inflammasome-related protein expression that may consequently result in attenuating septic AKI.

The finding of this study showed that NO levels after sepsis induction did not significantly increase until 24 h, while Arg-treated groups showed significantly higher NO levels

since 12 h onwards. Poeze et al. [27] observed that in the porcine endotoxemia model, plasma NO levels increased significantly in the LPS-infused animals pretreated with Arg, while there was no difference in NO of the untreated animals. This phenomenon may be due to the compartmentalization of NO, where some organs could be deprived of NO even when the plasma levels are not changed [28]. Moreover, sepsis also induces the activation of arginase. The competition between arginase and NOS for using Arg as a substrate may delay the elevation of plasma NO that may explain the late response of increased NO in the saline sepsis group. iNOS has been known to contribute to excessive, long-lasting production of NO which is possibly responsible for hypotension and shock [28]. Excessive iNO production is considered as a

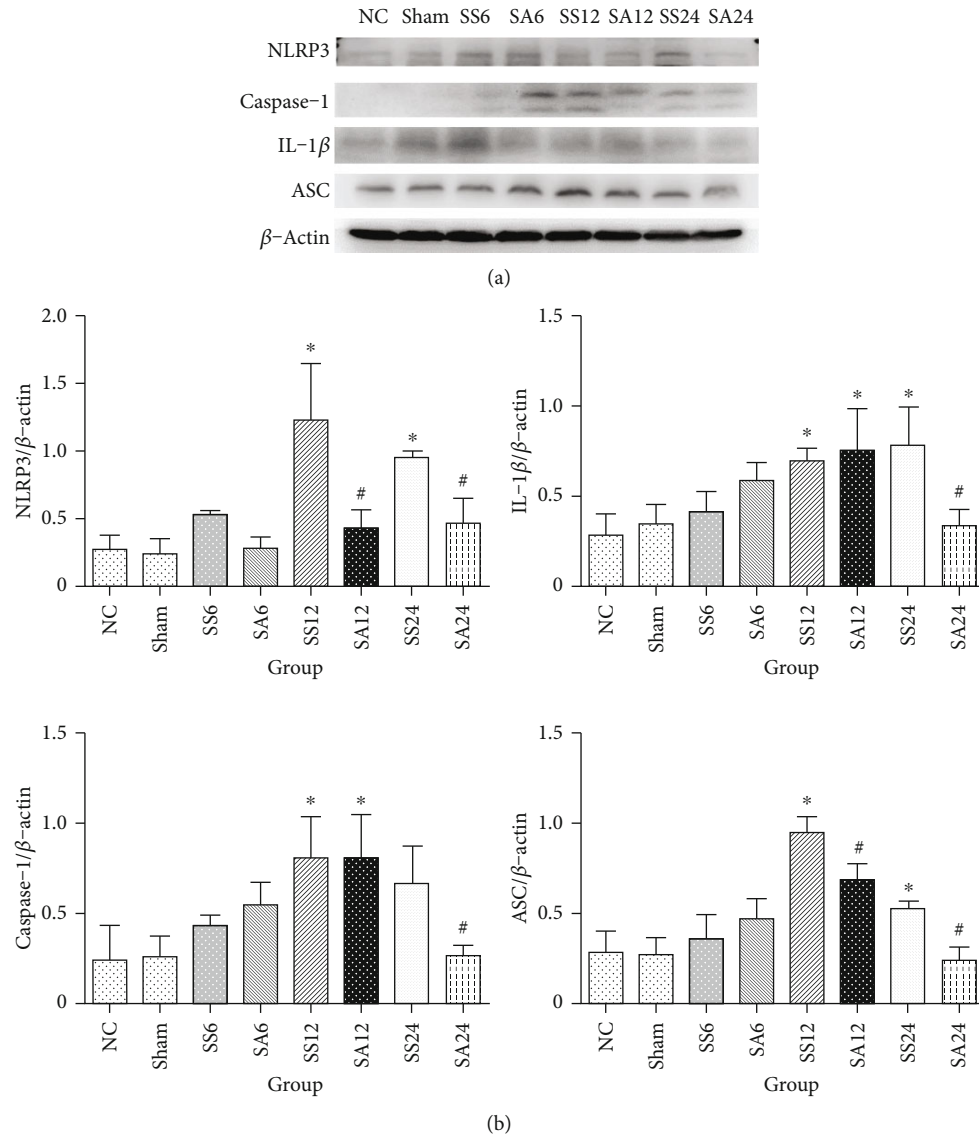


FIGURE 4: Protein levels of the nucleotide-binding domain-like receptor protein 3 (NLRP3) inflammasome complex in renal tissues. (a) Protein expressions of NLRP3, apoptosis-associated speck-like protein containing CARD (ASC), interleukin (IL)-1 β , and caspase-1. Whole-tissue lysates were analyzed by immunoblotting, and β -actin was used as a loading control. (b) Densitometric analysis of blots corrected by the protein loading control. NC: normal control group; Sham: sham group; SS: sepsis group with saline injection sacrificed at 6, 12, and 24 h after cecal ligation and puncture (CLP); SA: sepsis group with arginine injection sacrificed at 6, 12, and 24 h after CLP. Results of the densitometric analysis are presented as the mean \pm SD; $n = 6$ for each group. Differences among groups were analyzed using a one-way ANOVA with Tukey's post hoc test. *Significantly differs from the NC group; #significantly differs from SS groups at the same time point ($P < 0.05$).

source of reactive nitrogen species (RNS). Paradoxically, depletion of Arg also enhances the iNOS-derived formation of O_2^- due to iNOS uncoupling reaction [29]. Increased Arg availability also inhibits the production of O_2^- [30]. A previous in vitro study showed that decreasing concentrations of Arg enhanced iNOS-induced ROS/RNS production in cardiac myocytes [31]. In this study, Arg supplementation increased the availability of Arg to be converted to NO and may consequently prevent O_2^- and peroxynitrite formation in current sepsis condition.

In respect to kidney function, NGAL reflects activated neutrophils during innate immune activation [32] and is a

more-specific marker of tubular injury compared to kidney function parameters such as Cr and BUN [33]. A previous study reported that rats with Arg-supplemented diets had lower NGAL values after a uninephrectomy and kidney stone induction [34]. Significant reductions in plasma Cr, BUN, and NGAL levels observed in the Arg sepsis group compared to the saline sepsis group are suggestive of attenuated renal injury following Arg treatment.

Previous studies showed that resident mononuclear cells, such as macrophage and dendritic cells, express all parts of the NLRP3 inflammasome (NLRP3, ASC, and procaspase-1) in kidney tissues, but the expression levels are low in

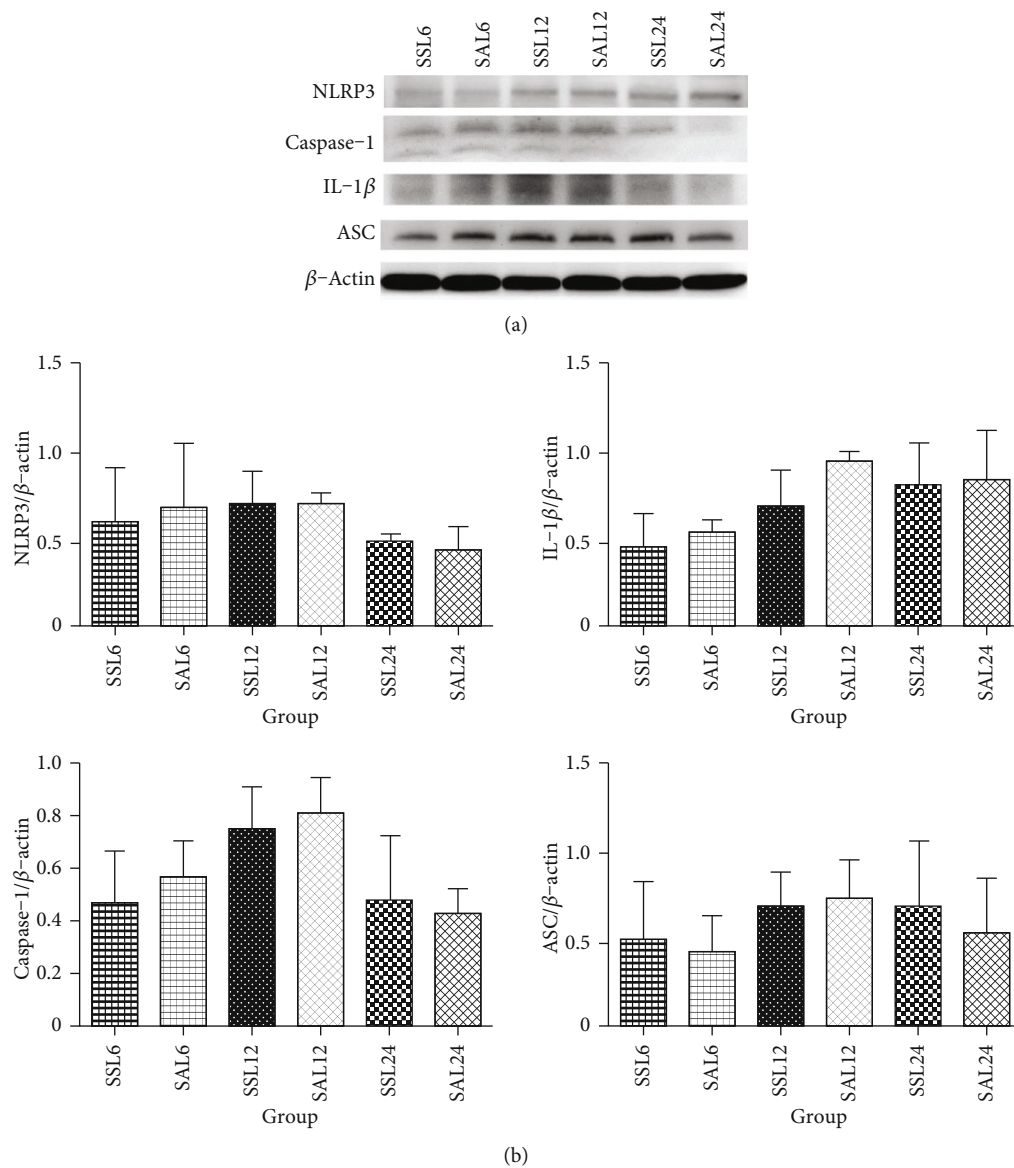
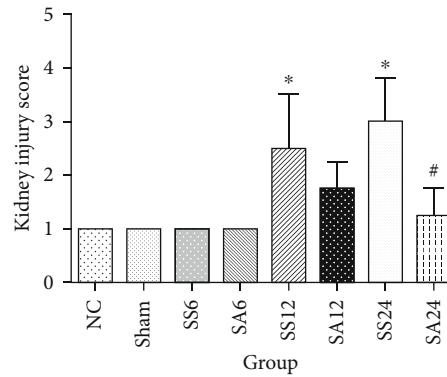
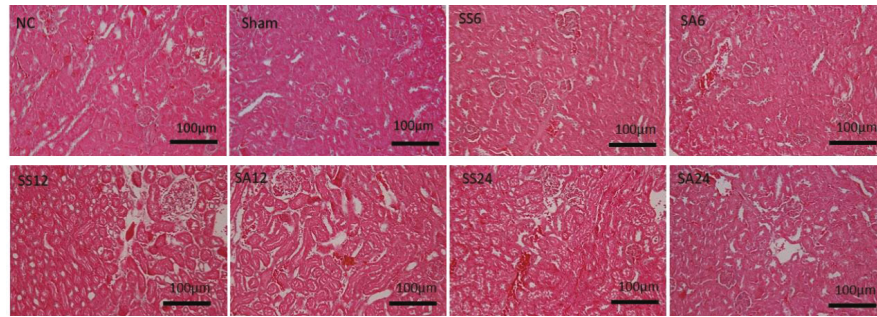


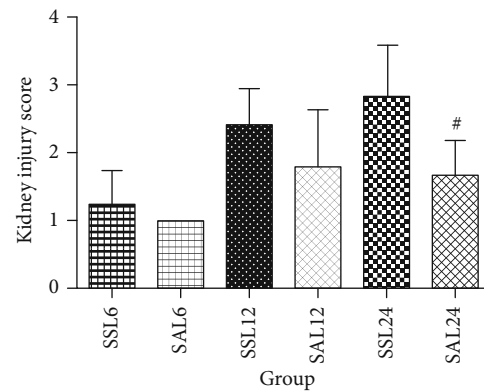
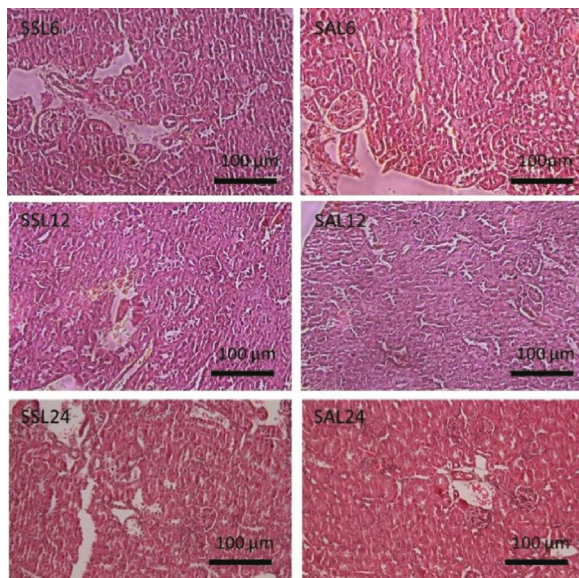
FIGURE 5: Kidney nucleotide-binding domain-like receptor protein 3 (NLRP3) inflammasome-associated protein expressions in groups treated with the nitric oxide synthase (iNOS) inhibitor, L-N (6)-iminoethyl-lysine (L-NIL). (a) Protein expressions of NLRP3, apoptosis-associated speck-like protein containing CARD (ASC), interleukin- (IL-) 1 β , and caspase-1. Whole-tissue lysates were analyzed by immunoblotting, and β -actin was used as a loading control. (b) Densitometric analysis of blots corrected by the protein loading control. SSL: sepsis group with saline plus L-NIL, sacrificed at 6, 12, and 24 h after CLP; SAL: sepsis group with Arg plus L-NIL, sacrificed at 6, 12, and 24 h after CLP. Results of the densitometric analysis are presented as the mean \pm SD; $n = 6$ for each group. Differences among group were analyzed using a one-way ANOVA with Tukey's post hoc test.

normal condition [35–37]. In the septic AKI state, NLRP3 inflammasome expressed by resident mononuclear cells and the recruited leukocytes are upregulated to secrete mature inflammatory cytokines [38]. On the other hand, renal parenchymal cells such as renal tubular epithelial cells, podocytes, glomerular endothelial cells, and mesangial cells contain significant amount of NLRP3 that expressed under inflammatory conditions [39, 40]. In this study, we evaluated the role of NO on septic AKI because NO is one of the suppressors of NLRP3. A previous study showed that NO could suppress caspase-1 in murine macrophages, resulting in decreased IL-1 β [41]. Macrophages treated with S-nitroso-

N-acetylpenicillamine, an NO donor, showed lower NLRP3 activation and IL-1 β production [42]. *In vivo*, mice treated with the NOS inhibitor, N ω -nitro-L-arginine methyl ester hydrochloride (L-NAME), showed significantly increased IL-1 β [43]. In this study, we found that the expression of NLRP3-associated proteins, including NLRP3, ASC, caspase-1, and IL-1 β , was significantly upregulated at 12 and 24 h after sepsis. Arg administration downregulated expressions of NLRP3 inflammasome-related proteins. However, the favorable effects were abrogated when Arg sepsis groups were treated with L-NIL. These findings suggest that Arg administration alleviates sepsis-induced renal NLRP3



(a)



(b)

FIGURE 6: Histology and quantification of kidney tissues. Images were assessed using Image-Pro Plus software, and representative histological images are shown at 200x magnification. Microphotographs and semiquantification of H&E staining in (a). NC: normal control group; Sham: sham group; SS: sepsis group with a saline injection sacrificed at 6, 12, and 24 h after cecal ligation and puncture (CLP); SA: sepsis group with an arginine injection sacrificed at 6, 12, and 24 h after CLP; (b) SSL: sepsis group with saline plus L-NIL, sacrificed at 6, 12, and 24 h after CLP; SAL: sepsis group with Arg plus L-NIL, sacrificed at 6, 12, and 24 h after CLP. Results are presented as the mean \pm SD; $n = 6$ for each group. Differences between groups were analyzed using a one-way ANOVA with Tukey's post hoc test. *Significantly differs from the NC group ($P < 0.05$); # significantly differs from the SS groups at the same time point ($P < 0.05$).

inflammasome activation, and NO plays an important role in suppressing NLPR3 inflammasome expression.

A characteristic hallmark of septic AKI is tubular cell vacuolization and displacement of the nucleus to the periphery of the cell [44], which could be caused by increased ROS

production in tubules with sluggish blood flow [2]. In this study, we found that sepsis-induced tubular cell damage was obvious, and the kidney injury score was elevated since 12 h after CLP. Although the iNOS inhibitor, L-NIL provided in this study, proved that the Arg/NO pathway participates in

suppressing renal lipid peroxide production and NLRP3 inflammasome activation, kidney histological improvements were independent of NO-mediated regulation.

Regardless of whether or not L-NIL was administered, Arg supplementation decreased the severity of tubular damage at the late phase of sepsis. This result indicated that the NO-mediated suppression of NLRP3 inflammasome expression might only be one of the mechanisms responsible for attenuating septic AKI. It is possible that the benefits of Arg may be mediated through other process. Firstly, restored Arg levels needed for physiological demand may help to attenuate organ injury. Arg degradation occurs via multiple pathways which produce numerous metabolites with biological importance that participate in the pathogenesis of kidney and other diseases [45]. In addition to NO and citrulline synthesis via NOS, Arg is also a substrate for ornithine production through urea cycle, which can be converted by ornithine aminotransferase into pyrroline-5-carboxylase and subsequently proline. In this study, the findings showed that septic mice administered with Arg maintained plasma glutamine levels, reversed sepsis-induced Arg decrement, and increased proline levels after sepsis. Glutamine is a specific amino acid with immunomodulatory properties. Previous studies found that glutamine improved vascular function [46], elicited a more-balanced lymphocyte regulation, and thus reduced kidney injury in septic mice [47]. Proline is an essential component of collagen [48]. The amino acid profile presented here in the Arg sepsis group may provide favorable effects in attenuating damage to kidney tissues. Secondly, Arg replacement may improve organ perfusion by restoring constitutive endothelial NOS. A previous study found that heterogeneous peritubular flow led to hypoxia in the cortical areas and increased flow in the medulla [49]. Uneven microcirculatory flow in the kidney tubules is one of the causes that drives septic AKI [2]. Arg administration may promote NO production by constitutive endothelial NOS causing improved organ perfusion. A previous study also revealed that Arg administration after CLP enhanced the mobilization of proangiogenic cells, which may play important roles in resolving vascular endothelium inflammation and ameliorating remote organ injury in a septic condition [17]. Thirdly, the effect of Arg on leukocytes during sepsis may also play roles in attenuating organ inflammatory response. A previous study carried out by Wang et al. [50] demonstrated that Arg supplementation enhanced macrophage phagocytic activity and promoted bacterial clearance in septic rats. In an *in vitro* study performed by our laboratory, we found that Arg administration with comparable or higher than physiological levels reduced cellular adhesion molecule expression, decreased neutrophil transendothelial migration, and thus attenuated inflammatory response in abdominal surgical condition [51]. However, the exact mechanism through which Arg is involved in attenuating septic AKI requires further investigation. There was a limitation in this study. Since the inflammasome immunohistochemistry staining was not performed, the effects of Arg on the exact location of the inflammatory cells in kidney tissues cannot be displayed here and therefore needed to be elucidated.

In summary, this study showed that Arg administration immediately after sepsis increased plasma Arg and NO concentrations, Arg/NO-mediated regulation decreased lipid peroxide levels and downregulated NLRP3 inflammasome-associated protein expressions. Since Arg plus L-NIL administration also attenuated kidney injury after CLP, the favorable effect of Arg resulting from NO-mediated NLRP3 inflammasome inhibition may be partly responsible for attenuating septic AKI. The findings of this study provide basic information and imply that a single dose of Arg administration may have benefits in restoring Arg levels and alleviating remote kidney injury in abdominal surgical patients at risk of postoperative infectious complications.

Data Availability

All data described in the manuscript are available from the first author upon request.

Conflicts of Interest

The authors declare that there are no competing financial or personal interests in this study.

Authors' Contributions

Chiu-Li Yeh and Sharon Angela Tanuseputero contributed to the acquisition of the data and drafted the manuscript. Ming-Tsan Lin and Sung-Ling Yeh critically helped to interpret the data and revised the manuscript. All authors agreed to be fully accountable for ensuring the integrity and accuracy of the work and read and approved the manuscript.

Acknowledgments

This study was supported by research grant MOST 107-2320-B-038-014 from the Ministry of Science and Technology (Taipei, Taiwan). We thank the technical support provided by the TMU Core Facility and Ms. Yuan-Chin Hsiung for her excellent technical support at the TMU Core Facility.

References

- [1] M. Singer, C. S. Deutschman, C. W. Seymour et al., "The third international consensus definitions for sepsis and septic shock (sepsis-3)," *The Journal of the American Medical Association*, vol. 315, no. 8, pp. 801–810, 2016.
- [2] H. Gomez, C. Ince, D. de Backer et al., "A unified theory of sepsis-induced acute kidney injury: inflammation, microcirculatory dysfunction, bioenergetics, and the tubular cell adaptation to injury," *Shock*, vol. 41, no. 1, pp. 3–11, 2014.
- [3] S. Uchino, J. A. Kellum, R. Bellomo et al., "Acute renal failure in critically ill patients: a multinational, multicenter study," *The Journal of the American Medical Association*, vol. 294, no. 7, pp. 813–818, 2005.
- [4] G. M. Gonçalves, D. S. Zamboni, and N. O. S. Câmara, "The role of innate immunity in septic acute kidney injuries," *Shock*, vol. 34, Supplement 1, pp. 22–26, 2010.

- [5] J. Fan, K. Xie, L. Wang, N. Zheng, and X. Yu, "Roles of inflammasomes in inflammatory kidney diseases," *Mediators of Inflammation*, vol. 2019, Article ID 2923072, 14 pages, 2019.
- [6] L. Vande Walle and M. Lamkanfi, "Pyroptosis," *Current Biology*, vol. 26, no. 13, pp. R568–R572, 2016.
- [7] B.-Z. Shao, Z.-Q. Xu, B.-Z. Han, D.-F. Su, and C. Liu, "NLRP3 inflammasome and its inhibitors: a review," *Frontiers in Pharmacology*, vol. 6, p. 262, 2015.
- [8] Y. Cao, D. Fei, M. Chen et al., "Role of the nucleotide-binding domain-like receptor protein 3 inflammasome in acute kidney injury," *FEBS Journal*, vol. 282, no. 19, pp. 3799–3807, 2015.
- [9] L. He, X. Peng, J. Zhu et al., "Mangiferin attenuate sepsis-induced acute kidney injury via antioxidant and anti-inflammatory effects," *American Journal of Nephrology*, vol. 40, no. 5, pp. 441–450, 2014.
- [10] P. Wang, J. Huang, Y. Li et al., "Exogenous carbon monoxide decreases sepsis-induced acute kidney injury and inhibits NLRP3 inflammasome activation in rats," *International Journal of Molecular Sciences*, vol. 16, no. 9, pp. 20595–20608, 2015.
- [11] I. E. P. Quirino, M. B. H. Carneiro, V. N. Cardoso et al., "Arginine supplementation induces arginase activity and inhibits TNF- α synthesis in mice spleen macrophages after intestinal obstruction," *Journal of Parenteral and Enteral Nutrition*, vol. 40, no. 3, pp. 417–422, 2016.
- [12] Y. C. Luiking, M. Poeze, G. Ramsay, and N. E. P. Deutz, "The role of arginine in infection and sepsis," *Journal of Parenteral and Enteral Nutrition*, vol. 29, Supplement 1, pp. S70–S74, 2005.
- [13] Y. C. Luiking, M. Poeze, C. H. Dejong, G. Ramsay, and N. E. Deutz, "Sepsis: an arginine deficiency state?," *Critical Care Medicine*, vol. 32, no. 10, pp. 2135–2145, 2004.
- [14] M. Zhou and R. G. Martindale, "Arginine in the critical care setting," *The Journal of Nutrition*, vol. 137, 6, Supplement 2, pp. 1687S–1692S, 2007.
- [15] M. D. Rosenthal, E. L. Vanzant, R. G. Martindale, and F. A. Moore, "Evolving paradigms in the nutritional support of critically ill surgical patients," *Current Problems in Surgery*, vol. 52, no. 4, pp. 147–182, 2015.
- [16] Z.-L. Dai, X.-L. Li, P.-B. Xi, J. Zhang, G. Wu, and W.-Y. Zhu, "Regulatory role for L-arginine in the utilization of amino acids by pig small-intestinal bacteria," *Amino Acids*, vol. 43, no. 1, pp. 233–244, 2012.
- [17] C. L. Yeh, M. H. Pai, Y. M. Shih, J. M. Shih, and S. L. Yeh, "Intravenous arginine administration promotes proangiogenic cells mobilization and attenuates lung injury in mice with polymicrobial sepsis," *Nutrients*, vol. 9, no. 5, p. 507, 2017.
- [18] Y. M. Kim, R. V. Talanian, J. Li, and T. R. Billiar, "Nitric oxide prevents IL-1 β and IFN- γ -inducing factor (IL-18) release from macrophages by inhibiting caspase-1 (IL-1 β -converting enzyme)," *Journal of Immunology*, vol. 161, no. 8, pp. 4122–4128, 1998.
- [19] Y.-F. Kuo, C.-L. Yeh, J.-M. Shih, Y.-M. Shih, and S.-L. Yeh, "Arginine pretreatment enhances circulating endothelial progenitor cell population and attenuates inflammatory response in high-fat diet-induced obese mice with limb ischemia," *Nutrition Research*, vol. 53, pp. 67–76, 2018.
- [20] C. Pasten, C. Alvarado, J. Rocco et al., "I-NIL prevents the ischemia and reperfusion injury involving TLR-4, GST, clusterin, and NFAT-5 in mice," *American Journal of Physiology, Renal Physiology*, vol. 316, no. 4, pp. F624–F634, 2019.
- [21] M. Kuruş, M. Ugras, and M. Esrefoglu, "Effect of resveratrol on tubular damage and interstitial fibrosis in kidneys of rats exposed to cigarette smoke," *Toxicology and Industrial Health*, vol. 25, no. 8, pp. 539–544, 2009.
- [22] G. Bertolini, D. Luciani, and G. Biolo, "Immunonutrition in septic patients: a philosophical view of the current situation," *Clinical Nutrition*, vol. 26, no. 1, pp. 25–29, 2007.
- [23] M. D. Rosenthal, P. W. Carrott, J. Patel, L. Kiraly, and R. G. Martindale, "Parenteral or enteral arginine supplementation safety and efficacy," *The Journal of Nutrition*, vol. 146, no. 12, pp. 2594S–2600S, 2016.
- [24] Y. C. Luiking, M. Poeze, and N. E. Deutz, "Arginine infusion in patients with septic shock increases nitric oxide production without haemodynamic instability," *Clinical Science*, vol. 128, no. 1, pp. 57–67, 2015.
- [25] P. J. Popovic, H. J. Zeh III, and J. B. Ochoa, "Arginine and immunity," *The Journal of Nutrition*, vol. 137, no. 6, 6 Supplement 2, pp. 1681S–1686S, 2007.
- [26] M. J. Lortie, J. Satriano, F. B. Gabbai et al., "Production of arginine by the kidney is impaired in a model of sepsis: early events following LPS," *American Journal of Physiology-Regulatory, Integrative and Comparative Physiology*, vol. 287, no. 6, pp. R1434–R1440, 2004.
- [27] M. Poeze, M. J. Bruins, F. Kessels, Y. C. Luiking, W. H. Lamers, and N. E. P. Deutz, "Effects of L-arginine pretreatment on nitric oxide metabolism and hepatosplanchnic perfusion during porcine endotoxemia," *The American Journal of Clinical Nutrition*, vol. 93, no. 6, pp. 1237–1247, 2011.
- [28] K. Wijnands, T. Castermans, M. Hommen, D. Meesters, and M. Poeze, "Arginine and citrulline and the immune response in sepsis," *Nutrients*, vol. 7, no. 3, pp. 1426–1463, 2015.
- [29] Y. Xia and J. L. Zweier, "Superoxide and peroxynitrite generation from inducible nitric oxide synthase in macrophages," *Proceedings of the National Academy of Sciences*, vol. 94, no. 13, pp. 6954–6958, 1997.
- [30] K. Murakami, P. Enkhbaatar, Y. M. Yu et al., "L-arginine attenuates acute lung injury after smoke inhalation and burn injury in sheep," *Shock*, vol. 28, no. 4, pp. 477–483, 2007.
- [31] J. Ramachandran and R. D. Peluffo, "Threshold levels of extracellular L-arginine that trigger NOS-mediated ROS/RNS production in cardiac ventricular myocytes," *American Journal of Physiology Cell Physiology*, vol. 312, no. 2, pp. C144–C154, 2017.
- [32] J. Mårtensson, M. Bell, S. Xu et al., "Association of plasma neutrophil gelatinase-associated lipocalin (NGAL) with sepsis and acute kidney dysfunction," *Biomarkers*, vol. 18, no. 4, pp. 349–356, 2013.
- [33] A. Leelahavanichkul, P. Somparn, J. Issara-Amphorn et al., "Serum neutrophil gelatinase associated lipocalin (NGAL) outperforms serum creatinine in detecting sepsis-induced acute kidney injury, experiments on bilateral nephrectomy and bilateral ureter obstruction mouse models," *Shock*, vol. 45, no. 5, pp. 570–576, 2016.
- [34] A. D. Kandhare, M. V. K. Patil, and S. L. Bodhankar, "L-arginine attenuates the ethylene glycol induced urolithiasis in in-nephrectomized hypertensive rats: role of KIM-1, NGAL, and NOs," *Renal Failure*, vol. 37, no. 4, pp. 709–721, 2015.

- [35] M. Correa-Costa, T. T. Braga, P. Semedo et al., "Pivotal role of toll-like receptors 2 and 4, its adaptor molecule MyD88, and inflammasome complex in experimental tubule-interstitial nephritis," *PLoS One*, vol. 6, no. 12, p. e29004, 2011.
- [36] I. Ludwig-Portugall, E. Bartok, E. Dhana et al., "An NLRP3-specific inflammasome inhibitor attenuates crystal-induced kidney fibrosis in mice," *Kidney International*, vol. 90, no. 3, pp. 525–539, 2016.
- [37] A. Lau, H. Chung, T. Komada et al., "Renal immune surveillance and dipeptidase-1 contribute to contrast-induced acute kidney injury," *The Journal of Clinical Investigation*, vol. 128, no. 7, pp. 2894–2913, 2018.
- [38] S. R. Mulay, O. P. Kulkarni, K. V. Rupanagudi et al., "Calcium oxalate crystals induce renal inflammation by NLRP3-mediated IL-1 β secretion," *The Journal of Clinical Investigation*, vol. 123, no. 1, pp. 236–246, 2013.
- [39] S. M. Kim, Y. G. Kim, D. J. Kim et al., "Inflammasome-independent role of NLRP3 mediates mitochondrial regulation in renal injury," *Frontiers in Immunology*, vol. 9, article 2563, 2018.
- [40] H. J. Anders, B. Suarez-Alvarez, M. Grigorescu et al., "The macrophage phenotype and inflammasome component NLRP3 contributes to nephrocalcinosis-related chronic kidney disease independent from IL-1-mediated tissue injury," *Kidney International*, vol. 93, no. 3, pp. 656–669, 2018.
- [41] J. S. Eun, Y. H. Suh, D. K. Kim, and H. Jeon, "Regulation of cytokine production by exogenous nitric oxide in murine splenocyte and peritoneal macrophage," *Archives of Pharmacal Research*, vol. 23, no. 5, pp. 531–534, 2000.
- [42] E. Hernandez-Cuellar, K. Tsuchiya, H. Hara et al., "Cutting edge: nitric oxide inhibits the NLRP3 inflammasome," *Journal of Immunology*, vol. 189, no. 11, pp. 5113–5117, 2012.
- [43] K. Mao, S. Chen, M. Chen et al., "Nitric oxide suppresses NLRP3 inflammasome activation and protects against LPS-induced septic shock," *Cell Research*, vol. 23, no. 2, pp. 201–212, 2013.
- [44] O. Takasu, J. P. Gaut, E. Watanabe et al., "Mechanisms of cardiac and renal dysfunction in patients dying of sepsis," *American Journal of Respiratory and Critical Care Medicine*, vol. 187, no. 5, pp. 509–517, 2013.
- [45] A. A. Reyes, I. E. Karl, and S. Klahr, "Role of arginine in health and in renal disease," *American Journal of Physiology-Renal Physiology*, vol. 267, no. 3, Part 2, pp. F331–F346, 1994.
- [46] M. H. Pai, Y. M. Shih, J. M. Shih, and C. L. Yeh, "Glutamine administration modulates endothelial progenitor cell and lung injury in septic mice," *Shock*, vol. 46, no. 5, pp. 587–592, 2016.
- [47] Y.-M. Hu, Y.-C. Hsiung, M.-H. Pai, and S.-L. Yeh, "Glutamine administration in early or late septic phase downregulates lymphocyte PD-1/PD-L1 expression and the inflammatory response in mice with polymicrobial sepsis," *Journal of Parenteral and Enteral Nutrition*, vol. 42, no. 3, pp. 538–549, 2017.
- [48] G. Wu, F. W. Bazer, T. A. Davis et al., "Arginine metabolism and nutrition in growth, health and disease," *Amino Acids*, vol. 37, no. 1, pp. 153–168, 2009.
- [49] D. Di Giandomasso, H. Morimatsu, C. N. May, and R. Bellomo, "Intrarenal blood flow distribution in hyperdynamic septic shock: effect of norepinephrine," *Critical Care Medicine*, vol. 31, no. 10, pp. 2509–2513, 2003.
- [50] Y. Y. Wang, H. F. Shang, Y. N. Lai, and S. L. Yeh, "Arginine supplementation enhances peritoneal macrophage phagocytic activity in rats with gut-derived sepsis," *Journal of Parenteral and Enteral Nutrition*, vol. 27, no. 4, pp. 235–240, 2003.
- [51] C. L. Yeh, C. S. Hsu, S. C. Chen, Y. C. Hou, W. C. Chiu, and S. L. Yeh, "Effect of arginine on cellular adhesion molecule expression and leukocyte transmigration in endothelial cells stimulated by biological fluid from surgical patients," *Shock*, vol. 28, no. 1, pp. 39–44, 2007.